U.S. DEPARTMENT OF COMMERCE
National Technical Information Service

PB-277 733

Atmospheric Tracer Studies to Characterize the Transport and Dispersion of Pollutants in the California Delta Region. Volume I. Presentation and Discussion of Results

California Inst. of Technology, Pasadena

Prepared for

California State Air Resources Board, Sacramento

15 Jun 77

PB 277 733

ATMOSPHERIC TRACER STUDIES TO CHARACTERIZE THE TRANSPORT AND DISPERSION OF POLLUTANTS IN THE CALIFORNIA DELTA REGION

VOLUME I

PRESENTATION AND DISCUSSION OF RESULTS

Contract No. ARB-A5-065-87

June 15, 1977

Prepared for:

State of California
Air Resources Board
1709 11th Street
Sacramento, California 95814

by

Brian K. Lamb

and

Fredrick H. Shair
(Principal Investigator)

Division of Chemistry and Chemical Engineering
California Institute of Technology
Pasadena, California 91125

REPRODUCED BY
NATIONAL TECHNICAL
INFORMATION SERVICE
U.S. DEPARTMENT OF COMMERCE
SPRINGFIELD, VA. 22161

BIBLIOGRAPHIC DATA SHEET

1. Report No.
ARB-R-A5-065-87-77-69

2.

3. Recipient's Accession No.
PB277735

4. Title and Subtitle
Atmospheric Tracer Studies to Characterize the Transport and Dispersion of Pollutants in the California Delta Region.
Volume 1: Presentation and Discussion of Results

5. Report Date
June 1977

6.

7. Author(s)
Brian K. Lamb and Fredrick H. Shair

8. Performing Organization Rept. No.

9. Performing Organization Name and Address
Division of Chemistry and Chemical Engineering
California Institute of Technology
Pasadena, CA 91125

10. Project/Task/Work Unit No.

11. Contract/Grant No.
ARB - A5 - 065 - 87

12. Sponsoring Organization Name and Address
Air Resources Board
State of California
P.O. Box 2815
1102 Q Street
Sacto, CA 95812

13. Type of Report & Period Covered
final

14.

15. Supplementary Notes

16. Abstracts

Eight tracer studies were conducted during four designated meteorological periods in 1976 to quantitatively determine the transport and dispersion characteristics of the air passing over a proposed industrial site in the Montezuma Hills. On the average, plumes emitted from the Montezuma Hills during the test periods were transported southeast. Estimates of tracer concentrations based upon the Gaussian plume model were found to be reasonably accurate. A nomograph was developed to permit rapid calculation of non-reactive pollutant concentrations from tracer data and pollutant emission rates; in the case of NO_2, the oxidation of NO to NO_2 was assumed to be rapid relative to the transport time. The nomograph was used to predict ground level concentrations of pollutants resulting from the projected emissions associated with the proposed Dow complex in the Montezuma Hills. A reasonable correlation was found to exist between the horizontal standard deviation of the wind, σy , and the horizontal dispersion parameter of the plume, σy. The correlation between $\sigma\theta$ and σy, along with air parcel trajectory analysis provide a means for extending the results of this study to other periods of the year.

17. Key Words and Document Analysis

Air Pollution
Smog
Plume Detection
Tracer
Sulfur Hexafluoride

Nitrogen Oxides
Gas Chromatography

17b. Identifiers/Open-Ended Terms

Montezuma Hills
California Delta Region
Hino Correction
Plume Model
Pollutant Emission Rates
San Joaquin Valley
Industrial Growth
Environmental Impact
Bromotrifluoromethane

17c. COSATI Field/Group

18. Availability Statement Release unlimited. Available from National Technical Information Service 5285 Port Royal Road Springfield, VA 22161

19. Security Class (This Report) UNCLASSIFIED

20. Security Class (This Page) UNCLASSIFIED

21. No. of Pages
284

22. Price
PC A13 MF A01

The statements and conclusions in this report are those of the contractor and not necessarily those of the California Air Resources Board. The mention of commercial products, their source or their use in connection with material reported herein is not to be construed as either an actual or implied endorsement of such products.

Portions of this report may not be
clearly reproduced. Information about
any illegible portion may be obtained
from the author

SUMMARY

Eight atmospheric tracer studies, utilizing $CBrF_3$ and/or SF_6, were conducted from August 31, 1976, through September 14, 1976, within the California Delta Region during four designated meteorological periods. The purpose of these tests was to quantitatively determine the transport and dispersion characteristics of the air passing over the Montezuma Hills. The data base was comprehensive enough to permit accurate mass balances of the tracer; essentially all of the tracer was accounted for by this analysis. Due to the steadiness of the winds, the plume trajectories at 10 km and 50 km downwind of the Montezuma Hills were found to be quite similar. On the average, plumes emitted from the Montezuma Hills during the test periods were transported southeast over Stockton. As a result of the steady nature of the winds, the commonly used Hino correction was found to grossly underestimate the hourly-averaged tracer concentrations computed from 10-second averaged concentrations. A comparison of experimentally determined dispersion parameters with those associated with Pasquill atmospheric stability classes indicated that atmospheric stability generally decreases with increasing distance downwind from the Montezuma Hills. In spite of the complex meteorology and terrain, estimates of tracer concentrations based upon the Gaussian plume model were found to be reasonably accurate. A nomograph was developed to permit rapid calculation of non-reactive pollutant concentrations from tracer data and pollutant emission rates; in the case of NO_2, the oxidation of NO to NO_2 was assumed to be rapid relative to the transport time. The nomograph was used to predict ground level concentrations of pollutants resulting from the projected emissions associated with the proposed Dow complex in the Montezuma Hills. A reasonable correlation was found to exist between the horizontal standard deviation of the wind, σ_θ, and the horizontal dispersion parameter of the plume, σ_y. Air parcel trajectories, based upon Goodin's (1977) numerical solution to the two-dimensional mass balance equation were found to be in excellent agreement with the tracer data. The correlation between σ_θ and σ_y, along with the trajectory analysis provide a means for extending the results of this study to other periods of the year. This investigation indicates where emissions from the Montezuma Hills should be monitored. Finally, these results suggest that further study regarding the chemistry, transport and dispersion of pollutants entering the San Joaquin Valley will be of considerable interest.

ACKNOWLEDGMENT

We are very happy to acknowledge Charles L. Bennett and Jack K. Suder, both Senior Air Pollution Research Specialists with the California Air Resources Board, for their interest, helpful suggestions, and their help in coordinating this program.

The cooperation of William Anderson and David Bauer of the Dow Chemical Company was greatly appreciated. We wish to thank Art Schafer and L. Willard Richards of Rockwell International for their support.

We wish to thank John Pryshepa of Caltrans for the use of their portable anemometers. We thank Norman Baker for his support in providing airborne sampling and pertinent meteorological data. We thank Neal Moyer of the Air Resources Board for providing emission data, and Burton Okin of the Bay Area APCD for providing meteorological data.

Personnel from Meteorology Research, Incorporated provided meteorological support and also collected airborne samples. In particular, we wish to thank Ted B. Smith, Hans D. Giroux, and William Knuth for their cooperation throughout the field study.

We thank Joseph Spano of the San Joaquin APCD for his support in providing air sampling sites. We also thank the California State Police along with local firefighters for providing a number of air sampling sites. The Pinole police department was very cooperative in providing a release location. We express our thanks to the many people at APCD stations, private businesses, and homes who allowed us to operate the hourly air sampling systems.

We wish to thank C. Ray Dickson of the NOAA Laboratories in Idaho Falls, Idaho, for helpful suggestions regarding the development of chromatographic columns which were used to separate SF_6 and $CBrF_3$.

We thank Russell Bennett and Dave Suder for their help in obtaining air samples during the field study.

We wish to thank George Griffith, Henry Smith, Ray Reed, and John Yehle for their willingness to lend a hand when the need arose. We also thank Sharon ViGario for her patience in the typing of this report.

Finally, we thank the management of the California Holiday Lodge for permitting us to set up a small laboratory on their premises.

PERSONNEL

The following persons participated in the 1976 California Delta tracer field studies:

1. Mr. Bart Croes
2. Mr. Andrew Falls
3. Mr. Arthur Gooding
4. Mr. Jim Hickey
5. Mr. Eric Kaler
6. Mr. Brian Lamb
7. Mrs. Margaret Lamb
8. Mr. Wing Hong Lee
9. Mr. Ernest Sasaki
10. Dr. Fredrick Shair
11. Mr. Peter Shair
12. Mr. Jim Westover

TABLE OF CONTENTS

Volume I

Page

Summary: Volume I iii

Acknowledgment iv

Personnel v

Table of Contents: Volume I vi

Table of Contents: Volume II, Parts A and B viii

List of Tables x

List of Figures xi

1. Introduction 1
   - 1.1 Industrialization of the California Delta Region 1
   - 1.2 Literature Review 4
   - 1.3 Objectives of the California Delta Tracer Study 7
2. Meteorology and Topography of the California Delta Region 8
3. Experimental Procedure 15
   - 3.1 Field Test Design and Schedule 15
   - 3.2 Tracer Release System 15
   - 3.3 Air Sampling Systems 17
     - 3.31 Automobile Traverse System 17
     - 3.32 Airborne Air Sampling System 17
     - 3.33 Hourly Average Sequential Samples 17
   - 3.4 Chemical Analysis of Air Samples 27
   - 3.5 Meteorological Support Systems 33
     - 3.51 Surface Wind Data 33
     - 3.52 Upper Air Wind Data 33
4. Presentation and Discussion of Results 39
   - 4.1 Relation of Tracer Data to Industrial Pollutant Emissions 39
   - 4.2 Description of the Tracer Tests 48

Table of Contents, Volume I (Continued)

Page

4.21 Tracer Test 1 (8/31/76) 48
4.22 Tracer Test 2 (9/2/76) 54
4.23 Tracer Test 3 (9/5/76) 67
4.24 Tracer Test 4 (9/6/76) 76
4.25 Tracer Test 5 (9/9/76) 86
4.26 Tracer Test 6 (9/10/76) 91
4.27 Tracer Test 7 (9/13/76) 102
4.28 Tracer Test 8 (9/14/76) 116
4.3 Determination of Dispersion Parameters from Automobile Traverse and Airborne Spiral Tracer Data 122
4.4 Mass Balance of Tracer Data 134
4.5 Analysis of Dispersion 142
4.6 Use of Field Study Data for Air Quality Model Development 182
4.7 Applicability of the Gaussian Plume Model in the California Delta Region 182
4.8 Relation of Dispersion Data to Fluctuations of the Wind 210
4.9 Estimated Maximum Pollutant Concentrations 230

5. Calculation of the Surface Wind Field 236

Appendix A (Gas Chromatograph Calibration Results) 258

Appendix B (Calculation of Plume Parameters from Crosswind Traverses) 260

Literature Cited 264

TABLE OF CONTENTS
VOLUME II, PARTS A AND B

Part A

		Page
Summary: Volume II, Parts A and B		iii
Acknowledgment		v
Personnel		vi
Table of Contents		vii
List of Tables		ix
List of Figures		x
1.	Introduction	1
2.	Experimental Procedure	4
3.	Presentation of Tracer Data	21
3.1	Relation of Tracer Data to Industrial Pollutant Emissions	21
3.2	Overview of Tracer Data	25
3.3	Automobile Traverse Tracer Data	93
3.4	Airborne Traverse Tracer Data	122
3.5	Airborne Spiral Tracer Data	130
3.6	Automobile Traverse Best-fit Gaussian Curves	133
3.7	Airborne Spiral Best-fit Gaussian Curves	165
3.8	Hourly Averaged Tracer Data	168
3.9	Hourly Averaged Crosswind Tracer Concentrations	183
3.10	Mass Balance of Tracer Data	187
3.11	Crosswind Horizontal and Vertical Standard Deviations as Functions of Downwind Distance	193
3.12	Comparison of Experimental Dispersion Results with Pasquill Dispersion Parameters	228
4.	Relationship of Dispersion Data to Wind Data	257
4.1	Fluctuations in the Horizontal Winds	257
4.2	Horizontal Dispersion as a Function of Wind Fluctuations	260
4.3	Atmospheric Stability Classification	262

Part B

Page
5. Tabulation of Tracer Data 264
5.1 Automobile Traverse Tracer Data 264
5.2 Airborne Traverse Tracer Data 400
5.3 Airborne Spiral Tracer Data 438
5.4 Hourly Averaged Sequential 12-Hour Tracer Data 455
5.5 Hourly Averaged Sequential 3-Hour Tracer Data 468
6. Tabulation of Meteorological Data 475
6.1 Hourly Averaged Wind Speed and Direction Data 475
6.2 Montezuma Hills Pibal Summary 512
6.3 Estimation of Mixing Layer Depth 571
6.4 Upper Air Average Wind Speed and Direction Data 576

Literature Cited

LIST OF TABLES

Page

1. Daily Average Wind Summary for the Dow and Brentwood Stations. 12

2. Tracer Release Data. 16

3. Descriptions of Automobile and Airborne Traverses and Airborne Spirals. 18

4. Location of Hourly Averaged Sequential Air Samplers. 28

5. Wind Data Stations and Description of Wind Data. 34

6. Projected Dow Emissions and Associated Nomograph K Values. 43

7. Pollutant Emissions from Major Point Sources in the Northeastern Bay Area. 45

8. Average Meteorological Conditions During the Field Tests. 49

9. Best-fit Gaussian Curve Results. 129

10. Tracer Mass Balance Results. 138

11. Horizontal and Vertical Crosswind Dispersion Coefficients. 147

12. Stack Characteristics from the Dow Montezuma Hills Plant. 205

13. Comparison of 10-second and Hourly Averaged Maximum Tracer Concentrations. 220

14. Maximum Pollutant Concentrations Due to Projected Dow Emissions. 231

15. Comparison of NO_2 Concentration Measurements and Estimations. 234

A-1 Gas Chromatograph Calibration Results. 258

A-2 Gas Chromatograph Cross-Check Results. 259

LIST OF FIGURES

		Page
1.	The California Delta Region.	3
2.	Prevailing west and northwest wind flow types.	9
3.	Topographical map of the Bay Area, California Delta, and San Joaquin Valley.	13
4.	Typical tracer chromatogram.	30
5.	Gas chromatograph calibration curves for dual tracers.	32
6.	Location of surface wind and upper air data stations.	38
7.	Conversion nomograph for converting SF_6 tracer concentrations to pollutant concentrations.	41
8.	Conversion nomograph for converting $CBrF_3$ tracer concentrations to pollutant concentrations.	42
9.	Surface wind streamlines, 1600 PDT, 8/31/76.	50
10.	Overview of automobile traverse tracer data, Test 1.	52
11.	Hourly averaged crosswind SF_6 profiles measured along Highway 160, Test 1.	53
12.	Hourly averaged crosswind SF_6 profiles measured along Highway 99, Test 1.	55
13.	Overview of hourly averaged SF_6 data, Test 1.	56
14.	Surface wind streamlines, 1600 PDT, 9/2/76.	57.
15-17.	Overview of automobile traverse tracer data, Test 2.	59-61
18.	Hourly averaged crosswind $CBrF_3$ profiles measured along Highway 160, Test 2.	62
19.	Hourly averaged crosswind SF_6 profiles measured along Highway 160, Test 2.	64
20.	Overview of hourly averaged SF_6 data, Test 2.	55
21.	Hourly averaged crosswind SF_6 profiles measured along Highway 99, Test 2.	66
22.	Surface wind streamlines, 0100 PDT, 9/5/76.	68

List of Figures (Continued)

		Page
23-24.	Overview of automobile traverse SF_6 data, Test 3.	69-70
25.	Overview of hourly averaged SF_6 data, Test 3.	72
26-28.	Hourly averaged crosswind SF_6 profiles measured along Highway 99, Test 3.	73-75
29.	Surface wind streamlines, 1900 PDT, 9/6/76.	77
30-31.	Overview of automobile traverse SF_6 data, Test 4.	78-79
32.	Overview of hourly averaged SF_6 data, Test 4.	81
33-36.	Hourly averaged crosswind SF_6 profiles, measured along Highway 99.	82-85
37.	Surface wind streamlines, 1300 PDT, 9/9/76.	88
38-39.	Overview of automobile traverse SF_6 data, Test 5.	89-90
40.	Surface wind streamlines, 1000 PDT, 9/10/76.	92
41-42.	Overview of automobile traverse SF_6 data, Test 6.	93-94
43,45-46.	Overview of airborne traverse SF_6 data, Test 6	95, 98-99
44.	Vertical SF_6 profile observed over Frank's Tract Recreation Area, Test 6.	97
47.	Overview of hourly averaged SF_6 data, Test 6.	100
48.	Hourly averaged crosswind SF_6 profiles, Test 6.	101
49.	Surface wind streamlines, 1000 PDT, 9/13/76	103
50-54.	Overview of automobile traverse tracer data, Test 7.	104-108
55,57-58.	Overview of airborne traverse tracer data, Test 7.	111, 113-114
56.	Vertical SF_6 profiles observed 0.8 Km north of the Port Chicago Naval Depot.	112
59.	Overview of hourly averaged SF_6 data, Test 7.	115
60.	Surface wind streamlines, 1000 PDT, 9/14/76	117

List of Figures (Continued)

		Page
61-62.	Overview of automobile traverse SF_6 data, Test 8.	118- 119
63.	Overview of airborne traverse SF_6 data, Test 8.	120
64.	Vertical SF_6 profile observed 0.8 Km north of the Port Chicago Naval Depot.	121
65-66.	Typical best-fit Gaussian curves to automobile traverse tracer data.	125- 126
67-68.	Best-fit Gaussian curves to airborne spiral tracer data.	127- 128
69.	Horizontal crosswind dispersion parameter, σ_y, as a function of distance downwind of the Dow site.	143
70.	Vertical crosswind dispersion parameter, σ_z, as a function of distance downwind of the Dow site.	144
71.	Vertical crosswind dispersion parameter, σ_z, as a function of distance downwind of the Pinole site.	145
72.	Vertical crosswind dispersion parameter, σ_z, as a function of distance downwind of the Pinole site.	146
73-78.	Horizontal and vertical crosswind dispersion parameters, σ_y and σ_z, as functions of downwind distance (by meteorological period).	152- 157
79-92.	Comparison of horizontal and vertical dispersion of tracer plumes with the dispersion of plumes associated with Pasquill atmospheric stability classes (by test).	158- 171
93.	Horizontal crosswind dispersion parameter, σ_y, as a function of distance downwind of the Dow site compared with the dispersion parameter associated with Pasquill atmospheric stability classes (by meteorological period).	175
94.	Vertical crosswind dispersion parameter, σ_z, as a function of distance downwind of the Dow site compared with the dispersion parameter associated with Pasquill atmospheric stability classes (by meteorological period).	176
95.	Horizontal crosswind dispersion parameter, σ_y, as a function of distance downwind for tracer releases from Pinole and Martinez and the dispersion parameter associated with Pasquill atmospheric stability classes (by meteorological period).	177

List of Figures (Continued)

		Page
96.	Vertical crosswind dispersion parameter, σ_z, as a function of distance downwind for tracer releases from Pinole and Martinez, and the dispersion parameter associated with Pasquill atmospheric stability classes (by meteorological period).	178
97-108.	Centerline tracer concentrations compared with centerline concentrations predicted using the Gaussian plume model.	185-197
110-112.	Crosswind tracer profiles compared with crosswind profiles predicted using the Gaussian plume model.	201-203
113-115.	Centerline tracer concentrations compared with centerline concentrations predicted using the Briggs plume rise model and the Gaussian plume model.	207-209
116-117.	Horizontal standard deviation of the wind as a function of time of day.	211-212
118.	Plume centerline concentration as a function of distance north of the Highway 4 - Highway 160 junction along Highway 160.	214
119.	Plume centerline concentration as a function of distance south of Sacramento along Highway 99	215
120.	Average plume centerline positions for plumes emitted from the Dow site in the Montezuma Hills.	216
121.	Horizontal crosswind standard deviation, σ_y, as a function of the horizontal standard deviation of the wind, σ_θ.	222
122.	Horizontal standard deviation of the wind, σ_θ, as a function of time of day for different averaging periods.	225
123-125	Horizontal crosswind standard deviation, σ_y, as a function of the horizontal standard deviation of the wind, σ_θ, for different averaging times.	226-28
126.	Estimation of distance downwind of the Montezuma Hills where the concentration of NO$_2$ (caused by projected Dow emissions) equals maximum ambient levels.	233
127.	California Delta Region wind calculation grid system.	237

List of Figures (Continued)

		Page
128-139	Hourly surface wind vectors, 1200-2300 PDT, 8/31/76.	239-250
140-142.	Hourly upper air wind vectors, 1700 PDT, 8/31/76.	251-253
143.	Forward air parcel surface trajectories from the Montezuma Hills, 8/31/76.	255
144.	Forward air parcel surface trajectories from Pinole and Martinez, 8/31/76.	257

1. Introduction

1.1 Industrialization of the California Delta Region

Interbasin air flow between the Bay Area of San Francisco and the Sacramento and San Joaquin Valleys of central California is characterized during the summer months by a sharp low-level temperature inversion (Miller, 1968) and a strong diurnal sea breeze (Fosberg and Schroeder, 1966). A northern component of the marine air flows through the Bay Area, channels into the Carquinez Strait and fans across the Delta region of the Sacramento and San Joaquin Rivers (Smalley, 1957). Ultimately, the air passing over the heavily populated and industrialized Bay Area passes from the Delta region into the Sacramento and San Joaquin Valleys. The presence of large industrial complexes, projected for construction in the Montezuma Hills of the Delta region, may add to the levels of atmospheric pollutants already present in the air passing through the area. The existence of the urban centers upwind and downwind of the proposed construction sites, the rugged terrain surrounding the Bay Area, and the complex meteorological patterns in the region prohibit simple predictions of the impact associated with future industrialization. An analysis of the extent of adverse impact upon air quality which may result from industrial development of the Montezuma Hills requires a study of the transport and dispersion of pollutants emitted within the Delta region and the Bay Area. The use of atmospheric tracer techniques, utilizing gaseous tracers such as SF_6 and $CBrF_3$, provides a relatively simple and inexpensive means to obtain important data which can be used to assist in the impact analysis. The results from eight full-scale tracer studies conducted in the California Delta Region (shown in Figure 1) during September, 1976, are presented in this report. The cost of these tracer studies was less than .02% of the capital investments required for the construction of just one of the proposed industrial facilities.

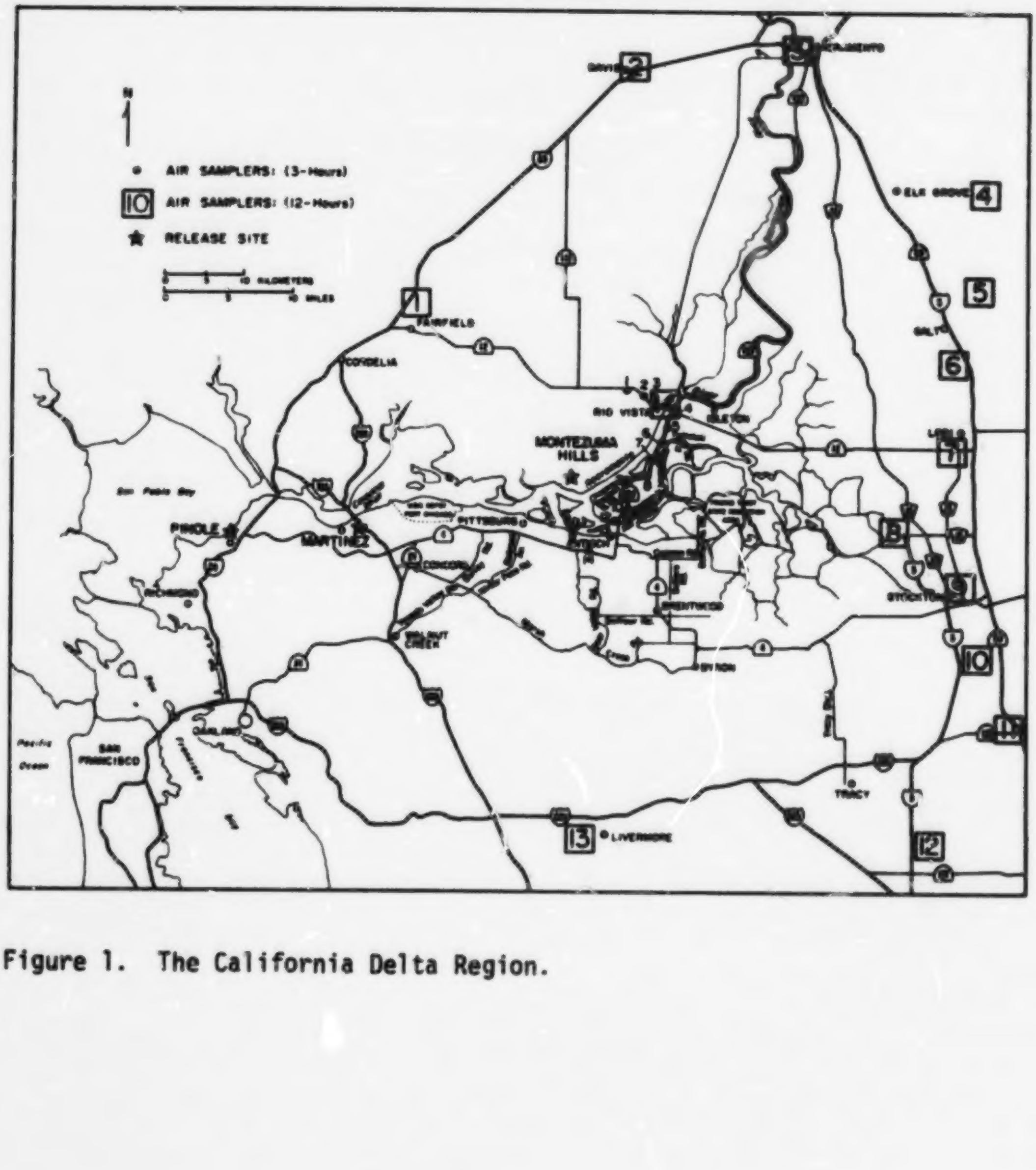
N
AIR SAMPLERS: (3-Hours)
10 AIR SAMPLERS: (12-Hours)
RELEASE SITE
0 5 10 KILOMETERS
0 5 10 MILES
SACRAMENTO
DAVIS
2
ELK GROVE
4
5
GALT
6
LODI
1
FAIRFIELD
CORDELIA
1 2 3
RIO VISTA
ISLETON
MONTEZUMA HILLS
San Pablo Bay
PINOLE
MARTINEZ
PITTSBURG
ANTIOCH
CONCORD
RICHMOND
BRENTWOOD
STOCKTON
WALNUT CREEK
BYRON
10
OAKLAND
Pacific Ocean
SAN FRANCISCO
TRACY
13
LIVERMORE
12

Figure 1. The California Delta Region.

1.2 Literature Review

The transport and dispersion of pollutants under complex topographical and meteorological conditions have been the concern of a growing list of workers (Pasquill, 1974). Start, et al. (1974) used tracer techniques in Utah to determine the amount of dilution which occurs for airborne material passing over and around mountains and canyons. They concluded that enhanced mechanical turbulence associated with rough terrain increased dilution over that found in flat regions. Terrain effects were found to increase with increasing stability. Similar conclusions were reached by Giroux, et al. (1974) from a tracer test conducted in southern California. In that test, the SF_6 tracer was followed as far as 40 km downwind of the release point. MacReady, et al. (1974) agreed with the preceding reports in suggesting that turbulence was generated from topographical-induced horizontal divergence patterns. From the results of diffusion tests in the Point Arguello area of southern California, Hinds (1970) found that "daytime (unstable) conditions minimized the importance of terrain whereas nighttime (stable) conditions led to apparently significant interactions between terrain and synoptic scale weather events." Angell, et al. (1966,1976) used tetroons to study pollutant trajectories through the southern California air basin. Tetroons released along the coast in some instances were carried out to sea and then, with the diurnal reversal of the winds, swept back into the interior of the basin. In the latter work (1976), tetroons released in early morning near Los Angeles were tracked eastward through the Puente Hills as far as San Bernardino. Other tetroons, released under more stagnant conditions, moved south before turning east into the Santa Ana Canyon.

Previous work in this laboratory has attempted to characterize the transport and dispersion of pollutants in California coastal areas. Drivas and Shair (1974) released 33.5 Kg of SF_6 over 45 minutes from Anaheim, California, and followed the tracer through five neighboring communities as far as Palm Springs, 124 km downwind. These authors (1975) also conducted full-scale tracer studies from power plant stacks in both the Moss Landing and Long Beach coastal zones of California. Afternoon tracer plumes from Moss Landing were observed to move southeast through the Salinas Valley. Afternoon tracer plumes from Long Beach were transported northeast toward Fullerton and Pomona, and then eastward toward San Bernardino. Lamb and Shair (1977) conducted a tracer study from the Oxnard Plain in Ventura County and found that plumes were transported east along the coast and along an inland route into the San Fernando Valley of the Los Angeles Air Basin. These studies reflect the usefulness of tracer techniques in studying the transport and dispersion of pollutants under complex coastal meteorological and topographical conditions.

Fosberg, et al. (1976) attempted to account for the effects of mass divergence upon pollutant dispersion by modifying the well-known Gaussian plume model. Inclusion of a divergence term in the Gaussian expression decreased calculated pollutant concentrations by as much as a factor of two. In other work using the Gaussian plume model, Peters and Richards (1977) developed a scheme to incorporate fast reversible chemical reactions into dispersion models. Application of the procedure to the conversion of NO to NO_2 by reaction with ozone and to the reaction of sulfuric acid with ambient ammonia was presented. This procedure is based on the assumption that local chemical equilibria is achieved at each receptor site. Liu, et al. (1976) showed how to modify the Gaussian dispersion terms to account for the roughness of the terrain. Their derivation of the modified dispersion parameters was based on development of the relationship of the eddy diffusivities and the Gaussian dispersion parameters. Liu, et al. found that for a surface roughness of 50 cm the modified dispersion parameters resulted in a decrease in concentration by a factor of two from the conventional Gaussian model.

Several authors have utilized forms of the diffusion equation to develop dispersion models which take into account the effects of terrain. Roffman and Grimble (1974) developed a three-dimensional model based on successive coordinate transformations where one coordinate was required to be parallel to the flow during each segment of the transport path. Reynolds, et al. (1973) used a coordinate transformation to take into account the irregularity of the floor of the Los Angeles Air Basin.

The experimental studies cited above generally indicate that pollutants are dispersed to a greater extent over complex terrain than over flat surfaces. Furthermore, under stable atmospheric conditions, the effects of terrain upon dispersion and transport are increased over that observed under unstable conditions. Transport paths over complex terrain within complicated meteorological patterns appear to be relatively difficult to predict on a quantitative basis. Efforts are progressing on the modification and development of atmospheric dispersion models to account for the effects of terrain and meteorology upon the transport and dispersion of pollutants.

1.3 Objectives of the California Delta Tracer Study

The purpose of this work was to determine the trajectories and dilution of pollutants emitted from the Montezuma Hills and from the northern portion of the Bay Area under typical and worst-case meteorological conditions. The quantitative examination of the tracer data was expected to provide a means of estimating the impact upon regional air quality of the operation of large industrial complexes in the Montezuma Hills. Such an impact analysis would include a comparison of the effects of emissions from existing and future pollutant sources.

The tracer data and accompanying meteorological data would provide a comprehensive data base for the validation and calibration of the Gaussian plume model and more detailed, large-scale numerical dispersion models. The meteorological data would be used to determine the applicability of the results of the tracer studies to other periods of the year.

2. Meteorology and Topography of the California Delta Region

Surface wind patterns from Smalley (1957) indicate that the Carquinez Strait is the major channel for air flow over the Delta Region. During September in the years 1952-1955, the surface wind patterns most prevalent in the area were the west and northwest wind flow types shown in Figure 2. According to Smalley, these patterns occurred 51% of the time, and light and variable winds accounted for 23% of the time. Patterns W5, W2, and W6 were most often observed; they occurred 14%, 10%, and 10% of the time, respectively. These surface patterns show how marine air can become laden with urban pollutants in the Bay Area, pass over the Delta Region, and then turn either north to Sacramento or south to Stockton. Fosberg and Schroeder (1966) explained the onshore summer flow patterns as the result of strong pressure and temperature gradients developed from the coexistence of the eastern Pacific subtropical high pressure area off the coast and a thermal trough in the interior.

Wind flow from the Bay Area through the Delta typically centers around the daily occurrence of an afternoon sea breeze. Fosberg and Schroeder (1966) pointed out that this sea breeze, which is caused by differential heating and cooling of the land and sea, is superimposed upon the summer marine air flow. Miller (1968) noted that the central California sea breeze was accompanied by a sharp, low-level temperature inversion extending inland as far as 40 km. The diurnal cycle can be divided into four periods of the day (Smith, 1976). During Sea Breeze conditions, from approximately 1300 to 1800, winds are relatively strong throughout the area. The average wind speeds at Martinez, Sacramento, and Stockton during the Sea Breeze test periods were respectively, 5 m/sec,

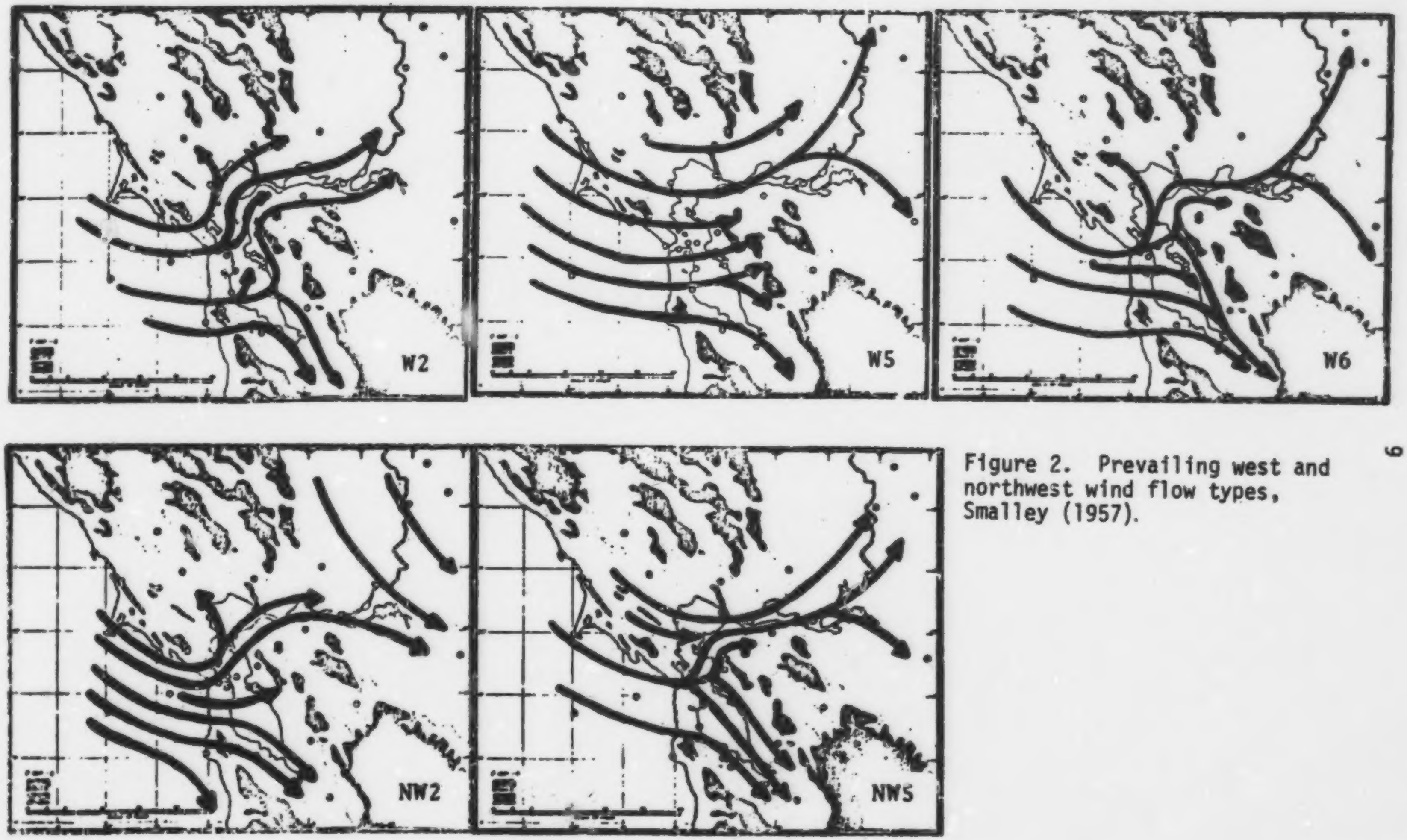
W2
W5
W6
NW2
NW5

Figure 2. Prevailing west and northwest wind flow types, Smalley (1957).

2 m/sec, 4 m/sec. Smalley noted that wind flow types W5 and W6 accounted for 40% of the patterns observed at 1600 hours. In the afternoon, the mixing depth reaches a maximum due to the heating of the land. Typical afternoon mixing depths during the test period were between 1000 and 3000 meters. This pattern is opposite to that which occurs during Nighttime conditions from approximately midnight to 0500. At night, the height of the mixing layer drops to a minimum, typically between 100 and 500 meters. Air flow stagnates as drainage from the Sierra Nevada Mountains meets the weak sea flow over the Central Valley. According to the Smalley report, light and variable winds occurred during 38% of the measurements taken at 0400; west wind types accounted for 39% of measurements in the early morning. Two transition periods separate the Sea Breeze and Nighttime regimes: Pre-Sea Breeze conditions occur from approximately 0600 to 1100 and are characterized by lifting of the nighttime mixing layer and development of the marine air flow. Wind type W2 was observed in 13% of the patterns at 1000, and light and variable winds were measured during 28% of the time at 1000. Sea Breeze Tail conditions follow the afternoon period and are typified by a decrease in mixing height and a decrease in the strength of the coastal flow. West wind flows in the Smalley work existed in 48% of the observations taken at 2200.

As a result of this summertime meteorological cycle, a strong, relatively constant jet of air issues from the Carquinez Strait and fans out into the reaches of the Delta Region and Central Valley. Fosberg and Schroeder (1966) indicated that the wind surge associated with the invading marine air gains speed as it passes through the Carquinez Strait where it combines with the intensely channeled summer marine flow. It appears that part of this jet maintains its strength past the Montezuma Hills and then dissipates fairly rapidly just beyond the area. For example, during the two-week test period in early September, the average surface wind speed at the Dow site in the Montezuma Hills was 7 m/sec; further downwind, at Brentwood, the average surface wind speed was 2 m/sec. The daily average wind speeds measured at two levels at the Dow site and at the surface at Brentwood are given in Table 1.

The existence of this jet suggests that material emitted from the Montezuma Hills may be carried into the Central Valley within a narrow, stable stream of air. Material emitted west of the Carquinez Strait into the marine flow may be widely dispersed by the divergence of air from the Strait. Pollutants emitted from sources located very near one another in the vicinity of the Carquinez Strait may be transported along widely different trajectories into the Sacramento or San Joaquin Valleys.

Terrain effects on air flow through the Carquinez Strait appear to be very important in determining pollutant trajectories through the Delta Region. In a Bay Area tracer study utilizing fluorescent particles, Sandberg, et al. (1970) found that the hilly terrain surrounding San Francisco Bay served to deflect westerly marine air flow into the northerly and southerly trajectories apparent in the Smalley wind patterns. Sandberg noted that the presence of low-level temperature inversions enhanced the effects of the Bay Area terrain upon air flow. Results from the tracer study showed that the hilly terrain increased pollutant dispersion, but channeling through such terrain caused higher concentrations to occur locally. The map in Figure 3 shows the topographical contour

TABLE 1

DAILY AVERAGE WIND SUMMARY FOR THE DOW AND BRENTWOOD STATIONS

Date	Dow (surface) 10 meters Ave. Speed (m/sec)	Dow (surface) 10 meters Prevailing Direction	Dow (tower) 56 meters Ave. Speed (m/sec)	Dow (tower) 56 meters Prevailing Direction	Brentwood (surface) 10 meters Ave. Speed (m/sec)	Brentwood (surface) 10 meters Prevailing Direction
Aug. 30	5.6	W	7.2	W	2.6	NW
" 31	7.3	W	8.5	W	2.5	N
Sept. 1	9.6	W	10.2	W	2.1	NNE
" 2	8.9	W	9.7	W	2.2	NNE
" 3	9.6	W	10.7	W	2.3	N
" 4	8.9	W	10.2	W	2.3	NNE
" 5	8.5	W	9.6	W	2.3	N
" 6	6.8	W	7.5	W	2.4	NNE
" 7	5.8	NE	7.6	N	3.0	NNE
" 8	3.0	WNW	4.2	WNW	2.9	NNE
" 9	5.0	W	6.5	W	2.5	N
" 10	6.3	W	7.0	W	1.8	NE
" 11	5.6	W	6.1	W	-	-
" 12	5.9	W	6.5	W	2.3	NNW
" 13	6.2	W	7.3	W	1.7	NNE
" 14	8.9	W	10.0	WSW	3.5	WSW
" 15	7.2	W	7.7	W	2.9	WSW
" 16	5.9	W	6.9	W	1.9	NW
AVE.	6.9 (m/sec) (16 mph)		AVE. 8.0 (m/sec) (18 mph)		AVE. 2.4(m/sec) (5 mph)	

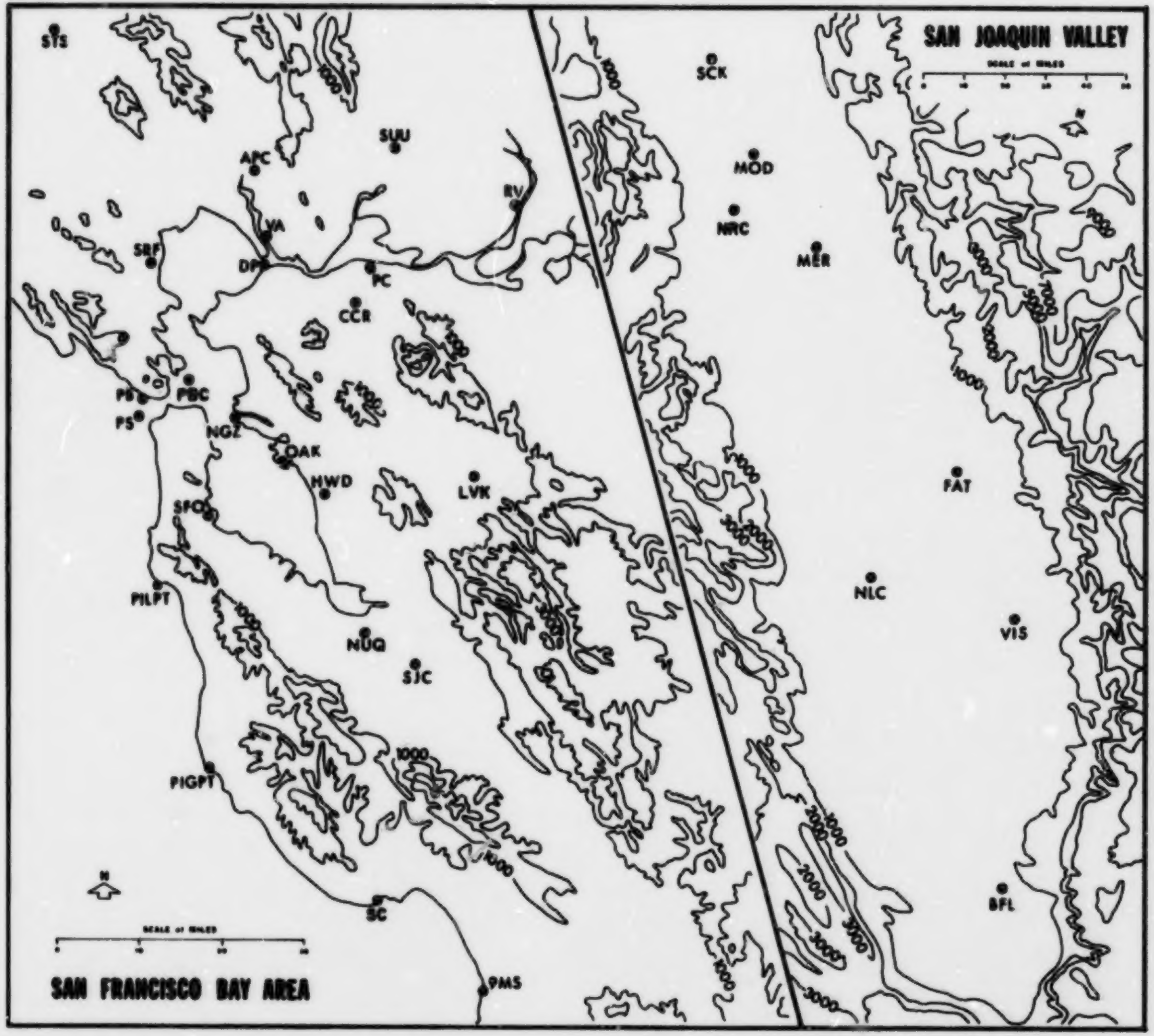
SAN FRANCISCO BAY AREA
SCALE of MILES
N
STS
APC
SUU
RV
VA
SRF
DP
PC
CCR
PB
PBC
PS
NGZ
OAK
HWD
LVK
SFO
PILPT
NUQ
SJC
PIGPT
SC
9MS
1000
SAN JOAQUIN VALLEY
SCALE of MILES
N
SCK
MOD
NRC
MER
FAT
NLC
VIS
BFL
1000
2000
3000
7000
9000

Figure 3. Topographical map of the Bay Area, California Delta, and San Joaquin Valley. Contour lines are given in feet.

lines in 1000 foot intervals for the field study region. Fosberg and Schroeder (1966) found that channeling and deflecting by topographic barriers is extremely noticeable on warm sea breeze days and to a lesser extent on cool days.

3. Experimental Procedure

3.1 Field Test Design and Schedule

Eight tracer studies were conducted from August 31, 1976, through September 14, 1976, within the Delta Region during the four designated meteorological periods. During seven of the tests, either SF_6 or $CBrF_3$ was released from property owned by Dow Chemical in the Montezuma Hills. During the two tests where $CBrF_3$ was used, the SF_6 tracer was emitted upstream from Martinez during Test 2 and from Pinole during Test 7 in order to determine the origin and dispersion of the air passing over the Montezuma Hills. The final test involved the release of SF_6 from Pinole. Releases from the Dow site covered all four meteorological periods; the releases from Martinez and Pinole were conducted during Sea Breeze and Pre-Sea Breeze conditions. The release schedule, the release locations, and tracer release rates are given in Table 2.

3.2 Tracer Release System

Tracers were released at a constant rate from gas cylinders using a manifold, regulator, and large volume flowmeter; the gases were released into the air through 1/2 inch copper tubing at a height of approximately 5 meters. The release system was secured in a truck which provided an easy means of moving the release system to new release locations. Release rates were set using the regulator and calibrated flowmeter; the average release rates listed in Table 2 were determined by weighing the gas cylinders before and after each release, and averaging the weight of the released tracer over the release period. The total amount of tracer released was within 2% of the rate determined from the calibrated rotameter. The release system was continuously monitored during every release.

TABLE 2

TRACER RELEASE DATA

Date	Test	Location* of SF_6 Release	Release Period (PDT)	Release Rate (grams/sec)	Location of $CBrF_3$ Release	Release Period	Release Rate
8/31/76	1	Montezuma Hills	1200-1700	10.6 1.01 tons/day	-	-	-
9/2/76	2	Martinez	1100-1600	11.4 1.08 tons/day	Montezuma Hills	1300-1500	16.6 1.58 tons/day
9/5/76	3	Montezuma Hills	0000-0500	9.5 0.90 tons/day	-	-	-
9/6/76	4	Montezuma Hills	1800-2300	10.8 1.03 tons/day	-	-	-
9/9/76	5	Montezuma Hills	1130-1330	10.7 1.02 tons/day	-	-	-
9/10/76	6	Montezuma Hills	0600-1100	10.5 1.00 tons/day	-	-	-
9/13/76	7	Pinole	0600-1500	11.5 1.09 tons/day	Montezuma Hills	0900-1100	16.0
						1300-1400	16.0 1.52 tons/day
9/14/76	8	Pinole	0730-1300	10.9 1.04 tons/day	-	-	-

* Exact Tracer Release Locations: (1) Montezuma Hills: tracer was released from a truck parked by the Dow Chemical air quality monitoring station. The monitoring station is located approximately 4.3 Km east of Collinsville and 2 Km north of the Sacramento River. (2) Martinez: tracer was released from the parking lot of the Mountain View Sanitary District Sewage Plant at the end of Arthur Road. (3) Pinole: tracer was released from the parking lot of the Pinole police station on Pear Street.

3.3 Air Sampling Systems

3.31 Automobile Traverse System

During each release day, a series of automobile air sampling traverses were conducted using from three to five, two-person teams. Automobile traverses were made by having the passenger in each car take 10-second grab samples in 30 cm^3 plastic syringes. Generally, samples were collected every 0.1, 0.2, 0.5 or 1.0 miles, depending upon the distance from the release point and the steadiness of the wind. Descriptions of the traverses are given in Table 3. Traverse paths were determined in the field based upon real time wind data obtained from various data collection agencies and from measurements taken by the traverse personnel. Samples taken during traverses in the early part of each test were analyzed during the test in order to determine the actual plume trajectory.

3.32 Airborne Air Sampling System

Personnel from Meteorology Research, Inc. (MRI) obtained air samples in a manner similar to the automobile traverse teams from an airplane traveling downwind of the release at various heights and locations. Air samples were also obtained during spirals from above the mixing layer to the surface. Samples were typically taken at vertical intervals of 100 or 200 feet. During Test 6, Caltrans provided a plane and personnel for three airborne traverses from Sacramento to Stockton. Descriptions of the airborne traverses and spirals are also given in Table 3.

3.33 Hourly Averaged Sequential Samplers

A total of 42 sequential air samplers were located at 28 sampling sites; the locations of the sites are shown in Figure 1. Samplers which

TABLE 3

AUTOMOBILE TRAVERSES

Date	Test No.	Traverse No.	Highway	Direction Traveled	Crossroad	Traverse Time (PDT)	Distance Traveled (km)	No. Samples
8/31/76	1	1	99,120,I205	South, west	Highway 12	1400-1450	58.7	74
		2	160	South	Twitchell Island Road	1420-1433	16.7	53
		3	160	North	Highway 4	1430-1445	14.8	47
		4	160	South	Twitchell Island Road	1515-1527	14.8	47
		5	I5,120,99	East, north	Interstate 205	1600-1652	68.3	86
		6	160	North	Highway 4	1630-1641	14.8	47
		7	99,120,I205	South, west	Boessow Road (Galt)	1701-1753	70.8	89
9/2/76	2	1	I680	South	Interstate 780	1130-1143	20.0	63
		2	I680	North	Highway 24 (Walnut Creek)	1215-1228	20.0	63
		3	4,160	East, north	Loveridge Road	1240-1350	25.7	17
		4	160	North	Highway 4	1400-1415	18.7	59
		5	160	South	Highway 12	1445-1503	18.7	59
		6	160	North	Highway 4	1515-1530	18.3	39
		7	Railroad Ave.	Southwest	Highway 4	1545-1635	29.8	69
		8	Empire Mine Road	South	Lone Tree Road	1625-1640	10.4	14

TABLE 3 (cont.)

AUTOMOBILE TRAVERSES

Date	Test No.	Traverse No.	Highway	Direction Traveled	Crossroad	Traverse Time (PDT)	Distance Traveled (km)	No. Samples
9/2/76 (cont.)	2 (cont.)	9	99,120,I205	South	Collier Road	1630-1715	63.6	80
		10	I580,I205,120,99	East, north	Foothill Road (Dublin)	1630-1737	90.9	114
		11	I205,120,99	East, north	MacArthur Dr.	1731-1815	63.6	80
9/5/76	3	1	160	North	Highway 4	0100-0112	18.7	59
		2	99,120	South, west	Highway 12	0130-0210	63.6	80
		3	99	South, west	Boessow Road	0213-0259	63.6	80
		4	160	South	(Emmaton)	0240-0300	6.6	42
		5	4	West	Interstate 5	0247-0320	47.5	60
		6	160	South	Highway 12	0259-0306	5.1	65
		7	4	West	Interstate 5	0332-0415	63.6	80
		8	4,J3,12	East, north, west	Byron Road	0414-0545	74.8	93
		9	160	North	Highway 4	0430-0445	8.9	56
		10	12,J8	East, south	Highway 160	0432-0517	38.1	80
		11	160	South	Bean pot	0441-0450	6.1	77
		12	160	North	San Joaquin River	0502-0511	7.6	48
		13	12	East	Terminous	0630-0637	8.7	18
		14	J8	North	Highway 12	0637-0647	14.5	19

TABLE 3 (cont.)

AUTOMOBILE TRAVERSES

Date	Test No.	Traverse No.	Highway	Direction Traveled	Crossroad	Traverse Time (PDT)	Distance Traveled (km)	No. Samples
9/6/76	4	1	160	South	Highway 12	1928-1946	18.7	59
		2	99,120,I205	South, west	Highway 12	2130-2217	63.6	80
		3	160	South	Bean pot	2132-2140	6.4	80
		4	99,120,I205	South, west	Kettleman Lane	2200-2246	63.6	80
		5	160	North	San Joaquin River Bridge	2214-2222	6.3	79
		6	I205,120,99	East, north	Tracy Blvd.	2232-2320	63.6	80
		7	I205,120,99	East, north	Patterson Pass Rd. (1.4 mi e of)	2315-2400	63.6	80
9/9/76	5	1	4	East	Railroad Ave.	1255-1315	15.0	94
		2	4, 160	East, north	Railroad Ave.	1314-1330	25.4	80
		3	Sellers Rd., Cypress Rd., Bethel Island Rd.	North, east, north	Highway 4	1349-1417	14.9	38
		4	Balfour Rd.	East	Deer Valley Rd.	1351-1405	12.1	26
		5	Marsh Creek Rd.	East	Deer Valley Rd.	1356-1428	35.7	75
		6	160,4	South, west	Twitchell Island Road	1359-1416	25.4	80
		7	Balfour Road	West	Byron Highway	1413-1426	12.1	26
		8	Balfour Road	East	Deer Valley Rd.	1436-1450	12.1	26

TABLE 3 (cont.)

AUTOMOBILE TRAVERSES

Date	Test No.	Traverse No.	Highway	Direction Traveled	Crossroad	Traverse Time (PDT)	Distance Traveled (km)	No. Samples
9/10/76	6	1	Sherman Island Road	Southwest	160	0800-0815	5.8	37
		2	160	South	12	0740-0753	15.9	100
		3	99,120,I205	South, west	Highway 12	1001-1051	63.6	80
		4	Sherman Levee Road	South	Highway 160	1023-1033	9.5	60
		5	99	South, west	Highway 12	1030-1115	63.6	80
		6	160	North	San Joaquin River Bridge	1022-1033	6.4	80
		7	160	North	San Joaquin River Bridge	1103-1112	6.4	80
		8	I205,120,99	East, north	Patterson Pass Rd. (1.5 mi e of)	1105-1203	63.6	80
		9	I205,120,99	East, north	Tracy Blvd.	1145-1230	63.6	80
9/13/76	7	1	24,I680,I780	East, north	Highway 13	0924-0956	48.3	100
		2	Sherman Island Road	Northeast	S. end of Sherman Island Rd.	0940-1155	7.0	88
		3	12,160,4	East, south, west	Interstate 80	1113-1217	75.6	48
		4	I780,I680	South	Interstate 80	1130-1146	24.9	32
		5	I580,I205,120	East	Vasco Road	1335-1458	138.4	87
		6	I780,I680,24	South, west	Interstate 80	1340-1414	51.5	33

TABLE 3 (cont.)

AUTOMOBILE TRAVERSES

Date	Test No.	Traverse No.	Highway	Direction Traveled	Crossroad	Traverse Time (PDT)	Distance Traveled (km)	No. Samples
9/13/76 (cont.)	7 (cont.)	7	I580	East	Highway 238	1429-1451	33.8	22
		8	I80,17,238, I580 Vasco, Walnut 4,160,12	S,S,E,E N,N N,N,W	W. Texas (Fairfield)	1450-1706	191.5	120
		9	I580	West	Highway 84	1458-1532	33.8	22
		10	24,I680,I780	East, north	Interstate 580	1537-1611	53.1	34
		11	99,120,I205, I580	S, west	Mack Road	1654-1820	132.0	83
		12	I580,17	West, north	Highway 84	1835-1901	25.7	17
9/14/76	8	1	I680	South	Interstate 80	0906-0931	38.6	49
		2	I680	North	Highway 24	0941-1007	38.6	49
		3	12,160,4,24	E,S,W,S	W. Texas Ave. (Fairfield)	1047-1151	91.7	58
		4	I680	North	Highway 24 (Walnut Creek)	1154-1220	38.6	49

TABLE 3 (cont.)

AIRBORNE TRAVERSES AND SPIRALS

Date	Test No.	Traverse No.	Traverse Path and Direction	Altitude (meters, MSL)	Traverse Time	Distance Traveled (km)	No. Samples
9/10/76	6	1	VACA-Dixon Airport south to Isleton	305	0934-0946	38.1	11
		2	Isleton s. to 4 mi. e. of Brentwood	305	0950-1005	24.3	59
		3	4 mi. e. of Brentwood s. to I580-I205 junction	305	1012-1020	23.1	9
		4	I580-I205 junction n. to 4 mi. e. of Brentwood	183	1044-1052	23.1	8
		5	4 mi. e. of Brentwood n. to Isleton	183	1054-1107	24.3	52
		6	Isleton n. to VACA-Dixon Airport	183	1109-1122	38.1	14
		7	Isleton s. to 4 mi. e. of Brentwood	427	1140-1153	24.3	25
		8	Junction S.P.T. Co. Railroad & I580 n. to I5 and I205	305	1229-1235	17.8	7
		9	I5-I205 n. to Wilson Way & Highway 99	305	1238-1251	27.5	27
		10	Sacramento Executive Airport s. to Ripon	183	1000-1039	94.1	40
		11	Ripon n. to Sacramento Executive Airport	183	1100-1139	94.1	40
		12	Sacramento Executive Airport s. to Ripon	183	1200-1239	94.1	40

TABLE 3 (cont.)

AIRBORNE TRAVERSES AND SPIRALS

Date	Test No.	Traverse No.	Traverse Path and Direction	Altitude (meters, MSL)	Traverse Time	Distance Traveled (km)	No. Samples
9/10/76 (cont.)	6 (cont.)	13	Ripon n. to Sacramento Executive Airport	183	1300-1339	94.1	40
9/13/76	7	1	Cordelia s. to I680 and Highway 24 (Walnut Creek)	427	0736-0748	36.5	50
		2	I680 and Highway 24 n. to Cordelia	305	0757-0810	36.5	53
		3	Cordelia s. to I680 and Highway 24	183	0819-0832	36.5	53
		4	Cordelia s. to I680 and Highway 24	427	0906-0918	36.5	12
		5	I680 & 24 to Cordelia	305	0925-0938	36.5	53
		6	Cordelia to I680 & 24	183	0945-0958	36.5	53
		7	VACA-Dixon Airport s. to Isleton	183	1112-1324	38.1	26
		8	Isleton s. to I580 & I205	183	1327-1343	47.0	62
		9	I205 & I580 n. to Isleton	305	1348-1404	47.0	68
		10	Isleton n. to VACA-Dixon Airport	305	1409-1422	38.1	27
		11	VACA-Dixon Airport s. to Isleton s. to I580 & I205	427	1428-1456	85.1	55
		12	Livermore Airport East to I5-205	457	1759-1812	44.1	27
		13	I5 & I205 Northeast to Stockton Airport	457	1815-1822	16.2	13

TABLE 3 (cont.)

AIRBORNE TRAVERSES AND SPIRALS

Date	Test No.	Traverse No.	Traverse Path and Direction	Altitude (meters, MSL)	Traverse Time	Distance Traveled (km)	No. Samples	ΔH (meters)
9/13/76 (cont.)	7 (cont.)	14	Stockton Airport n. to 5.7 mi ssw of Sacramento Executive Airport	457	1850-1912	66.4	45	
9/14/76	8	1	I680-Highway 24 (Walnut Creek) n. to Cordelia	366	0826-0839	36.5	53	
		2	Cordelia s. to I680-Highway 24	274	0843-0856	36.5	53	
		3	I680-24 n. to Cordelia	183	0858-0911	36.5	53	
		4	Cordelia s. to I680-24	427	0942-0955	36.5	27	
		5	I680-24 n. to Cordelia	305	0959-1012	36.5	52	
		6	Cordelia s. to I680-24	183	1016-1028	36.5	51	
			SPIRALS					
9/10/76	6	1	Over Frank's Tract Recreation Area	914 to 488	1158-1203	-	8	61
		2	Over Frank's Tract Recreation Area	472 to 30	1203-1208	-	31	15
9/13/76	7	1	0.5 mi n. of the Port Chicago Naval Magazine	914 to 488	0845-0850	-	8	61
		2	0.5 mi n. of the Port Chicago Naval Magazine	472 to 15	0850-0854	-	33	15

TABLE 3 (cont.)

AIRBORNE TRAVERSES AND SPIRALS

Date	Test No.	Traverse No.	Traverse Path and Direction	Altitude (meters, MSL)	Traverse Time	Distance Traveled (km)	No. Samples	ΔH (meters)
9/13/76 (cont.)	7 (cont.)	3	0.5 mi n. of the Port Chicago Naval Magazine	914 to 488	1008-1013	-	8	61
		4	0.5 mi n. of the Port Chicago Naval Magazine	457 to 0	1013-1017	-	31	15
		5	Rio Vista	1829 to 914	1518-1526	-	16	61
		6	Rio Vista	884 to 30	1526-1534	-	29	31
		7	Tracy	1829 to 914	1553-1559	-	16	61
		8	Tracy	884 to 91	1559-1603	-	27	31
		9	Stockton	1524 to 762	1832-1838	-	14	61
		10	Stockton	732 to 30	1838-1844	-	24	31
9/14/76	8	1	0.5 mi n. of Port Chicago Naval Magazine	1067 to 457	0921-0926	-	11	61
		2	0.5 mi.n. of Port Chicago Naval Magazine	442 to 15	0926-0930	-	29	15
		3	0.5 mi n. of Port Chicago Naval Magazine	1372 to 457	1039-1044	-	16	61
		4	0.5 mi n. of Port Chicago Chicago Naval Magazine	442 to 15	1044-1049	-	29	15

permitted the collection of hourly averaged air samples each hour for 12 hours were positioned at 14 locations, primarily along Highway 99. An additional 14 locations along Highway 160, 10 km east of the Dow site, were designated for the positioning of battery-powered samplers which permitted the collection of hourly averaged samples each hour for three hours. These samplers were used during Tests 1 and 2. Table 4 lists the site locations, crosswind distances from a reference point and downwind distances from the three release points.

3.4 Chemical Analysis of Air Samples

Air samples were analyzed for SF_6 and $CBrF_3$ using electron capture gas chromatography. The tracers were separated in a stainless steel column (39" x 0.25" OD, 0.18" ID) packed with 80-100 mesh 5A Molecular Sieve. Prepurified nitrogen flowing at 10 psig, caused the SF_6 to elute in 18 seconds and the $CBrF_3$ to elute in 40 seconds. Both column and detector were operated at ambient temperatures. A typical chromatogram is shown in Figure 4; additional details concerning the gas chromatographs are available elsewhere (Drivas, 1974).

Twelve chromatographs and two digital integrators were set up in a room at the California Holiday Lodge, Fairfield, California. Only eight of the chromatographs were used during the test; four were used to analyze for SF_6 alone and four were set up to analyze for both tracers. Field samples were returned each day to the lab for analysis. All of the samples from one test were analyzed before the next test began. Calibration was done using an exponential dilution method. Calibration results show that concentrations down to 10^{-12} parts SF_6 per part air and 10^{-11} parts $CBrF_3$ per part air could be detected at a signal-to-noise ratio of

TABLE 4

LOCATION OF HOURLY AVERAGE SEQUENTIAL SAMPLERS

Hourly Average 12-Hour Sequential Sampling Stations

Location of 12-Hour Samplers	Distance from Release Points (Km)			Distance S. of Sacramento (Km)
	Montezuma Hills	Martinez	Pinole	
1 Fairfield	28.6	28.1	36.0	-
2 Davis	50.4	64.6	73.7	-
3 Sacramento	61.1	81.1	92.5	0
4 Elk Grove	59.3	84.4	99.6	18.0
5 Herald	54.0	80.6	96.3	29.9
6 Collier Road	48.9	75.8	92.0	39.3
7 Lodi	46.6	73.2	90.2	49.9
8 Hammer Lane	41.3	66.6	83.9	62.7
9 Stockton	48.7	73.2	90.0	67.0
10 French Camp	51.9	74.5	91.5	76.0
11 Manteca	59.3	79.6	96.3	84.8
12 Tracy	61.8	77.5	93.0	99.3
13 Livermore	44.3	47.1	59.5	-
14 Rio Vista	13.4	39.0	55.0	-

TABLE 4 (cont.)

3-hour Boards	Distance from Release Points (Km)		Distance N. of Highway 4 - Highway 160 Junction (Km)
	Montezuma Hills	Martinez	
1	12.2	36.2	26.4
2	12.9	37.5	23.8
3	12.9	38.3	22.2
4	13.7	39.5	30.0
5	12.4	38.3	17.9
6	10.9	37.0	15.0
7	9.4	35.5	13.4
8	8.1	34.2	10.9
9	5.8	31.4	8.8
10	6.1	30.9	7.4
11	7.6	31.2	6.1
12	7.1	29.1	4.2
13	8.4	28.6	4.2
14	9.4	26.1	3.4 (south of 4&160)

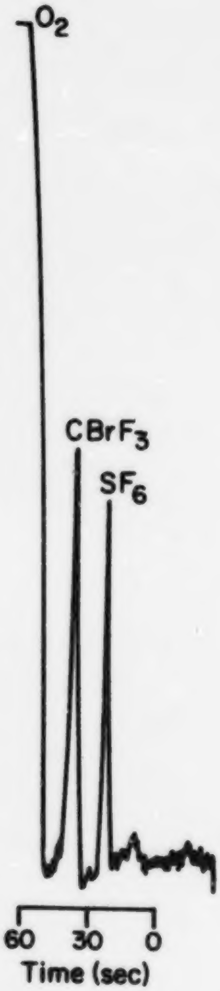

Figure 4. Typical tracer chromatogram: $[SF_6]$ = 6 ppt; $[CBrF_3]$ = 310 ppt.

better than 3 to 1. A typical calibration curve is shown in Figure 5. The chromatogram peaks were integrated with an Autolab System I electronic digital integrator (Spectra-Physics, Santa Clara, California). The gas chromatographs were calibrated before and after the field test period. During the tests, the instruments were cross-checked periodically for reproducibility. The calibration of the tracer data changed by approximately 7% among the gas chromatographs used to analyze SF_6 alone. Calibration results for the remaining gas chromatographs changed by 25% for SF_6 and 20% for $CBrF_3$. Degradation of the columns and detectors due to atmospheric contaminants in the air samples is the probable cause for the changes in the calibration results. Previous experience has shown that the presence of halogenated solvents in air samples can, over an extended period of use of the chromatograph, contaminate the detector and column. Uncertainty in the tracer data is estimated to range from less than 5% to no more than 25%. Details of the calibration results are given in Appendix A of this volume.

Z9

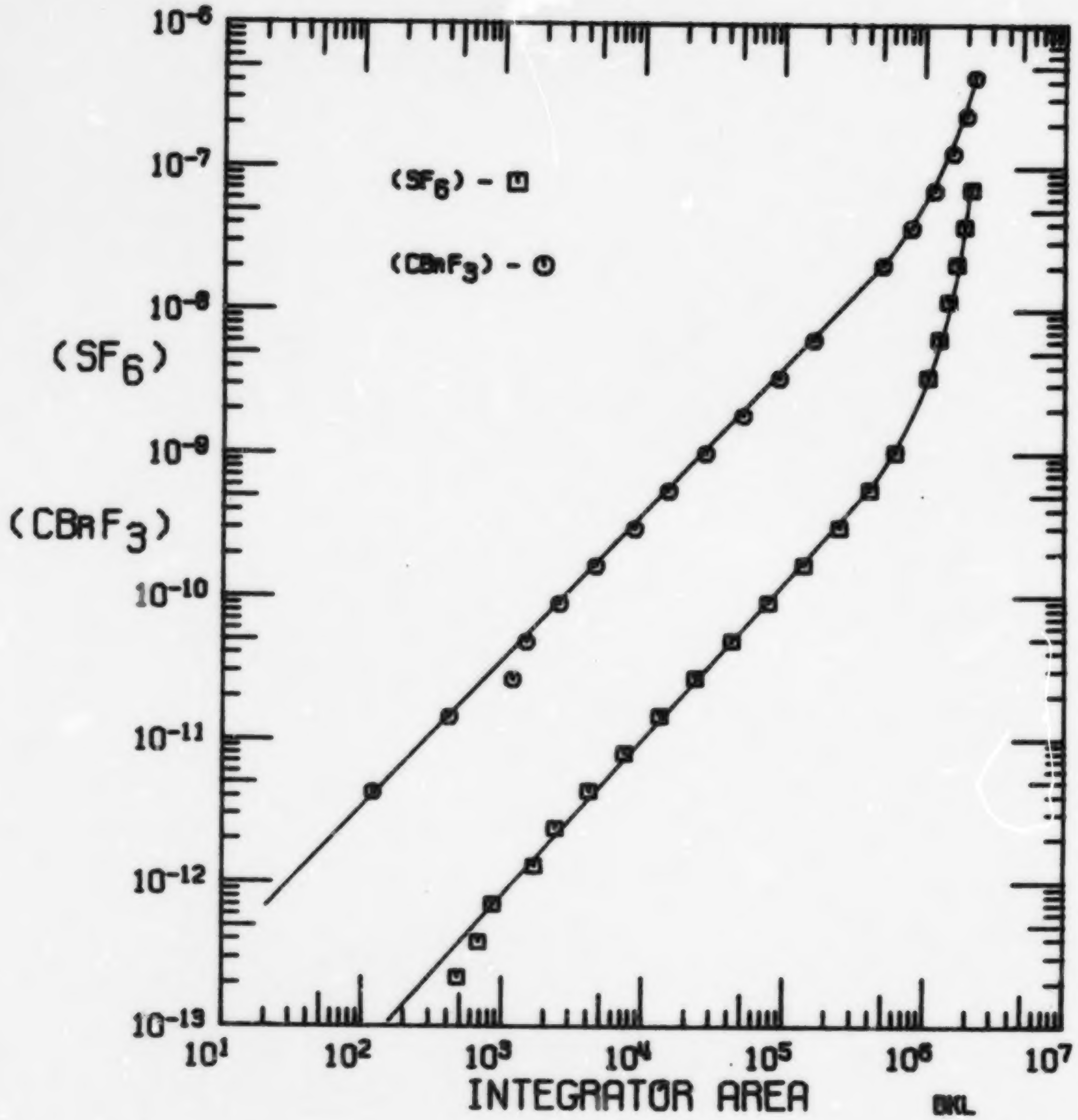

BKL
8/21/76

Figure 5. Gas chromatograph calibration curves for dual tracers.

3.5 Meteorological Support Systems

3.51 Surface Wind Data

Data obtained from MRI were collected from the various agencies listed in Table 5. Table 5 also contains stations maintained by the Bay Area Air Pollution Control District and various industrial companies. The data for these stations were obtained directly from the Bay Area APCD. The data for each station during the test period are tabulated in Table 17 of Volume II, Part B. Measurements from 27 of the 36 wind stations provided hourly averaged wind direction and velocity data; 3 stations measured 2 or 3-hour averaged data. Data from the remaining 6 stations were recorded as single hourly observations. The locations of the stations are shown in Figure 6.

3.52 Upper Air Wind Data

Pilot balloon upper air wind speed and direction measurements (pibal measurements) were taken by MRI at the times and locations indicated in Table 5. The data obtained from these measurements are given in Table 18 of Volume II, Part B. MRI also provided estimates of the mixing depth at various locations and times during the test based upon upper air wind and temperature measurements. These data are given in Table 19 of Volume II, Part B. Vector-averaged wind speed and direction data from the surface to the height of the mixing layer are given in Table 20 of Volume II, Part B. The locations of the upper air stations are shown in Figure 6.

TABLE 5

WIND DATA STATIONS AND DESCRIPTION OF WIND DATA

Station	Station Code	Description of Data
1 Dow Surface (Rockwell)	DW01	Hourly averaged wind speed, wind direction at 5-minute intervals
2 Brentwood (Rockwell)	BR02	Hourly averaged wind speed, wind direction at 5-minute intervals
3 Venice Ferry (MRI)	VF03	Hourly averaged speed and direction
4 Rio Cosumnes (MRI)	RC04	Hourly averaged speed and direction
5 Stockton (NWS)	SK05	Single hourly observations
6 Livermore (NWS)	LV06	Single hourly observations
7 Rio Vista (NWS)	RV07	Single hourly observations
8 Sacramento (Metropolitan Airport) (NWS)	SA08	Single hourly observations
9 Concord (Buchanan Field) (NWS)	CC09	Single hourly observations
10 Benicia (BAAPCD)	BE10	Hourly averaged speed and direction
11 Voice of America Radio Tower	VA11	Hourly averaged speed and direction
12 Pittsburg PG&E Company	PB12	Hourly averaged speed and direction
13 Martinez Shell Oil	MZ13	Hourly averaged speed and direction
14 Martinez Lion Oil	MZ14	Hourly averaged speed and direction
15 Antioch Fibreboard	AT15	Hourly averaged speed and direction

TABLE 5 (cont.)

Station	Station Code	Description of Data
16 Benicia Exxon	BE16	Hourly averaged speed and direction
17 Richmond Allied Chemical	RM17	Hourly averaged speed and direction
18 Pittsburg Allied Chemical	PB18	Hourly averaged speed and direction
19 Rodeo Union Oil	RD19	Hourly averaged speed and direction
20 Concord BAAPCD	CC20	Hourly averaged speed and direction
21 Vallejo BAAPCD	VL21	Hourly averaged speed and direction
22 San Rafael BAAPCD	SR22	Hourly averaged speed and direction
23 San Francisco BAAPCD	SF23	Hourly averaged speed and direction
24 Redwood City BAAPCD	RC24	Hourly averaged speed and direction
25 Livermore BAAPCD	LV25	Hourly averaged speed and direction
26 Fremont BAAPCD	FR26	Hourly averaged speed and direction
27 Pittsburg BAAPCD	PB27	Hourly averaged speed and direction
28 Rancho Seco Nuclear Power Plant Site	RS28	Hourly averaged speed and direction
29 Sacramento Caltrans	SA29	Hourly averaged speed and direction
30 Davis Caltrans	DV30	Hourly averaged speed and direction

TABLE 5 (cont.)

Station	Station Code	Description of Data
31 Wilton Caltrans	WT31	Hourly averaged speed and direction
32 Rio Vista Yolo-Solano APCD	RV32	3-Hourly averaged speed and direction
33 Woodland Yolo-Solano APCD	WD33	2-Hourly averaged speed and direction
34 Davis Yolo-Solano APCD	DV34	2-Hourly averaged speed and direction
35 Stockton San Joaquin APCD	SK35	Miles of wind/hr by quadrant
36 Travis Travis Air Force Base	TR36	Single hourly observations

TABLE 5 (cont.)

UPPER AIR WIND SPEED AND DIRECTION MEASUREMENTS

Station	Station Code	Date and Time (PDT)	
Dow Tower	DW50	Continuous 8/31/76 through 9/14/76	
Dow Pibal	DW51	8/31/76	1100-1700
		9/2/76	1000-1700
		9/5/76	0000-0500
		9/6/76	1700-2300
		9/9/76	1100-1400
		9/10/76	0700-1200
		9/13/76	0700-1700
		9/14/76	0800-1600
B & W Resort Pibal	BW52	8/31/76	1000-1800
		9/2/76	1000-1800
		9/5/76	0000-0600
		9/6/76	1600-2400
		9/9/76	1000-1400
		9/10/76	0800-1900
Livermore Pibal	LV53	8/31/76	1000-1800
		9/2/76	0900-1000
		9/9/76	0900-1900
		9/10/76	1100-1800
		9/13/76	0800-1800
		9/14/76	0800-1500
Pinole Pibal	PN54	9/13/76	0600-1600
		9/14/76	0600-1700
Junction J2 & CAL4 Pibal	JC55	9/14/76	1600-1900
Benicia Pibal	BE56	9/10/76	1400
Rancho Seco Nuclear Power Plant Site Tower	RS57	Continuous at 200 feet, hourly standard deviation of the wind	
Oakland International Airport Pibal	OK58	8/31/76 through 9/14/76 2 measurements per day	

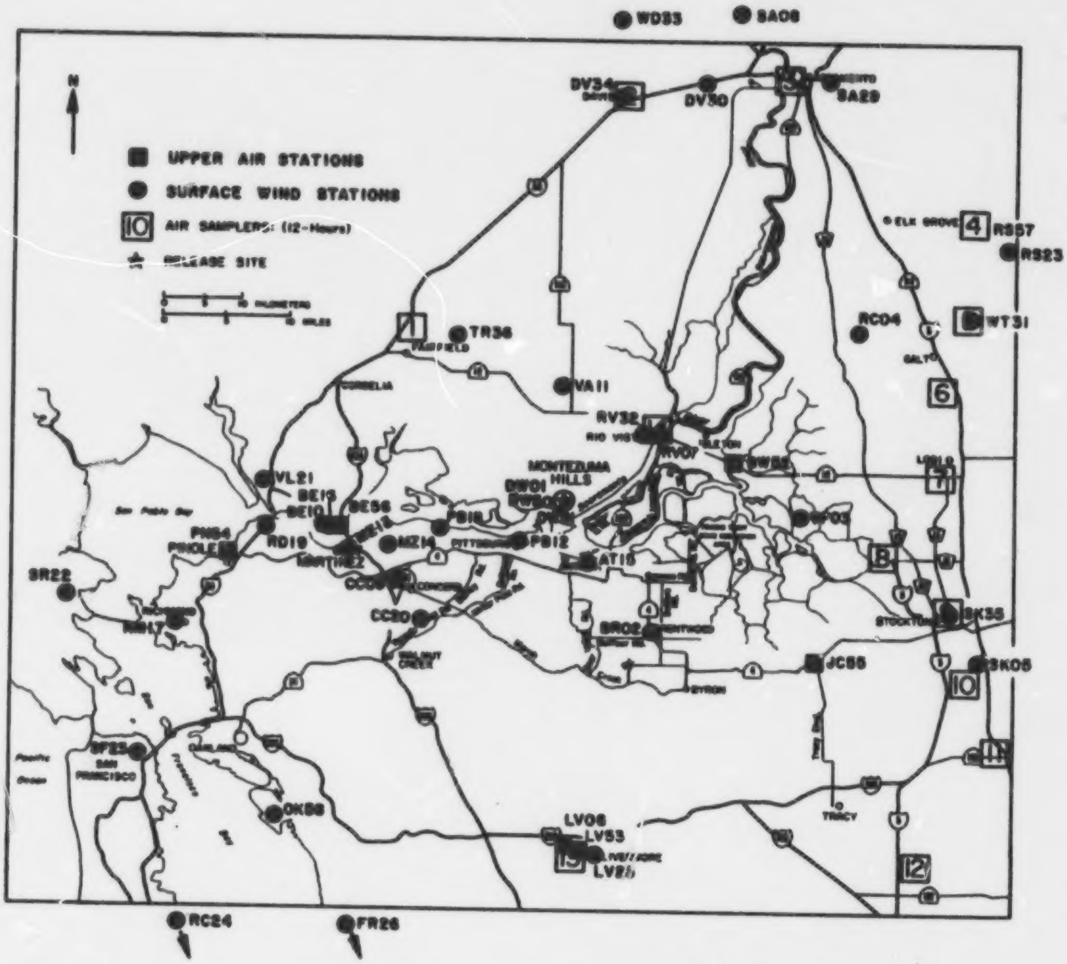
N
UPPER AIR STATIONS
SURFACE WIND STATIONS
10 AIR SAMPLERS (12-Hours)
RELEASE SITE
KILOMETERS
MILES
WD33
SA08
DV34
DAVIS
DV30
SA29
ELK GROVE
4
RS57
RS23
RC04
WT31
GALT
6
1
TR36
FAIRFIELD
VA11
RV32
RIO VISTA
RV07
ISLETON
DW88
MONTEZUMA HILLS
DW01
CORDELIA
VL21
BE15
BE10
BE56
PS18
PN34
PINOLE
RD19
MZ14
PITTSBURG
PS12
AT15
MARTINEZ
LODI
7
SP03
8
SR22
RICHMOND
CC05
CONCORD
CC20
BR02
BRENTWOOD
STOCKTON
SK35
JC55
SK05
10
WALNUT CREEK
BYRON
SF25
SAN FRANCISCO
OAKLAND
Pacific Ocean
San Pablo Bay
11
TRACY
OK56
LV06
LV53
LIVERMORE
LV25
13
12
RC24
FR26

Figure 6. Location of surface wind and upper air data stations.

4. Presentation and Discussion of Results

The tracer and meteorological data have been presented graphically in Volume II, Part A, and tabulated in Volume II, Part B, of this report. Results from a portion of the data reduction procedures are also given in Volume II, Part A. In the remainder of this volume, we will present detailed summaries of the qualitative and quantitative results of each test period; we will examine and discuss the atmospheric dispersion characteristics of the Delta Region, and perform a consistency check of the tracer data based on mass balance considerations. We will seek to determine the applicability of the Gaussian plume model to the description of pollutant impact within the test region, and we will present an important relationship between the standard deviation of the wind direction and the Gaussian horizontal dispersion parameter.

4.1 Relation of Tracer Data to Industrial Pollutant Emissions

As a means of interpreting the results of the California Delta tracer tests in terms of existing or projected industrial pollutant emissions, we have developed a simple nomograph to be used to convert measured tracer concentrations to pollutant concentrations. Such a conversion necessarily implies that the pollutant emissions of interest are suitably characterized by the tracer release. The conversion of concentrations also implies that either the pollutant is essentially unreactive (like the tracer) or that its rate of reaction is very rapid. For example, carbon monoxide may be considered unreactive over the time scale involved in tracer transport. Sulfur dioxide has been shown to have a relatively slow (15%/hr) reaction rate (Roberts, 1975); nitrogen oxide (NO) can be converted rapidly to nitrogen dioxide (NO_2) in the presence of high oxidant concentrations. In cases like SO_2, the conversion of tracer concentrations to pollutant concentrations gives an upper bound on the pollutant concentration. If, as in the example of NO, a pollutant reacts fairly rapidly, then the conversion of tracer concentrations to the product concentrations (NO_2) will yield an upper bound on the product concentrations.

The tracer concentrations obtained during the California Delta field study can be converted to pollutant concentrations using the nomographs in Figures 7 and 8. In order to use the nomographs, a value of K, the ratio of the pollutant molecular weight (in grams) to the pollutant's existing or projected emission rate (in tons/day) must be specified. Any tracer concentration measured during the Delta field study can then be converted to the concentration of the pollutant by selecting the point along the specified K-line where the tracer concentration occurs. As examples, the projected emissions of NO_x (as NO_2), SO_2 and CO associated with the Dow complex have been used to specify the K-lines which are shown in the nomographs. A concentration of 100 ppt SF_6 converts to 2.93 ppb NO_2, .242 ppb SO_2, and .499 ppb CO. In the case of NO_2 we have assumed that NO reacts rapidly to form NO_2. A summary of the preliminary estimates of emissions from the Dow project are given in Table 6 (Moyer, 1977). A more detailed list is tabulated in Volume II, Part A, Table 6.

The nomographs are based upon the following equation:

$$[P] = [T] \cdot \frac{MW_T}{RR_T} \cdot \frac{RR_P}{MW_P} = [T] \cdot \frac{K_T}{K_P} \tag{1}$$

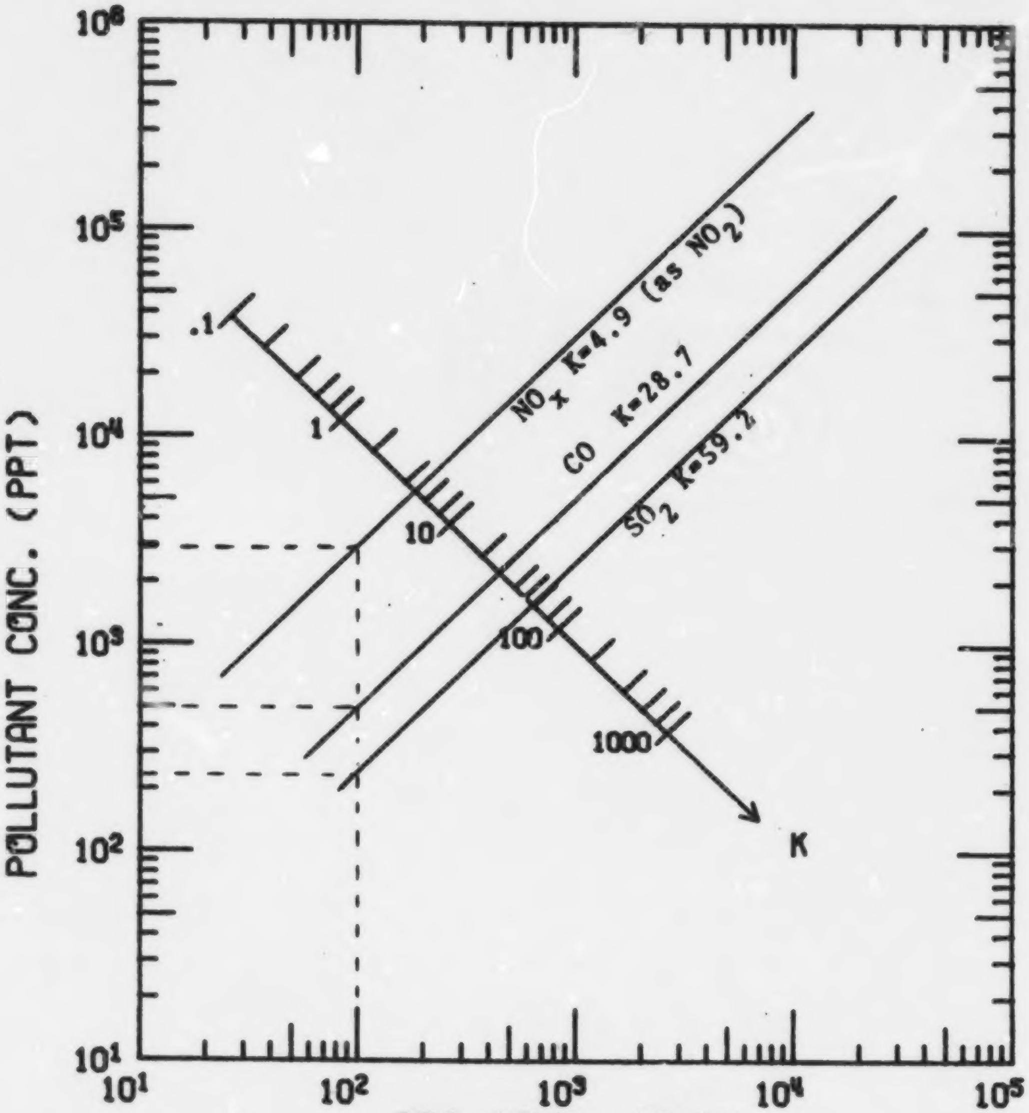

Figure 7. Conversion nomograph for converting SF_6 tracer concentrations measured during the field study to pollutant concentrations. K = (pollutant molecular wt., grams) / (pollutant emission rate, tons/day). Values of K shown above are based on projected pollutant emissions from the Montezuma Hills Dow chemical complex. Dashed line indicates the corresponding tracer-to-pollutant concentration conversions.

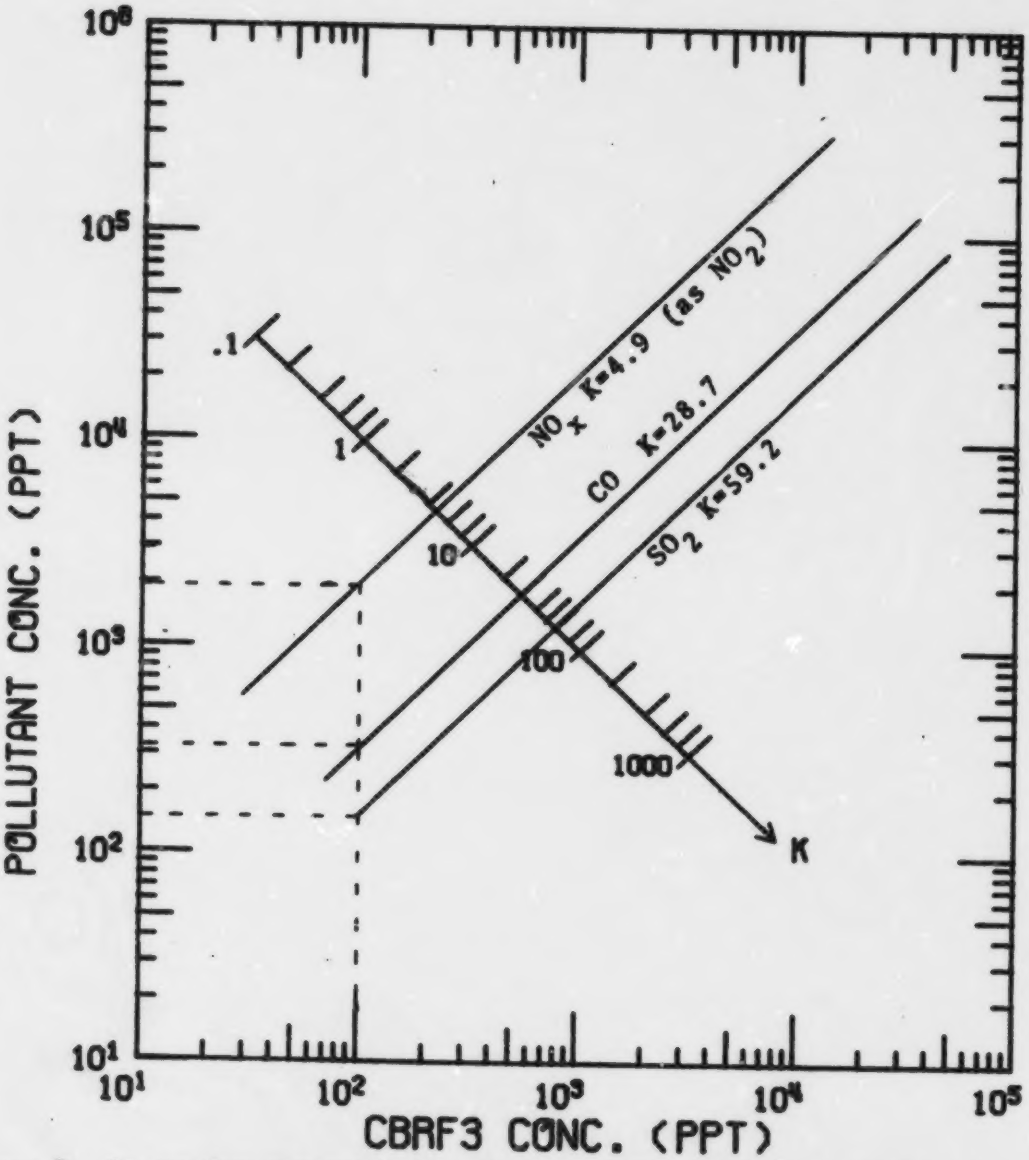

Figure 8. Conversion nomograph for converting $CBrF_3$ tracer concentrations measured during the field study to pollutant concentrations. K = (pollutant molecular wt, grams) / (pollutant emission rate, tons/day). Values of K shown above are based on projected pollutant emissions from the Montezuma Hills Dow chemical complex. Dashed line indicates the corresonding tracer-to-pollutant concentrations conversions.

TABLE 6

NOMOGRAPH K-VALUES FOR PROJECTED DOW EMISSIONS*

$$K \equiv \frac{\text{Mol. Wt. of Pollutant (grams)}}{\text{Emission Rate (tons/day)}} = \frac{MW_p}{RR_p}$$

Pollutant	MW_p (grams)	RR_p* (tons/day)	K Dow only	RR_p** Dow + Turbine	K Dow + Turbine
NO_x (as NO_2)	46	9.41	4.89	23.10	1.99
SO_2	64	1.08	59.2	1.252	51.12
CO	28	0.976	28.68	4.796	5.84
NMHC+	-	1.516	-	2.900	-

MW_p = molecular weight of pollutant (grams/mole)

RR_p = emission rate of pollutant (tons/day)

* Projected Dow emissions for Montezuma Hills chemical complex from Moyer (1977).

** Plans concerning the development of the Dow project indicated a 146 megawatt gas turbine might be necessary as an on-site power source. The emissions resulting from the operation of such a turbine were obtained from Moyer (1977).

+ Values of K for nonmethane hydrocarbons (NMHC) hava not been calculated because the complex reaction mechanisms prevent simple descriptions of the rates of conversion.

where [P] is the pollutant concentration in ppt, [T] is the tracer concentration in ppt, RR_T and RR_P are the tracer and pollutant release rates in tons/day, respectively, and $MW_T$and MW_P are the associated molecular weights in grams. The terms K_T and K_P are the respective ratios of tracer and pollutant molecular weights to emission rates. The K-lines shown in the nomographs are based on the average tracer release rates during the eight tests (1.02 tons SF_6/day, 1.55 tons $CBrF_3$/day). This introduces only a small error (4%) since the release rates were relatively constant from test to test.

Table 7 gives an indication of how emissions from existing sources in the northern Bay Area and near the Montezuma Hills compare with the projected Dow emissions. Pollutant emission rates and the corresponding values of K are listed for the major point sources in the region of interest. These emission rates were taken from the Bay Area APCD Emissions Inventory Summary Report (Base Year, 1975), (Moyer, 1977). We have listed the calculated values of K for these sources as a comparison to the Dow values. Using these values of K to predict pollutant concentrations due to any of the listed sources can only yield a very rough approximation. The tracer source characteristics, in general, may be expected to differ in several important aspects from the source characteristics of these industrial facilities. The effects of the exact location, stack height, or stack velocity are difficult to extrapolate without additional experimental data.

TABLE 7

POLLUTANT EMISSIONS FROM MAJOR POINT SOURCES IN THE NORTHEASTERN BAY AREA

The following list shows the larger point sources and their annual average emissions for 1975. The emissions shown are the total for the whole source site.

The symbol (--) indicates a quantity less than 0.01 Tons/Day.

1975 MAJOR SOURCES (NORTHEASTERN BAY AREA APCD)	ANNUAL AVERAGE EMISSIONS (T/D) AND NOMOGRAPH K-VALUES (K = MOLECULAR WT./EMISSION RATE)						
	ORG	NOX	K_{NOX}	SO_2	K_{SO_2}	CO	K_{CO}
ALLIED CHEMICAL CORP. BAY POINT	.04	.04	1200	5.6	11	.6	47
ANTIOCH BUILDING MATERIALS PITTSBURG	.05	.01	4600	---		.2	140
ATLANTIC RICHFIELD BULK PLANT, RICHMOND	.7	---	----	---	--	--	---
CALIFORNIA & HAWAIIAN SUGAR CO., CROCKETT	.04	2.5	18	---	--	.3	93
CHEVRON CHEMICAL CO. RICHMOND	.2	.06	770	.03	2100	.2	140
COLLIER CARBON & CHEM. CORP., NICHOLS	--	2.1	22	4.1	16	--	---
CROWN-ZELLERBACH CORP. ANTIOCH	0.1	.8	58	.02	3200	--	---
CROWN CORK & SEAL RICHMOND	.7	.03	1500	--	--	.04	700
DOW CHEMICAL COMPANY PITTSBURG	.3	4.0	12	.09	710	1.6	18
E. I. DUPONT COMPANY ANTIOCH	.4	.5	92	--	19	1.5	---
EXXON CO., U.S.A. BENICIA	9.1	9.8	4.7	40	1.6	4.2	6.7

NO_x emissions are assumed to be in terms of tons NO_2/day.

1975 MAJOR SOURCES (NORTHEASTERN BAY AREA APCD)	ANNUAL AVERAGE EMISSIONS - T/D ORG	NOX	K_{NOX}	SO_2	K_{SO_2}	CO	K_{CO}
EXXON CO., U.S.A. BULK PLANT, BENICIA	.3	---	----	---	----	--	---
FIBREBOARD CORP. ANTIOCH	.6	.8	58	.03	2100	22	1.3
GLASS CONTAINERS CORP. ANTIOCH	---	.5	92	.2	320	--	---
GULF OIL CO. - CALIF. BULK PLANT, HERCULES	2.5	1.3	35	.4	160	--	---
GULF OIL CO. - CALIF. BULK PLANT, HERCULES	3.1	---	---	--	---	--	---
HERCULES INC. HERCULES	.02	.5	92	--	---	--	---
JOHNS-MANVILLE CORP. PITTSBURG	--	.1	460	--	---	--	---
MARE ISLAND NAVAL SHIPYARD VALLEJO	.4	.8	58	.03	2100	.04	700
MARTINEZ PETROLEUM BULK PLANT, MARTINEZ	.08	--	---	--	---	--	---
MONSANTO COMPANY MARTINEZ	--	.3	150	26	2.5	2.2	13
MYERS DRUM COMPANY SAN PABLO	.3	.01	4600	--	---	--	---
PACIFIC GAS & ELECTRIC CO. (AVON PLANT), AVON	.01	3.7	12	2.8	23	--	---
PACIFIC GAS & ELECTRIC CO. (CONTRA COSTA PLANT),ANTIOCH	.06	11	4.2	5.4	12	.01	2800
PACIFIC GAS & ELECTRIC CO. (PITTSBURG PLANT)PITTSBURG	.1	34	1.4	14	4.6	.03	930
PHILLIPS PETROLEUM CO. MARTINEZ	14	9.2	5.0	18	3.6	.08	350
PHILLIPS PETROLEUM CO. BULK PLANT, MARTINEZ	.4	--	---	--	---	--	---

1975 MJAOR SOURCES (NORTHEASTERN BAY AREA APCD)	ANNUAL AVERAGE EMISSIONS - T/D ORG	NOX	K_{NOX}	SO_2	K_{SO_2}	CO	K_{CO}
QUARRY PRODUCTS, INC. RICHMOND	--	.02	2300	--	---	--	---
RADIANT COLOR CO. RICHMOND	.2	--	---	--	---	--	---
SAFEWAY STORES, INC. (HOFFMAN BLVD),RICHMOND	.3	.02	2300	--	---	--	---
SHELL OIL COMPANY MARTINEZ	20	6.9	6.7	11	5.8	4.7	6.0
STANDARD OIL CO. OF CALIF., RICHMOND	22	20	2.3	12	5.3	9.8	2.9
STANDARD OIL CO. OF CA. BULK PLANT, AVON	.3	--	---	--	---	--	---
STANDARD OIL CO. OF CA. BULK PLANT, RICHMOND	.5	--	---	--	---	--	---
STAUFFER CHEMICAL CO. MARTINEZ	--	.05	920	7.9	8.1	.1	280
TEXACO, INC. BULK PLANT, RICHMOND	.4	--	---	--	---	--	---
UNION OIL CO. OF CALIF. RODEO	10	5.1	9.0	8.2	7.8	1.4	20
UNION OIL CO. OF CALIF. BULK PLANT, RICHMOND	.6	--	---	--	---	--	---
U. S. STEEL CORP. PITTSBURG	.02	.6	77	--	---	.04	700

4.2 Description of the Tracer Tests

In this section, a brief synopsis of each tracer test will be presented. The purpose of the test, the test schedule, and the test meteorology will be outlined; typical results for each test will be presented in the form of overview maps of the automobile and airborne traverse data and the hourly averaged data.

Turner's (1961) method of determining stability class based upon wind speed and insolation was used to classify the stability for each test period. The average insolation or cloud cover, the average wind speed, the average mixing layer depth, and the resulting stability class are given in Table 8. The average wind vector at the tracer release point during the release period is also given.

4.21 Tracer Test 1 (8/31/76)

The purpose of the first tracer test was to probe the transport and dispersion of pollutants emitted from the Montezuma Hills under afternoon Sea Breeze conditions. SF_6 was released at a steady rate of 10.6 g/sec (1.10 tons/day) from 1200 to 1700 PDT.

The average wind vector at the Dow site during the release was 270° at 5.3 m/sec; the overall average wind for the area during the afternoon was 300° at 3.4 m/sec. The sky was clear, and Pasquill classes B-C were assumed to exist. The average standard deviation of the wind at Dow was 9°. The average mixing height during the test was approximately 960 meters, and maximum mixing height reached 2300 m after 1500 PDT. The wind pattern observed at 1600 PDT shown in Figure 9 is typical of the afternoon. The pattern appears to be similar to the Smalley wind flow type NW-5; this pattern occurred 13% of the time in August and

TABLE 8

AVERAGE METEOROLOGICAL CONDITIONS DURING FIELD TESTS

Test	Time PDT	L^{*} m	u^{**} deg/m/sec	u_r^{***} (release point)	Cloud cover	Stability class
1	1200-1800	960	300/3.4	270/5.3	clear	B-C
2	1100-1700	830	290/4.3	270/4.0 (Mart.)	clear	B-C
	1300-1500			270/9.2 (Dow)		
3	0000-0600	860	290/3.3	280/9.3	scattered	D-F
4	1800-0000	510	290/3.3	280/7.1	broken	D-F
5	1100-1500	1910	340/2.6	17/1.8	scattered	B-C
6	0600-1400	1250	270/1.2	280/6.3	overcast	D
7	0600-1900	830	280/2.3	240/2.6 (Pinole)	scattered	B-C
				270/4.6 (Dow)		
8	0700-1300	1200	250/3.6	220/3.7	scattered	B-C

[*] The average height of the mixing depth, L, was calculated from available hourly mixing depths for all stations over the indicated time period.

[**] The average wind direction and speed was obtained by vector averaging data from all downwind stations over the time indicated.

[***] u_r is the average wind direction and speed at the tracer release point during the time of the release. Surface data from Rodeo (4 Km northeast of Pinole) were used for determining u_r at Pinole.

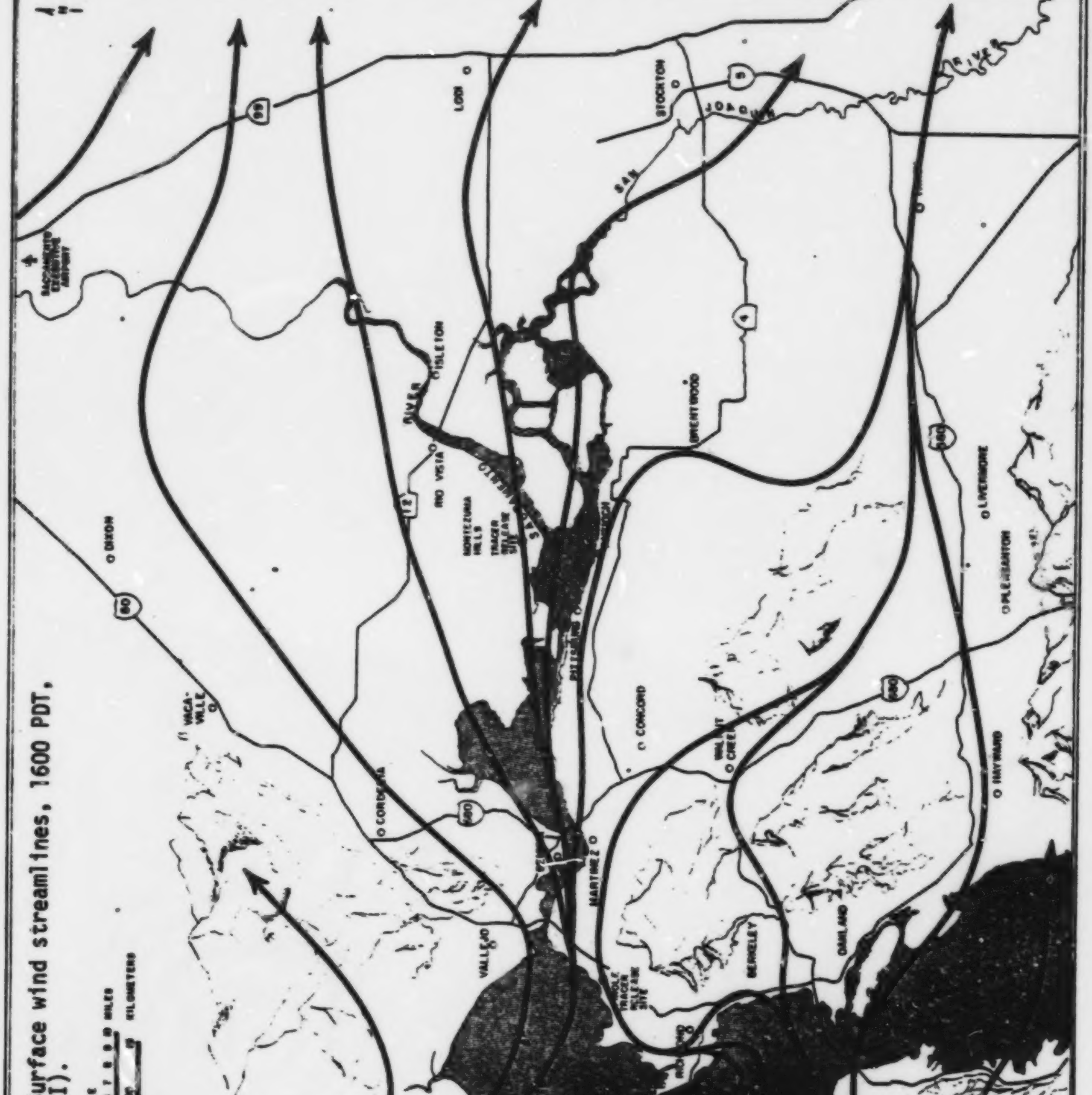
SCALE
0 1 2 3 4 5 6 7 8 9 10 MILES
0 1 2 3 4 5 10 15 KILOMETERS
N
SACRAMENTO EXECUTIVE AIRPORT
DIXON
VACAVILLE
CORDELIA
VALLEJO
RICHMOND
BERKELEY HILLS TRACER RELEASE SITE
BERKELEY
OAKLAND
SAN FRANCISCO
HAYWARD
WALNUT CREEK
CONCORD
MARTINEZ
PITTSBURG
ANTIOCH
BRENTWOOD
MONTEZUMA HILLS TRACER RELEASE SITE
RIO VISTA
SACRAMENTO
RIVER
ISLETON
LODI
STOCKTON
SAN
JOAQUIN
RIVER
TRACY
LIVERMORE
PLEASANTON
99
80
680
12
4
5
580
101

Figure 9. Surface wind streamlines, 1600 PDT, 8/31/76 (MRI).

6% of the time over a year in the Smalley study. A quantitatve description of the Test 1 wind patterns and tracer trajectories based upon a numerical solution of the mass balance equation is given in Section 5 of this volume. Peak ozone concentrations in the area reached .16 ppm at Livermore during the afternoon.

Four automobile traverses were conducted along Highway 160 7 km downwind between 1420 and 1641 PDT. The plume crossed Highway 160 approximately 9 km north of the Highway 160-Highway 4 junction. Peak concentrations observed in the traverses ranged from 611 ppt to 1223 ppt. Three automobile traverses were conducted along Highway 99 from Galt to Tracy; the two traverses conducted between 1400 and 1700 PDT indicated the plume had not yet crossed Highway 99. Traverse 7, conducted from 1701 to 1753 PDT, showed the center of the plume, 52 km downwind, to be 6 km east of Tracy at the intersection of I5 and I205. The plume had a centerline concentration of 64 ppt and an observable width of approximately 39 km. Traverses 6 and 7 are shown in Figure 10. As indicated in Traverse 7, emissions from the Dow site ultimately can impact in the San Joaquin Valley, south of Tracy. The average wind speed associated with the transport of the plume from the Montezuma Hills to Highway 99 was about 3 m/sec.

Hourly averaged samples were collected at points along Highway 160 and Highway 99. Peak hourly concentrations along the two routes were 636 ppt and 103 ppt, respectively. The hourly averaged plume crossing Highway 160, 7 km downwind, was centered 8.8 km north of the Highway 160-Highway 4 junction and was approximately 5.6 km wide; hourly crosswind profiles are shown in Figure 11. Further downwind at 45 km, the

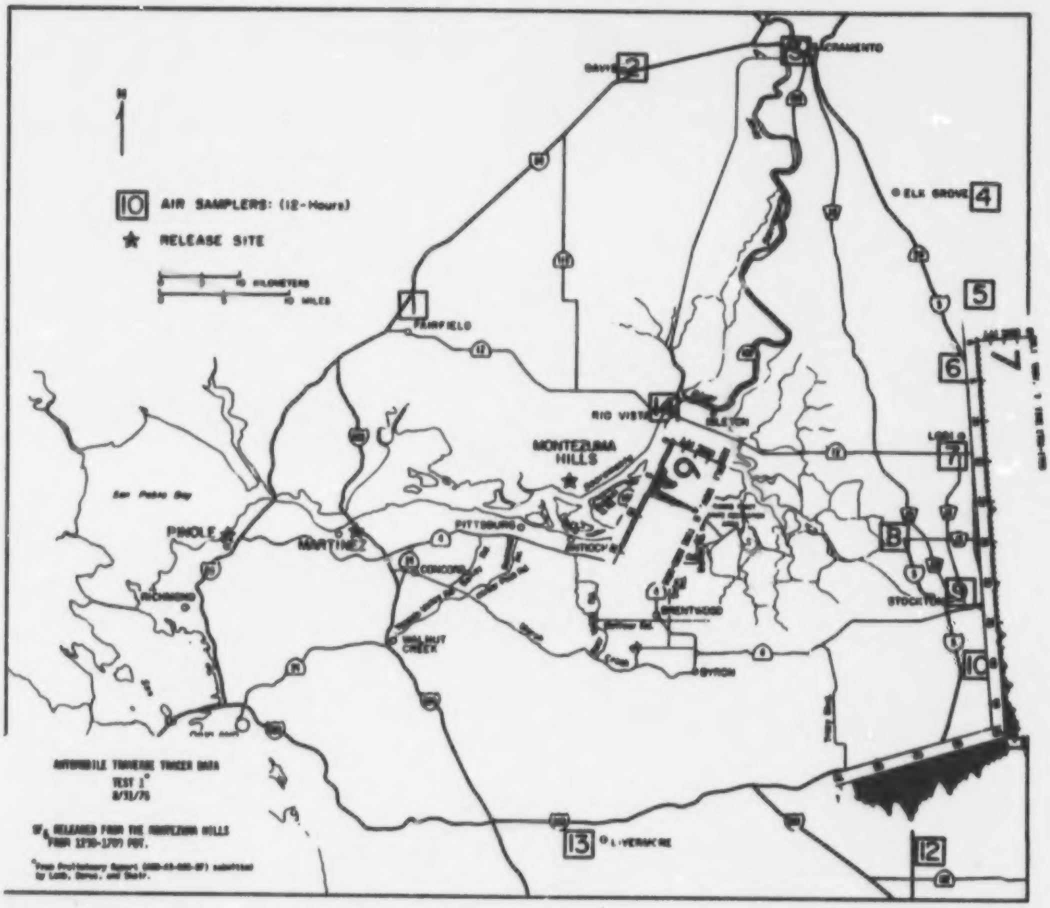
N
10 AIR SAMPLERS: (12-Hours)
RELEASE SITE
10 KILOMETERS
10 MILES
SACRAMENTO
DAVIS
ELK GROVE
FAIRFIELD
RIO VISTA
ISLETON
MONTEZUMA HILLS
LODI
STOCKTON
PITTSBURG
ANTIOCH
CONCORD
MARTINEZ
PINOLE
RICHMOND
San Pablo Bay
WALNUT CREEK
BRENTWOOD
BYRON
LIVERMORE
1
2
3
4
5
6
7
8
9
10
11
12
13

AUTOMOBILE TRAVERSE TRACER DATA
TEST 1*
8/31/76

SF_6 RELEASED FROM THE MONTEZUMA HILLS FROM 1200-1700 PDT.

Figure 10. Overview of automobile traverse SF_6 data.

TEST 1

8/31/76

Auto Traverses:

6 1630 - 1641 PDT, SF_6(max) = 1223 ppt

7 1701 - 1753 PDT, SF_6(max) = 64 ppt

SF_6 released from the Montezuma Hills from 1200-1700 PDT.

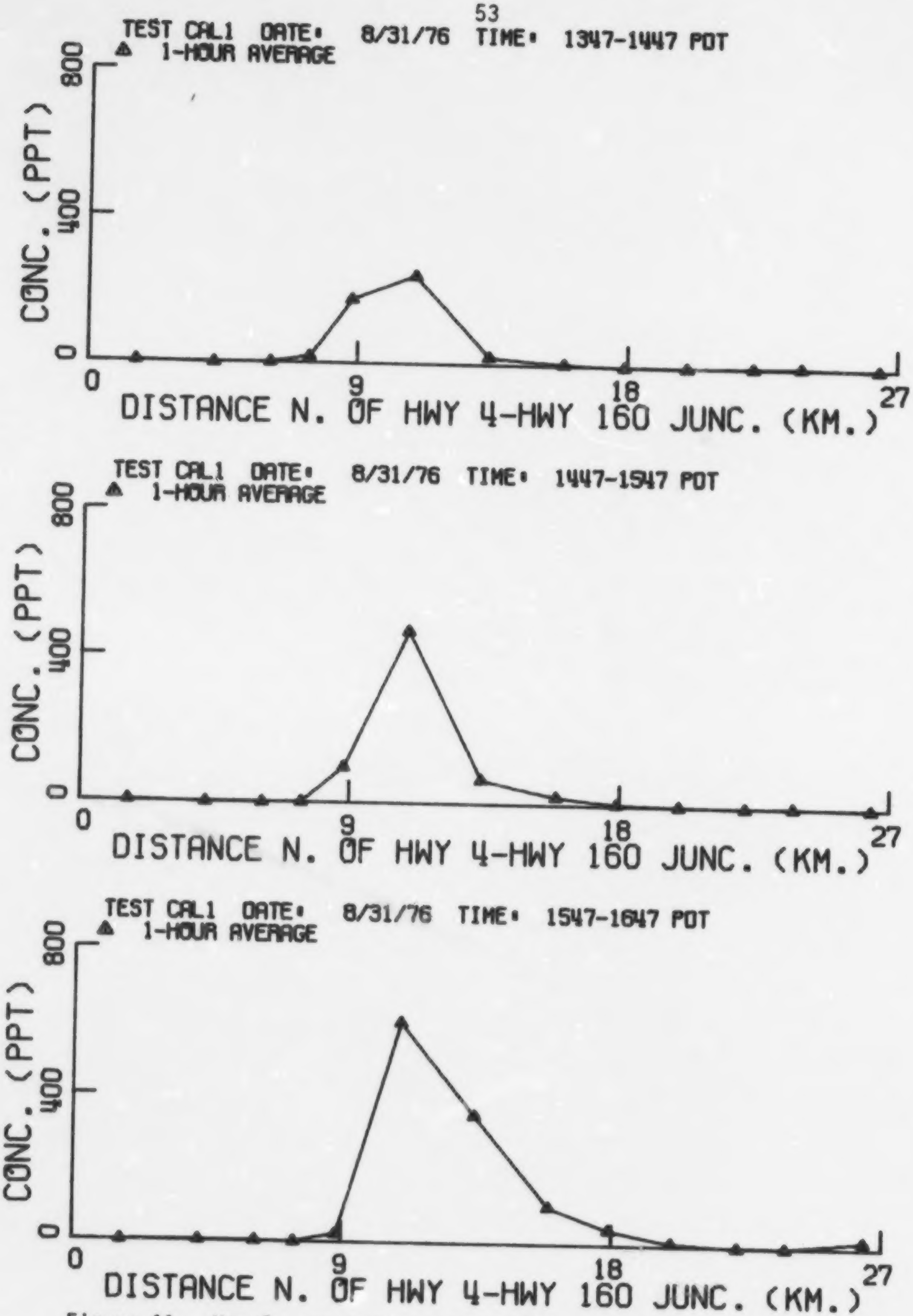

Figure 11. Hourly averaged crosswind SF_6 profiles measured along Highway 160.

hourly plume was 72 km wide and was centered approximately 10 km north of Stockton. Significant levels of SF_6 were detected during three hours along Highway 99. The tracer emitted during a five-hour period took only three hours to pass, implicating the existence of somewhat stagnant conditions downwind of the Montezuma Hills earlier in the afternoon. The hourly averaged concentrations are plotted as a function of the distance south of Sacramento in Figure 12. An overview of the hourly averaged results is provided in Figure 13.

4.22 Tracer Test 2 (9/2/76)

The purpose of Test 2 was to tag the air moving over the Montezuma Hills during the afternoon Sea Breeze period. Two atmospheric tracers were used: SF_6 was introduced upstream at Martinez near existing industrial pollutant sources; $CBrF_3$ was released from the Montezuma Hills. SF_6 was released at a steady rate of 11.4 g/sec (1.08 tons/day) from 1100 to 1600 PDT. The release of $CBrF_3$ was not started until 1300 PDT in hopes of waiting for the SF_6-tagged air to reach the Montezuma Hills. The $CBrF_3$ was released at a constant rate of 16.6 g/sec (1.58 tons/day) until 1500 PDT.

The average surface wind vectors at Martinez and at the Dow site were 270^0 at 4.0 m/sec and 270^0 at 9.2 m/sec, respectively. The overall area average wind direction and speed for the release period was 290^0 at 4.3 m/sec. The horizontal standard deviation of the winds at the Dow site was 7^0 for the day. The average mixing height in the area was 830 meters with a maximum of 1500 meters occurring during the late afternoon. There were no clouds, and Pasquill stability classes B-C were assumed to exist. The wind pattern at 1600 PDT shown in Figure 14 was typical for

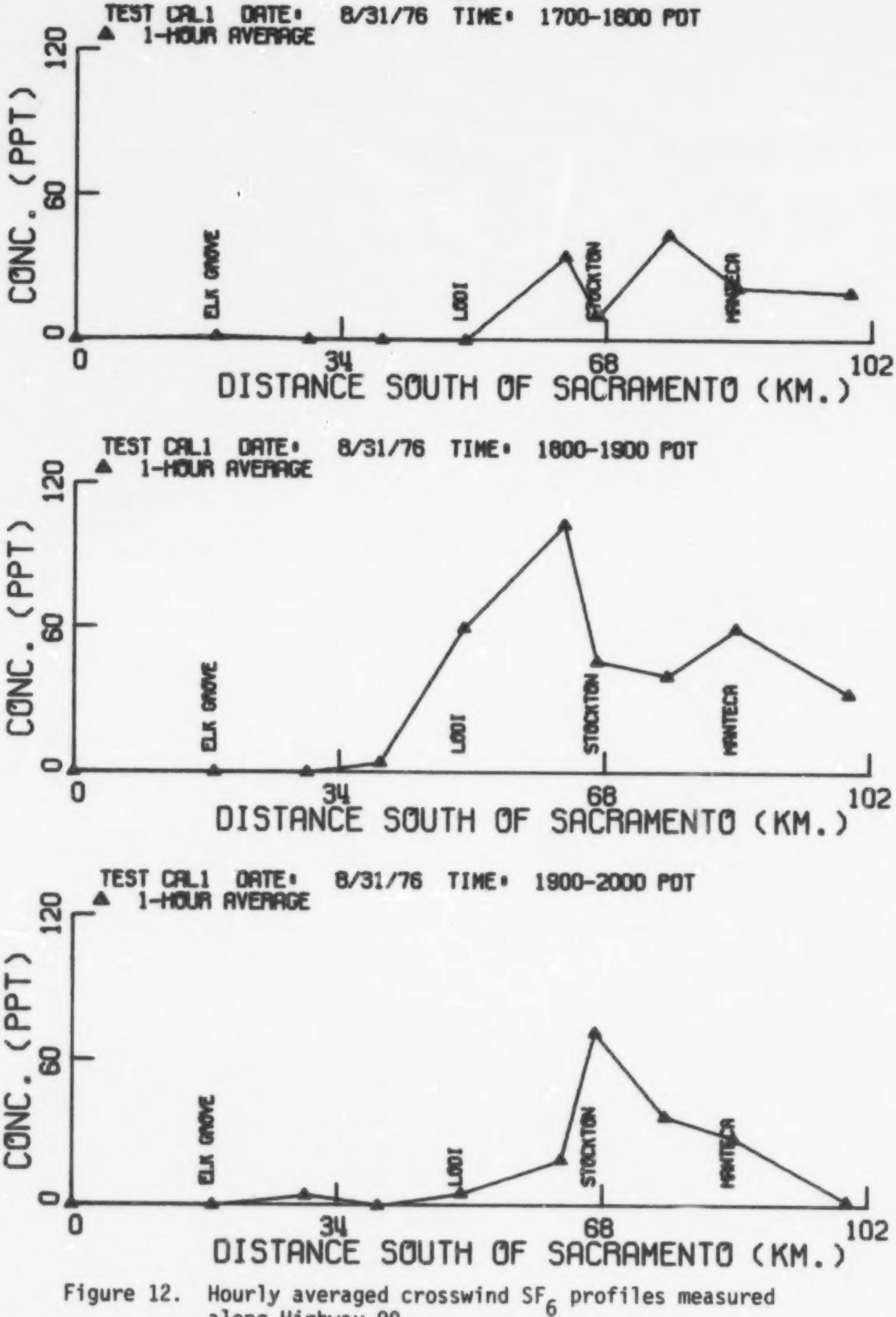

Figure 12. Hourly averaged crosswind SF_6 profiles measured along Highway 99.

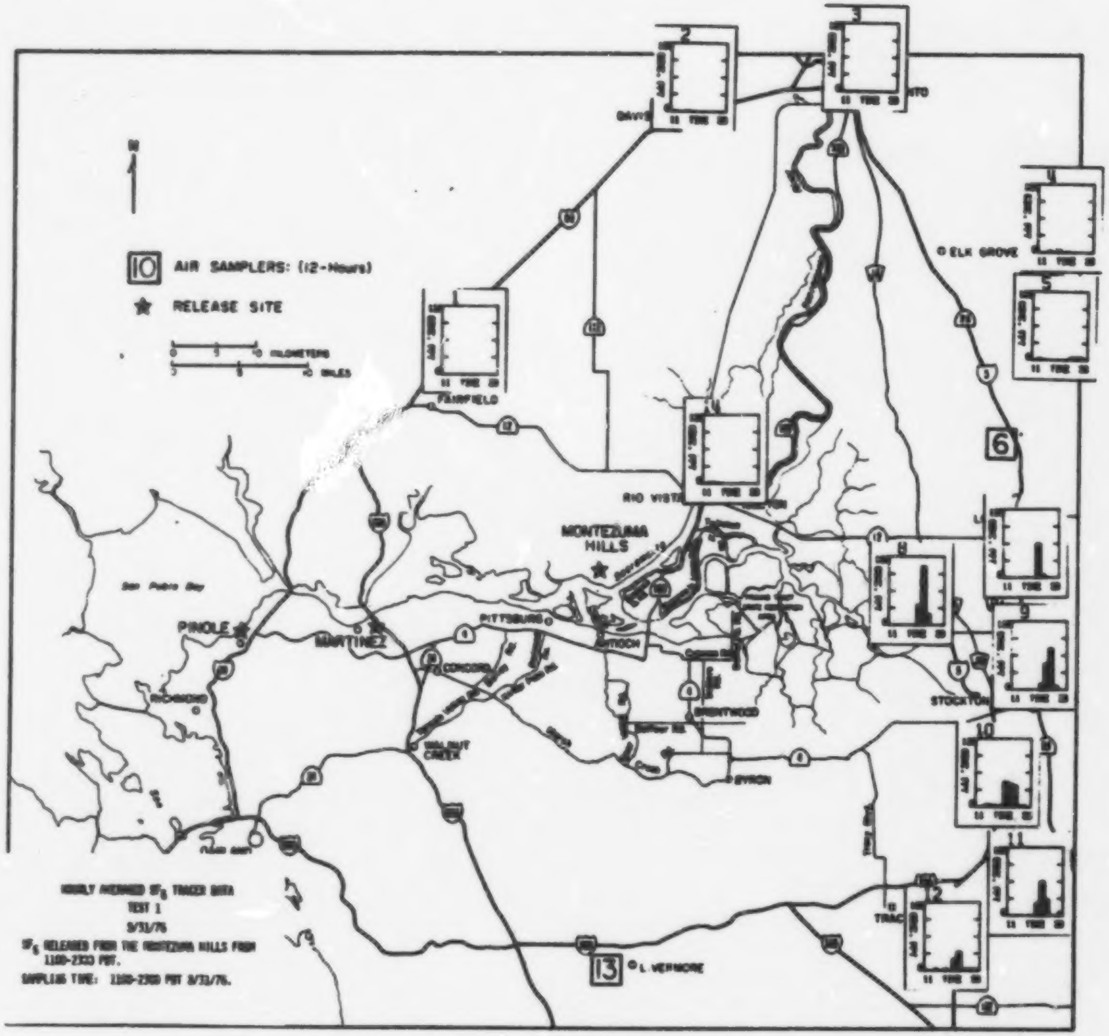
AIR SAMPLERS: (12-Hours)
RELEASE SITE
KILOMETERS
MILES
N
10
6
13
2
3
4
5
7
8
9
10
11
12
CONC. PPT
TIME
DAVIS
ELK GROVE
FAIRFIELD
RIO VISTA
MONTEZUMA HILLS
PITTSBURG
ANTIOCH
PINOLE
MARTINEZ
CONCORD
RICHMOND
WALNUT CREEK
BRENTWOOD
BYRON
STOCKTON
TRACY
L. VERMORE
San Pablo Bay
HOURLY AVERAGED SF6 TRACER DATA
TEST 1
5/31/76
SF6 RELEASED FROM THE MONTEZUMA HILLS FROM 1100-2330 PDT.
SAMPLING TIME: 1100-2300 PDT 5/31/76.

Figure 13. Overview of hourly averaged SF_6 data. Full-scale SF_6 = 120 ppt.

9/2 15

Figure 14. Surface wind streamlines, 1600 PDT, 9/2/76 (MRI).

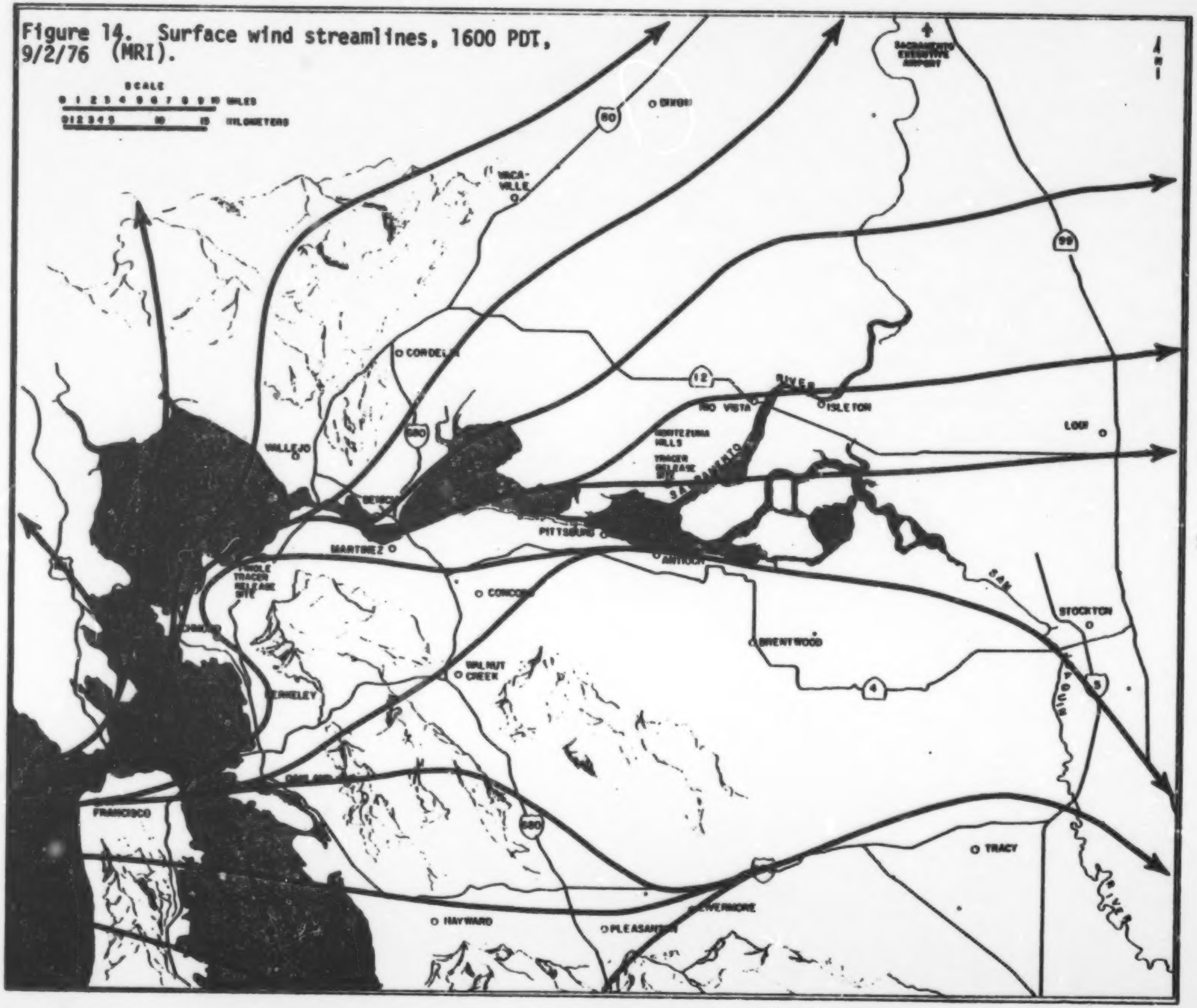
SCALE
0 1 2 3 4 5 6 7 8 9 10 MILES
0 1 2 3 4 5 10 15 KILOMETERS
N
SACRAMENTO EXECUTIVE AIRPORT
DIXON
80
VACA-VILLE
99
CORDELIA
12
RIVER
RIO VISTA
ISLETON
MONTEZUMA HILLS
TRACER RELEASE SITE
SACRAMENTO
LODI
VALLEJO
680
BENICIA
MARTINEZ
PITTSBURG
ANTIOCH
PINOLE TRACER RELEASE SITE
CONCORD
SAN
STOCKTON
BRENTWOOD
WALNUT CREEK
4
JOAQUIN
5
BERKELEY
OAKLAND
FRANCISCO
680
TRACY
RIVER
LIVERMORE
HAYWARD
PLEASANTON

the afternoon. The pattern appears to be similar to Smalley wind flow type W-6 which occurred 10% of the time in September and 6% of the time on a yearly basis between 1952 and 1955. The peak ozone level was 0.16 ppm observed at Stockton.

Eleven automobile traverses were conducted. The majority of the air tagged by the SF_6 tracer did not pass over the Montezuma Hills. However, it did pass through the same downwind zone (i.e., the Tracy-Stockton area) as did the emissions from Montezuma Hills. Traverses 2 and 3 in Figure 15, Traverse 4 in Figure 16, and Traverse 10 in Figure 17 show the sharp, spiked SF_6 and $CBrF_3$ plumes immediately downwind of Martinez and Montezuma Hills, respectively, the broad SF_6 plume crossing Highway 160, and the location of both tracer plumes crossing Highway 99 south of Stockton. The maximum SF_6 concentration observed along Highway 160, 35 km downwind of Martinez, was 33 ppt, while the maximum level seen along Highway 99, 67 km downwind, was 91 ppt. The profile in Traverse 3 indicates that the SF_6 trajectory passed south of the Montezuma Hills below Pittsburg and Antioch. The SF_6 profile in Traverse 10 suggests that a portion of the tracer from Martinez moved south through the Walnut Creek area towards Livermore.

The $CBrF_3$ plume behaved in a manner similar to that observed during Test 1. The plume crossed Highway 160 approximately 8.2 km north of the Highway 160-Highway 4 junction with a peak concentration of 2168 ppt. It appeared to curve south toward Stockton, crossing Highway 99 with a peak concentration of 300 ppt, 57 km downwind.

Hourly averaged data obtained along Highway 160 and shown in Figure 18 confirm the description drawn from the traverse data. The

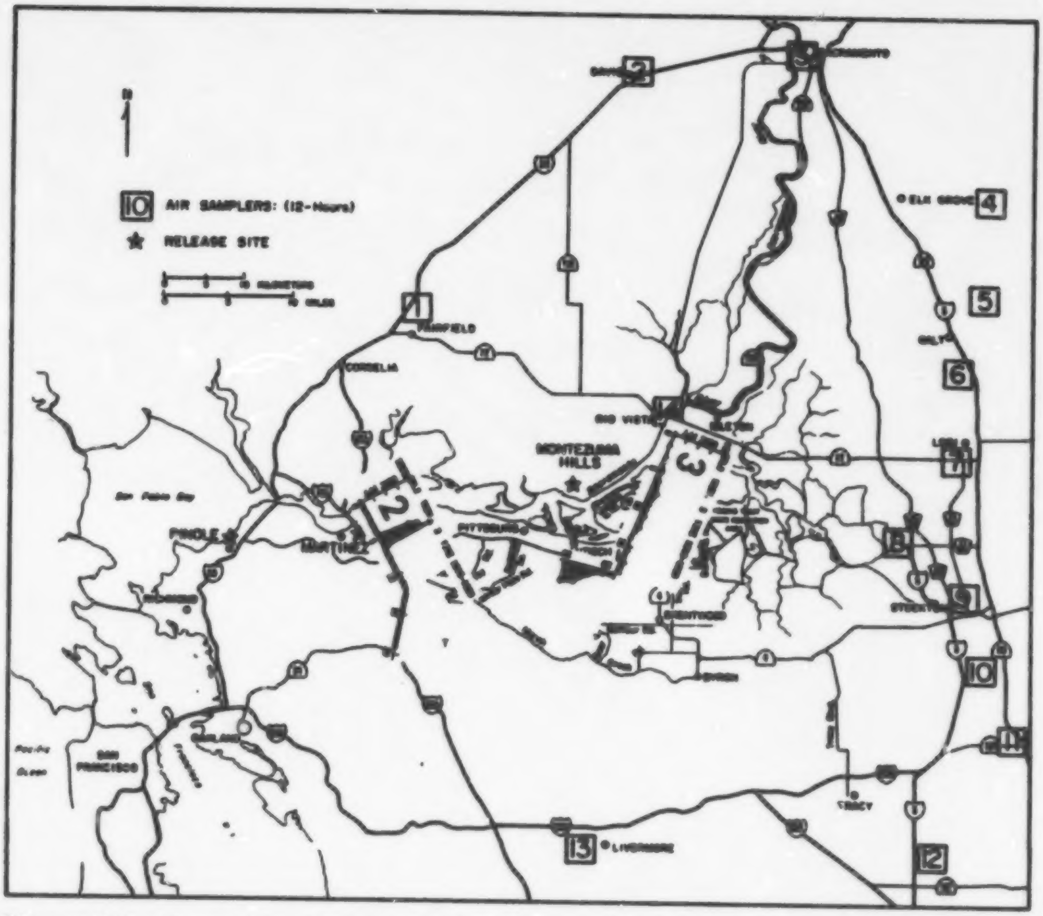
N
10 AIR SAMPLERS: (12-Hours)
RELEASE SITE
DAVIS
SACRAMENTO
ELK GROVE
FAIRFIELD
CORDELIA
GALT
RIO VISTA
MONTEZUMA HILLS
LODI
San Pablo Bay
PINOLE
MARTINEZ
PITTSBURG
STOCKTON
BRENTWOOD
Pacific Ocean
SAN FRANCISCO
TRACY
LIVERMORE
1
2
3
4
5
6
7
8
9
10
11
12
13

Figure 15. Overview of automobile traverse SF_6 data.

TEST 2

9/2/76

Autc Traverses:

2 1215 - 1228 PDT, SF_6(max) = 30,000 ppt

3 1240 - 1328 PDT, SF_6(max) - 41 ppt

SF_6 released from Martinez from 1100-1600 PDT.

$CBrF_3$ released from the Montezuma Hills from 1300-1500 PDT.

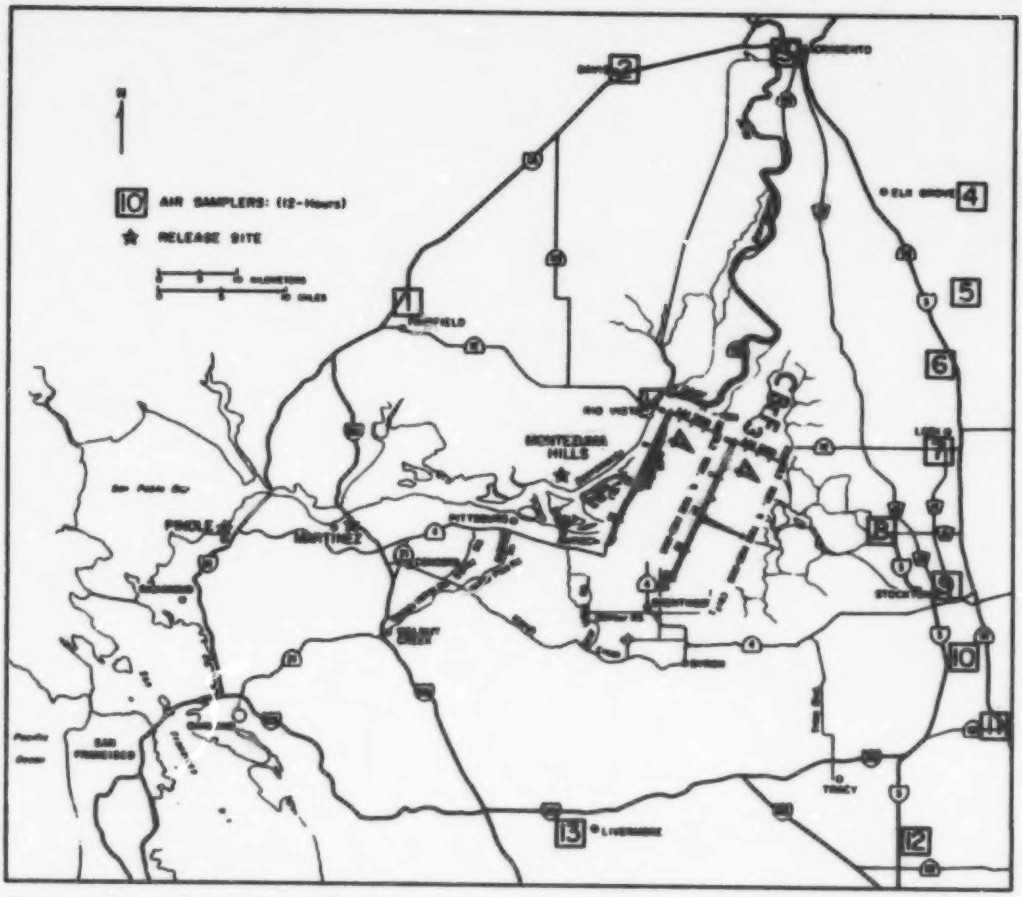
N
10
AIR SAMPLERS: (12-Hours)
RELEASE SITE
0 5 10 KILOMETERS
0 5 10 MILES
1
2
4
5
6
7
8
9
10
12
13
SACRAMENTO
ELK GROVE
FAIRFIELD
RIO VISTA
MONTEZUMA HILLS
LODI
San Pablo Bay
PINOLE
MARTINEZ
PITTSBURG
WALNUT CREEK
STOCKTON
SAN FRANCISCO
TRACY
LIVERMORE
4

Figure 16. Overview of automobile traverse SF_6 and $CBrF_3$ data.

TEST 2

9/2/76

Auto Traverse:

4 1400-1415 PDT, SF_6(max) = 33 ppt.

1400-1415 PDT, $CBrF_3$(max) = 2168 ppt.

SF_6 released from Martinez from 1100-1600 PDT.

$CBrF_3$ released from the Montezuma Hills from 1300-1500 PDT.

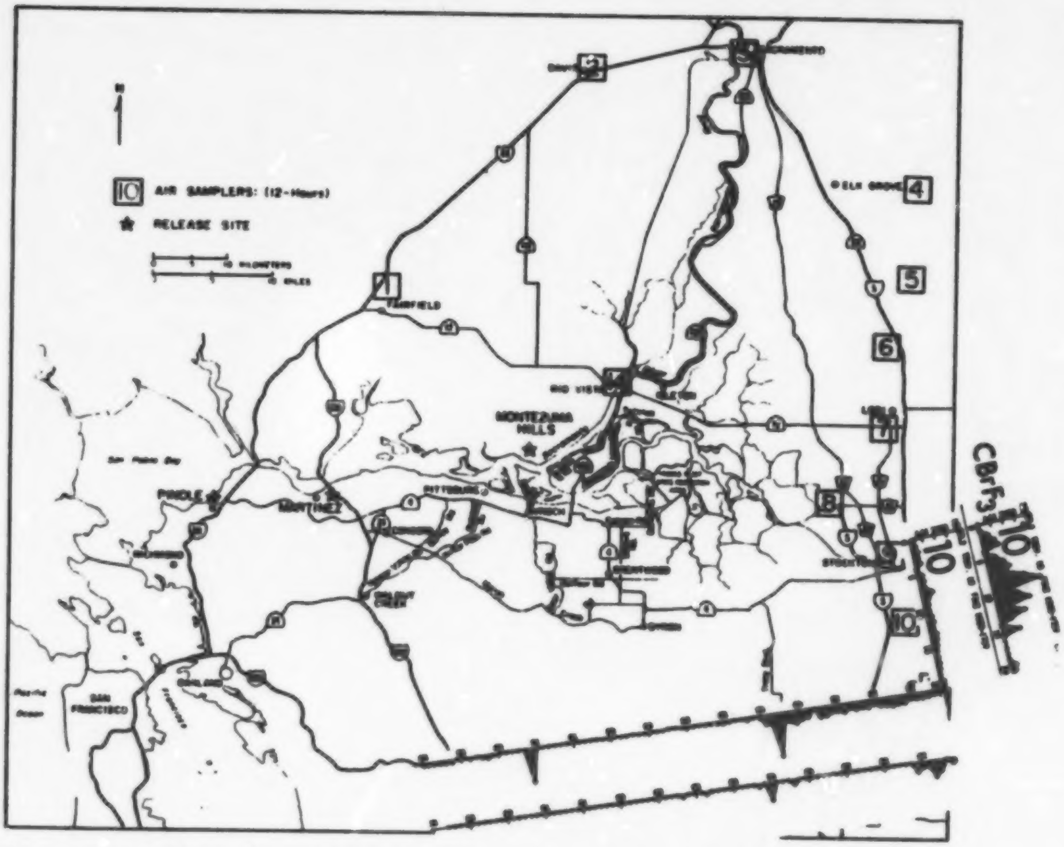
N
10 AIR SAMPLERS: (12-Hours)
RELEASE SITE
MONTEZUMA HILLS
FAIRFIELD
RIO VISTA
ELK GROVE
PITTSBURG
MARTINEZ
STOCKTON
SAN FRANCISCO
Pacific Ocean
CBrF3
10
1
2
4
5
6
7
8
9

Figure 17. Overview of automobile traverse SF_6 and $CBrF_3$ data.

TEST 2

9/2/76

Auto Traverse:

10 1630-1737 PDT, SF_6(max) = 91 ppt.

1630-1737 PDT, $CBrF_3$(max) = 300 ppt.

SF_6 released from Martinez from 1100-1600 PDT.

$CBrF_3$ released from the Montezuma Hills from 1300-1500 PDT.

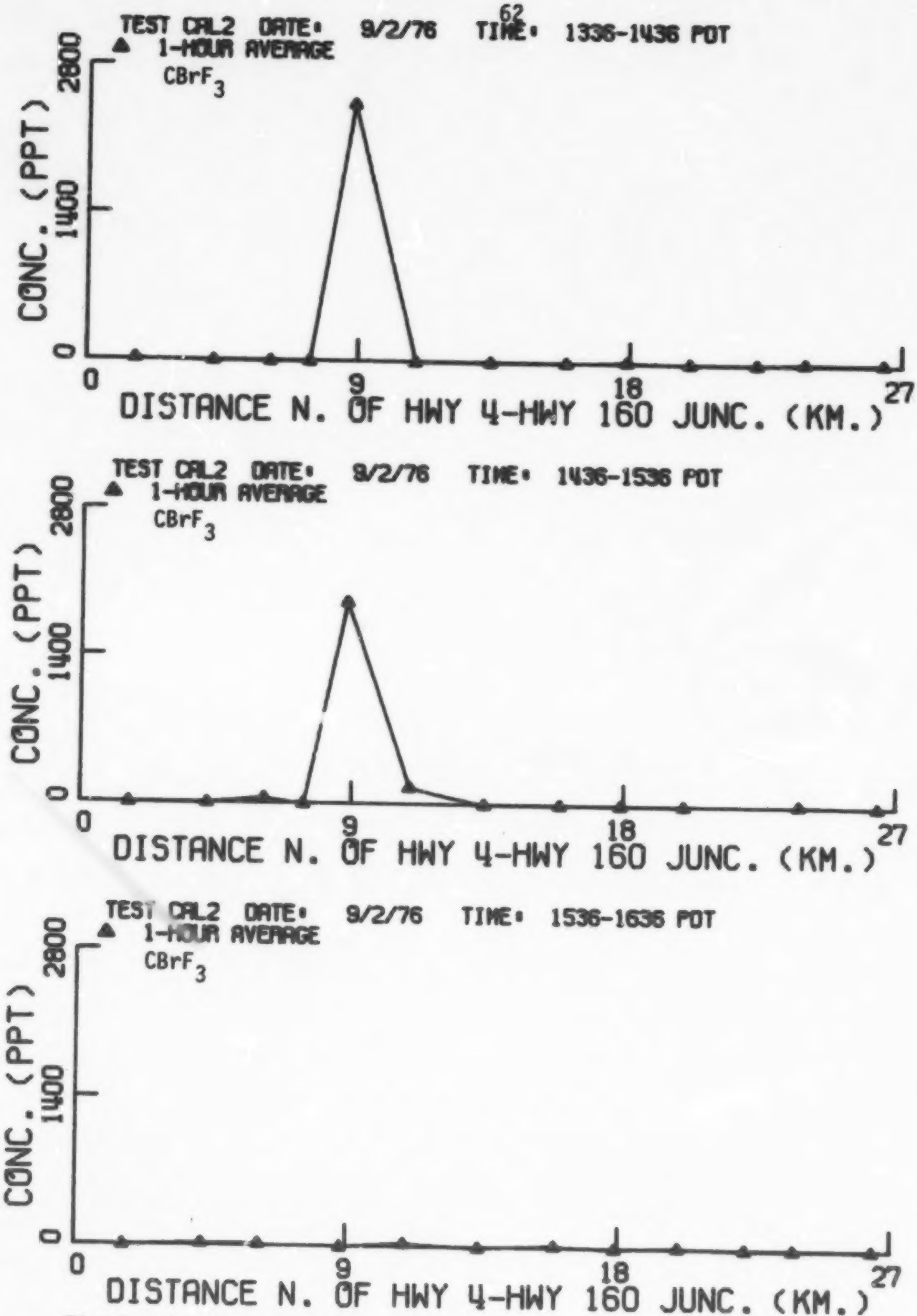

Figure 18. Hourly averaged crosswind $CBrF_3$ profiles measured along Highway 160.

SF_6 profile stretches along Highway 160 for 26 km with a maximum of 17 ppt as shown in Figure 19. The maximum hourly averaged concentration of CBrF3 along Highway 160 was 2427 ppt observed 8.8 km north of the Highway 160-Highway 4 junction. The overview map in Figure 20 shows the widespread detection of SF_6 during the test period. The data shown in Figure 21 indicate that the plume reached Stockton at about 1600 PDT, which corresponds to an average transport wind speed of 4 m/sec (14 km/hr). The maximum SF_6 concentration along Highway 99 was 21 ppt observed approximately 9 km south of Stockton at 1800 PDT. In this test, measurable levels of SF_6 were obtained during the night and early morning at several stations along Highway 99. These levels were less that 10 ppt; they suggest that possibly the tracer emitted near the end of the release period from Martinez was transported into the Stockton-Tracy area where it remained for several hours under nighttime stagnant conditions. As in the first test, material emitted from the Montezuma Hills reached the Stockton area and was directed south into the San Joaquin Valley. In addition, material emitted from Martinez, near the Carquinez Strait, reached the same area and appeared to be moving south into the San Joaquin Valley.

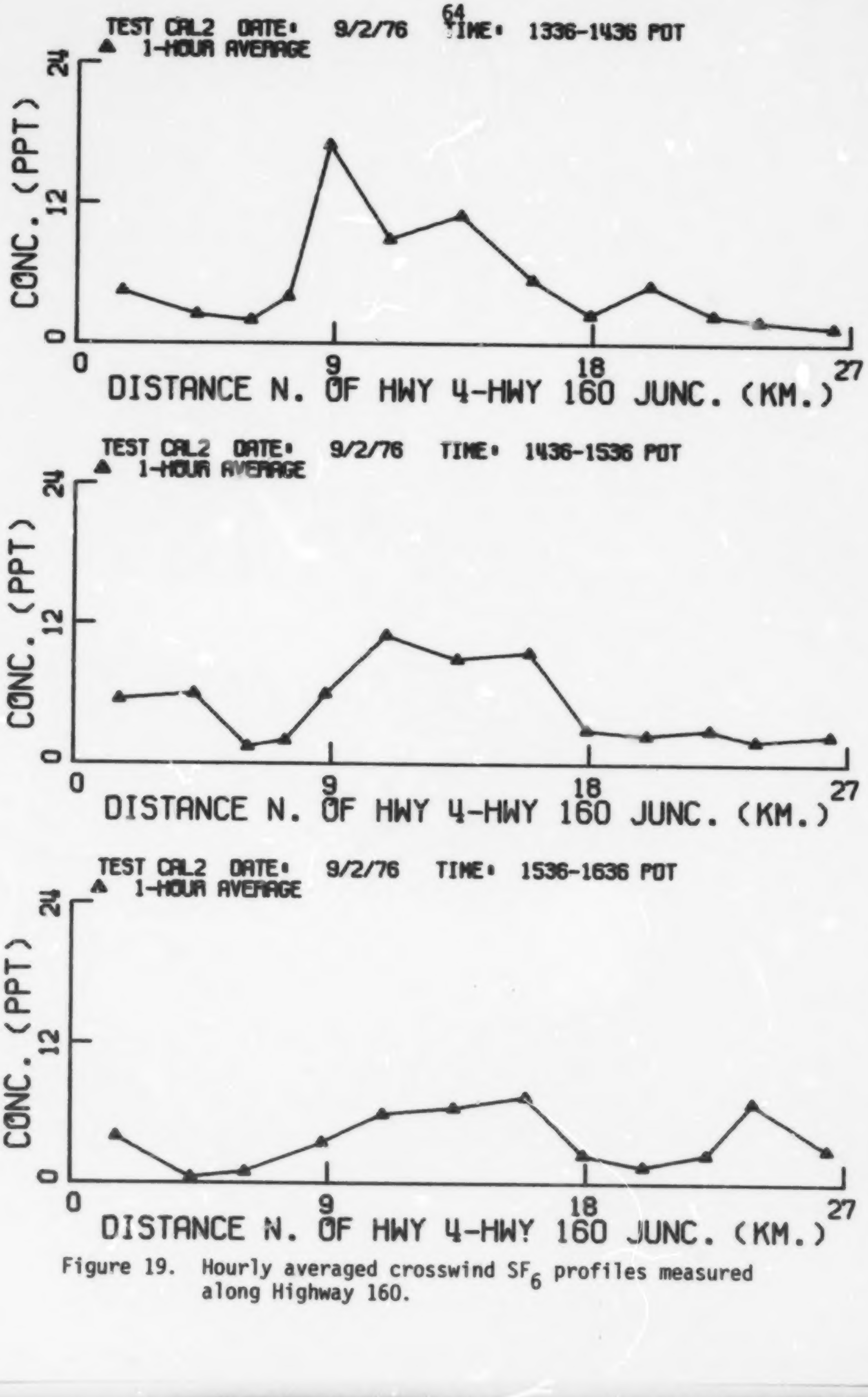

Figure 19. Hourly averaged crosswind SF_6 profiles measured along Highway 160.

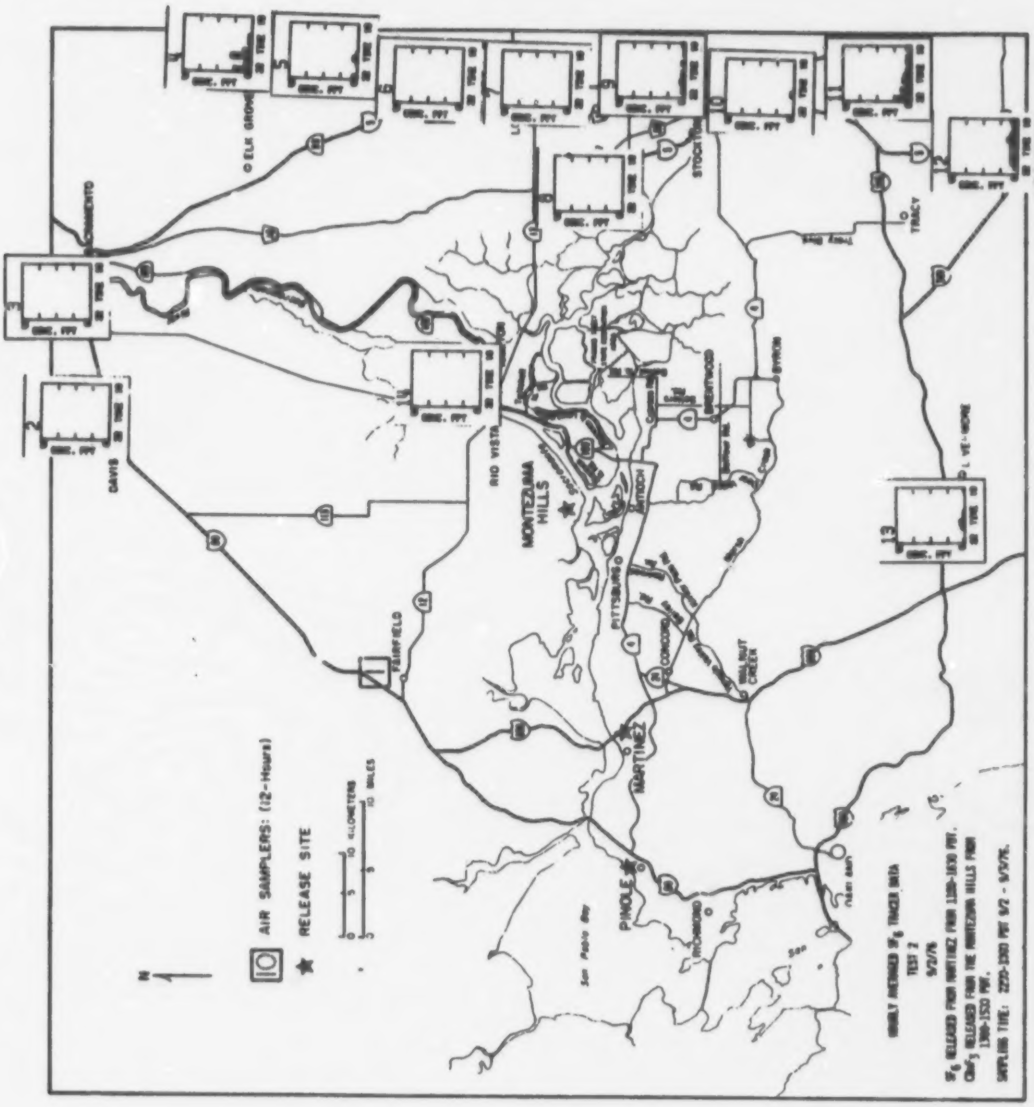
AIR SAMPLERS: (12-Hours)
RELEASE SITE
10 KILOMETERS
10 MILES
CONC. PPT
TIME
MONTEZUMA HILLS
RIO VISTA
PITTSBURG
ANTIOCH
MARTINEZ
PINOLE
RICHMOND
CONCORD
WALNUT CREEK
BRENTWOOD
BYRON
FAIRFIELD
DAVIS
SACRAMENTO
ELK GROVE
STOCKTON
TRACY
LIVERMORE
San Pablo Bay
12
13

Figure 20. Overview of hourly averaged SF_6 data. Full scale SF_6 = 40 ppt.

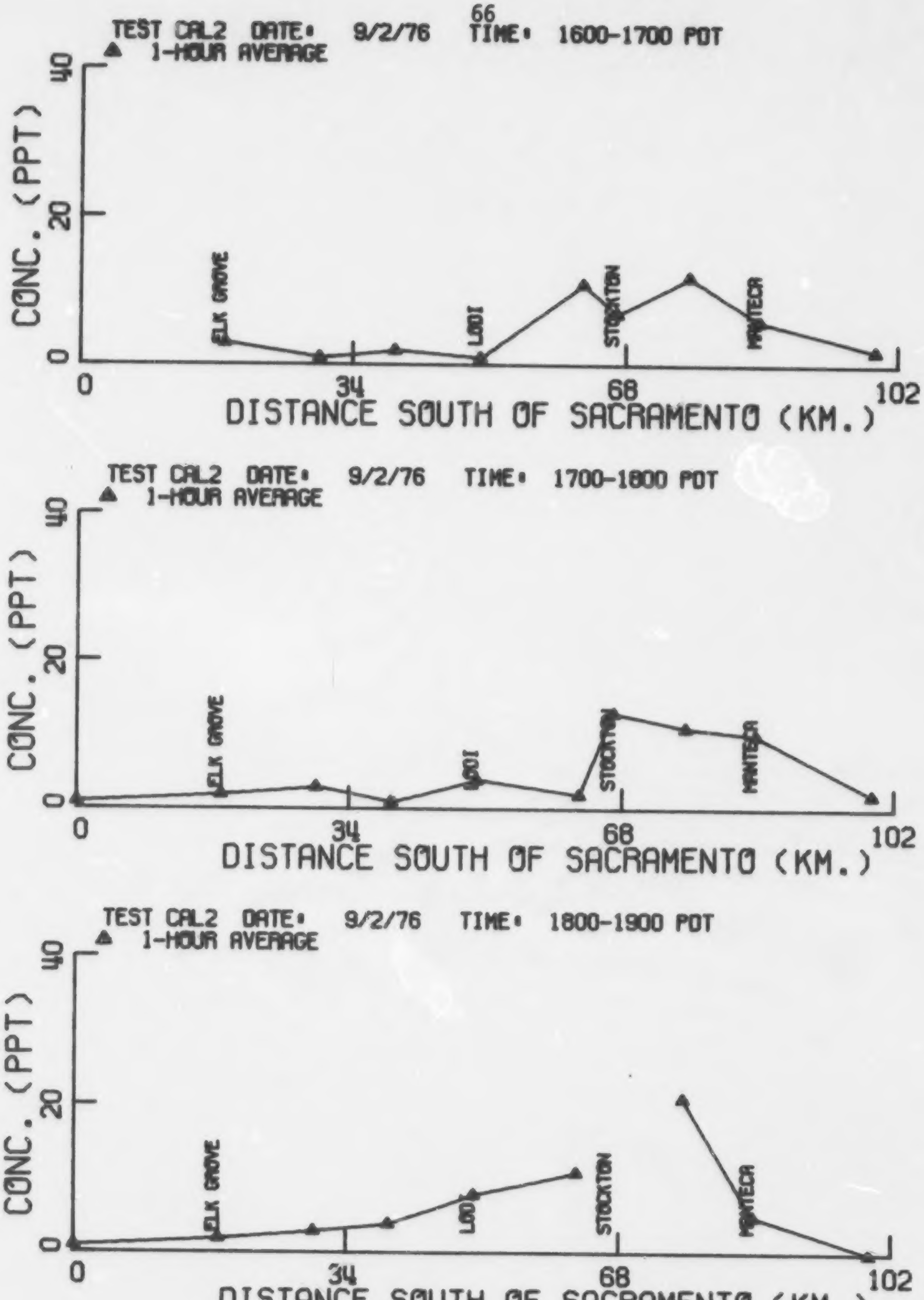

Figure 21. Hourly averaged SF_6 profiles measured along Highway 99.

4.23 Tracer Test 3 (9/5/76)

The purpose of the third tracer test was to characterize the transport and dispersion associated with the Nighttime meteorological period. SF_6 was released from the Dow site at a steady rate of 9.5 g/sec (0.90 ton/day) from midnight to 0500 PDT.

Average winds at the Dow site and throughout the area were 280^{o} at 9.3 m/sec and 290^{o} at 3.3 m/sec, respectively. The average standard deviation of the wind at Dow was 7^{o}. There were scattered clouds, and stability conditions were considered to be Pasquill classes D-F. This predicted range of stability classes results from the wide range of wind speeds observed in the area. The average mixing height during the test was 860 meters with a maximum of 1300 meters observed near the end of the tracer release. The wind pattern given in Figure 22 agrees with the results of the tracer data. Later patterns showed the sea flow meeting the mountain drainage winds between Lodi and Stockton. Under those conditions, one layer, presumably the sea flow, is pushed aloft by the opposite flow field. However, as will be apparent, the tracer trajectory throughout the night followed the streamlines drawn from 0100 PDT wind data.

Fourteen automobile traverses were conducted from 0100 to 0511 PDT. These traverses indicated that the plume crossed Highway 160 6.9 km north of the Highway 160-Highway 4 junction with an average peak concentration of 4992 ppt. The maximum level observed in these traverses was 8660 ppt. Typical crosswind SF_6 profiles are shown in Figures 23 and 24. Traverses along Highway 99 indicated the tracer trajectory passed through Stockton

9/40 2Y

Figure 22. Surface wind streamlines, 0100 PDT, 9/5/76 (MRI).

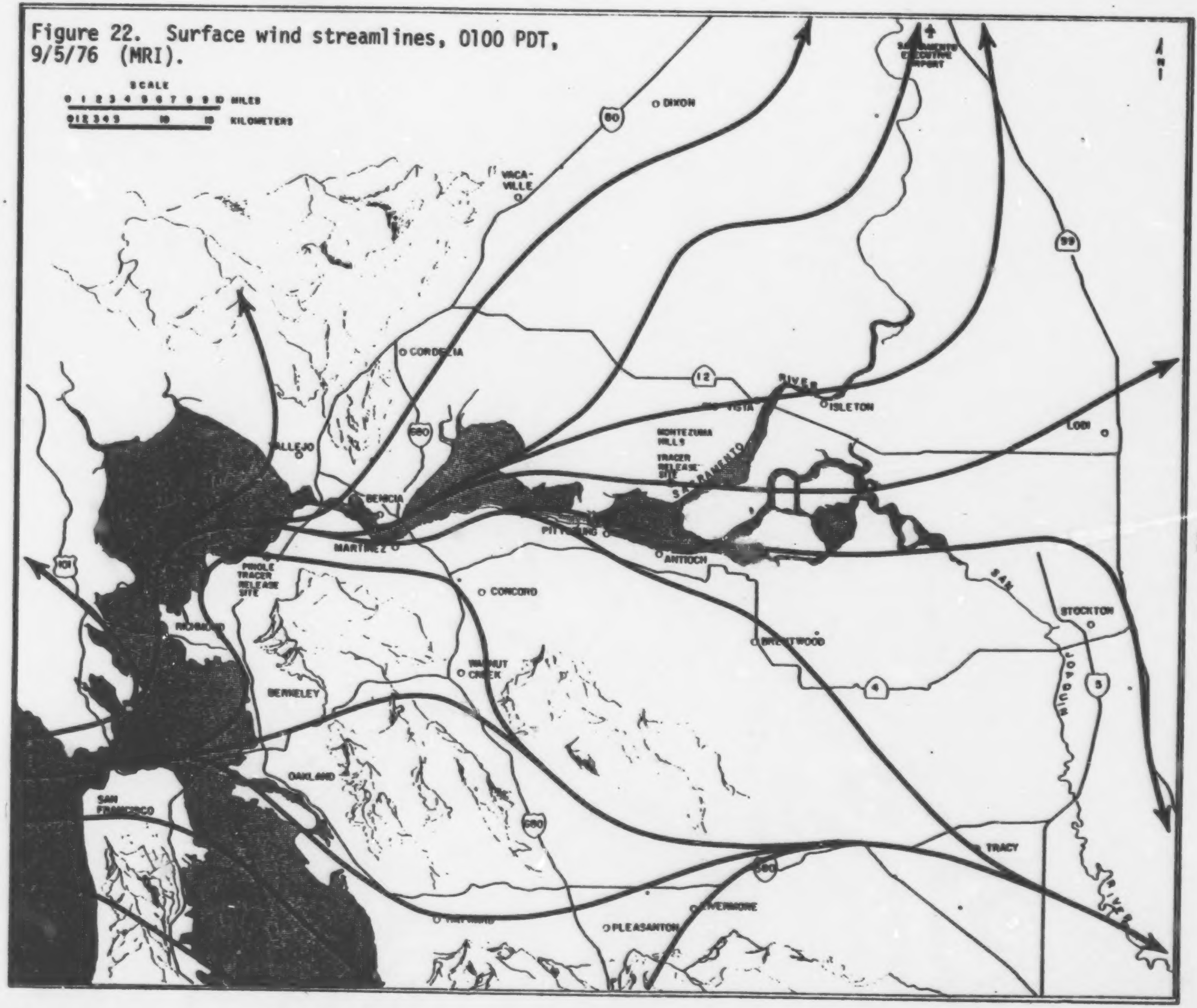
SCALE
0 1 2 3 4 5 6 7 8 9 10 MILES
0 1 2 3 4 5 10 15 KILOMETERS
N
SACRAMENTO EXECUTIVE AIRPORT
DIXON
80
VACA-VILLE
99
CORDELIA
12
RIVER
RIO VISTA
ISLETON
LODI
VALLEJO
680
MONTEZUMA HILLS
TRACER RELEASE SITE
SACRAMENTO
BENICIA
PITTSBURG
MARTINEZ
ANTIOCH
101
PINOLE TRACER RELEASE SITE
CONCORD
SAN
STOCKTON
RICHMOND
BRENTWOOD
WALNUT CREEK
JOAQUIN
5
BERKELEY
4
OAKLAND
SAN FRANCISCO
680
TRACY
580
LIVERMORE
HAYWARD
PLEASANTON
RIVER

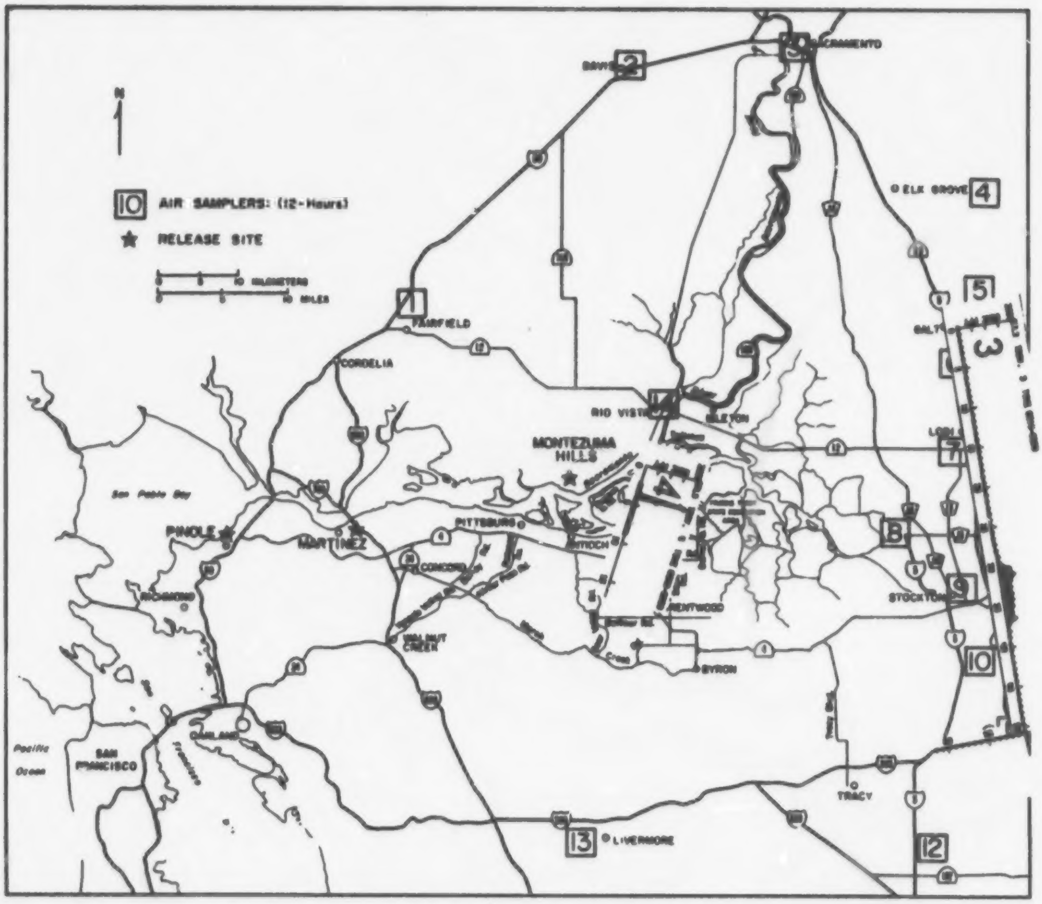
N
10 AIR SAMPLERS: (12-Hours)
RELEASE SITE
0 5 10 KILOMETERS
0 5 10 MILES
SACRAMENTO
DAVIS
2
ELK GROVE
4
5
GALT
3
1
FAIRFIELD
CORDELIA
RIO VISTA
ISLETON
MONTEZUMA HILLS
LODI
7
San Pablo Bay
PINOLE
MARTINEZ
PITTSBURG
ANTIOCH
8
CONCORD
RICHMOND
STOCKTON
9
BRENTWOOD
WALNUT CREEK
BYRON
10
Pacific Ocean
SAN FRANCISCO
OAKLAND
TRACY
13
LIVERMORE
12

Figure 23. Overview of automobile traverse SF_6 data.

TEST 3

9/5/76

Auto Traverses:

3 0213 - 0259 PDT, SF_6(max) = 537 ppt

4 0240 - 0300 PDT, SF_6(max) = 1856 ppt

SF_6 released from the Montezuma Hills from 0000-0500 PDT.

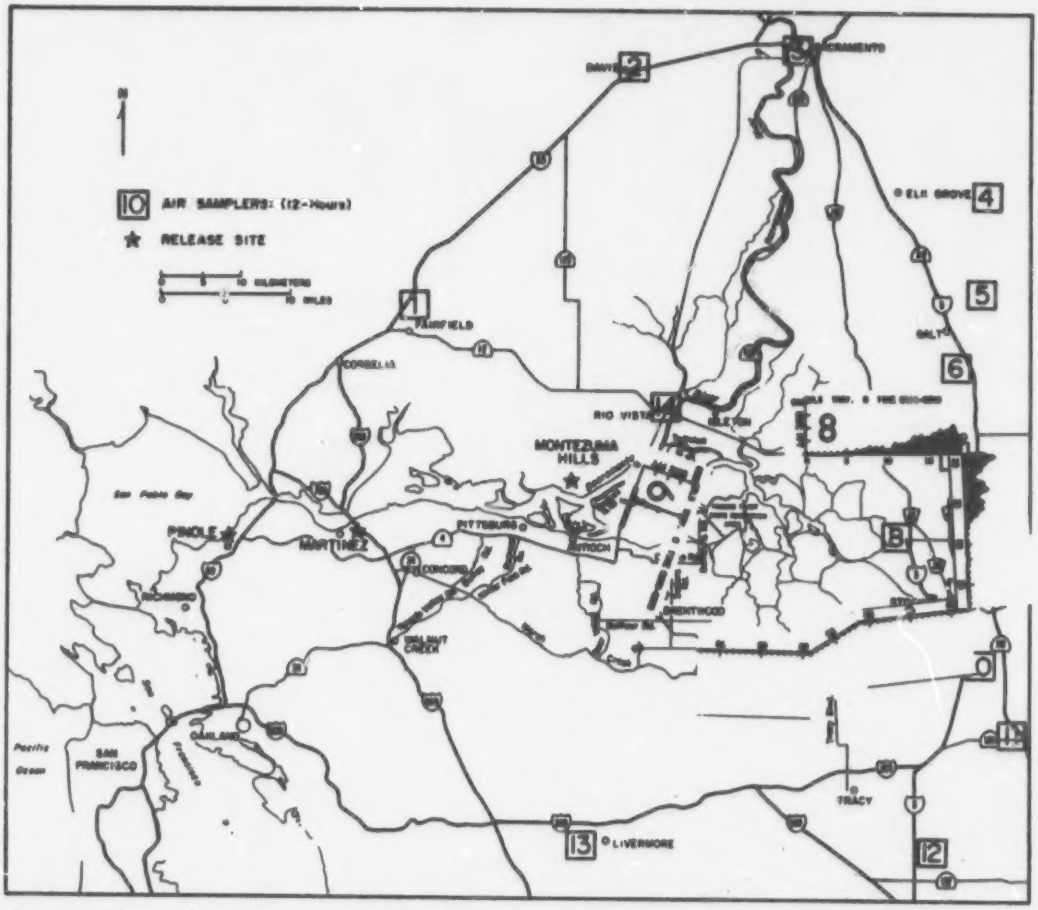
N
10 AIR SAMPLERS: (12-Hours)
RELEASE SITE
0 5 10 KILOMETERS
0 5 10 MILES
DAVIS
2
SACRAMENTO
ELK GROVE
4
5
GALT
6
1
FAIRFIELD
CORDELIA
RIO VISTA
ISLETON
8
MONTEZUMA HILLS
9
San Pablo Bay
PINOLE
MARTINEZ
PITTSBURG
ANTIOCH
CONCORD
BRENTWOOD
WALNUT CREEK
RICHMOND
Pacific Ocean
SAN FRANCISCO
OAKLAND
TRACY
13
LIVERMORE
12
10
11

Figure 24. Overview of automobile traverse SF_6 data.

TEST 3

9/5/76

Auto Traverses:

6 0259 - 0306 PDT, SF_6(max) = 8660 ppt

8 0414 - 0545 PDT, SF_6(max) = 370 ppt

SF_6 released from the Montezuma Hills from 0000-0500 PDT.

around 0200 PDT, but shifted north to Lodi by 0400 PDT. These data yield a transport speed of 7 m/sec (25 km/hr). Maximum levels measured in Stockton and near Lodi were 537 ppt and 608 ppt, respectively. During the daytime in Test 1, the plume widths along Highway 99 were 40 km; at night during Test 3, the plume widths along the same route were only 20 km.

The maximum SF_6 concentration observed in the hourly averaged air samples was 918 ppt, which occurred from 0600 to 0700 PDT at Station 8, 6 km north of Stockton. The data in the overview map in Figure 25 suggest that the wind shifted twice during the night. The plume impacted in the Stockton area from 0200 to 0400; it moved north towards Lodi from 0400 to 0600 PDT, and then shifted back towards Stockton and further south for the remaining hours. This shift in winds is more clearly seen in Figures 26-28 where the hourly crosswind tracer profiles are shown. Concentrations as high as 22 ppt were observed in Manteca as late as 1200 PDT.

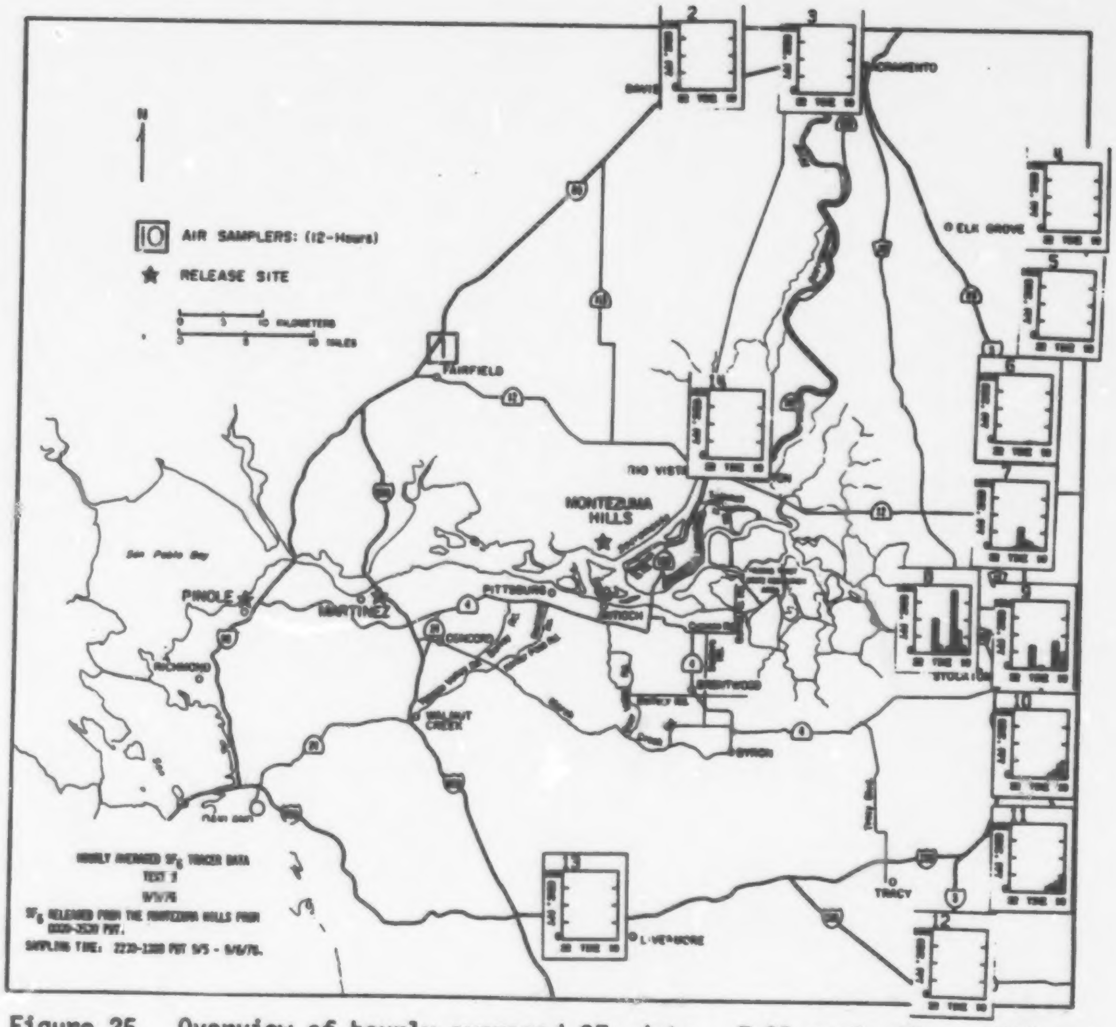
N
10 AIR SAMPLERS: (12-Hours)
RELEASE SITE
0 5 10 KILOMETERS
0 5 10 MILES
1
2
3
4
5
6
7
8
9
10
11
12
13
14
DAVIS
SACRAMENTO
ELK GROVE
FAIRFIELD
RIO VISTA
MONTEZUMA HILLS
San Pablo Bay
PINOLE
MARTINEZ
PITTSBURG
ANTIOCH
CONCORD
RICHMOND
WALNUT CREEK
BRENTWOOD
BYRON
STOCKTON
TRACY
LIVERMORE
HOURLY AVERAGED SF_6 TRACER DATA
TEST 3
SAMPLING TIME: 2220-1320 PST 9/5 - 9/6/78.
CONC. PPT
TIME

Figure 25. Overview of hourly averaged SF_6 data. Full scale SF_6 = 1000 ppt.

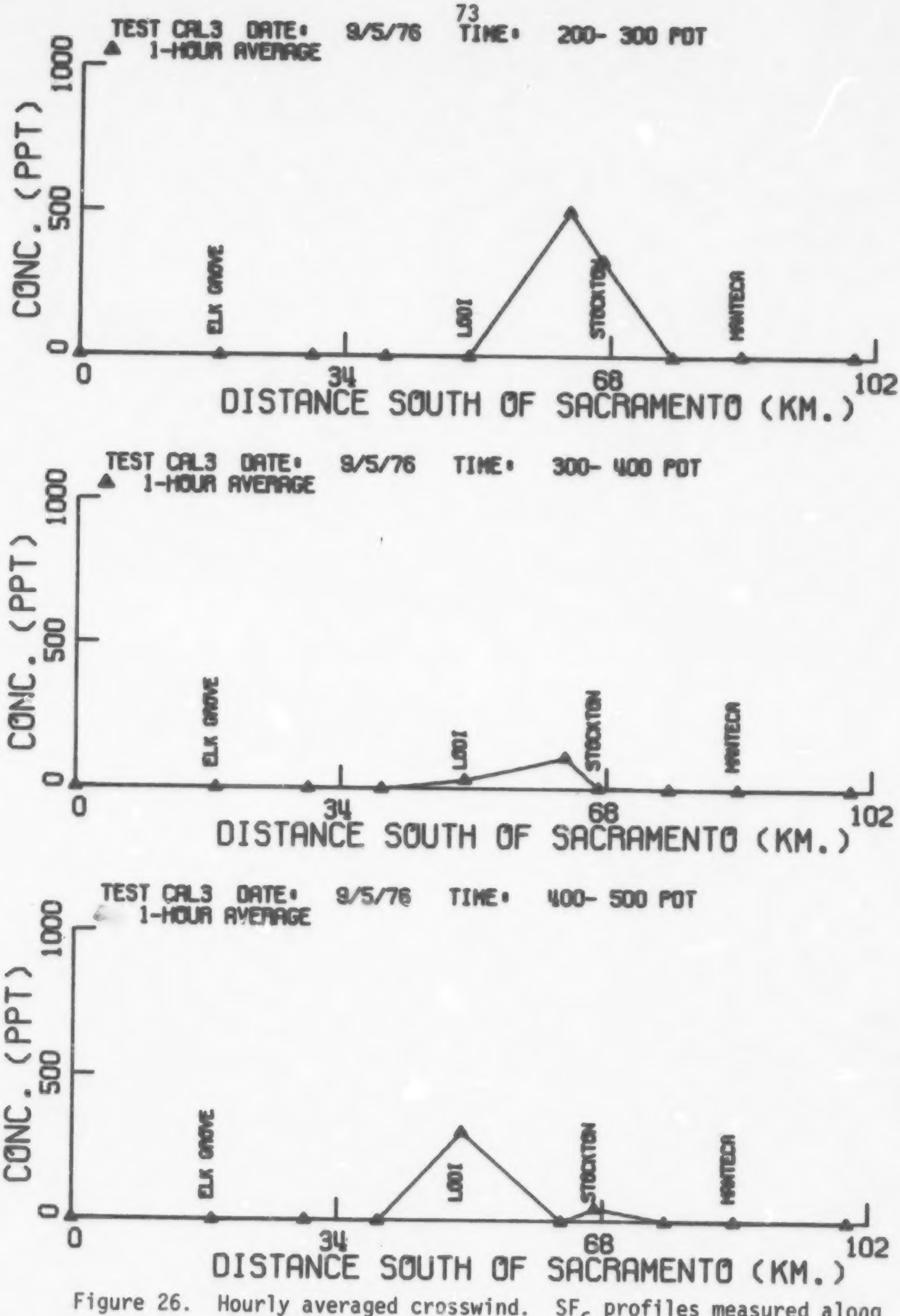

Figure 26. Hourly averaged crosswind. SF_6 profiles measured along Highway 99.

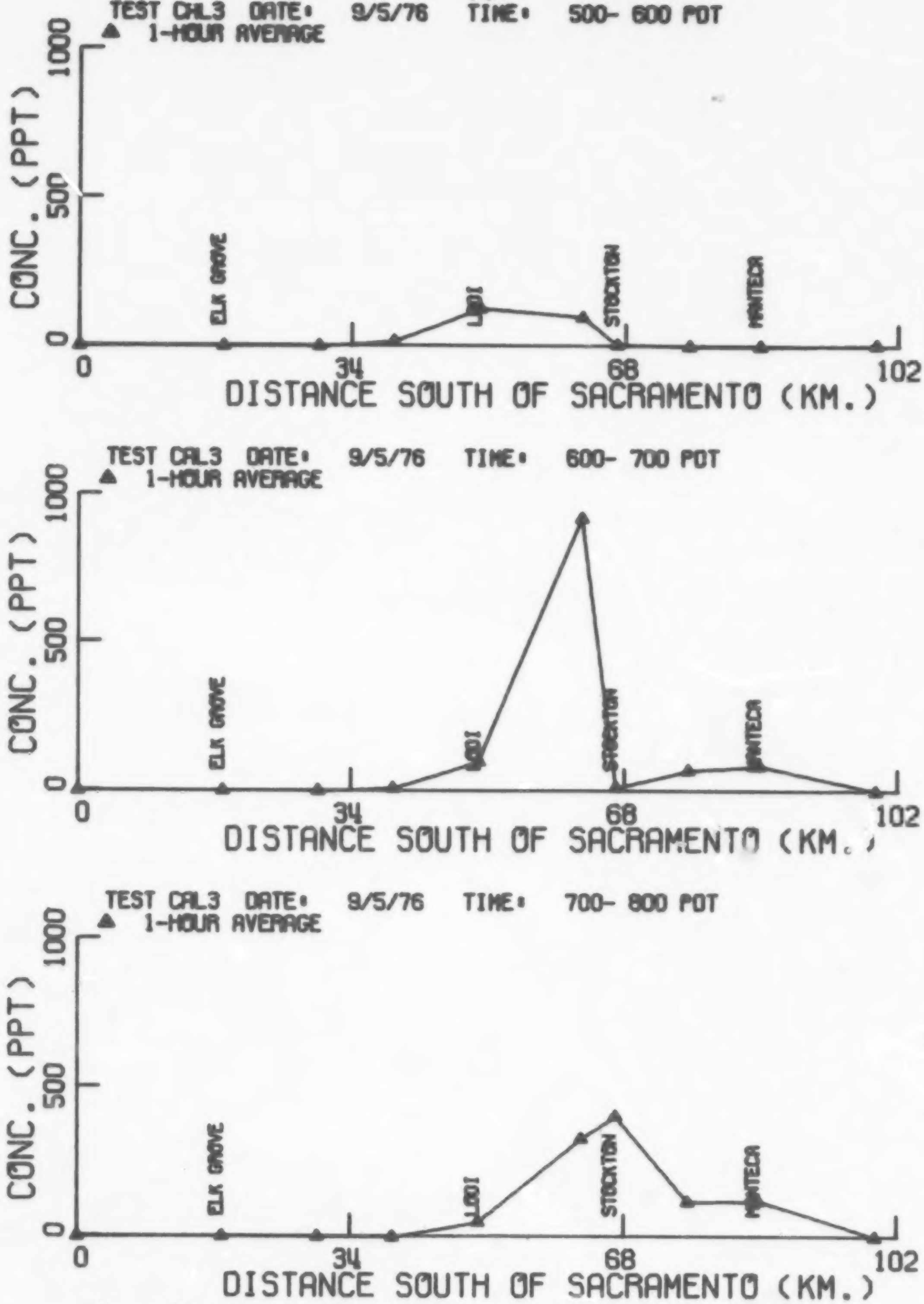

TEST CAL3 DATE: 9/5/76 TIME: 500- 600 PDT

TEST CAL3 DATE: 9/5/76 TIME: 600- 700 PDT

TEST CAL3 DATE: 9/5/76 TIME: 700- 800 PDT

Figure 27. Hourly averaged crosswind SF_6 profiles measured along Highway 99.

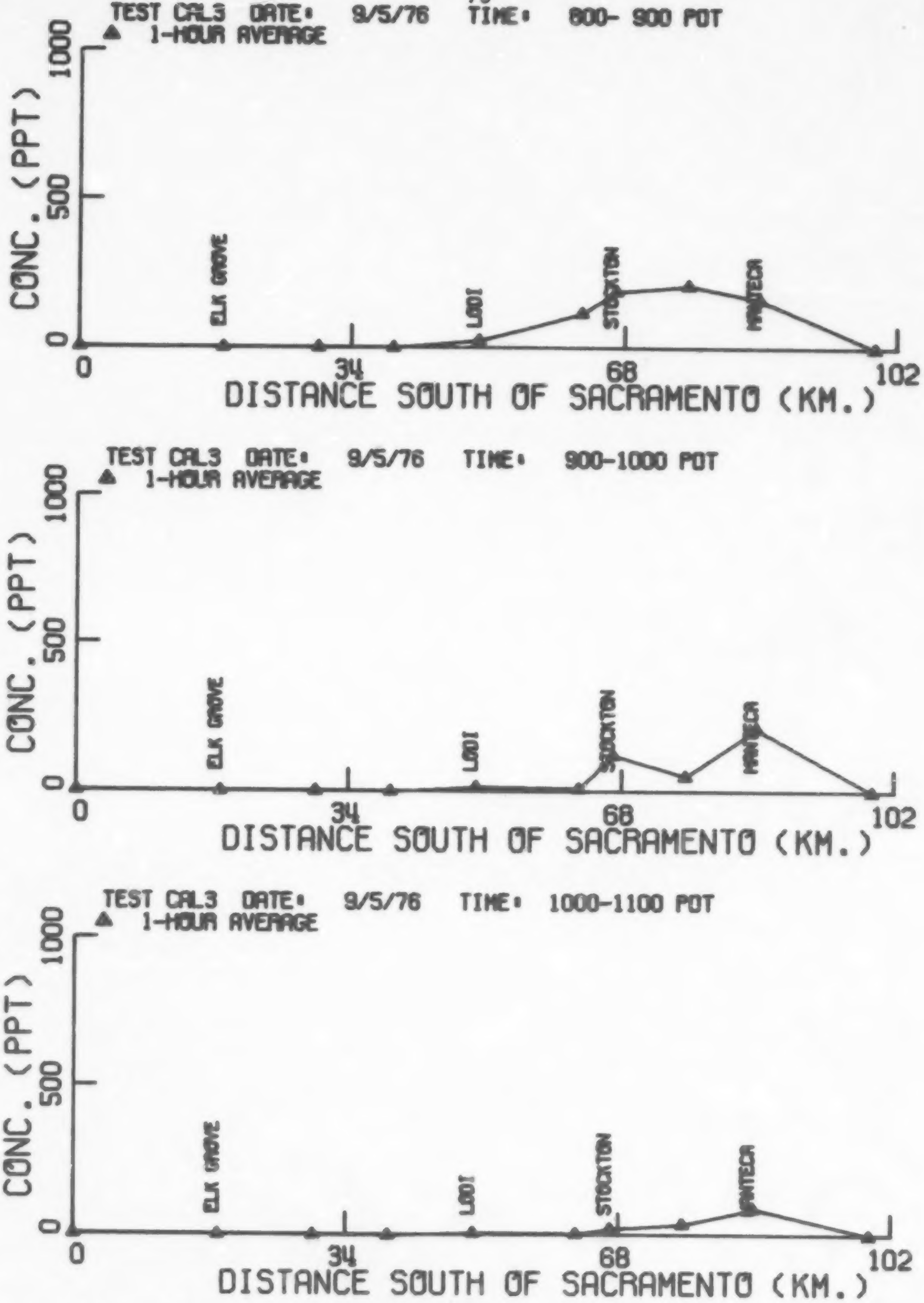

Figure 28. Hourly averaged crosswind SF_6 profiles measured along Highway 99.

4.24 Tracer Test 4 (9/6/76)

The purpose of Test 4 was to determine the characteristics of the transport and dispersion of pollutants emitted from the Montezuma Hills under the Sea Breeze Tail meteorological condition. SF_6 was released at a constant rate of 10.8 g/sec (1.02 tons/day) from 1800 to 2300 PDT.

The average wind vector at the Dow site during the release was 280° at 7.1 m/sec; the overall area average was 290° at 3.3 m/sec. The average value of σ_θ at the Dow site during the test was 7°. The cloud cover was broken, with Pasquill classes D-F assumed to exist. The average mixing height during the release was 510 meters with a maximum height of 650 meters measured at 1800 PDT. This was somewhat lower than that observed during the nighttime test. The wind field during the night generally consisted of westerly flow past the Montezuma Hills as shown in Figure 29. However, the tracer data indicate that the streamline over the Dow site curved to the south throughout the night. Ozone concentrations in the area during the day of the test were about .08 ppm.

Three automobile traverses were conducted along Highway 160 from 1928 through 2222 PDT, and four traverses were completed along Highway 99 between 2130 and 2400 PDT. The data obtained along Highway 160, shown in Figure 30, indicated that the plume from the Montezuma Hills, although narrow with high concentrations, appeared to behave similarly to those in previous tests. The maximum concentration observed along HIghway 160 was 11,900 ppt in Traverse 5 shown in Figure 31. The traverses crossed Highway 160 5.7 km north of the Highway 160-Highway 4 junction. The data measured along Highway 99 again showed that emissions from the Dow site curved south on a trajectory through Stockton. The maximum

9/6 JB

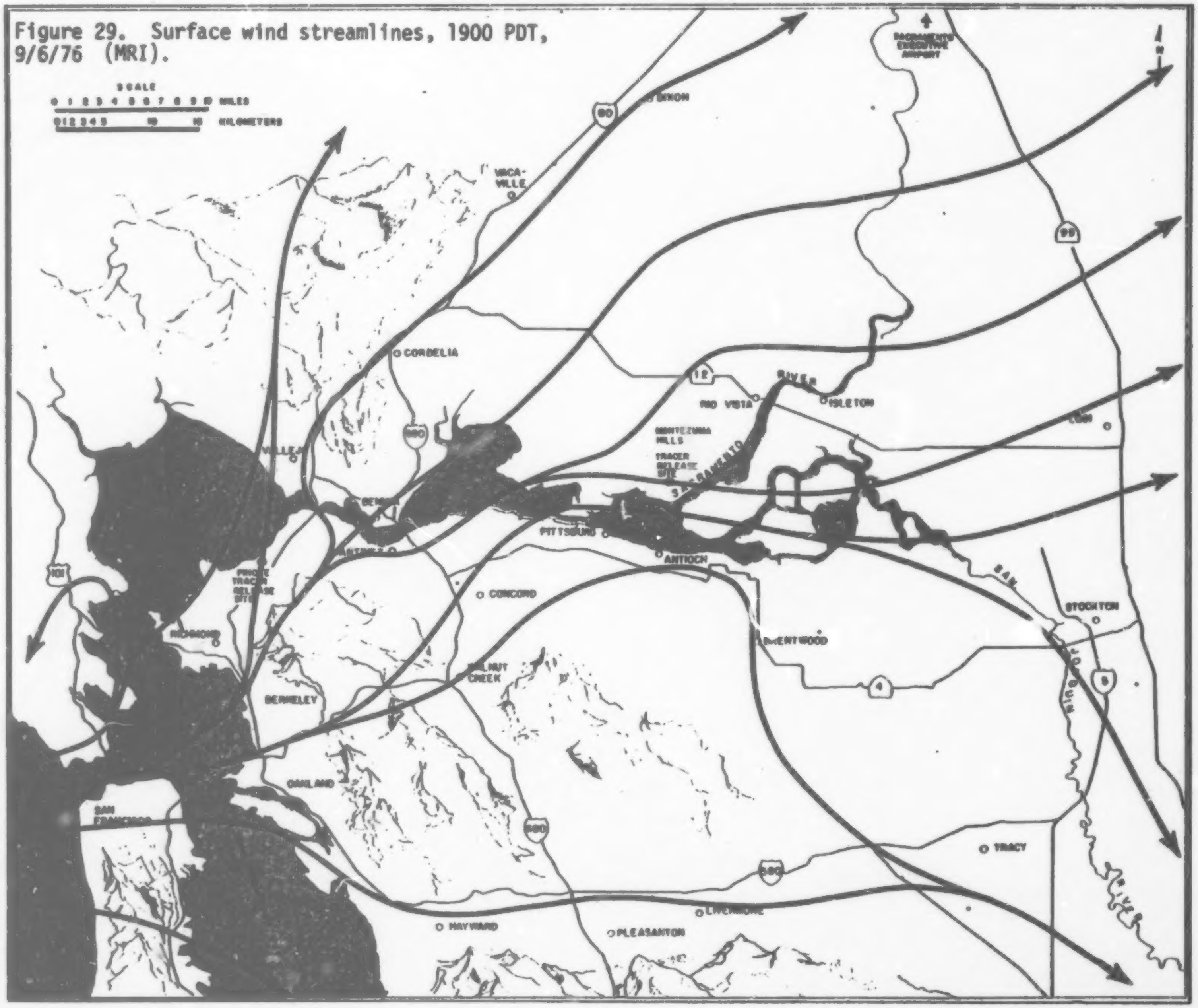

Figure 29. Surface wind streamlines, 1900 PDT, 9/6/76 (MRI).

SCALE
0 1 2 3 4 5 6 7 8 9 10 MILES
0 1 2 3 4 5 10 15 KILOMETERS
N
SACRAMENTO EXECUTIVE AIRPORT
DIXON
VACA-VILLE
CORDELIA
VALLEJO
BENICIA
MARTINEZ
PINOLE TRACER RELEASE SITE
RICHMOND
BERKELEY
OAKLAND
SAN FRANCISCO
HAYWARD
PLEASANTON
LIVERMORE
TRACY
WALNUT CREEK
CONCORD
PITTSBURG
ANTIOCH
BRENTWOOD
RIO VISTA
ISLETON
LODI
STOCKTON
MONTEZUMA HILLS
TRACER RELEASE SITE
SACRAMENTO RIVER
SAN JOAQUIN RIVER
80
99
12
680
101
4
5
580

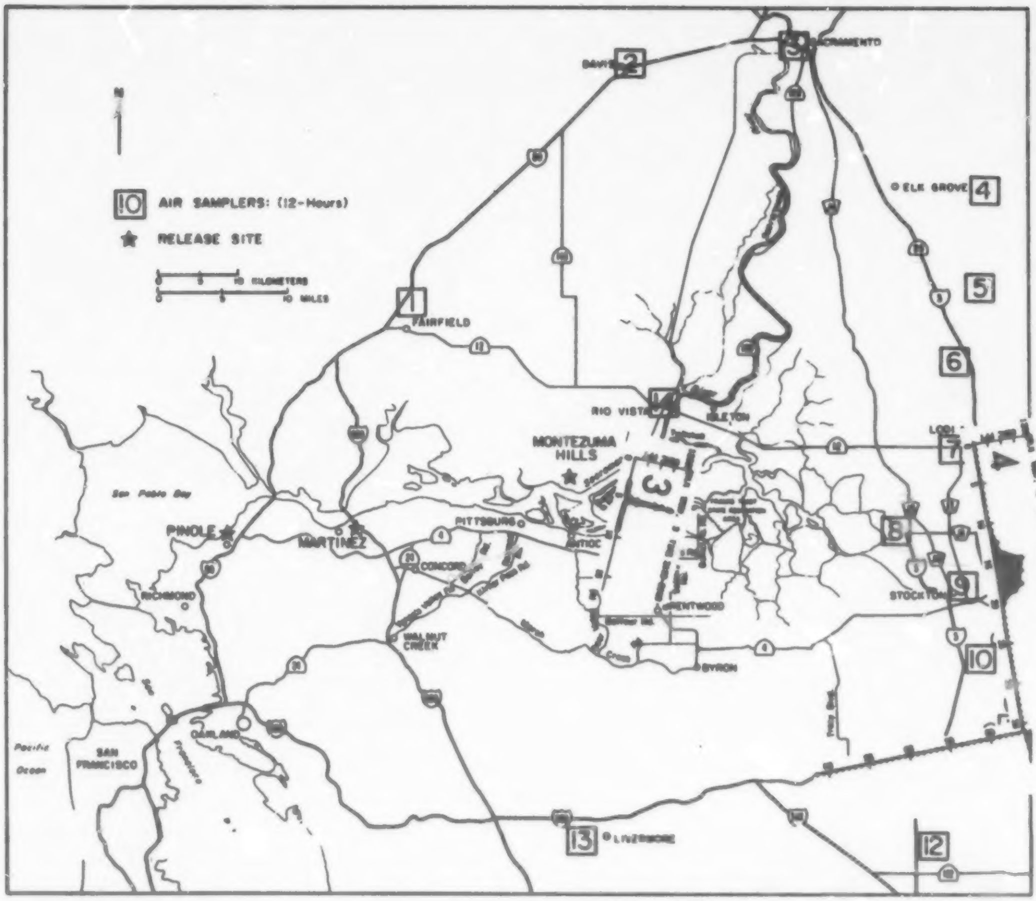
N
10 AIR SAMPLERS: (12-Hours)
RELEASE SITE
0 5 10 KILOMETERS
0 5 10 MILES
DAVIS
2
SACRAMENTO
ELK GROVE
4
5
6
1
FAIRFIELD
RIO VISTA
ISLETON
MONTEZUMA HILLS
3
LODI
7
4
8
9
STOCKTON
10
San Pablo Bay
PINOLE
MARTINEZ
PITTSBURG
ANTIOC
CONCORD
RICHMOND
WALNUT CREEK
BRENTWOOD
BYRON
Pacific Ocean
SAN FRANCISCO
OAKLAND
13
LIVERMORE
12

Figure 30. Overview of automobile traverse tracer data.

TEST 4

9/6/76

Auto Traverses:

3 2132 - 2140 PDT, SF_6(max) = 10,570 ppt

4 2200 - 2246 PDT, SF_6(max) = 628 ppt

SF_6 released from the Montezuma Hills from 1800-2300 PDT.

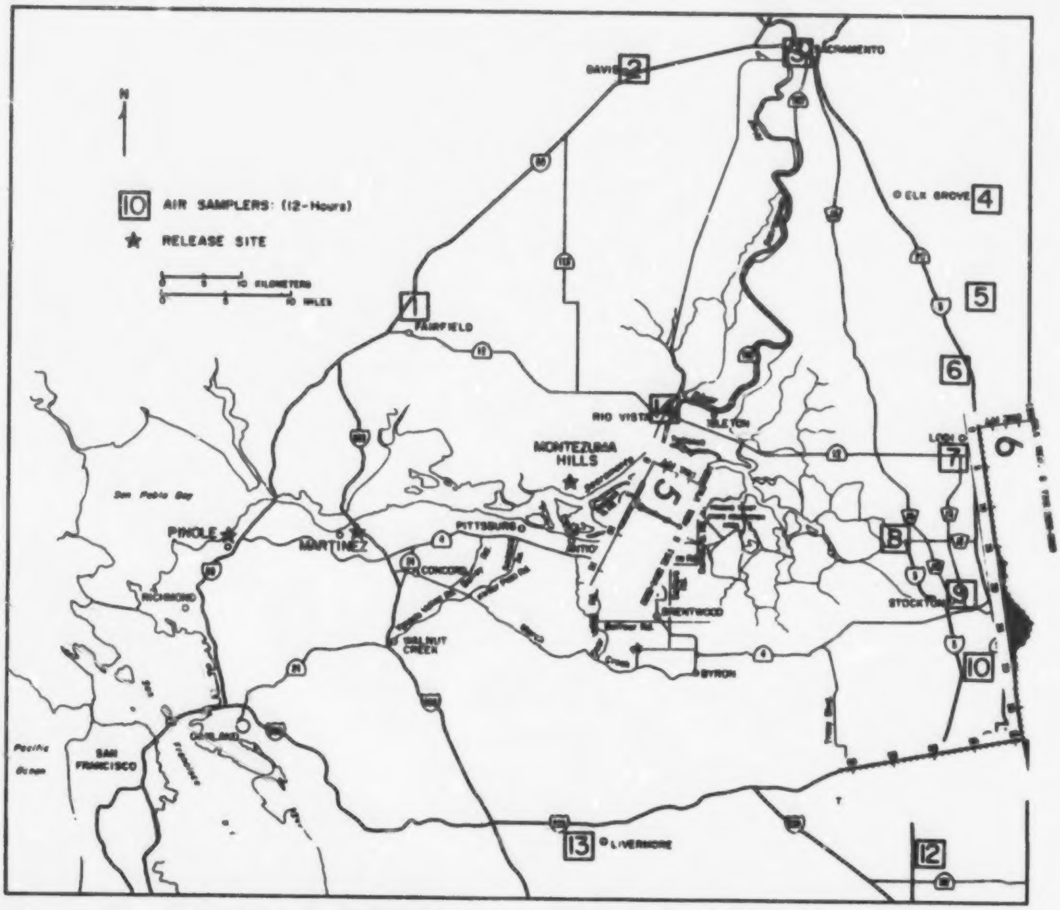
N
10 AIR SAMPLERS: (12-Hours)
RELEASE SITE
0 5 10 KILOMETERS
0 5 10 MILES
1
2
3
4
5
6
7
8
9
10
12
13
14
5
9
DAVIS
SACRAMENTO
ELK GROVE
FAIRFIELD
RIO VISTA
ISLETON
LODI
MONTEZUMA HILLS
San Pablo Bay
PINOLE
MARTINEZ
PITTSBURG
CONCORD
RICHMOND
WALNUT CREEK
BRENTWOOD
BYRON
STOCKTON
OAKLAND
SAN FRANCISCO
Pacific Ocean
LIVERMORE

Figure 31. Overview of automobile traverse tracer data.

TEST 4

9/6/76

Auto Traverses:

5 2214 - 2222 PDT, SF_6(max) = 11,900 ppt

6 2232 - 2320 PDT, SF_6(max) = 553 ppt

SF_6 released from the Montezuma Hills from 1800-2300 PDT.

concentration observed along Highway 99 was 746 ppt. The profiles in Figure 31 suggest that the plume had shifted slightly to the south by 2300 PDT.

The hourly averaged concentration profiles in the overview map in Figure 32 also show that the plume moved south during the latter part of the test. The maximum concentration in the hourly averaged samples was 556 ppt, which was found between 2200 and 2300 PDT in downtown Stockton. The hourly crosswind profiles given in Figure 33 indicate that between 2000 and 2300 PDT, the tracer trajectory was very steady over Stockton. As shown in Figure 34, the winds shifted south to French Camp between 2300 and midnight PDT. The data in Figures 35 and 36 indicate that tracer concentrations on the order of 20 ppt were observed south of Manteca as late as 0700 PDT. The results indicate again that material emitted from the Montezuma Hills follow trajectories into the San Joaquin Valley.

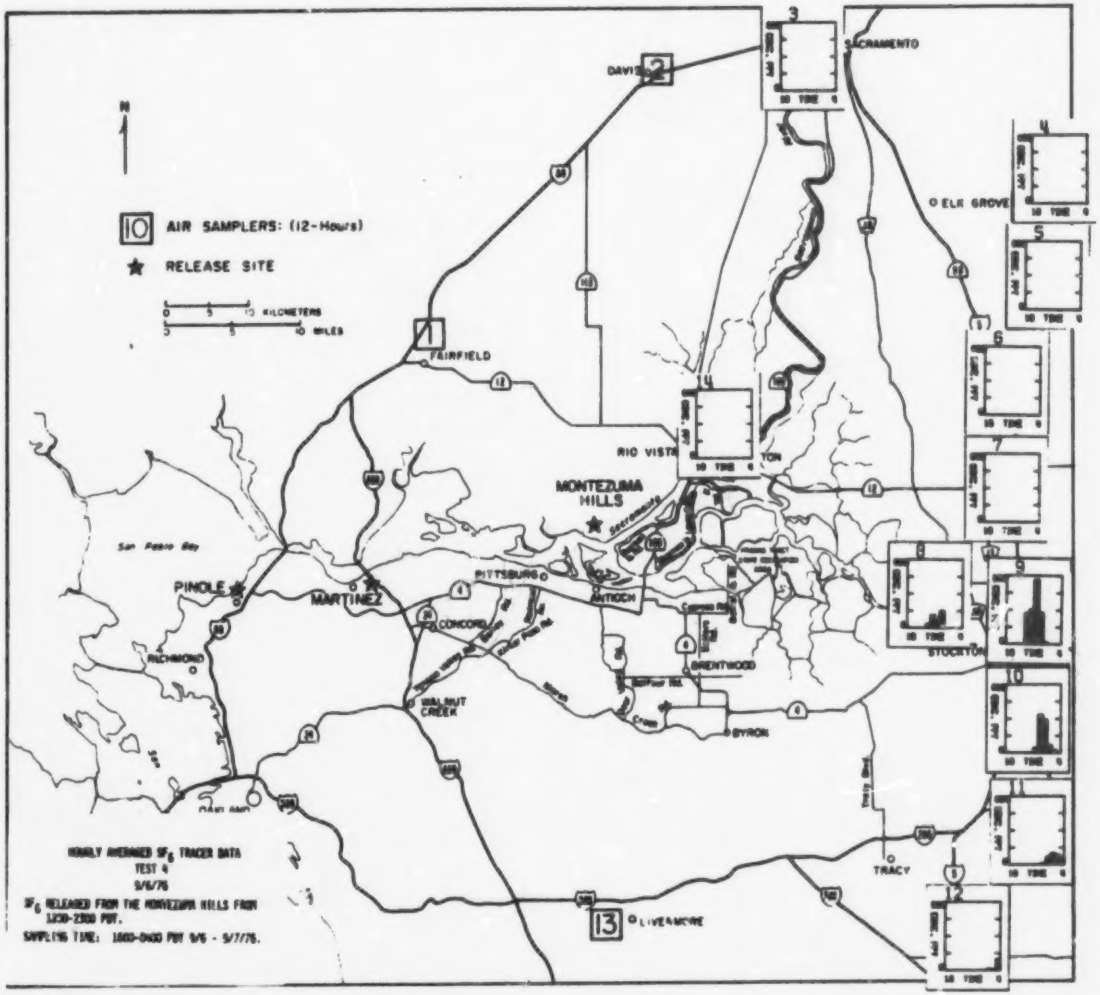
N
10 AIR SAMPLERS: (12-Hours)
RELEASE SITE
0 5 10 KILOMETERS
0 5 10 MILES
DAVIS
SACRAMENTO
ELK GROVE
FAIRFIELD
RIO VISTA
MONTEZUMA HILLS
San Pablo Bay
PINOLE
MARTINEZ
PITTSBURG
ANTIOCH
CONCORD
RICHMOND
WALNUT CREEK
BRENTWOOD
BYRON
STOCKTON
TRACY
LIVERMORE
OAKLAND
1
2
3
4
5
6
7
8
9
10
11
12
13
14
CONC. PPT
10 TIME 0
HOURLY AVERAGED SF6 TRACER DATA
TEST 4
9/6/76
SF6 RELEASED FROM THE MONTEZUMA HILLS FROM 1230-2300 PDT.
SAMPLING TIME: 1800-0400 PDT 9/6 - 9/7/76.

Figure 32. Overview of hourly averaged SF_6 data. Full scale SF_6 = 600 ppt.

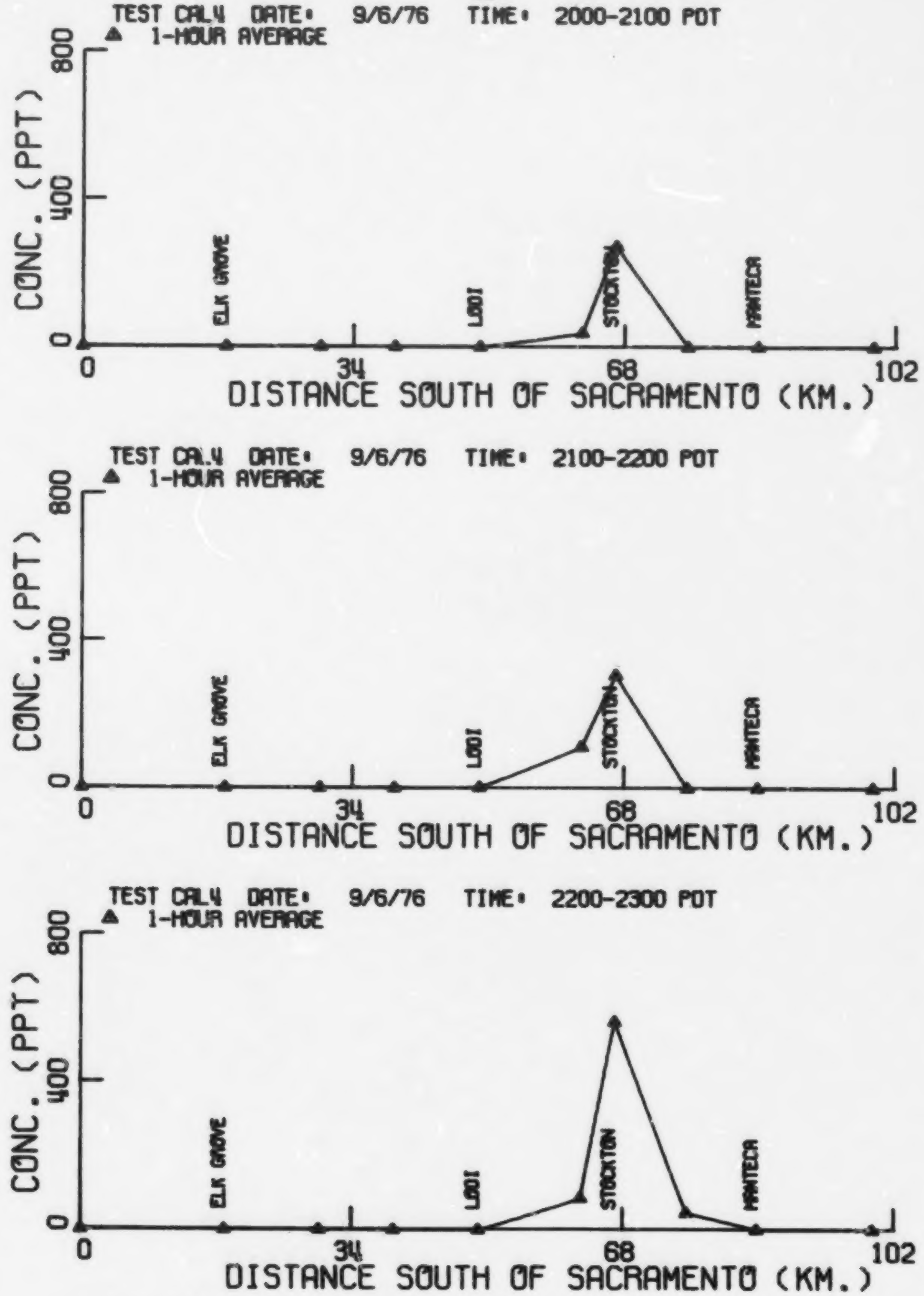

Figure 33. Hourly averaged crosswind SF_6 profiles measured along Highway 99.

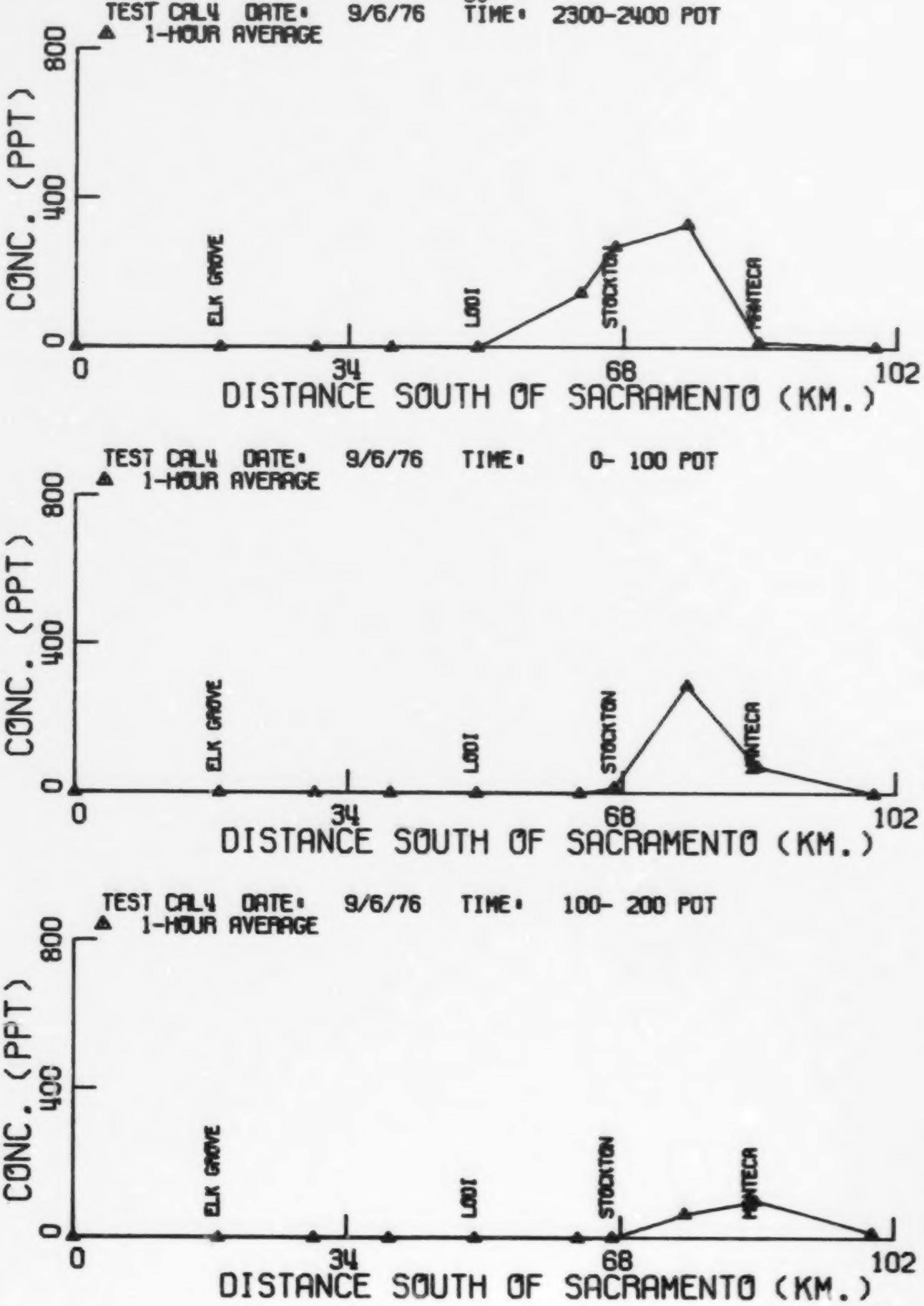

Figure 34. Hourly averaged crosswind SF_6 profiles measured along Highway 99.

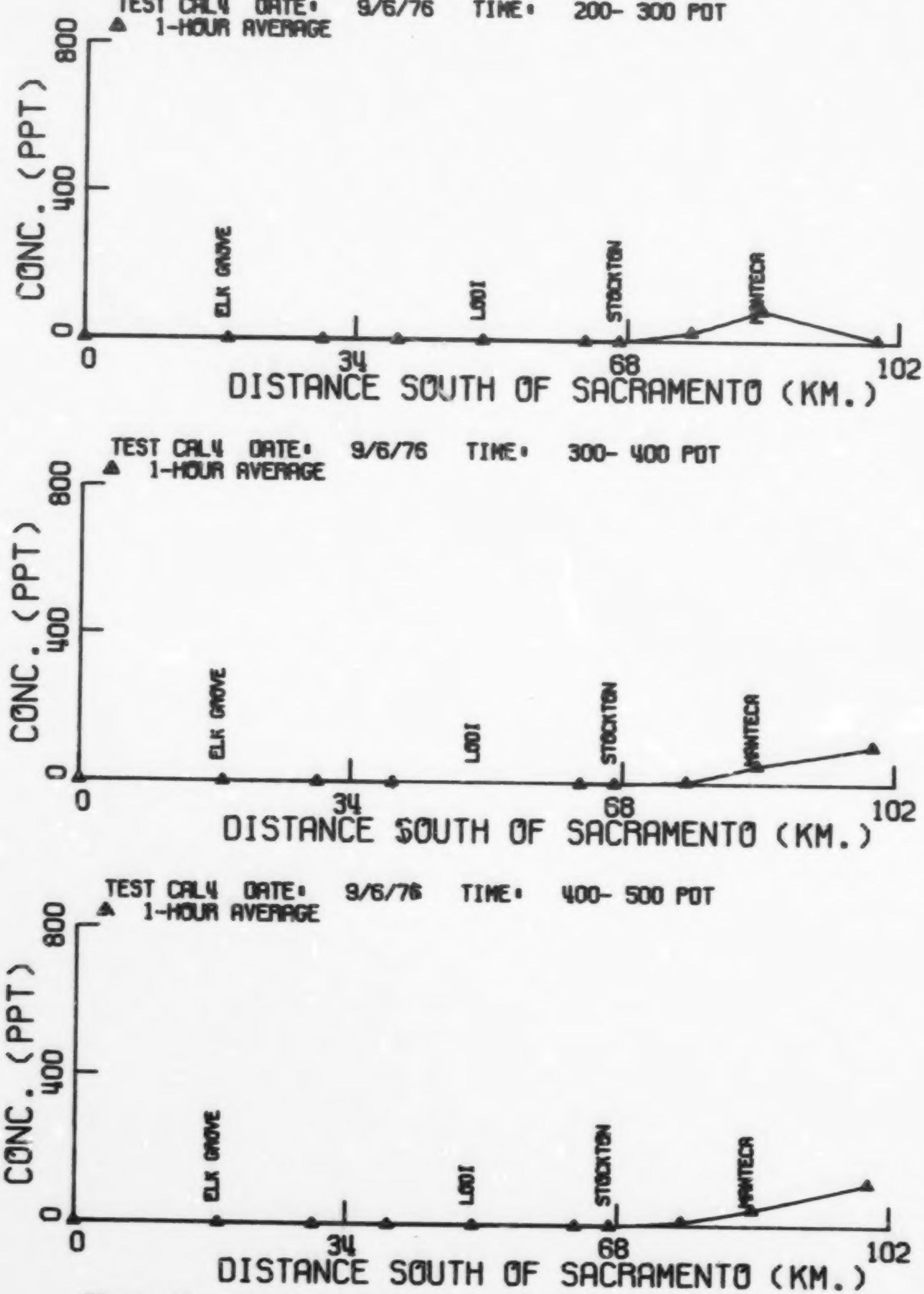

Figure 35. Hourly averaged crosswind SF_6 profiles measured along Highway 99.

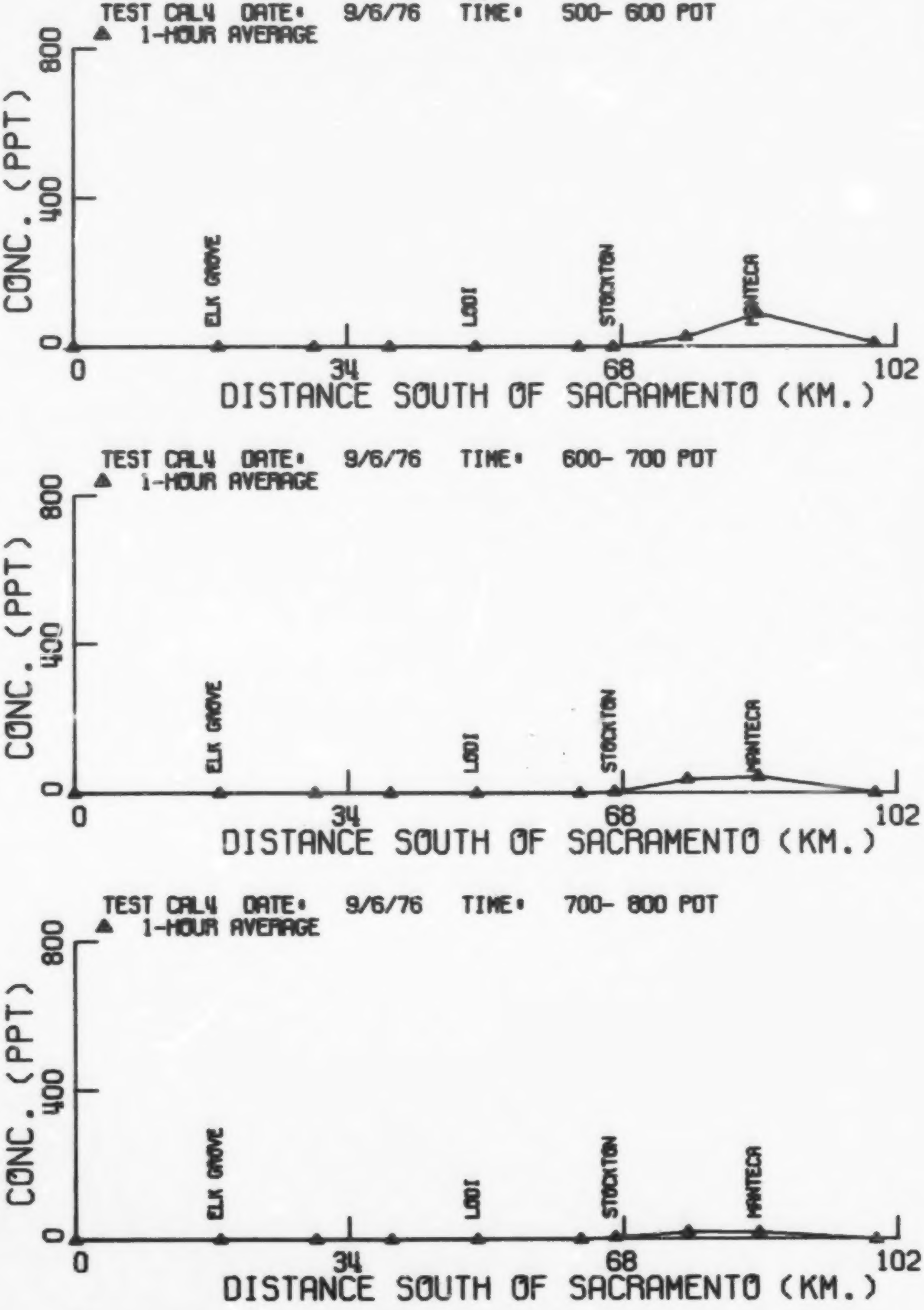

Figure 36. Hourly averaged crosswind SF_6 profiles measured along Highway 99.

4.25 Tracer Test 5 (9/9/76)

The purpose of this test was to study the transport and dispersion of pollutants emitted from the Montezuma Hills as the sea breeze developed. SF_6 was released at a constant rate of 10.7 g/sec (1.01 tons/day) from 1130 to 1330 PDT. The release was stopped after it became apparent that the afternoon sea breeze was not developing.

Because the winds were not steady through the test period, the calculated average wind is not significant. Winds at the Dow site during the test were between 270° and 40° at around 4 m/sec. The average standard deviation of the wind at the Dow site was 21°. There were only scattered clouds resulting in Pasquill class B-C conditions. The mixing height averaged 1910 meters with a maximum of 3000 meters during the afternoon. The wind pattern in Figure 37 for 1300 PDT shows the northerly flow sweeping through the area. This flow is similar to Smalley wind flow type NW-1, which occurred only 3.5% of the time on a yearly basis between 1952 and 1955; in September, this pattern occurred 0.6% of the time. In the Delta region, ozone levels reached 0.15 ppm; maximum levels of 0.25 ppm were observed in San Jose.

Eight automobile traverses were completed between 1255 and 1450 PDT. The tracer data are consistent with the wind streamlines; the plume moved south through Antioch towards Livermore. The maximum level observed along Highway 4, 9 km from the Dow site, was 801 ppt. Typical profiles of the tracer are shown in Figures 38 and 39. The traverses in the latter figure were taken along the same path at different times.

Although a maximum hourly averaged concentration of 47 ppt was observed near Stockton between 1700-1800 PDT, the lack of a plume pattern in the remaining stations suggests that the main plume trajectory crossed Highway 99 between Tracy and Livermore. Only 12 hours of data were collected during the test.

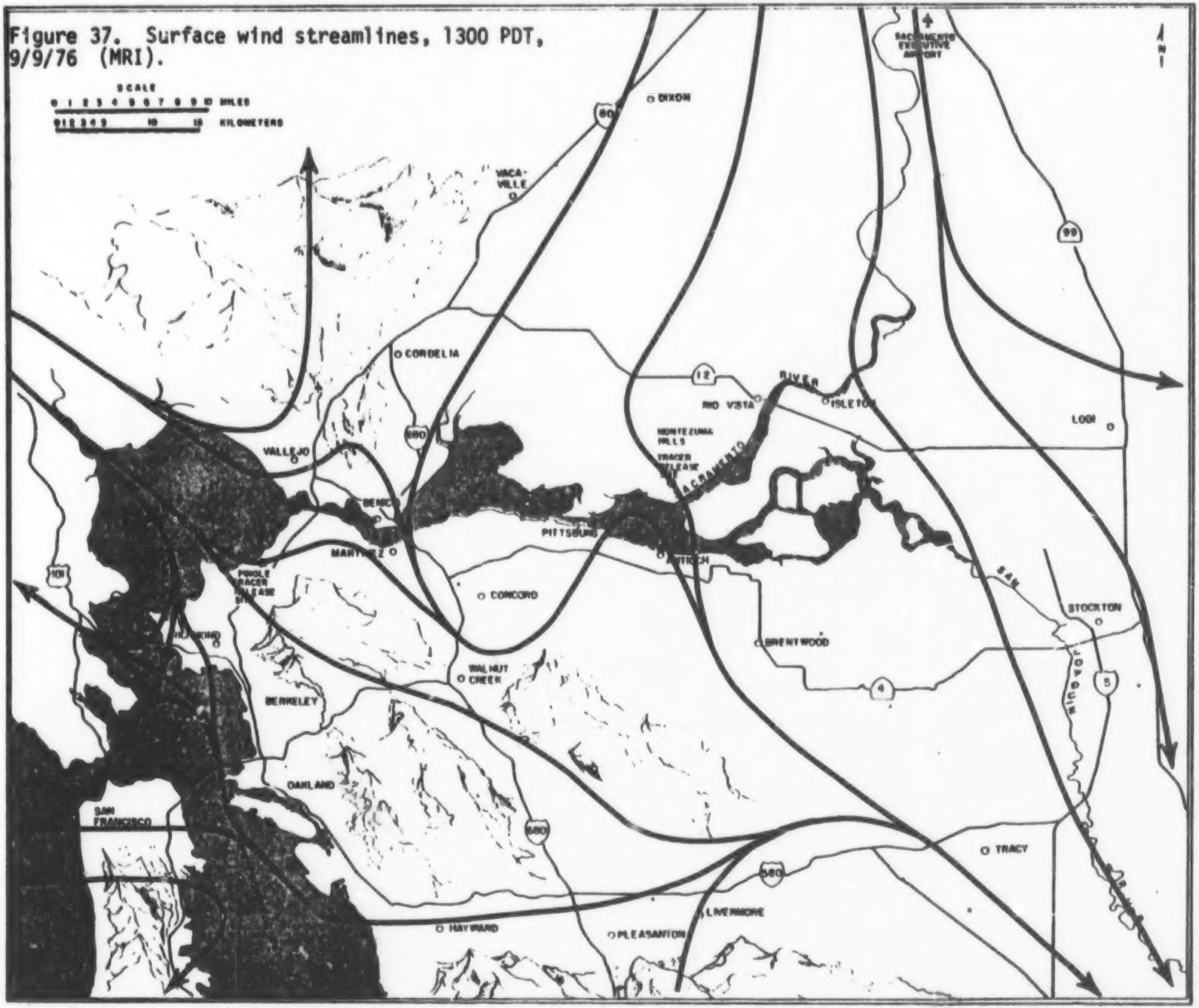
SCALE
0 1 2 3 4 5 6 7 8 9 10 MILES
0 1 2 3 4 5 10 15 KILOMETERS
N
SACRAMENTO EXECUTIVE AIRPORT
DIXON
VACA-VILLE
CORDELIA
RIO VISTA
ISLETON
RIVER
LODI
MONTEZUMA HILLS
TRACER RELEASE
SACRAMENTO
VALLEJO
BENICIA
MARTINEZ
PITTSBURG
ANTIOCH
SAN
JOAQUIN
STOCKTON
CONCORD
BRENTWOOD
PINOLE TRACER RELEASE
WALNUT CREEK
BERKELEY
OAKLAND
SAN FRANCISCO
TRACY
LIVERMORE
PLEASANTON
HAYWARD
80
12
99
680
101
4
5
580

Figure 37. Surface wind streamlines, 1300 PDT, 9/9/76 (MRI).

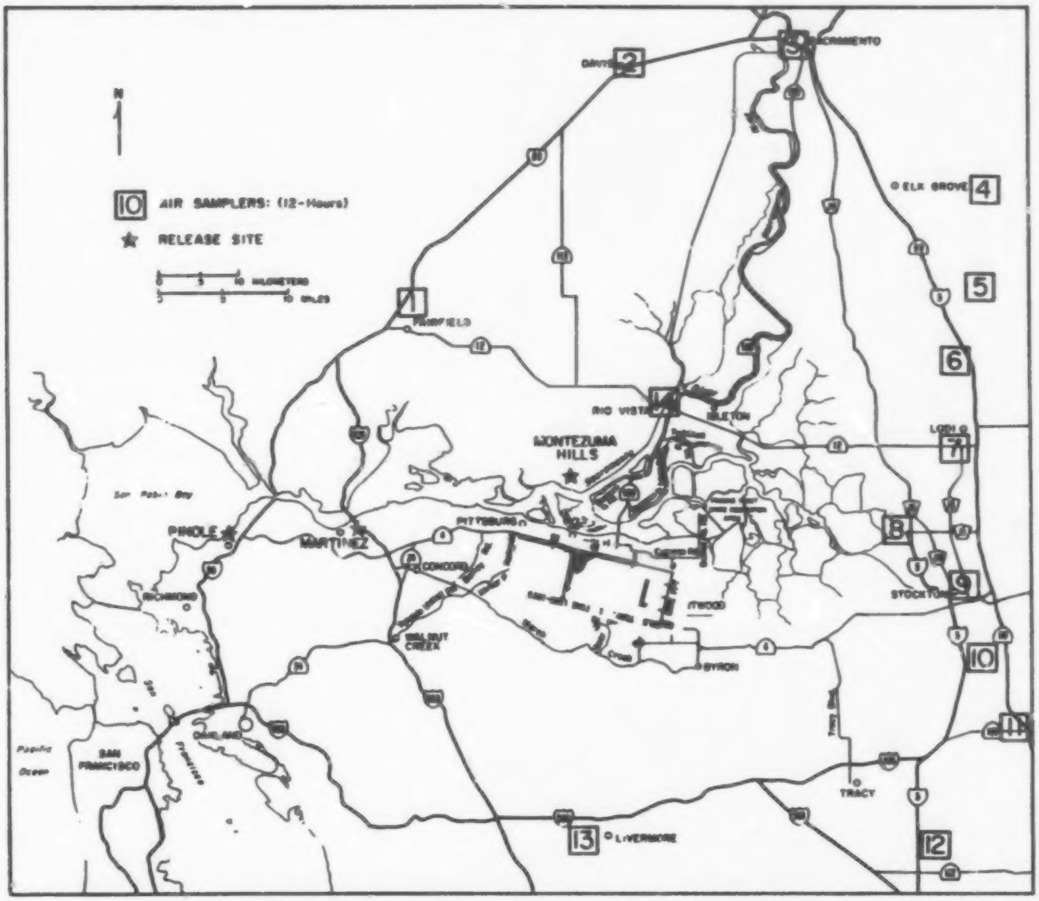
N
10 AIR SAMPLERS: (12-Hours)
★ RELEASE SITE
0 5 10 KILOMETERS
0 5 10 MILES
SACRAMENTO
DAVIS
2
3
ELK GROVE
4
5
6
1
FAIRFIELD
RIO VISTA
14
ISLETON
MONTEZUMA HILLS
LODI
7
8
San Pablo Bay
PINOLE
MARTINEZ
PITTSBURG
CONCORD
STOCKTON
9
RICHMOND
WALNUT CREEK
BYRON
10
11
Pacific Ocean
SAN FRANCISCO
OAKLAND
TRACY
13
LIVERMORE
12

Figure 38. Overview of automobile traverse SF_6 data.

TEST 5

9/9/76

Auto Traverse:

1 1255 - 1315 PDT, $SF_6(\max) = 801$ ppt

SF_6 released from the Montezuma Hills from 1130-1330 PDT.

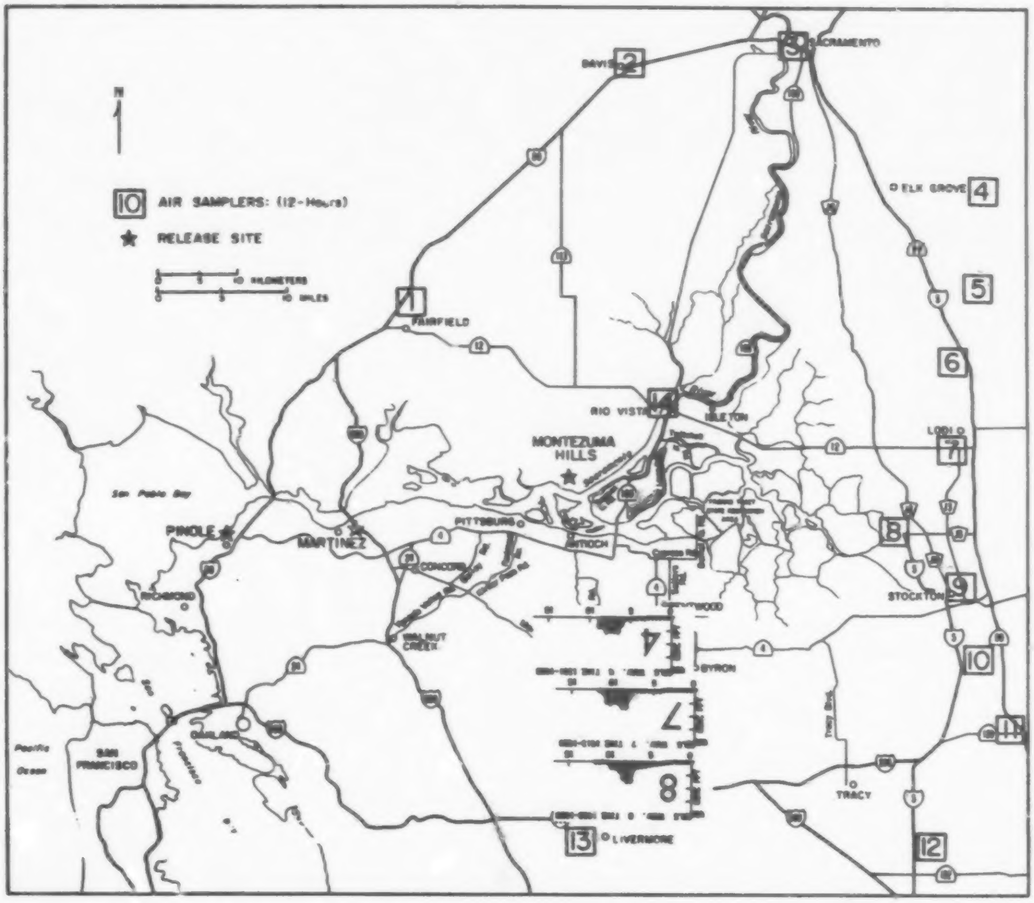
N
10 AIR SAMPLERS: (12-Hours)
RELEASE SITE
KILOMETERS
MILES
SACRAMENTO
DAVIS
ELK GROVE
FAIRFIELD
RIO VISTA
ISLETON
MONTEZUMA HILLS
LODI
San Pablo Bay
PINOLE
MARTINEZ
PITTSBURG
ANTIOCH
CONCORD
RICHMOND
WALNUT CREEK
STOCKTON
BYRON
TRACY
LIVERMORE
Pacific Ocean
SAN FRANCISCO
OAKLAND
1
2
3
4
5
6
7
8
9
10
11
12
13
14
4
7
8

Figure 39. Overview of automobile traverse SF_6 data.

TEST 5

9/9/76

Auto Traverses: (along Balfour Road)

4 1351 - 1405 PDT, SF_6(max) = 138 ppt.

7 1413 - 1426 PDT, SF_6(max) = 141 ppt.

8 1436 - 1450 PDT, SF_6(max) = 183 ppt.

SF_6 released from the Montezuma Hills from 1130-1330 PDT.

4.26 Tracer Test 6 (9/10/76)

The purpose of the sixth tracer test was to examine the transport and dispersion of pollutants emitted from the Montezuma Hills under Pre-Sea Breeze conditions. SF_6 was released at a constant rate of 10.5 g/sec (0.99 tons/day) from 0600 to 1100 PDT.

The average wind vector at the Dow site at 1100 PDT was 280° at 6.3 m/sec, no data were available for earlier times. The average wind for the area was 270° at 1.2 m/sec. The average standard deviation of the wind was 8° at the Dow site at 1100 PDT. The sky was overcast, and Pasquill class D conditions existed. The mixing layer extended to 1250 meters on an average, with a maximum of 3000 meters occurring during the afternoon. The streamline map at 1000 PDT in Figure 40 suggests that westerly flow had almost reached Stockton by midmorning. Maximum ozone levels of 0.08 ppm were observed at the Dow site during the day.

Nine automobile traverses conducted from 0800 to 1230 PDT indicated the plume crossed Highway 160 7.2 km north of the Highway 160-Highway 4 junction and reached I 580 in the Tracy area. Although maximum levels observed along Highway 160 reached 9526 ppt, levels along Highway 99 and I 580 were no greater than 20 ppt. It is possible that the traverses far downwind did not cross the centerline of the plume. Typical traverses are shown in Figures 41 and 42.

Thirteen airborne traverses were completed from 0934 to 1339 PDT. Data obtained during Traverse 5 in Figure 43 indicated the plume moved directly east and mixed to at least 183 meters after traveling 18 km downwind. The maximum concentration at that height was 1387 ppt. As

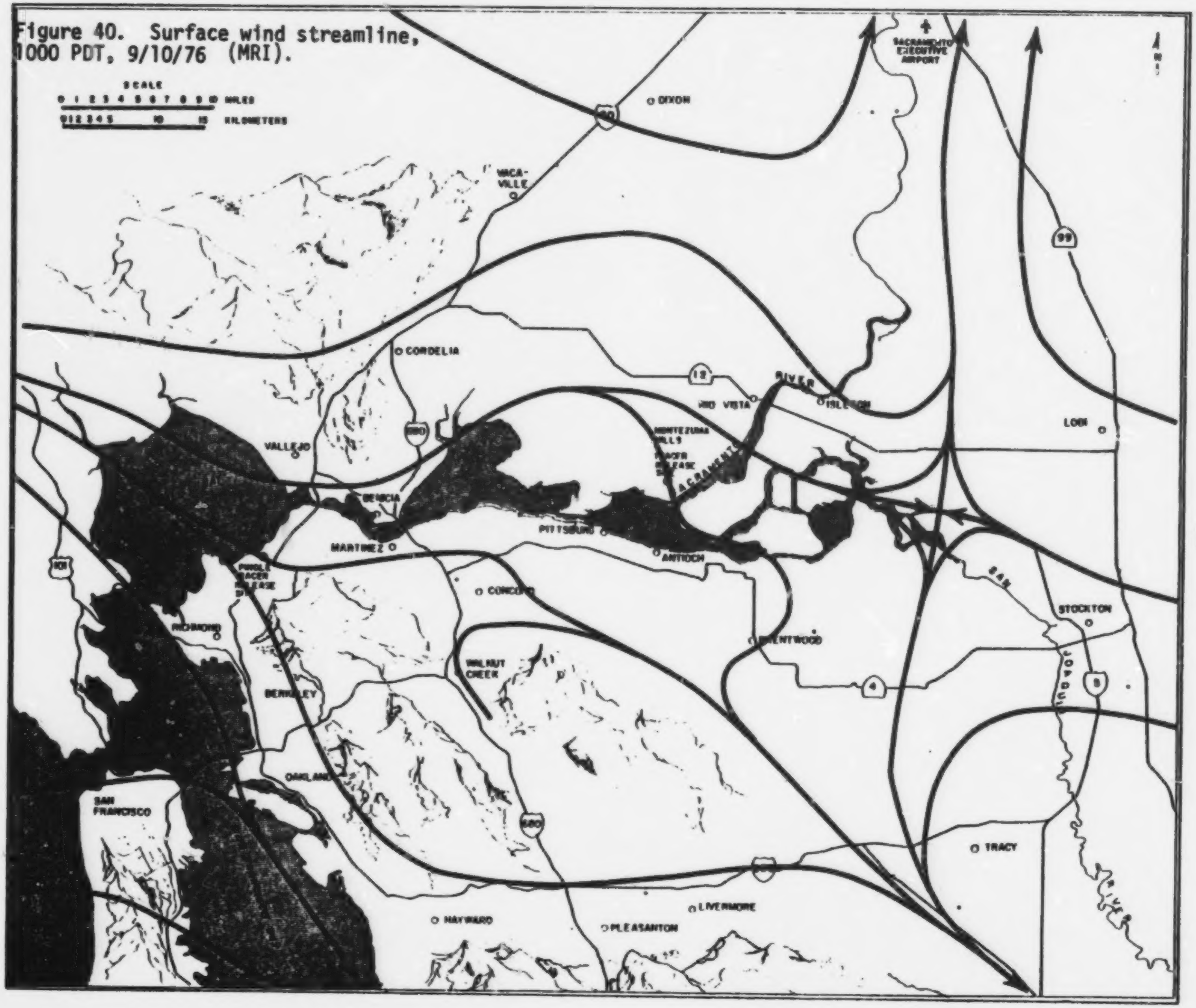

Figure 40. Surface wind streamline, 1000 PDT, 9/10/76 (MRI).

SCALE
0 1 2 3 4 5 6 7 8 9 10 MILES
0 1 2 3 4 5 10 15 KILOMETERS
N
SACRAMENTO EXECUTIVE AIRPORT
DIXON
VACA-VILLE
CORDELIA
VALLEJO
BENICIA
MARTINEZ
RIO VISTA
ISLETON
RIVER
SACRAMENTO
MONTEZUMA HILLS
PITTSBURG
ANTIOCH
CONCORD
WALNUT CREEK
BRENTWOOD
PINOLE TRACER RELEASE SITE
RICHMOND
BERKELEY
OAKLAND
SAN FRANCISCO
HAYWARD
PLEASANTON
LIVERMORE
TRACY
STOCKTON
LODI
SAN JOAQUIN RIVER
80
12
680
101
99
4
5

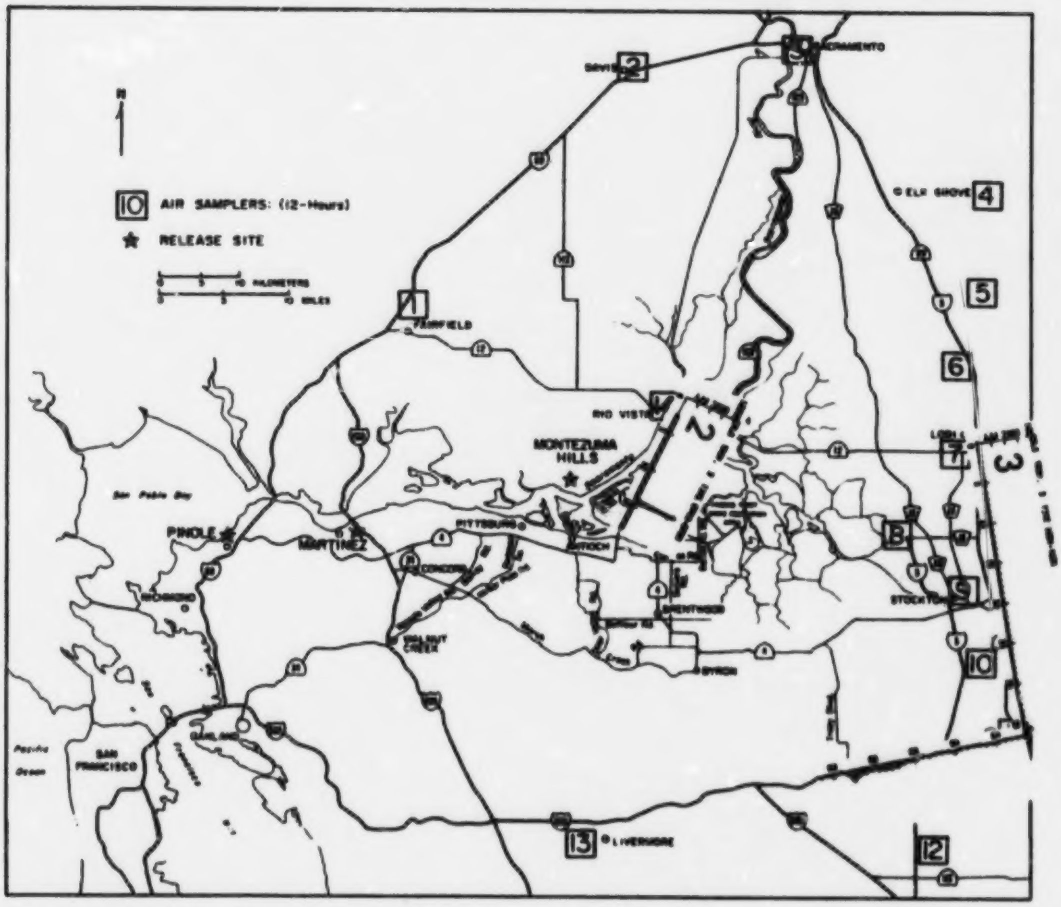
N
10 AIR SAMPLERS: (12-Hours)
RELEASE SITE
10 KILOMETERS
10 MILES
DAVIS 2
SACRAMENTO
ELK GROVE 4
5
6
1
FAIRFIELD
RIO VISTA
2
MONTEZUMA HILLS
LODI
7
3
San Pablo Bay
PINOLE
MARTINEZ
PITTSBURG
ANTIOCH
CONCORD
RICHMOND
WALNUT CREEK
BRENTWOOD
BYRON
8
STOCKTON
9
10
Pacific Ocean
SAN FRANCISCO
OAKLAND
13
LIVERMORE
12

Figure 41. Overview of automobile traverse SF_6 data.

TEST 6

9/10/76

Auto Traverses:

2 0740 - 0753 PDT, SF_6(max) = 7981 ppt

3 1001 - 1051 PDT, SF_6(max) = 20 ppt

SF_6 released from the Montezuma Hills from 0600-1100 PDT.

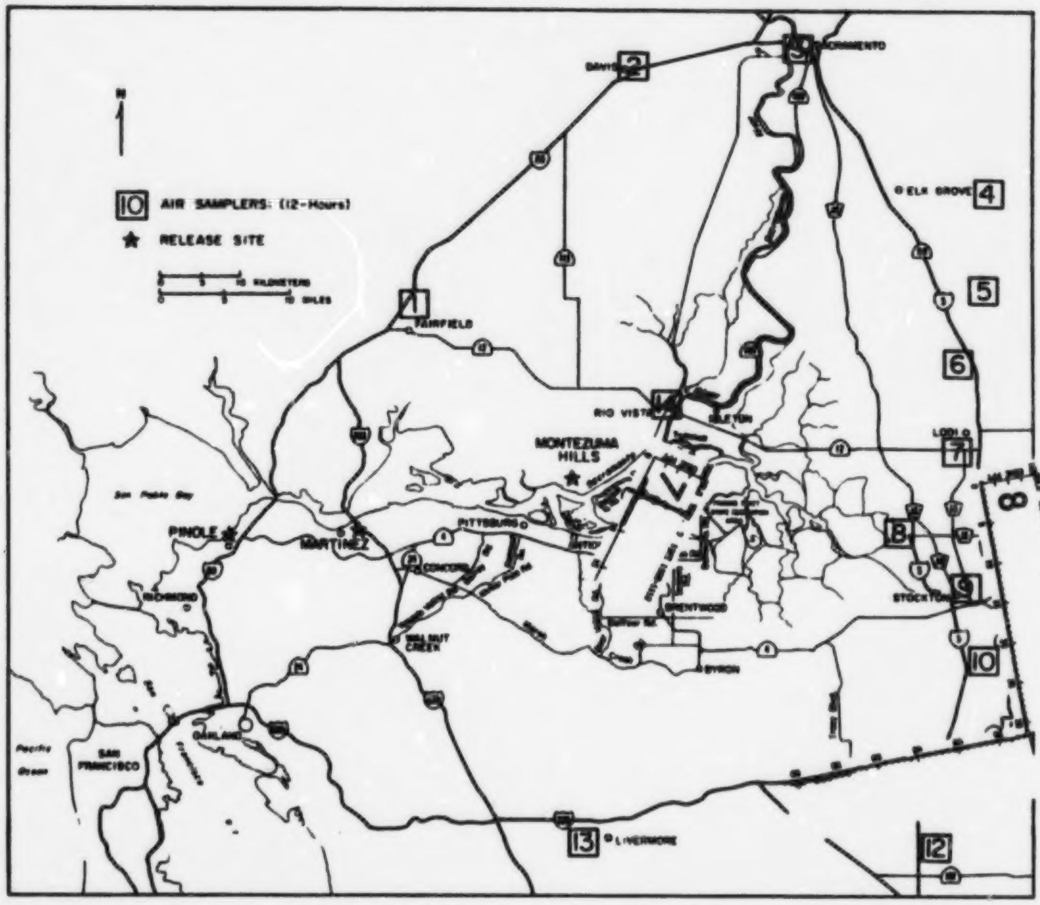
N
10 AIR SAMPLERS: (12-Hours)
RELEASE SITE
0 5 10 KILOMETERS
0 5 10 MILES
DAVIS
2
SACRAMENTO
ELK GROVE
4
5
6
1
FAIRFIELD
RIO VISTA
ISLETON
MONTEZUMA
HILLS
LODI
7
8
San Pablo Bay
PINOLE
MARTINEZ
PITTSBURG
CONCORD
RICHMOND
WALNUT
CREEK
BRENTWOOD
BYRON
STOCKTON
9
10
Pacific
Ocean
SAN
FRANCISCO
OAKLAND
13
LIVERMORE
12

Figure 42. Overview of automobile traverse SF_6 data.

TEST 6

9/10/76

Auto Traverses:

7 1103 - 1112 PDT, SF_6(max) = 7155 ppt

8 1105 - 1203 PDT, SF_6(max) = 12 ppt

SF_6 released from the Montezuma Hills from 0600-1100 PDT.

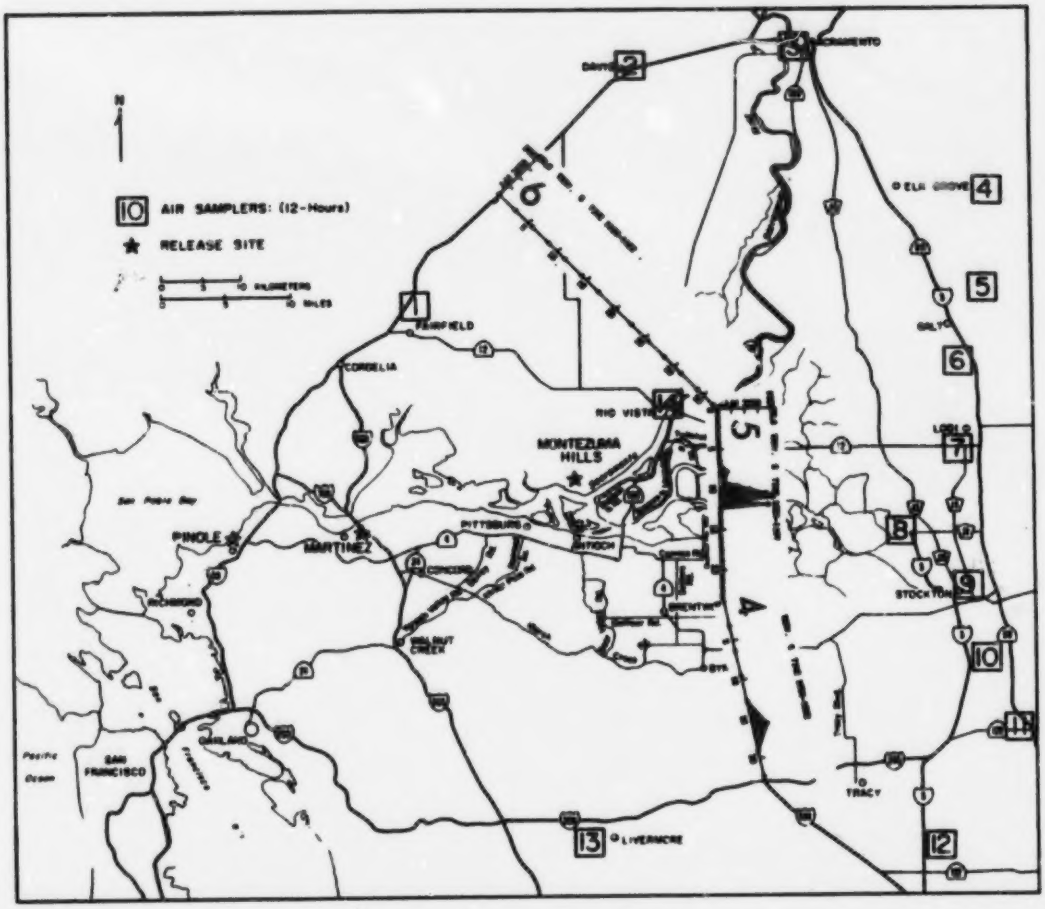
N
10 AIR SAMPLERS: (12-Hours)
RELEASE SITE
KILOMETERS
MILES
DAVIS
2
3
SACRAMENTO
ELK GROVE
4
5
GALT
6
1
FAIRFIELD
CORDELIA
14
RIO VISTA
MONTEZUMA HILLS
LODI
7
San Pablo Bay
PINOLE
MARTINEZ
PITTSBURG
ANTIOCH
CONCORD
8
9
STOCKTON
RICHMOND
BRENTWOOD
WALNUT CREEK
10
BYRON
11
Pacific Ocean
SAN FRANCISCO
OAKLAND
TRACY
13
LIVERMORE
12

Figure 43. Overview of airborne traverse SF_6 data.

TEST 6

9/10/76

Airborne Traverses:

4 1044 - 1052 PDT, 183 m, SF_6(max) = 396 ppt

5 1054 - 1107 PDT, 183 m, SF_6(max) = 1387 ppt

6 1109 - 1122 PDT, 183 m, SF_6(max) = 0 ppt

SF_6 released from the Montezuma Hills from 0600-1100 PDT.

shown in Figure 44, an airborne spiral over Frank's Tract Recreation Area indicated the plume possibly moved aloft with a centerline at 122 meters. At higher elevations, data from only one traverse reached significant levels. In Traverse 7 in Figure 45 at 427 meters, a single grab sample indicated SF_6 was present at 33 ppt. Further downwind above Highway 99, a traverse taken by Caltrans at 183 meters had a maximum concentration of 21 ppt as shown in Figure 46.

The hourly averaged data covered 12 hours from 0400 to 1600 PDT. Maximum levels of 83 and 73 ppt were measured in the 1500-1600 PDT samples at stations 7 and 8 as indicated in Figures 47 and 48. These were the only stations where significant tracer levels were detected.

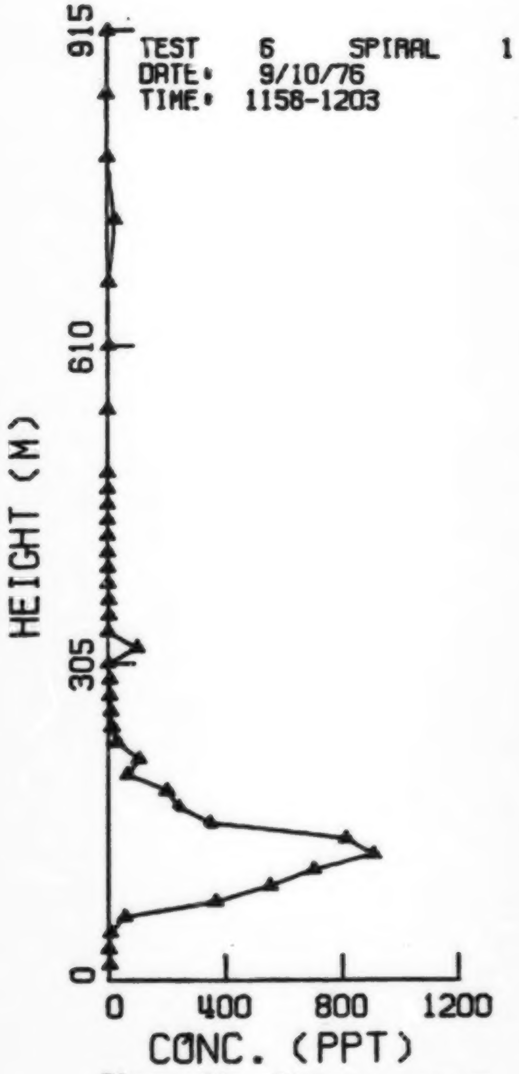

Figure 44. Airborne spiral over Frank's Tract Recreation Area.

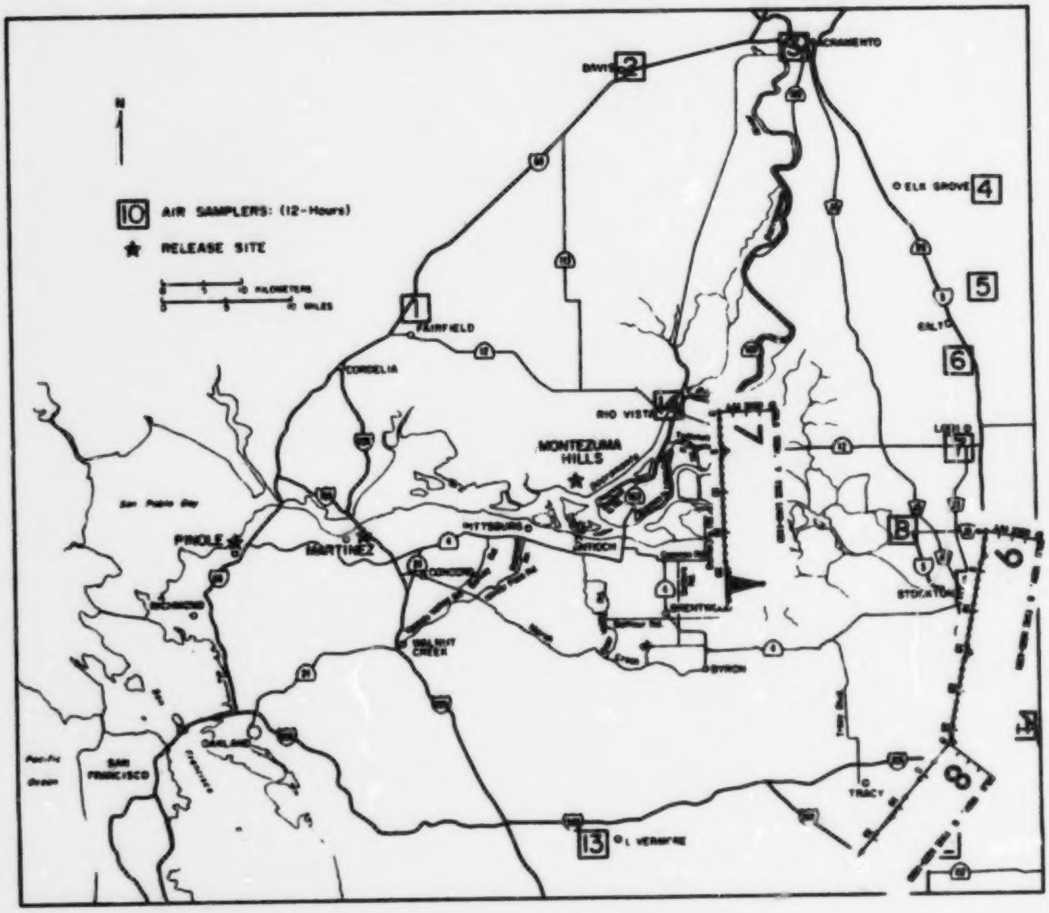
N
10 AIR SAMPLERS: (12-Hours)
RELEASE SITE
0 5 10 KILOMETERS
0 5 10 MILES
SACRAMENTO
DAVIS
2
ELK GROVE
4
5
GALT
6
1
FAIRFIELD
CORDELIA
RIO VISTA
MONTEZUMA HILLS
LODI
7
8
9
San Pablo Bay
PINOLE
MARTINEZ
PITTSBURG
ANTIOCH
CONCORD
BRENTWOOD
RICHMOND
WALNUT CREEK
BYRON
STOCKTON
Pacific Ocean
SAN FRANCISCO
OAKLAND
TRACY
13
L VERMORE

Figure 45. Overview of airborne traverse SF_6 data.

TEST 6

9/10/76

Airborne Traverses:

7 1140 - 1153 PDT, 427 m, SF_6(max) = 33 ppt
8 1229 - 1235 PDT, 305 m, SF_6(max) = 2 ppt
9 1238 - 1251 PDT, 305 m, SF_6(max) = 4 ppt

SF_6 released from the Montezuma Hills from 0600-1100 PDT.

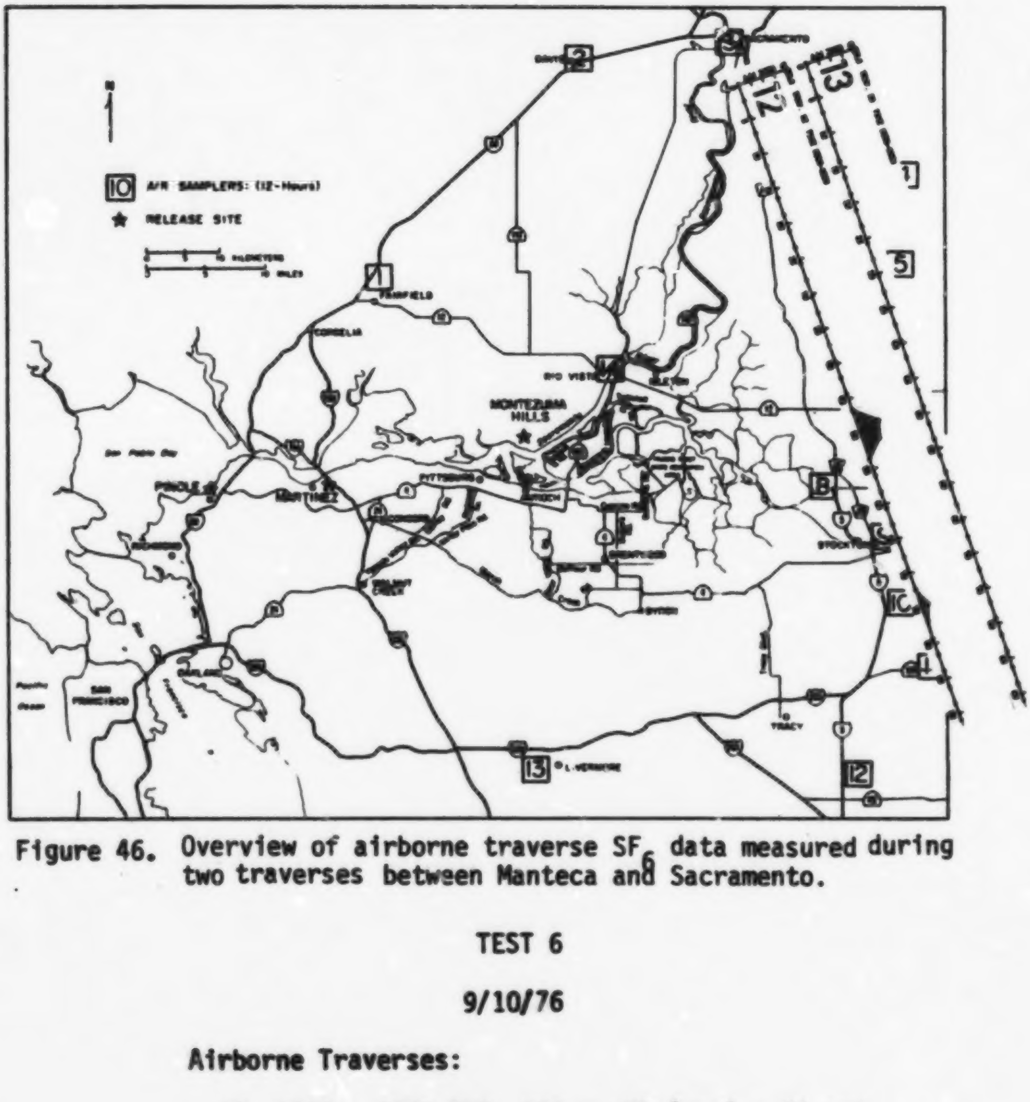
N
10 AIR SAMPLERS: (12-Hours)
RELEASE SITE
KILOMETERS
MILES
SACRAMENTO
2
13
12
1
5
FAIRFIELD
CORDELIA
RIO VISTA
ISLETON
MONTEZUMA HILLS
San Pablo Bay
PINOLE
MARTINEZ
PITTSBURG
RICHMOND
WALNUT CREEK
B
STOCKTON
C
IC
BYRON
TRACY
13
L.VERMORE
12
SAN FRANCISCO
OAKLAND
Pacific Ocean

Figure 46. Overview of airborne traverse SF$_6$ data measured during two traverses between Manteca and Sacramento.

TEST 6

9/10/76

Airborne Traverses:

12 1200 - 1239 PDT, 183 m, SF$_6$(max) = 21 ppt

13 1300 - 1339 PDT, 183 m, SF$_6$(max) = 0 ppt

SF$_6$ released from the Montezuma Hills from 0600-1100 PDT.

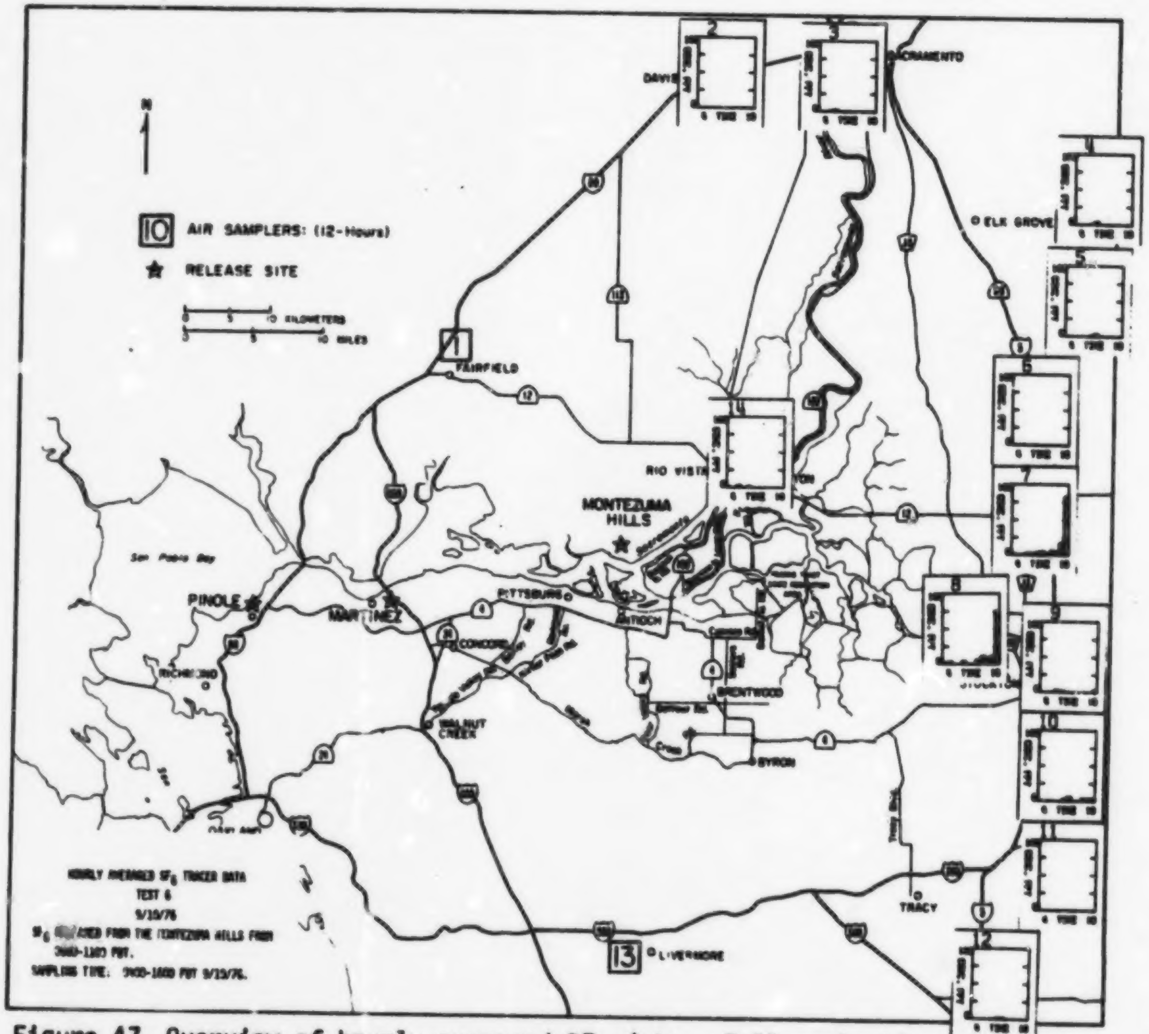
N
10 AIR SAMPLERS: (12-Hours)
RELEASE SITE
0 5 10 KILOMETERS
0 5 10 MILES
1
2
3
4
5
6
7
8
9
10
11
12
13
DAVIS
SACRAMENTO
ELK GROVE
FAIRFIELD
RIO VISTA
MONTEZUMA HILLS
San Pablo Bay
PINOLE
MARTINEZ
PITTSBURG
ANTIOCH
CONCORD
RICHMOND
WALNUT CREEK
BRENTWOOD
BYRON
STOCKTON
TRACY
LIVERMORE
HOURLY AVERAGED SF6 TRACER DATA
TEST 6
9/15/76
SF6 RELEASED FROM THE MONTEZUMA HILLS FROM 0800-1100 PDT.
SAMPLING TIME: 0400-1600 PDT 9/15/76.

Figure 47. Overview of hourly averaged SF_6 data. Full scale SF_6 = 100 ppt.

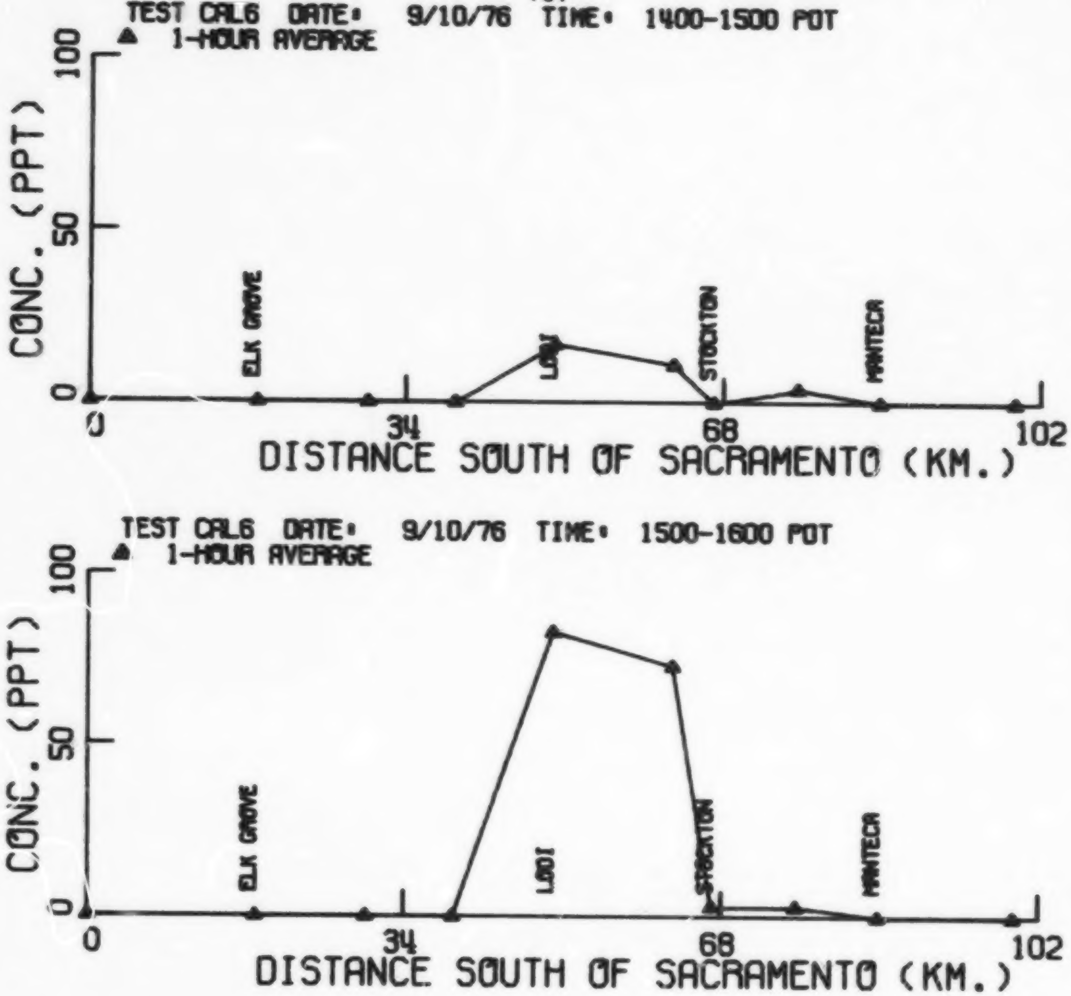

Figure 48. Hourly averaged crosswind SF_6 profiles measured along Highway 99.

4.27 Tracer Test 7 (9/13/76)

The purpose of this test was to tag the air upstream of the Montezuma Hills during the development and onset of the afternoon sea breeze. SF_6 was released at a constant rate of 11.6 g/sec (1.09 tons/day) from Pinole between 0600 and 1500 PDT. $CBrF_3$ was released from the Dow site at a constant rate of 16.0 g/sec (1.52 tons/day) from 0900-1100 PDT and from 1300-1400 PDT.

The average winds at Pinole as measured at Rodeo were 240° at 2.6 m/sec; at the Dow site winds were 270° at 4.6 m/sec. The average standard deviation of the winds at Dow was 8°. Pasquill conditions B-C were assumed to exist under scattered clouds. The average mixing height was 830 meters with a maximum of 1500 meters after 1200 PDT. The wind pattern observed at 1000 PDT in Figure 49 gives a general indication of the wind conditions during the test. Maximum ozone levels of 0.12 ppm were measured at the Montezuma Hills during the day.

Between 0924 and 1901 PDT twelve automobile traverses were conducted. The data from the traverses indicate that the SF_6 plume from Pinole diverged from the Carquinez Strait east past the Montezuma Hills and south through the Walnut Creek area towards Livermore. Figures 50 and 51 show the presence of SF_6 and $CBrF_3$ along Highway 160 downwind of the Montezuma Hills. The maximum $CBrF_3$ concentration was 12,140 ppt. SF_6 levels along I 680 15 km downwind of Pinole reached 614 ppt. Along Highway 160, the levels dropped to 94 ppt. Later traverses shown in Figures 52, 53, and 54 indicate that the SF_6 plume impacted in Livermore passing through Walnut Creek and also reached Tracy, possibly coming from both Livermore and

Figure 49. Surface wind streamlines, 1000 PDT, 9/13/76 (MRI).

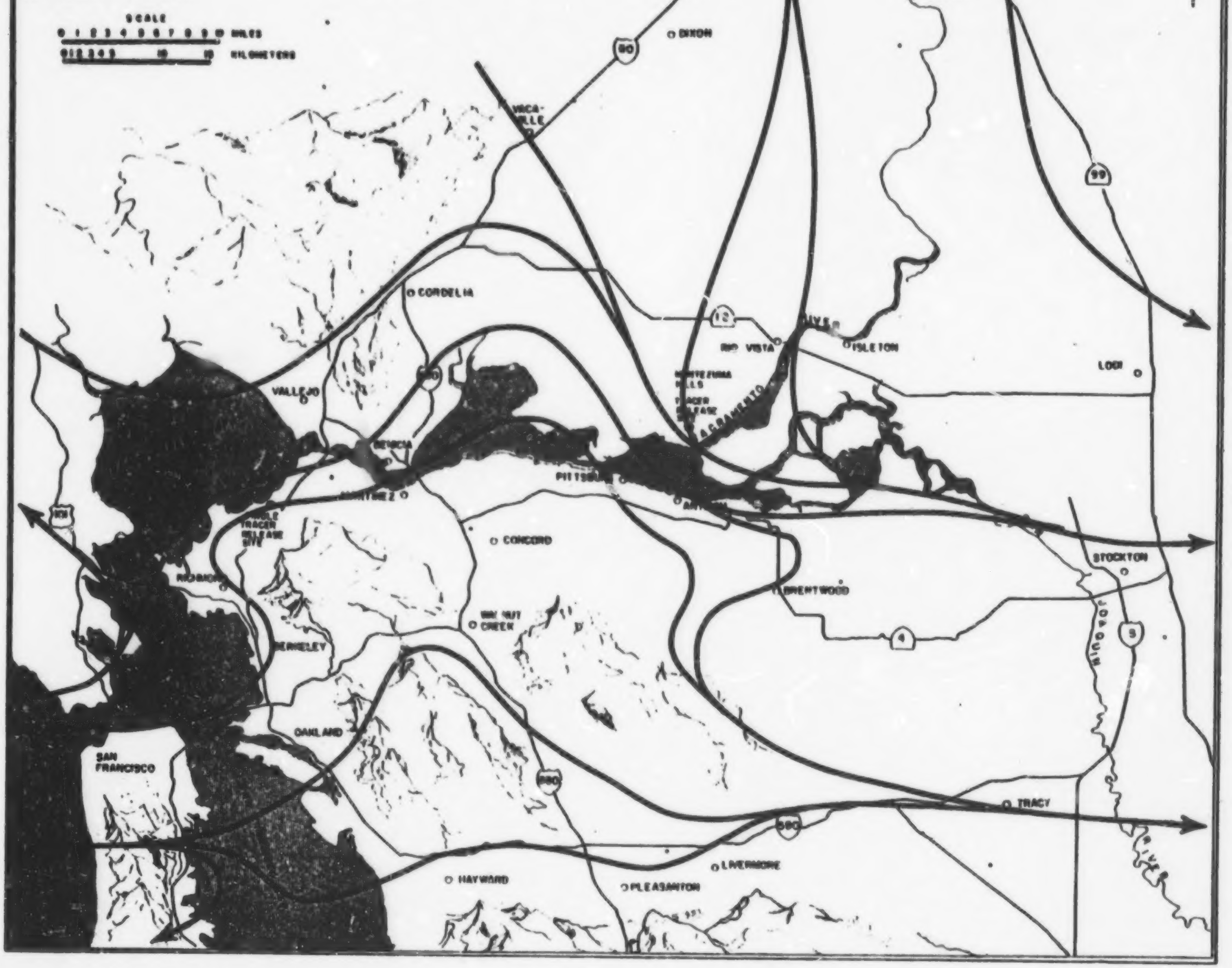
SCALE
0 1 2 3 4 5 6 7 8 9 10 MILES
0 1 2 3 4 5 10 15 KILOMETERS
N
SACRAMENTO EXECUTIVE AIRPORT
DIXON
80
VACAVILLE
99
CORDELIA
12
RIO VISTA
ISLETON
LODI
VALLEJO
MONTEZUMA HILLS TRACER RELEASE SITE
SACRAMENTO
BENICIA
PITTSBURG
ANTIOCH
MARTINEZ
CONCORD
STOCKTON
BRENTWOOD
WALNUT CREEK
4
5
JOAQUIN
RIVER
RICHMOND
BERKELEY
101
OAKLAND
SAN FRANCISCO
580
TRACY
HAYWARD
PLEASANTON
LIVERMORE

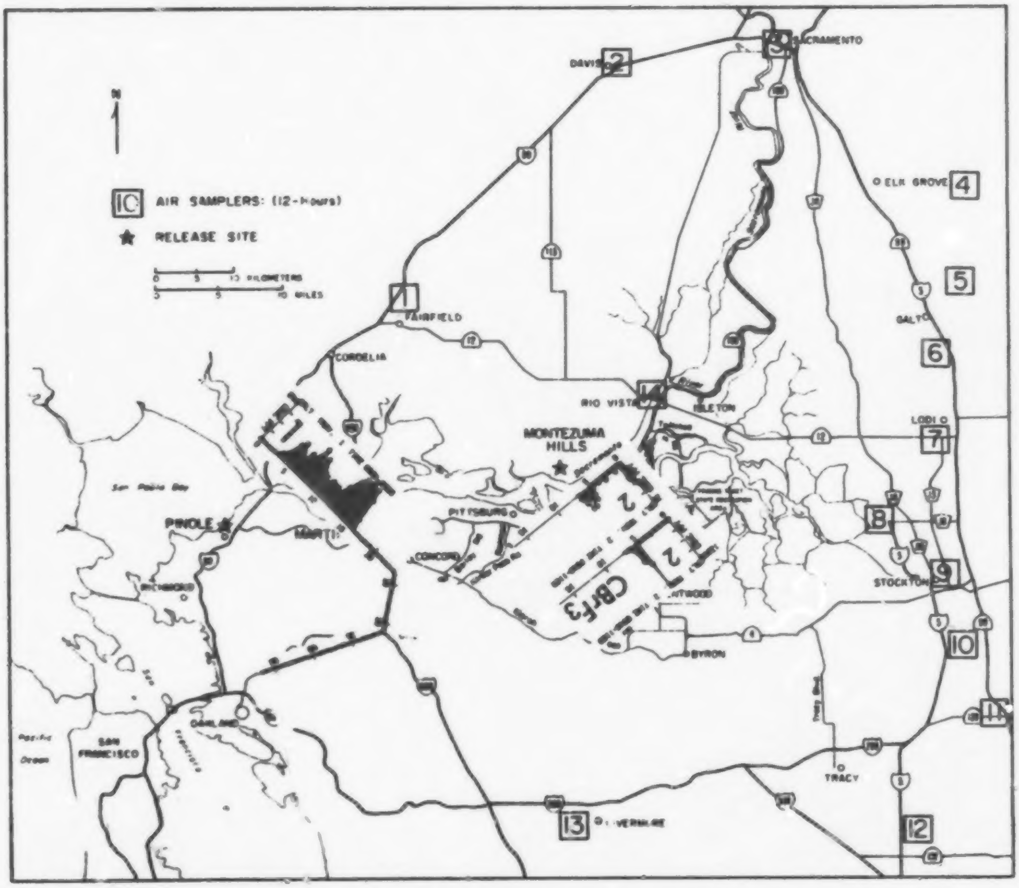
N
10
AIR SAMPLERS: (12-Hours)
RELEASE SITE
0 5 10 KILOMETERS
0 5 10 MILES
DAVIS
2
SACRAMENTO
3
ELK GROVE
4
5
GALT
6
LODI
7
8
STOCKTON
9
10
11
12
13
LIVERMORE
TRACY
BYRON
BRENTWOOD
RIO VISTA
14
ISLETON
MONTEZUMA HILLS
FAIRFIELD
1
CORDELIA
San Pablo Bay
PINOLE
MARTINEZ
PITTSBURG
CONCORD
RICHMOND
OAKLAND
SAN FRANCISCO
Pacific Ocean
1
2
2
CBrF3

Figure 50. Overview of automobile traverse SF_6 and $CBrF_3$ data.

TEST 7

9/13/76

Auto Traverses:

1 0924-0925 PDT, SF_6(max) = 614 ppt.

2 0940-1100 PDT, SF_6(max) = 11 ppt.

0940-1100 PDT, $CBrF_3$(max) = 12,140 ppt.

SF_6 released from Pinole from 0600-1500 PDT.

$CBrF_3$ released from the Montezuma Hills from 0900-1100 PDT, and from 1300-1400 PDT.

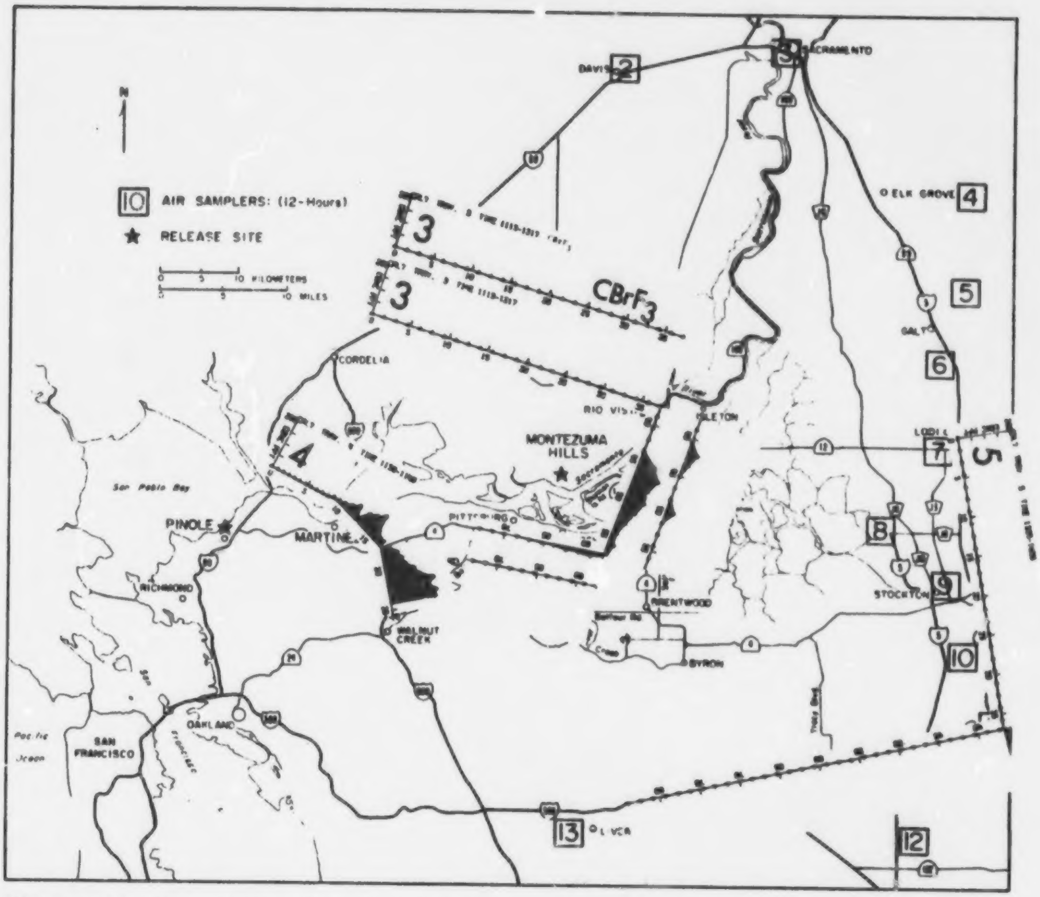
N
AIR SAMPLERS: (12-Hours)
RELEASE SITE
0 5 10 KILOMETERS
0 5 10 MILES
DAVIS
SACRAMENTO
ELK GROVE
GALT
LODI
STOCKTON
CORDELIA
RIO VISTA
MONTEZUMA HILLS
PINOLE
MARTINEZ
RICHMOND
WALNUT CREEK
BRENTWOOD
BYRON
OAKLAND
SAN FRANCISCO
Pacific Ocean
San Pablo Bay
CBrF3
3
3
4
5
2
4
5
6
7
8
9
10
12
13

Figure 51. Overview of automobile traverse SF_6 and $CBrF_3$ data.

TEST 7

9/13/76

Auto Traverses:

3 1113-1217 PDT, SF_6(max) = 94 ppt.
1113-1217 PDT, $CBrF_3$(max) = 37 ppt.
4 1130-1146 PDT, SF_6(max) = 180 ppt.
5 1335-1458 PDT, SF_6(max) = 3 ppt.

SF_6 released from Pinole from 0600-1500 PDT.

$CBrF_3$ released from the Montezuma Hills from 0900-1100 PDT and from 1300-1400 PDT.

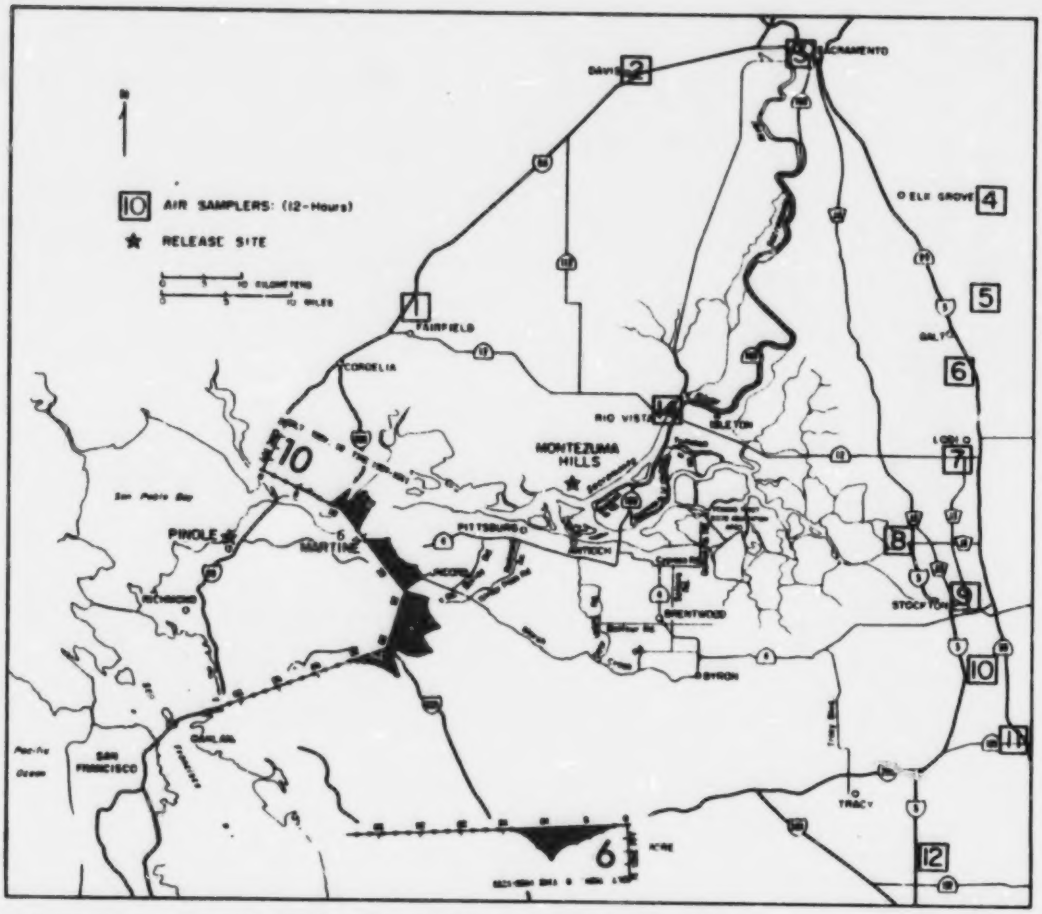
N
10 AIR SAMPLERS: (12-Hours)
★ RELEASE SITE
0 5 10 KILOMETERS
0 5 10 MILES
SACRAMENTO
DAVIS
2
ELK GROVE
4
5
GALT
6
1
FAIRFIELD
CORDELIA
RIO VISTA
14
ISLETON
LODI
7
MONTEZUMA HILLS
10
San Pablo Bay
PINOLE
6
MARTINEZ
PITTSBURG
ANTIOCH
8
STOCKTON
9
BRENTWOOD
BYRON
10
11
Pacific Ocean
SAN FRANCISCO
OAKLAND
TRACY
12
6

Figure 52. Overview of automobile traverse SF_6 data.

TEST 7

9/13/76

Auto Traverses:

9 1458 - 1522 PDT, SF_6(max) = 12 ppt.

10 1537 - 1611 PDT, SF_6(max) = 16 ppt.

SF_6 released from Pinole from 0600-1500 PDT.

$CBrF_3$ released from the Montezuma Hills from 0900-1100 PDT and from 1300-1400 PDT.

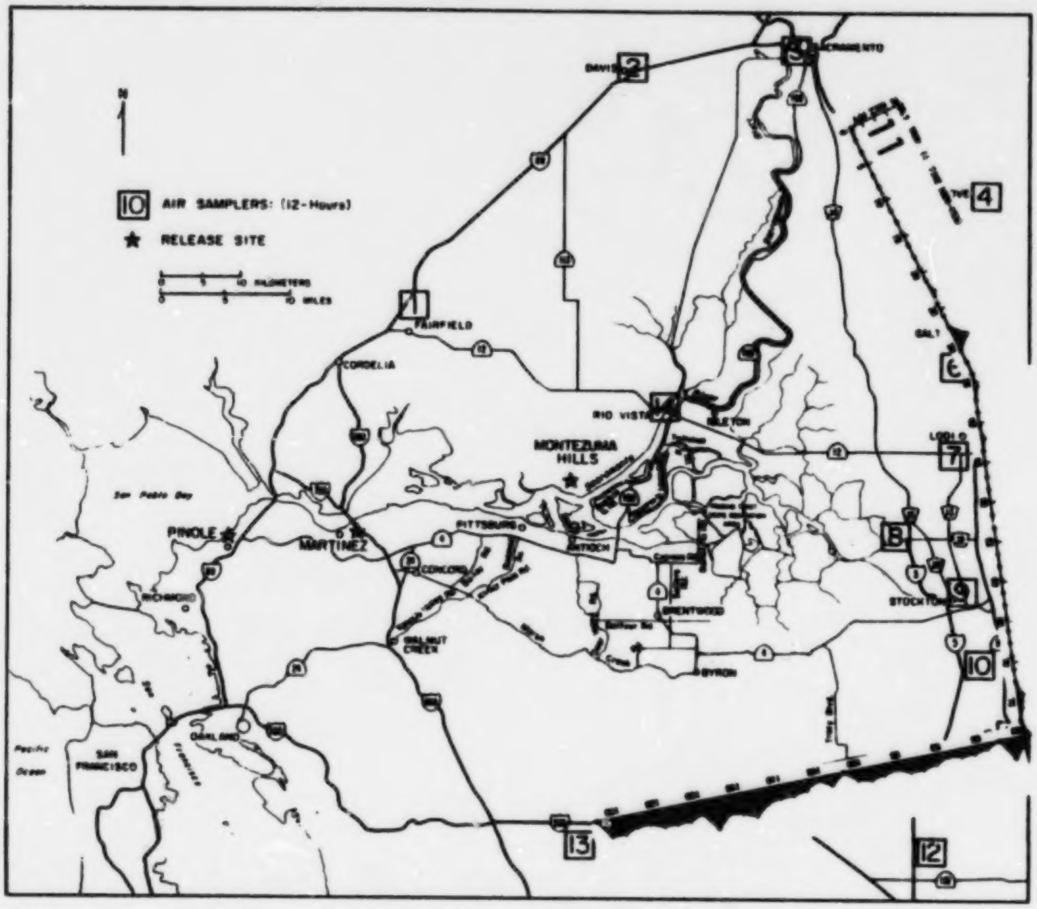
N
10 AIR SAMPLERS: (12-Hours)
RELEASE SITE
0 5 10 KILOMETERS
0 5 10 MILES
DAVIS
2
SACRAMENTO
4
1
FAIRFIELD
CORDELIA
GALT
6
RIO VISTA
ISLETON
MONTEZUMA HILLS
LODI
7
San Pablo Bay
PINOLE
MARTINEZ
PITTSBURG
ANTIOCH
8
CONCORD
STOCKTON
9
RICHMOND
BRENTWOOD
WALNUT CREEK
BYRON
10
Pacific Ocean
SAN FRANCISCO
OAKLAND
13
12

Figure 53. Overview of automobile traverse SF_6 data.

TEST 7

9/13/76

Auto Traverse:

11 1654 - 1820 PDT, SF_6(max) = 12 ppt.

SF_6 released from Pinole from 0600-1500 PDT.

$CBrF_3$ released from the Montezuma Hills from 0900-1100 PDT and from 1300-1400 PDT.

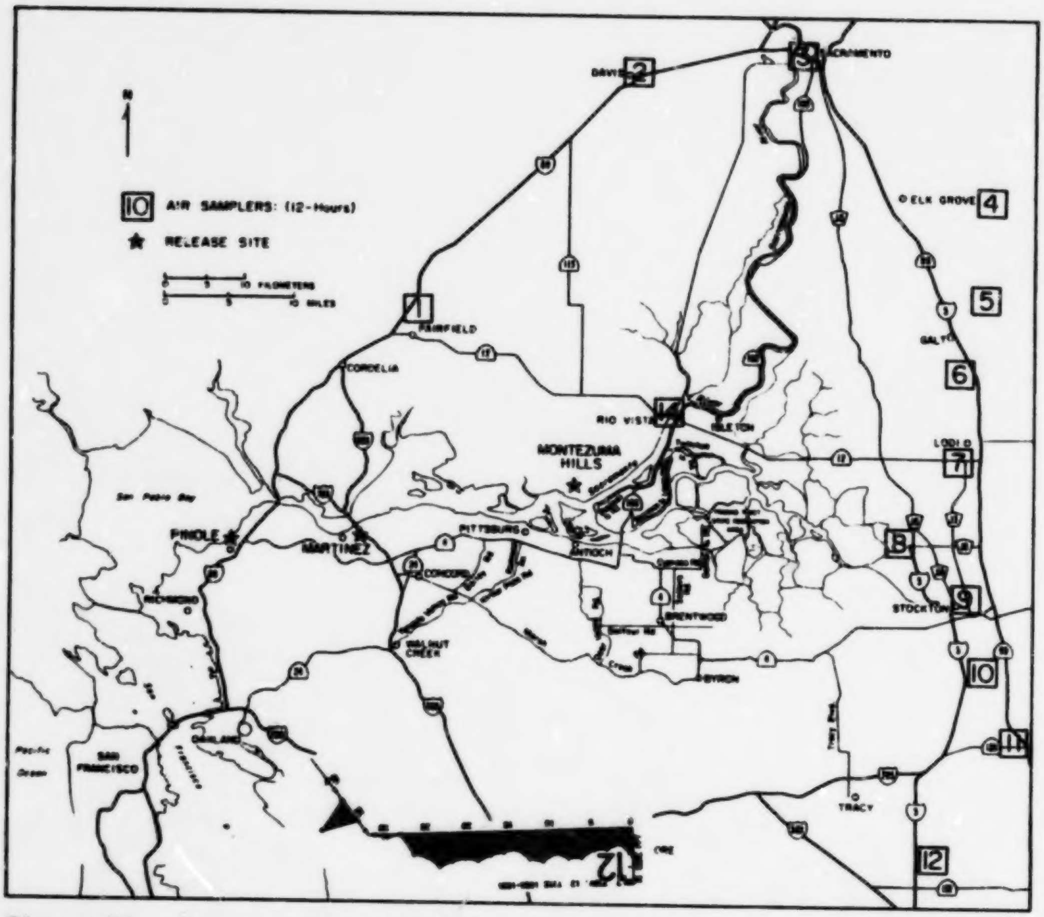
N
10 AIR SAMPLERS: (12-Hours)
RELEASE SITE
0 5 10 KILOMETERS
0 5 10 MILES
DAVIS
2
SACRAMENTO
3
ELK GROVE
4
5
GALT
6
1
FAIRFIELD
CORDELIA
RIO VISTA
ISLETON
MONTEZUMA HILLS
LODI
7
San Pablo Bay
PINOLE
MARTINEZ
PITTSBURG
ANTIOCH
CONCORD
8
STOCKTON
9
RICHMOND
WALNUT CREEK
BRENTWOOD
BYRON
10
11
Pacific Ocean
SAN FRANCISCO
OAKLAND
TRACY
12

Figure 54. Overview of automobile traverse SF_6 data.

Reproduced from best available copy.

TEST 7

9/13/76

Auto Traverse:

12 1835 - 1901 PDT, SF_6(max) = 13 ppt

SF_6 released from Pinole from 0600-1500 PDT.

$CBrF_3$ released from the Montezuma Hills from 0900-1100 PDT, and from 1300-1400 PDT.

the Pittsburg-Antioch area. Concentration levels along I 580 reached 16 ppt.

Fourteen airborne traverses were conducted from Cordelia to Walnut Creek, from Vacaville to Tracy, and from Livermore to Stockton to Sacramento. Data from three traverses at three altitudes above I 680 are shown in Figure 55. Apparently, the plume had mixed no higher than 305 meters after traveling 17 km downwind. The maximum concentration at 183 meters was 199 ppt. The vertical profile of the plume is shown in Figure 56 where data from spirals 22 km downwind of Pinole are plotted. By 1000 PDT, the plume appeared to be vertically well-mixed to a height of about 300 meters. The crosswind data indicate that the spirals were taken very near the centerline of the plume. Further downwind between Isleton and Tracy, elevated concentration profiles also indicate that the plume was vertically well-mixed. As shown in Figure 57, maximum concentrations at 183, 305, and 427 meters were 19, 25, and 15 ppt, respectively. The data indicate that the plume was wider at the higher elevations, suggesting either increased wind shear or reflectance from an inversion layer. The last set of airborne traverses above I 580 and Highway 99 in Figure 58 show that the SF_6 plume was present at 457 meters between Livermore and Tracy. The maximum concentration was 29 ppt.

A spiral over Stockton at 1832 PDT suggested that a portion of the plume was transported between 900 m and 1200 m. Concentration levels were on the order of 30 ppt; however, the concentration in one sample at 1036 m was analyzed as 952 ppt. Since none of the data collected during the spiral or during the other traverses in the area were over 50 ppt, it is assumed that the sample was contaminated and the data point should be disregarded.

As indicated in Figure 59, SF_6 was detected in hourly samples at very low levels (less than 10 ppt) from Elk Grove to Livermore along Highway 99. The major impact did not appear until after 1800 PDT. In general, the hourly averaged data also show that SF_6 reached Livermore and Tracy. Again, it appears that material emitted from the northern portions of the Bay Area can follow trajectories south through Stockton and Tracy into the San Joaquin Valley.

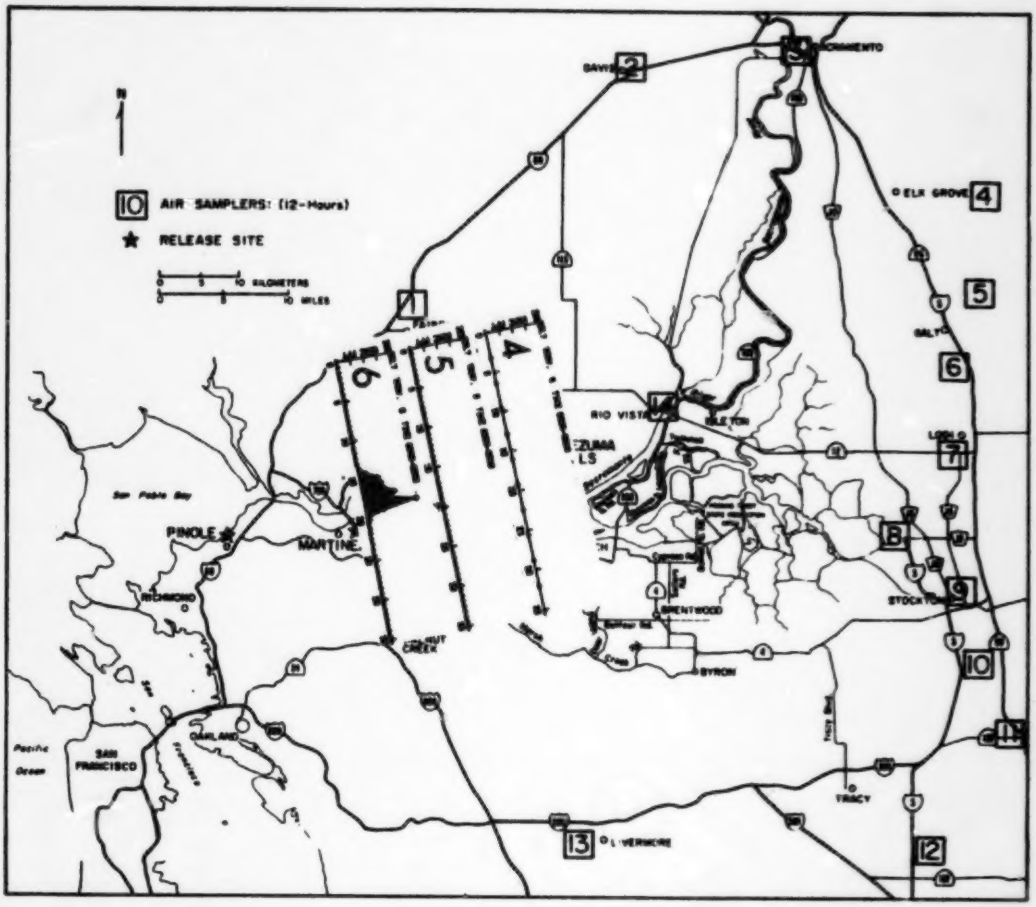
N
10 AIR SAMPLERS: (12-Hours)
RELEASE SITE
0 5 10 KILOMETERS
0 5 10 MILES
DAVIS
2
SACRAMENTO
3
ELK GROVE
4
5
GALT
6
LODI
7
8
STOCKTON
9
10
11
12
13
LIVERMORE
TRACY
BYRON
BRENTWOOD
RIO VISTA
14
ISLETON
1
6
5
4
San Pablo Bay
PINOLE
MARTINEZ
RICHMOND
WALNUT CREEK
OAKLAND
SAN FRANCISCO
Pacific Ocean

Figure 55. Overview of airborne traverse SF_6 data measured at three altitudes between Cordelia and Walnut Creek.

TEST 7

9/13/76

Airborne Traverses:

4 0906 - 0918 PDT, 427 m, SF_6(max) = 0 ppt
5 0925 - 0938 PDT, 305 m, SF_6(max) = 1 ppt
6 0945 - 0958 PDT, 183 m, SF_6(max) = 199 ppt

SF_6 released from Pinole from 0600-1500 PDT.

$CBrF_3$ released from the Montezuma Hills from 0900-1100 PDT and from 1300-1400 PDT.

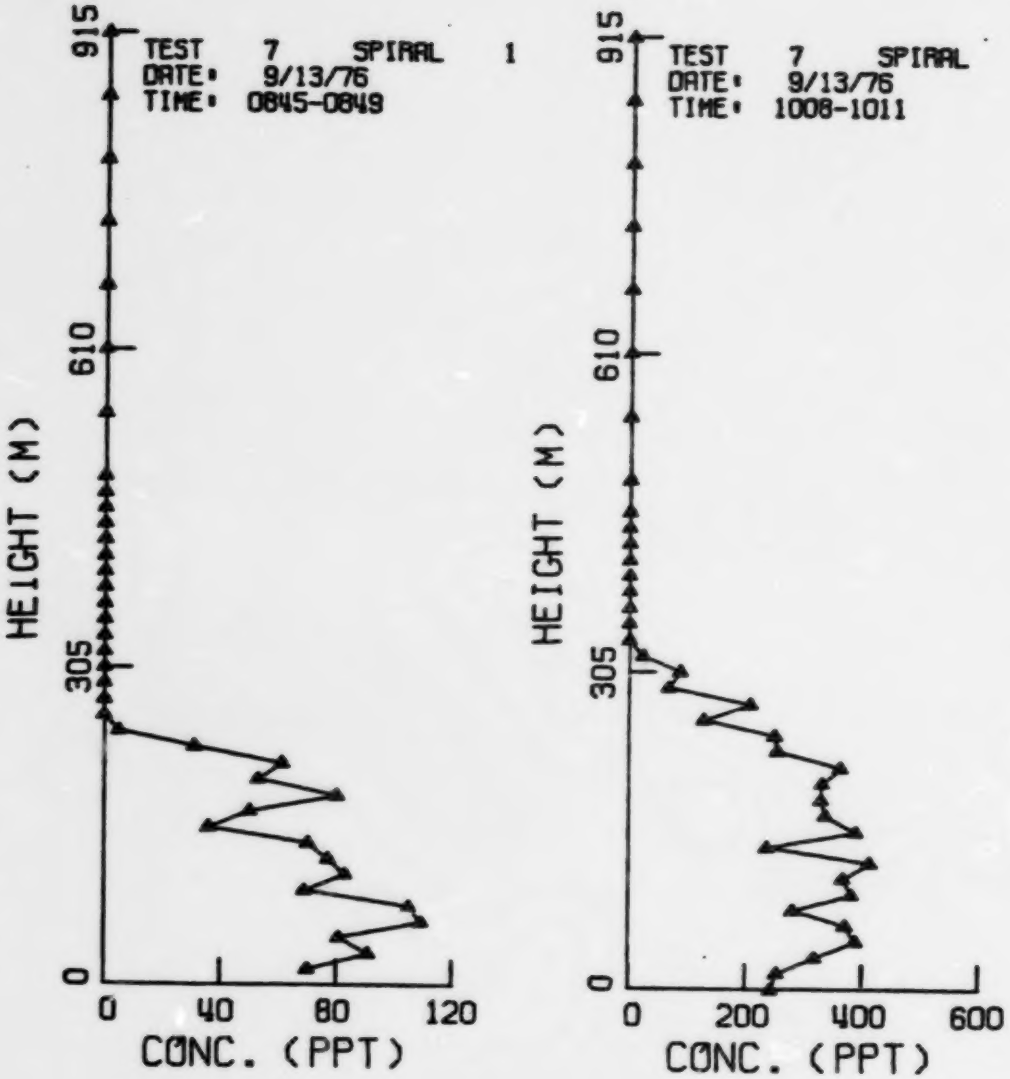

Figure 56. Vertical SF_6 profiles observed 0.8 Km north of the Port Chicago Naval Depot.

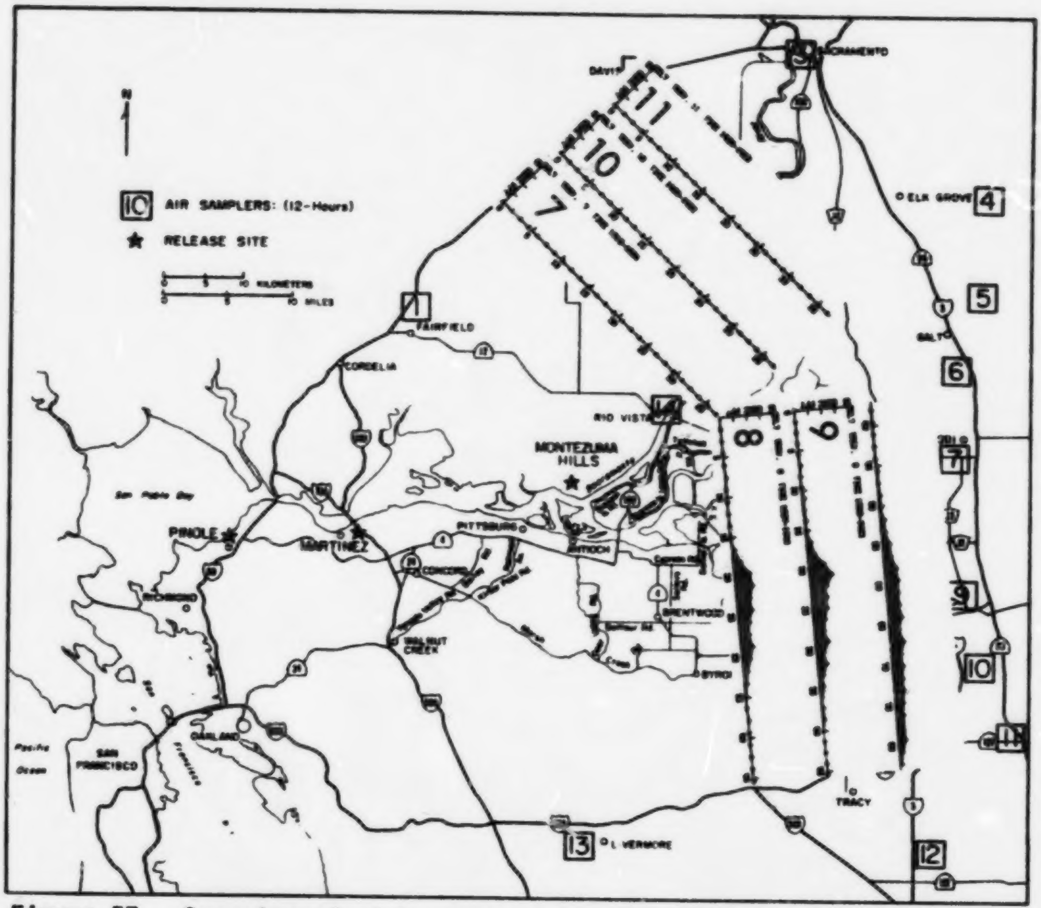
N
10 AIR SAMPLERS: (12-Hours)
RELEASE SITE
KILOMETERS
MILES
DAVIS
SACRAMENTO
ELK GROVE
4
5
6
7
9
10
11
12
13
14
1
FAIRFIELD
CORDELIA
RIO VISTA
MONTEZUMA HILLS
San Pablo Bay
PINOLE
MARTINEZ
PITTSBURG
ANTIOCH
CONCORD
BRENTWOOD
WALNUT CREEK
BYRON
OAKLAND
SAN FRANCISCO
Pacific Ocean
TRACY
LIVERMORE
7
8
9
10
11

Figure 57. Overview of airborne traverse SF_6 data measured at three altitudes between Vacaville, Isleton, and the I580-I205 junction.

TEST 7

9/13/76

Airborne Traverses:

7 1312-1324 PDT, 183 m, SF_6(max) = 0 ppt.
8 1327-1343 PDT, 183 m, SF_6(max) = 19 ppt.
9 1348-1408 PDT, 305 m, SF_6(max) = 25 ppt.
10 1409-1422 PDT, 305 m, SF_6(max) = 1 ppt.
11 1428-1456 PDT, 427 m, sF_6(max) = 15 ppt.

SF_6 released from Pinole from 0600-1500 PDT.

$CBrF_3$ released from the Montezuma Hills from 0900-1100 PDT and from 1300-1400 PDT.

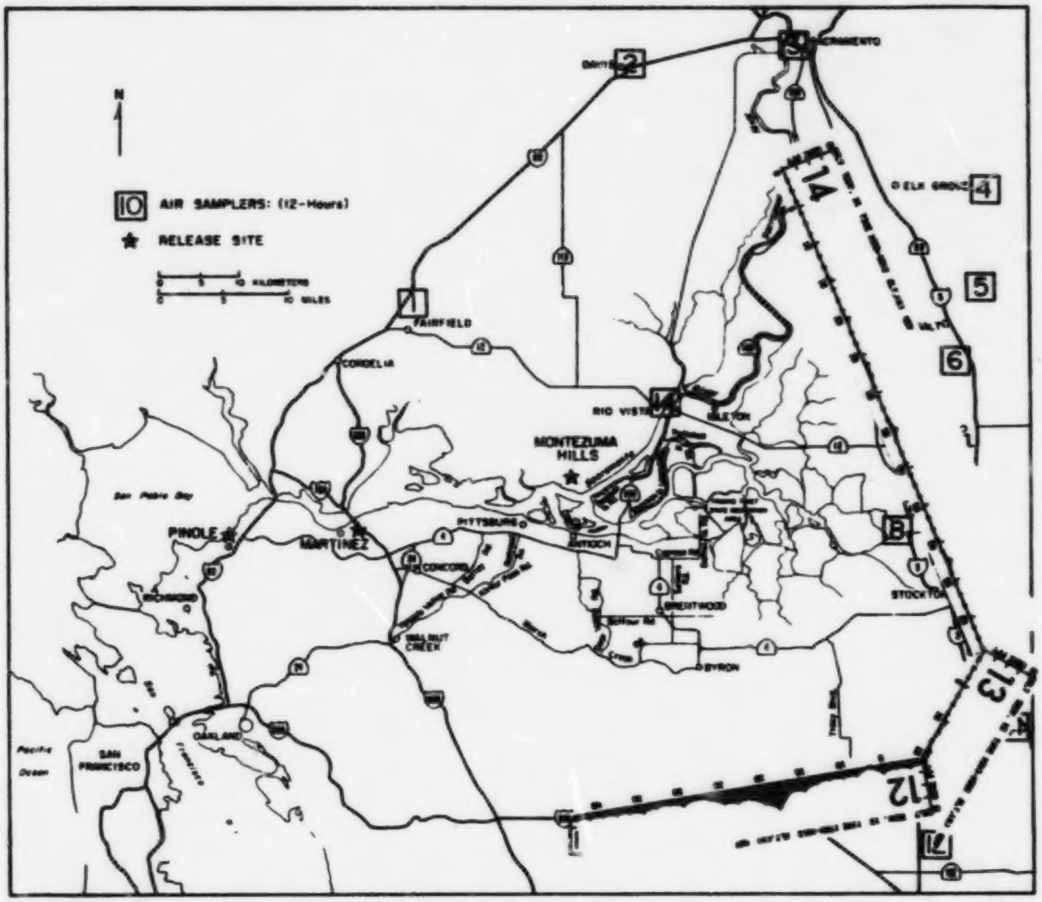
N
10 AIR SAMPLERS: (12-Hours)
RELEASE SITE
0 5 10 KILOMETERS
0 5 10 MILES
2
4
5
6
1
8
12
13
14
FAIRFIELD
CORDELIA
ELK GROVE
RIO VISTA
MONTEZUMA HILLS
San Pablo Bay
PINOLE
MARTINEZ
PITTSBURG
ANTIOCH
CONCORD
RICHMOND
WALNUT CREEK
BRENTWOOD
BYRON
STOCKTON
OAKLAND
SAN FRANCISCO
Pacific Ocean

Figure 58. Overview of airborne traverse SF_6 data.

TEST 7

9/13/76

Airborne Traverses:

12 1759 - 1812 PDT, 457 m, SF_6(max) = 29 ppt
13 1815 - 1822 PDT, 457 m, SF_6(max) = 5 ppt
14 1850 - 1912 PDT, 457 m, SF_6(max) = 4 ppt

SF_6 released from Pinole from 0600-1500 PDT.

$CBrF_3$ released from the Montezuma Hills from 0900-1100 PDT and from 1300-1400 PDT.

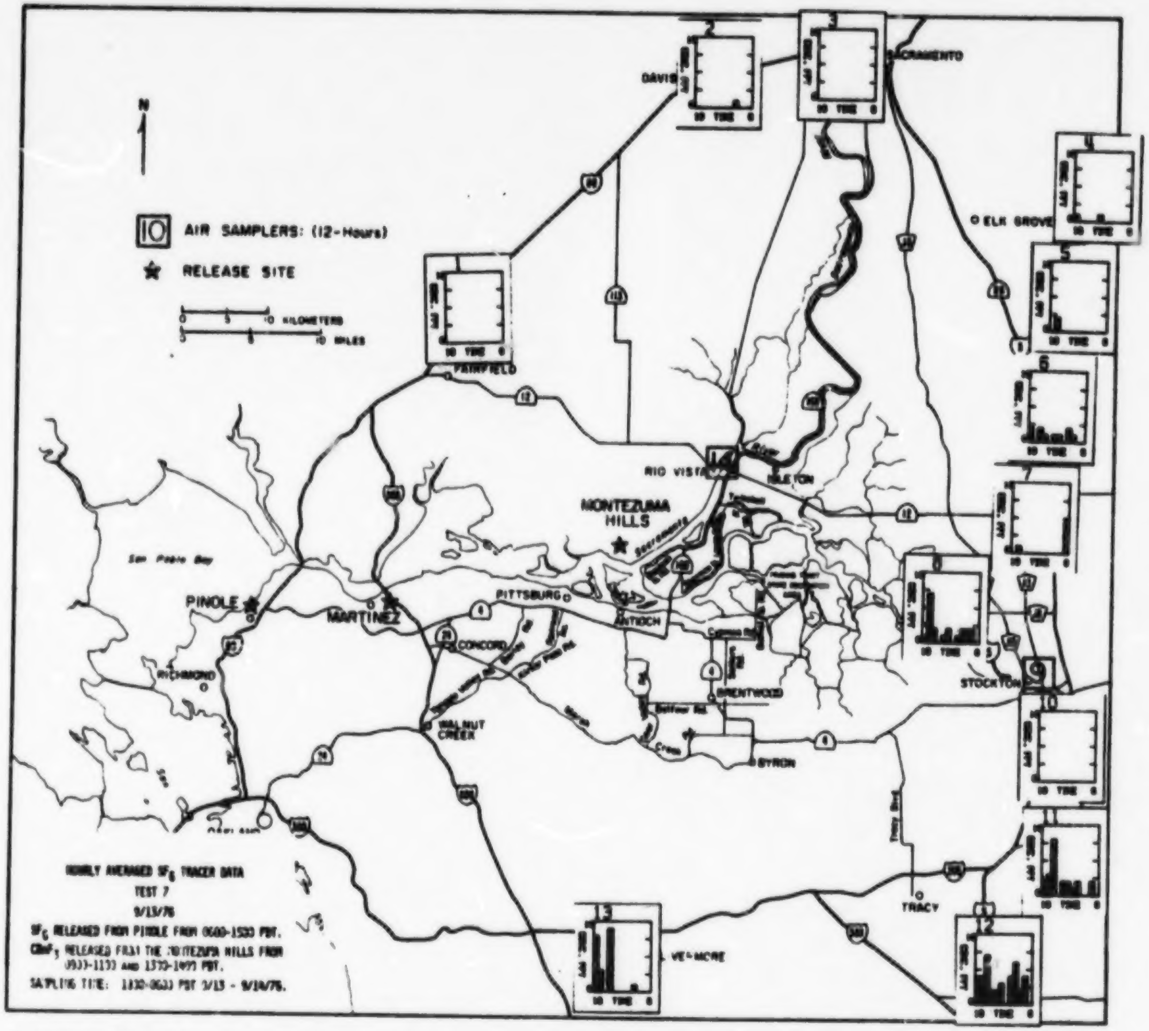
N
10 AIR SAMPLERS: (12-Hours)
RELEASE SITE
0 5 10 KILOMETERS
0 5 10 MILES
DAVIS
SACRAMENTO
ELK GROVE
FAIRFIELD
RIO VISTA
ISLETON
MONTEZUMA HILLS
PINOLE
MARTINEZ
PITTSBURG
ANTIOCH
CONCORD
RICHMOND
WALNUT CREEK
BRENTWOOD
BYRON
STOCKTON
TRACY
OAKLAND
LIVERMORE
San Pablo Bay
CONC. PPT
10 TIME 0
2
3
4
5
6
7
8
9
10
11
12
13
14
HOURLY AVERAGED SF6 TRACER DATA
TEST 7
9/13/76
SF6 RELEASED FROM PINOLE FROM 0600-1500 PDT.
CBrF3 RELEASED FROM THE MONTEZUMA HILLS FROM 0900-1100 AND 1300-1500 PDT.
SAMPLING TIME: 1100-0600 PDT 9/13 - 9/14/76.

Figure 59. Overview of hourly averaged SF_6 data. Full scale SF_6 = 10 ppt.

4.28 Tracer Test 8 (9/14/76)

The purpose of the final tracer test was to study the transport and dispersion of pollutants flowing through the Carquinez Strait during the development of the afternoon sea breeze. SF_6 was released at a constant rate of 10.9 g/sec (1.04 tons/day) from Pinole between 0730 and 1300 PDT.

The average winds at Rodeo near Pinole were 220° at 3.7 m/sec. The area averaged winds were from 250° at 3.6 m/sec. There were scattered clouds. Stability conditions were assumed to be Pasquill classes B-C. The average mixing height was 1200 meters, and the maximum height observed was 3000 meters around 1200 PDT. The winds during the test followed the streamlines shown in Figure 60 for 1000 PDT. Ozone levels reached no greater than 0.08 ppm in the area during the day.

Four automobile traverses were conducted between 0906 and 1218 PDT along I 680 and Highway 160. As indicated in Figures 61 and 62, the plume passed through the Carquinez Strait at levels as high as 1598 ppt. A wide SF_6 plume was detected along Highway 160 with a maximum level of 78 ppt. No data were collected along Highway 99.

Six airborne traverses were completed above I 680 17 km downwind of Pinole. The data shown in Figure 63 indicate that the plume mixed vertically to 427 meters by the time it passed over I 680. The vertical profile in Spiral 1, Figure 64 , agrees with the crosswind data. As will be discussed in Section 4.4, the elevated crosswind data provide a very accurate means of performing a mass balance on the tracer. In this case, 102% of the material emitted was accounted for by the traverse data. During the final test, no hourly data were collected.

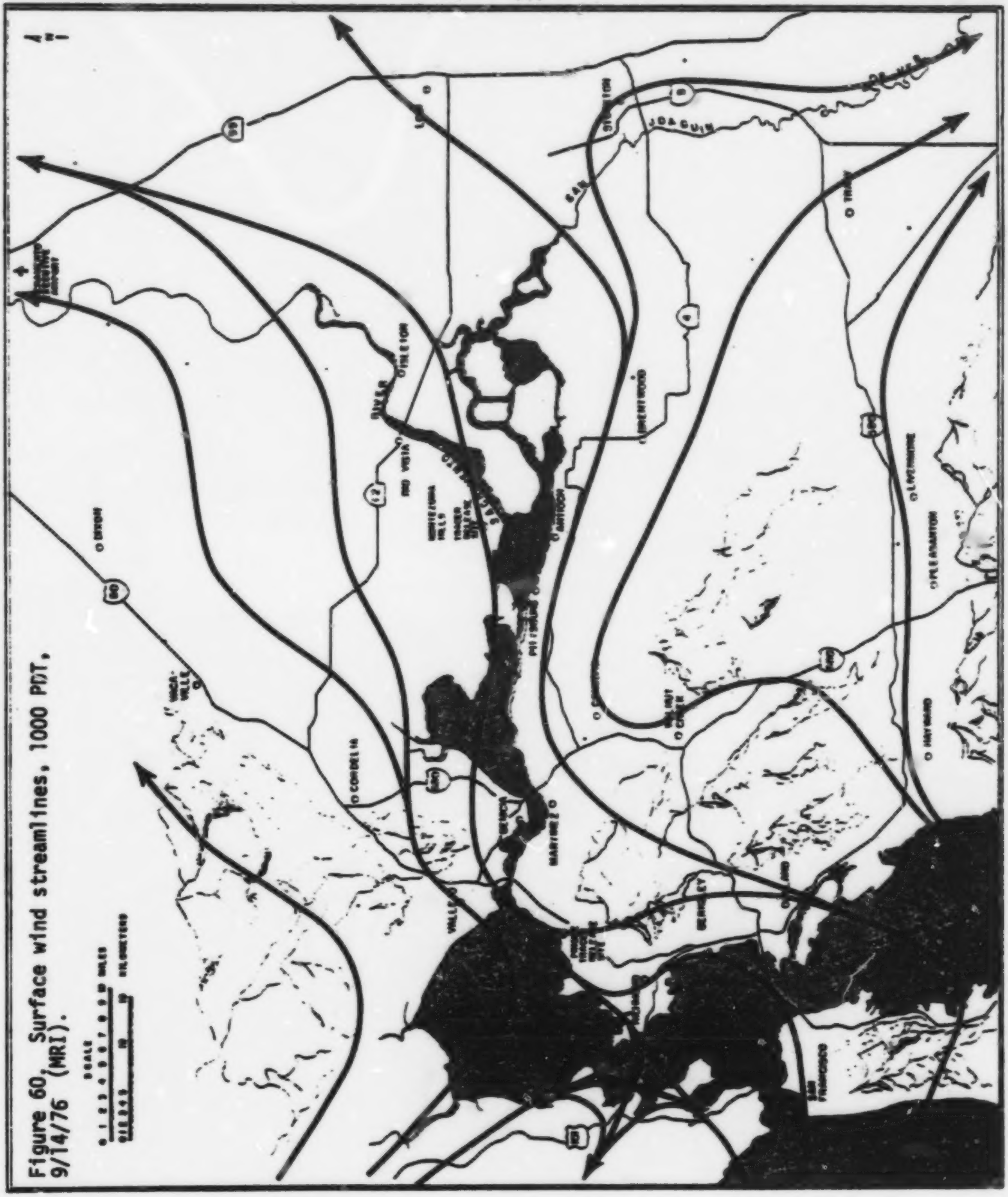
SAN JOAQUIN RIVER
STOCKTON
BRENTWOOD
ANTIOCH
PITTSBURG
RIO VISTA
DIXON
VACAVILLE
CORDELIA
BENICIA
MARTINEZ
VALLEJO
WALNUT CREEK
BERKELEY
OAKLAND
SAN FRANCISCO
HAYWARD
PLEASANTON
LIVERMORE
TRACY
SCALE
MILES
KILOMETERS

Figure 60, Surface wind streamlines, 1000 PDT, 9/14/76 (MRI).

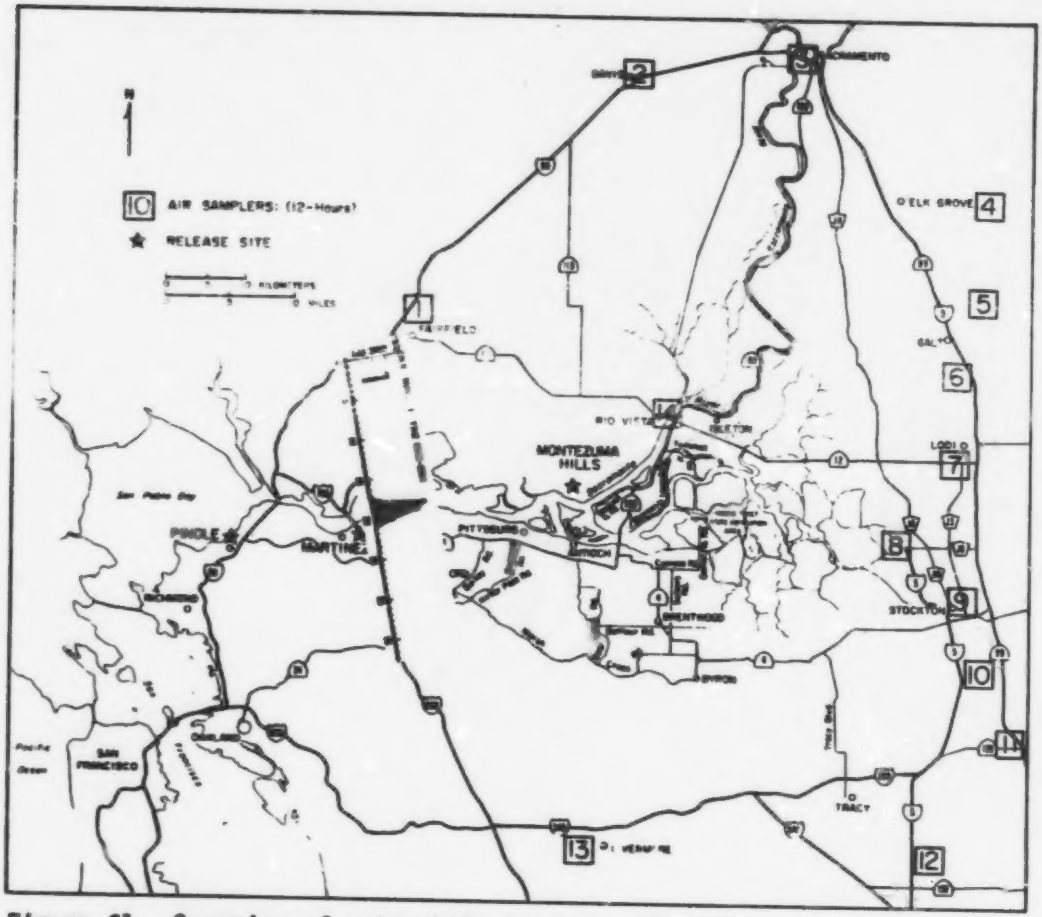
N
10 AIR SAMPLERS: (12-Hours)
RELEASE SITE
KILOMETERS
MILES
SACRAMENTO
DAVIS
2
3
ELK GROVE
4
5
GALT
6
1
FAIRFIELD
RIO VISTA
14
ISLETON
MONTEZUMA HILLS
LODI
7
San Pablo Bay
PINOLE
MARTINEZ
PITTSBURG
ANTIOCH
8
RICHMOND
BRENTWOOD
STOCKTON
9
BYRON
10
11
OAKLAND
Pacific Ocean
SAN FRANCISCO
TRACY
13
VERNALIS
12

Figure 61. Overview of automobile traverse SF_6 data.

TEST 8

9/14/76

Auto Traverse:

1 0906 - 0931 PDT, SF_6(max) = 1598 ppt

SF_6 released from Pinole from 0730-1300 PDT.

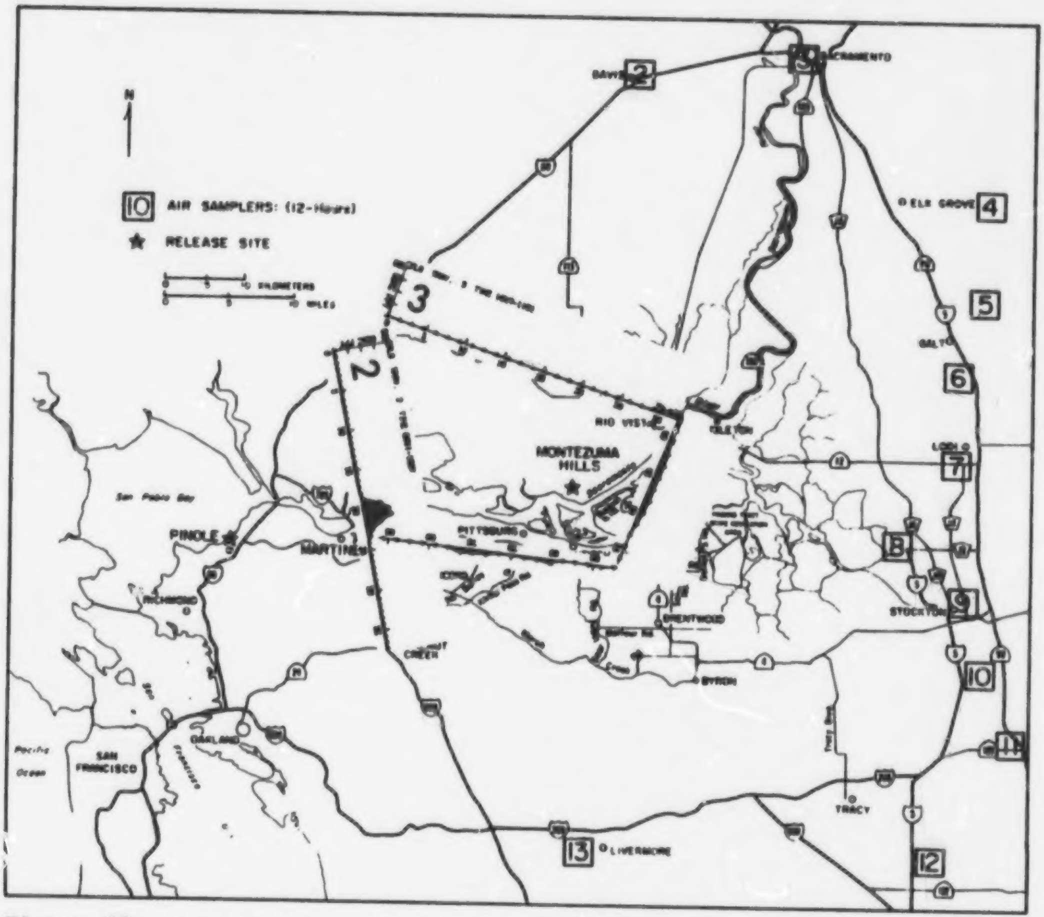
N
10 AIR SAMPLERS: (12-Hours)
★ RELEASE SITE
0 5 10 KILOMETERS
0 5 10 MILES
DAVIS 2
SACRAMENTO
ELK GROVE 4
5
GALT
6
LODI
7
8
STOCKTON 9
10
11
12
13 LIVERMORE
TRACY
BYRON
BRENTWOOD
RIO VISTA
ISLETON
MONTEZUMA HILLS
PITTSBURG
MARTINEZ
PINOLE
RICHMOND
San Pablo Bay
OAKLAND
SAN FRANCISCO
Pacific Ocean
WALNUT CREEK
3
2

Figure 62. Overview of automobile traverse SF_6 data.

TEST 8

9/14/76

Auto Traverses:

2 0941 - 1007 PDT, SF_6(max) = 412 ppt

3 1047 - 1151 PDT, SF_6(max) = 78 ppt

SF_6 released from Pinole from 0730-1300 PDT.

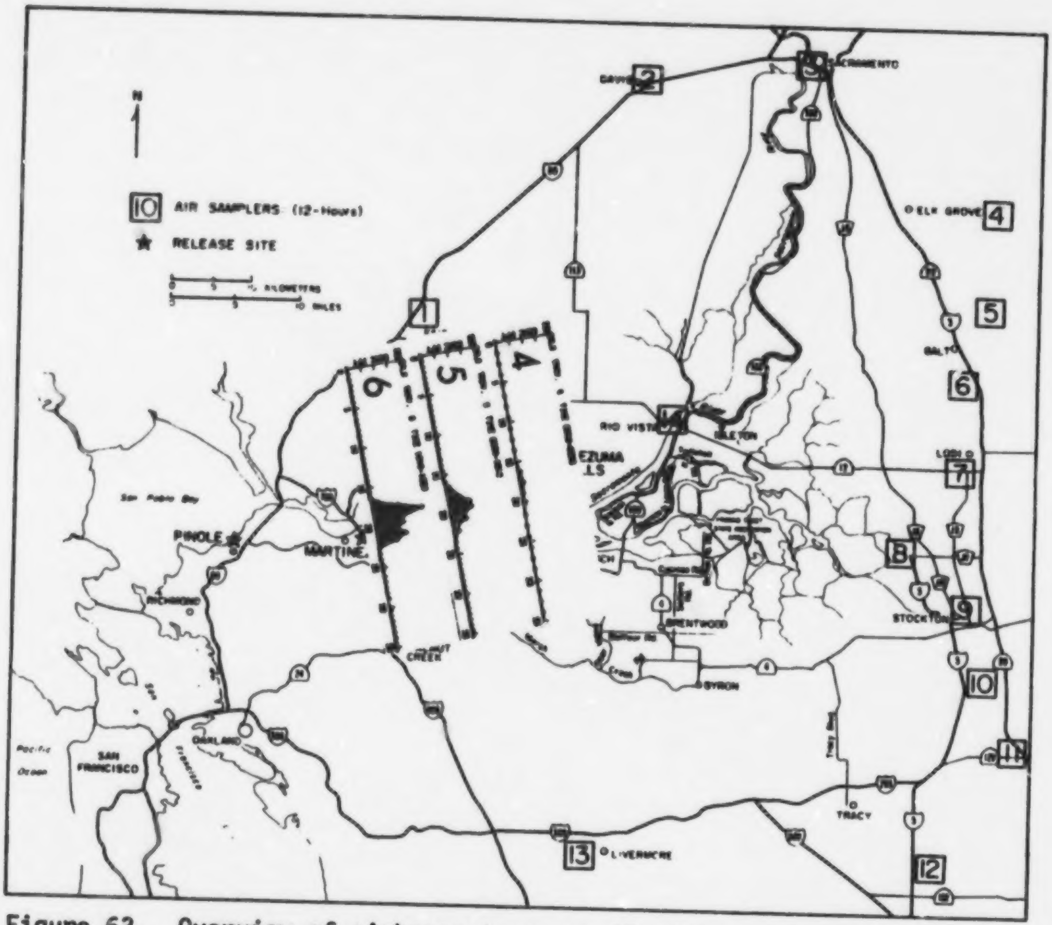
N
10 AIR SAMPLERS (12-Hours)
RELEASE SITE
KILOMETERS
MILES
DAVIS
2
SACRAMENTO
3
ELK GROVE
4
5
GALT
6
LODI
7
8
STOCKTON
9
10
11
12
13
LIVERMORE
TRACY
1
6
5
4
RIO VISTA
ISLETON
BRENTWOOD
BYRON
San Pablo Bay
PINOLE
MARTINEZ
RICHMOND
WALNUT CREEK
OAKLAND
SAN FRANCISCO
Pacific Ocean

Figure 63. Overview of airborne traverse SF_6 data measured at three altitudes between Cordelia and Walnut Creek.

TEST 8

9/14/76

Airborne Traverses:

4 0942-0955 PDT, 427 m, SF_6(max) = 22 ppt.

5 0959-1012 PDT, 305 m, SF_6(max) = 134 ppt.

6 1016-1028 PDT, 183 m, SF_6(max) = 304 ppt.

SF_6 released from Pinole from 0730-1300 PDT.

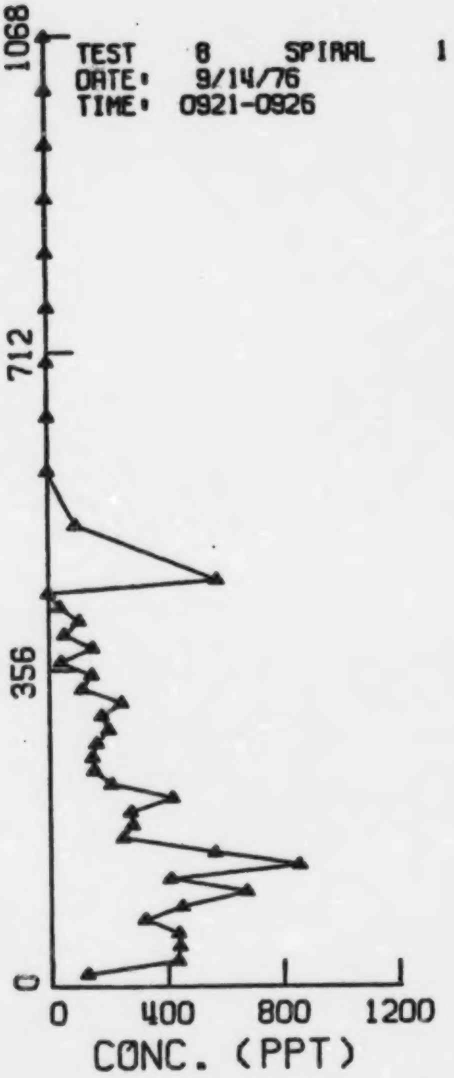

Figure 64. Vertical SF_6 profile observed 0.8 Km north of the Port Chicago Naval Depot.

4.3 Determination of Dispersion Parameters from Automobile Traverse and Airborne Spiral Tracer Data

In order to quantify the dispersion of tracer and pollutants along transport paths through the Delta Region, the Gaussian horizontal crosswind standard deviation for each automobile traverse was determined. By definition

$$Y_0 = \frac{\int_{-\infty}^{\infty} yC(y)dy}{\int_{-\infty}^{\infty} C(y)dy} \tag{2}$$

and

$$\sigma_y = \left[\frac{\int_{-\infty}^{\infty} y^2C(y)dy}{\int_{-\infty}^{\infty} C(y)dy} - Y_0{}^2\right]^{\frac{1}{2}} \tag{3}$$

where Y_0 is the distance along the traverse to the center line, C(y) is the concentration as a function of distance along the traverse, and σ_y is the horizontal crosswind standard deviation. The centerline concentration, C_0, is given by:

$$C_0 = \frac{\int_{-\infty}^{\infty} C(y)dy}{\sqrt{2\pi}\ \sigma_y} \tag{4}$$

These parameters were determined by numerical integration of the data; see Appendix B for details. When integrated in an iterative procedure, the parameters yield a best-fit Gaussian curve to the traverse data:

$$C(y) = C_0 \exp\left[-\frac{1}{2}\left(\frac{y-Y_0}{\sigma_y}\right)^2\right] \tag{5}$$

The best-fit curves resulting from this analysis are given in Section 3.6 of Volume II, Part A. Typical curves are shown in Figures 65 and 66 of this report; the experimental and best-fit parameters are listed in Table 9. As indicated in the figures, generally most of the traverses conform fairly well to a Gaussian profile.

A similar procedure can be applied to the airborne spiral data to give a best-fit Gaussian vertical profile. The results are shown in Figures 67 and 68. In this case, the curves do not fit the data as well as for the crosswind data. This is a result of the spiral pattern involved in obtaining the data. While we assume that the data represent a vertical profile at a constant crosswind distance from the plume centerline, in reality, the plane was spiraling around a radius of several hundred meters. Also, because the ground is a reflecting plane to the tracer, the tracer material connot be distributed in a perfect Gaussian form. However, determining σ_z from the data does give a measure of the extent of vertical spread. The best-fit results are given in Table 9. We have not presented best-fit crosswind curves to the airborne traverses because the release height was approximately $z = 0$. Correct determination of σ_y for use in the Gaussian model should occur at the plume centerline.

Although airborne data were collected only during the latter three tests, it is possible to estimate values of the vertical crosswind standard deviation, σ_z, for all the tests from the automobile traverse data. If one assumes that the Gaussian plume model can be used to describe the tracer results and, furthermore, that the tracer is conserved between the surface and the height of the mixing layer, then the crosswind integral of the experimental horizontal tracer data can be written

$$\int_{-\infty}^{\infty} C(y)\,dy \equiv C_{CWI} = \frac{Q}{\sqrt{2\pi}\,\sigma_z\,u}\left\{\exp\left[-\tfrac{1}{2}\left(\frac{Z+H}{\sigma_z}\right)^2\right] + \exp\left[-\tfrac{1}{2}\left(\frac{Z-H}{\sigma_z}\right)^2\right] + \sum_{n=1}^{4}\left(\exp\left[-\tfrac{1}{2}\left(\frac{z+H-2nL}{\sigma}\right)^2\right] + \exp\left[-\tfrac{1}{2}\left(\frac{z-H-2nL}{\sigma_z}\right)^2\right] + \exp\left[-\tfrac{1}{2}\left(\frac{z-H+2nL}{\sigma_z}\right)^2\right] + \exp\left[-\tfrac{1}{2}\left(\frac{z+H+2nL}{\sigma_z}\right)^2\right]\right)\right\} \tag{6}$$

when C_{CWI} has been defined as the crosswind-integrated concentration, Q is the average tracer release rate, u is the average wind velocity, H is the release height and L is the mixing layer height. The summation terms represent reflection of tracer from the top of the mixing layer. Equation (6) can be solved for σ_z using a numerical iterative procedure. The accuracy of such a solution is a function of the accuracy with which measured values of u and L represent the actual average meteorological conditions. In this analysis values of u were obtained by vector-averaging wind data available downwind of the release point. Values of L were obtained by averaging the data from the available measurements. The results of the analysis are presented in Table 9 for traverses where it appeared that the assumptions and necessary conditions were reasonable.

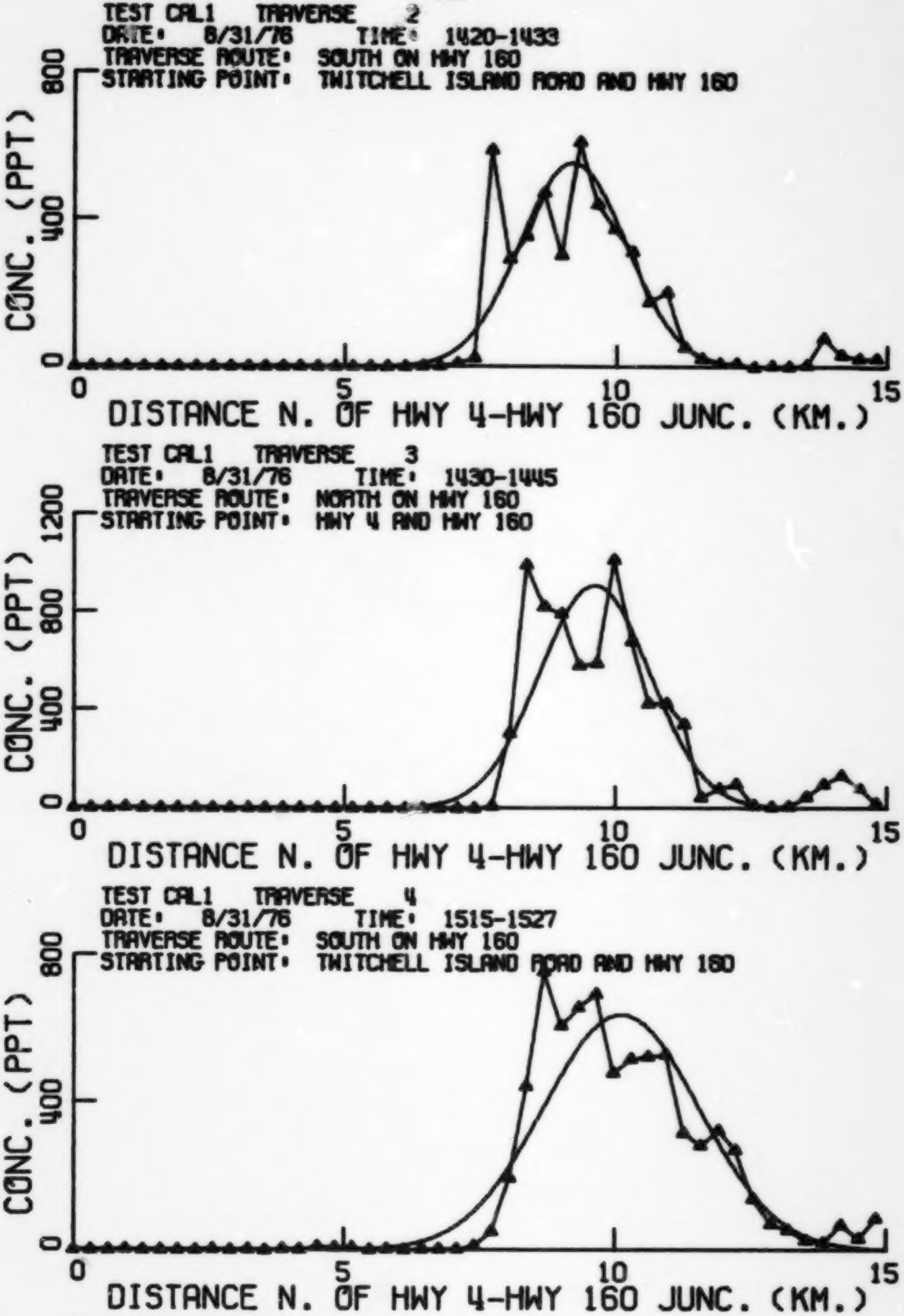

Figure 65. Gaussian best-fit curves through the automobile traverse tracer data.

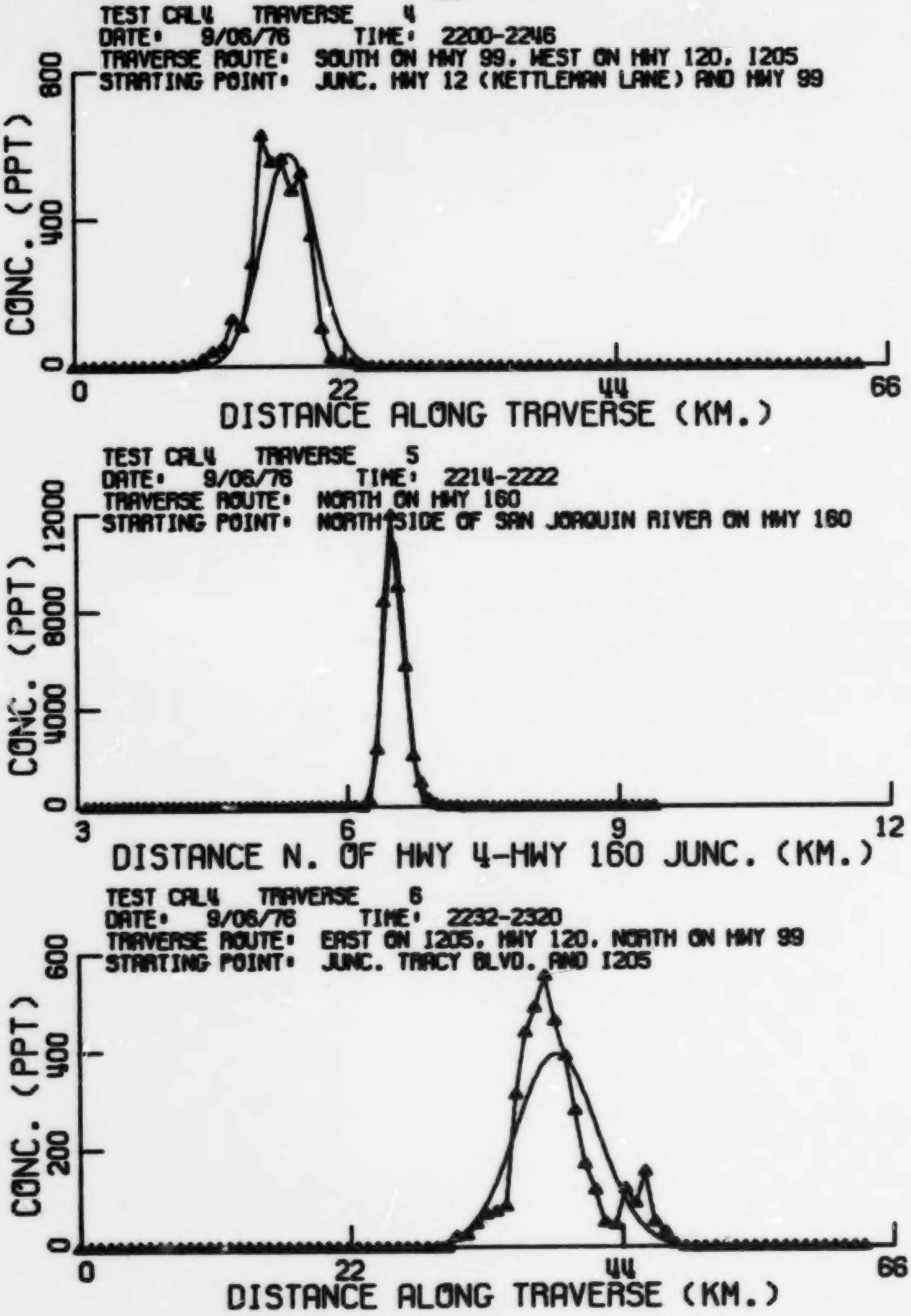

TEST CAL4 TRAVERSE 4
DATE: 9/06/76 TIME: 2200-2246
TRAVERSE ROUTE: SOUTH ON HWY 99, WEST ON HWY 120, I205
STARTING POINT: JUNC. HWY 12 (KETTLEMAN LANE) AND HWY 99

TEST CAL4 TRAVERSE 5
DATE: 9/06/76 TIME: 2214-2222
TRAVERSE ROUTE: NORTH ON HWY 160
STARTING POINT: NORTH SIDE OF SAN JOAQUIN RIVER ON HWY 160

TEST CAL4 TRAVERSE 6
DATE: 9/06/76 TIME: 2232-2320
TRAVERSE ROUTE: EAST ON I205, HWY 120, NORTH ON HWY 99
STARTING POINT: JUNC. TRACY BLVD. AND I205

CONC. (PPT)
0
200
400
600
0
22
44
66
DISTANCE ALONG TRAVERSE (KM.)

Figure 66. Gaussian best-fit curves through the automobile traverse tracer data.

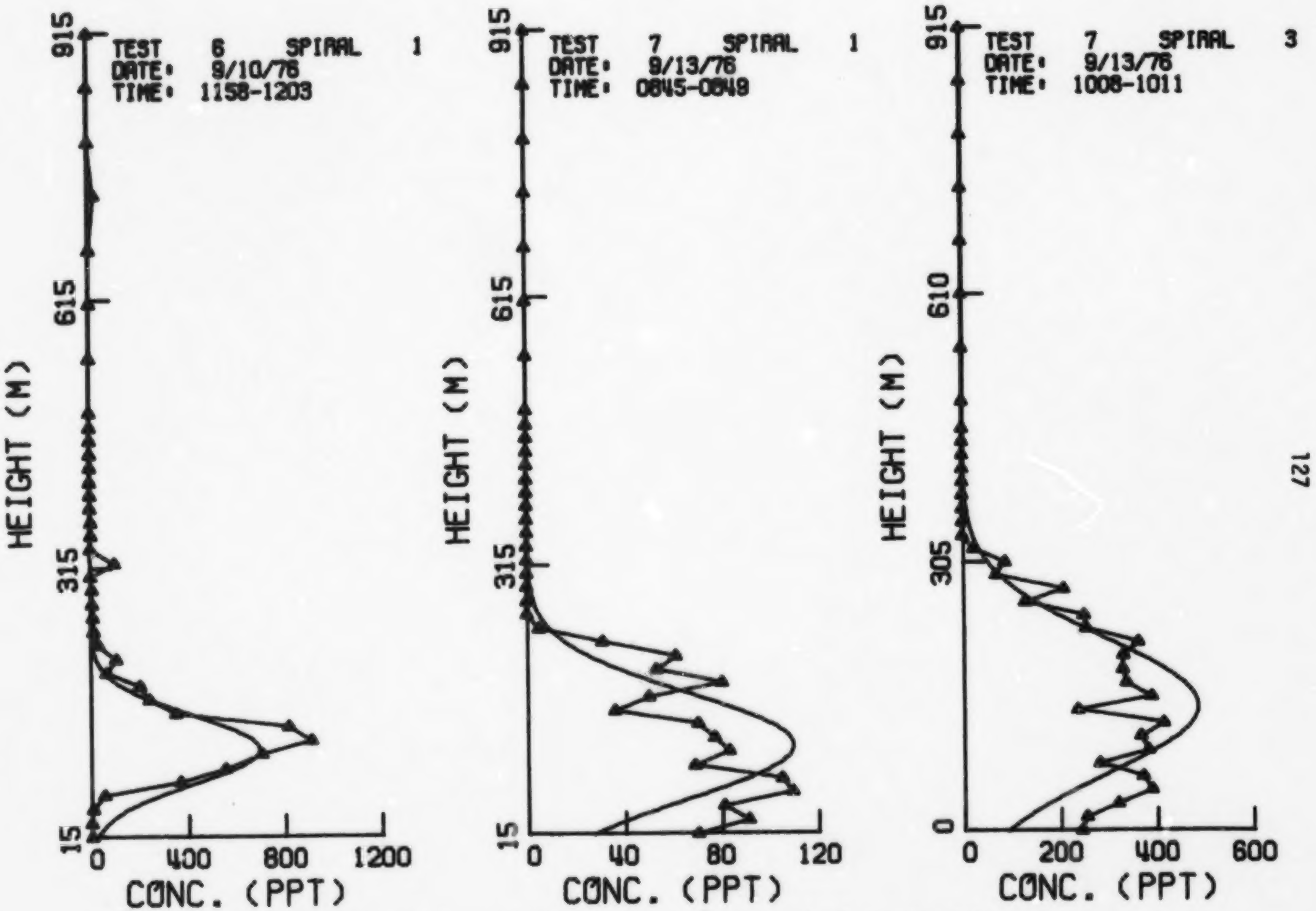

Figure 67. Gaussian best-fit curves through the airborne spiral tracer data.

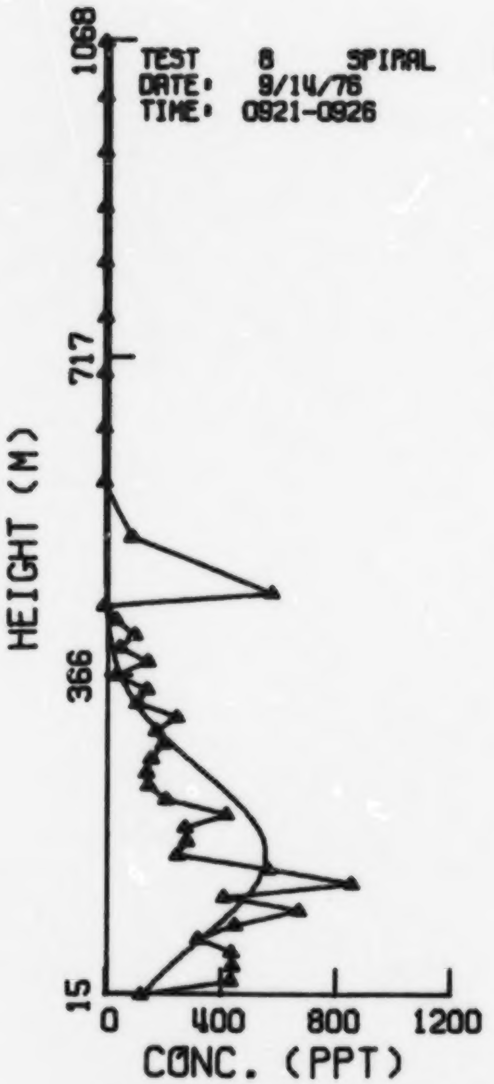

Figure 68. Gaussian best-fit curve through the airborne spiral tracer data.

TABLE 9

BEST-FIT GAUSSIAN CURVE RESULTS

Automobile Traverse Data

	Trav	Time PDT	C_0 exp (PPT)	C_0 fitted (PPT)	Y_0 exp (Km)	Y_0 fitted (Km)	X (km)	σ_y (meters)	σ_z* (meters)
Test 1 (8/31/76) SF_6 Release Rate = 10.6 grams/sec									
	2	1420-1433	611	554	9.3	9.2	7.3	879	200
	3	1430-1445	1013	908	10.0	9.6	8.1	909	118
	4	1515-1527	756	638	8.7	10.1	6.6	1299	126
	6	1630-1641	1223	560	8.0	8.9	6.5	946	198
	7	1701-1753	64	41	65.2	65.8	51.9	9446	626
Test 2 (9/02/76) SF_6 Release Rate = 11.4 g/sec $CBrF_3$ Release Rate = 16.6 g/sec									
	1	1130-1143	30000	21830	5.5	5.9	1.3	312	22
	2	1215-1228	30000	30210	13.8	14.2	0.8	296	17
	4	1400-1415	33	26	11.6	11.6	35.2	2235	
($CBrF_3$)	4	1400-1415	2168	1228	7.7	7.7	10.7	138	657
	5	1445-1503	19	10	10.6	11.4	34.1	2673	
($CBrF_3$)	5	1445-1503	840	510	8.7	9.1	10.0	487	405
	6	1515-1530	28	4	8.7	10.2	32.8	4289	
	7	1545-1635	304	251	6.8	5.0	25.3	115	394
	9	1630-1715	29	12	57.9	60.2	70.9	24950	1169
	10	1630-1737	91	16	48.3	61.2	67.4	10692	1014
($CBrF_3$)	10	1630-1737	300	111	82.1	80.6	57.0	6227	317
	11	1731-1815	32	17	49.1	35.2	73.5	18340	479

---

*Values of σ_z were determined from a mass-balance procedure using the horizontal crosswind traverse data.

TABLE 9 (cont.)

BEST-FIT GAUSSIAN CURVE RESULTS

Automobile Traverse Data

Trav	Time PDT	C_0		Y_0		X (km)	σ_y (meters)	σ_z* (meters)
		exp	fitted	exp	fitted			
		(PPT)		(Km)				
Test 3 (9/5/76) SF_6 Release Rate = 9.5 g/sec								
1	0100-0112	8146	9476	6.1	6.1	7.3	142	35
3	0213-0259	537	458	32.2	34.4	51.7	2480	72
4	0240-0300	1856	1944	7.4	7.4	7.3	141	166
6	0259-0306	8660	4298	6.8	6.8	7.3	136	97
8	0414-0545	370	283	54.7	55.8	47.4	4503	85
9	0430-0445	6178	6775	7.2	7.3	7.3	116	80
10	0432-0517	608	506	29.5	31.3	39.5	1936	100
11	0441-0450	2852	2288	7.1	7.2	7.3	151	183
12	0502-0511	2261	1502	6.6	6.6	7.3	195	229
14	0637-0647	173	121	1.6	0.5	37.2	4685	517
Test 4 (9/6/76) SF_6 Release Rate = 10.8 g/sec								
1	1928-1946	873	710	7.1	7.2	7.3	210	
2	2130-2217	746	680	15.3	15.8	50.9	2072	93
3	2132-2140	10570	8825	7.1	7.2	7.3	191	45
4	2200-2246	628	580	15.3	17.5	50.9	1987	109
5	2214-2222	11900	10820	6.5	6.5	7.3	118	59
6	2232-2320	553	396	37.8	38.7	54.5	2787	114
7	2315-2400	553	281	35.4	39.9	58.8	3819	142

*Values of σ_z were determined from a mass-balance procedure using the horizontal crosswind traverse data.

TABLE 9 (cont.)

BEST-FIT GAUSSIAN CURVE RESULTS

Automobile Traverse Data

Trav	Time PDT	C_o exp	C_o fitted	Y_o exp	Y_o fitted	X (km)	σ_y (meters)	σ_z[*] (meters)
		(PPT)		(Km)				
Test 5 (9/9/76) SF_6 Release Rate = 10.7 g/sec								
1	1255-1315	801	363	11.9	12.6	9.1	721	
2	1314-1330	528	288	8.4	8.9	9.4	877	
4	1351-1405	138	136	1.0	1.4	17.7	1192	
5	1356-1428	108	87	2.9	1.1	24.3	2416	
6	1359-1416	445	285	18.3	15.8	10.6	1636	1228
7	1413-1426	141	111	8.7	9.5	18.5	1525	
8	1436-1450	183	131	3.9	4.2	18.6	1382	
Test 6 (9/10/76) SF_6 Release Rate								
1	0800-0815	9526	21500	1.8	1.8	4.8	27	196
2	0740-0753	7981	9257	6.6	6.5	7.3	110	110
3	1001-1051	20	10	59.5	56.8	47.6	4164	
4	1023-1033	3739	2393	6.0	6.1	11.7	275	135
5	1030-1115	11	11	59.5	60.3	47.6	3062	
6	1022-1033	5954	4179	7.6	7.6	7.3	129	165
7	1103-1112	7155	6346	7.5	7.5	7.3	185	76
8	1105-1203	12	10	1.6	4.7	45.8	2975	
Airborne Spirals								
				(m)	(m)		σ_z[**]	
1	1158-1203	908	692	122	112	19.5	38	

---

[*] Values of σ_z were determined from a mass-balance procedure using the horizontal crosswind traverse data.

[**] Values of σ_z were obtained from a Gaussian best-fit of the spiral tracer data.

TABLE 9 (cont.)

BEST-FIT GAUSSIAN CURVE RESULTS

Automobile Traverse Data

Test 7 (9/13/76) SF_6 Release Rate = 11.5 g/sec
$CBrF_3$ Release Rate = 16.0 g/sec

	Trav	Time PDT	C_0 exp	C_0 fitted (PPT)	Y_0 exp	Y_0 fitted (Km)	X (km)	σ_y (meters)	σ_z* (meters
	1	0924-0956	614	459	33.8	37.2	15.3	3714	1388
($CBrF_3$)	2	0940	12140	5896	1.7	1.5	4.6	310	106
	3	1113-1217	94	60	48.3	52.3	50.7	4697	736
	4	1130-1146	180	151	24.1	25.1	22.0	6165	3481
	6	1340-1414	131	87	30.6	23.0	22.4	6944	792
	7	1429-1451	14	15	14.5	19.6	47.4	3881	
	8	1450-1706	200	95	29.0	27.8	5.6	375	492
	8	1450-1706	30	21	141.6	140.9	54.7	13203	
	9	1458-1532	12	10	9.7	8.5	52.7	1654	
	10	1537-1611	16	12	22.5	29.0	22.9	6746	
	11	1654-1820	12	7	117.5	118	65.9	14520	
	12	1654-1820	13	11	24.1	13.6	42.8	9881	
				Spirals					
					(m)	(m)		σ_z**	
	1	0854-0849	109	109	61	113	21.5	59	
	3	1008-1011	413	485	122	141	21.5	77	

*Values of σ_z were determined from a mass-balance procedure using the horizontal crosswind traverse data.

**Values of σ_z were obtained from a Gaussian best-fit of the spiral tracer data.

TABLE 9 (cont.)

BEST-FIT GAUSSIAN CURVE RESULTS

Automobile Traverse Data

Trav	Time PDT	C_0 exp (PPT)	C_0 fitted (PPT)	Y_0 exp (Km)	Y_0 fitted (Km)	X (km)	σ_y (meters)	σ_z* (meters)
Test 8 (9/14/76) SF_6 Release Rate = 10.9 g/sec								
1	0906-0931	1598	1461	19.3	19.9	14.4	713	273
2	0941-1007	412	440	16.9	17.2	15.7	953	
3	1047-1151	78	80	49.9	45.2	48.9	4604	380
4	1154-1220	129	103	12.9	11.6	18.4	1016	
Spirals								
				(m)	(m)		σ_z**	
1	0921-0926	858	541	137	169	21.5	91	

---

* Values of σ_z were determined from a mass-balance procedure using the horizontal crosswind traverse data.

**Values of σ_z were obtained from a Gaussian best-fit of the spiral tracer data.

4.4 Mass Balance of Tracer Data

The integration of the automobile and airborne traverse data over the crosswind traverse distance can be used to determine the average flux of tracer gas passing through the traverse vertical plane. This flux can then be compared to the amount of tracer released at the source to provide a mass balance on the experimental data:

$$\%\text{ tracer observed} = \left(\frac{\int_{-\infty}^{\infty} \int_{0}^{L} u(z) C(y,z)\, dz\, dy}{Q} \right) \cdot 100 \qquad (7)$$

where Q is the release rate, L is the height of the mixing layer, u(z) is the wind velocity, and C(y,z) is the tracer concentration. The accuracy of this mass balance is obviously subject to the uncertainties involved in determining the vertical profiles of the wind speed and tracer concentration. This expression may be simplified by considering a constant average wind velocity, $u(z) = \bar{u}$, and a uniform vertical tracer distribution, $C(z,y) = \bar{C}(y)$, over a height ℓ. For convenience in treating the data, the double integral is approximated by a series of single integrals:

$$\%\text{ tracer observed} = \bar{u} \sum_{i=1}^{n} \ell_i \left(\int_{-\infty}^{\infty} \bar{C}(y)\, dy \right)_i \cdot \frac{100}{Q} \qquad (8)$$

where $\sum_{i}^{n} \ell_i$ equals the height of the mixing layer. In the following calculations, $\bar{u}$ was obtained by vector averaging the available hourly wind data from points downwind of the source and the average mixing height was also obtained from the available data. For cases where only surface tracer data were available, we took n=1 and assumed that the tracer was vertically well-mixed from the surface to the height of the mixing layer, ℓ=L. Where traverse data were available at more than one height, n was taken to be the number of traverses and ℓ_i was taken to be a height arbitrarily assigned to each crosswind traverse. In this case, the tracer was assumed to be vertically well-mixed over a discrete portion of the mixing layer.

During Test 7 and 8, two sets of airborne traverses provided data for using the expression $n > 1$. In both cases, the mass balance results were remarkably accurate; the estimates of 113% and 102% of the tracer observed for Traverses 8, 9, 11 (Test 7) and for Traverses 4, 5, 6 (Test 8) give an indication of the usefulness of deriving the mass balance in this manner.

In many cases, particularly for automobile traverses close to the source, assuming a uniform vertical concentration distribution widely overestimates the flux of tracer. For this reason, we have performed the mass balance only where airborne data were available or transport distances were large. The results are given in Table 10.

In view of the assumptions necessary for the analysis, the mass balance results are very good. During the daytime tests when the extent of vertical mixing was the greatest, the results generally are no more than a factor of 2 over 100% of the tracer observed. In cases where the results are too low, closer examination of the traverses indicates that, in most cases, the traverses did not cover the entire plume. For example, in Test 2, Traverses 4, 5, and 6 were taken along Highway 160 where it appears that the SF_6 tracer plume was wider than the traverse paths.

The mass balance analysis can be reversed by assuming 100% of the tracer was observed and by predicting either the mixing height or wind velocity necessary to achieve this condition. These results are also given in Table 10. In traverses where the mass balance was overestimated, the predicted mixing height gives an indication of the extent of vertical mixing which did occur. During Tests 3 and 4 under nighttime stable conditions, the predicted heights are approximately between 100 and 200 meters while the estimated mixing height was between 500 and 800 meters. Although no airborne data were available, one can assume from the mass balance results that the plume remained within the lowest 100-200 meters of the atmosphere. Even though the estimated mixing heights were relatively low, the extent of vertical mixing of the tracer plume was not great enough to be influenced by the depth of the mixing layer. During nighttime conditions, the tracer was not well-mixed in the vertical direction even at downwind distances of 50 km.

Another means of determining the extent of vertical mixing is to solve the transient diffusion equation and estimate the distance in the vertical direction to which tracer diffuses. This leads to the approximation:

$$\frac{K_{zz}t}{L_z^2} \sim 1 \qquad (9)$$

or

$$L_z = \sqrt{K_{zz}t} \qquad (10)$$

where K_{zz} is the vertical eddy diffusivity, t is the transport time and L_z is the vertical distance to which tracer diffuses. Values of L_z can be calculated if one assumes that

$$\sigma_z = \sqrt{2K_{zz}t} \tag{11}$$

which is obtained from comparing the solution of the diffusion equation with the Gaussian plume model expression (Seinfeld, 1975).

Substituting for $K_{zz}t$ gives

$$L_z = \frac{\sigma_z}{\sqrt{2}} \tag{12}$$

where σ_z can be determined from the automobile traverse data. For example, using Test 3, Traverse 3 data, we take σ_z to equal 72 meters and calculate that L_z equals 51 meters. Thus, the tracer only diffuses to 51 meters over a transport distance of 52 km. The estimated depth of the mixing layer during this time was 700 meters.

The overall average % of tracer observed as given in Table 10 indicates that essentially all of the tracer released was accounted for in the traverse tracer data. During the daytime hours, the plumes appear to be relatively well-mixed in the vertical direction at downwind distances of 30 km or more. Results from the evening and nighttime tests indicate that the plumes were not vertically well-mixed even at downwind distances of 50 km. We have already seen in the individual test summaries that tracer concentrations measured during the evening and nighttime tests were much higher than concentrations observed during the daytime. The mass balance results confirm the description of evening and nighttime plumes as being narrow and having extremely low rates of dispersion with travel distance.

TABLE 10

TRACER MASS BALANCE RESULTS

Trav	Time	X (km)	L (m)	u (m/sec)	% tracer observed	L_{pred} (m)	u_{pred} (m/sec)
Test 1 (8/31/76)							
7*	1701-1753	51.9	1600	295/3.5	204	784	1.7
Test 2 (9/2/76)							
4*	1400-1415	35.2	780	290/6.2	36	2167	17.2
4	1400-1415	10.7	780	290/6.2	74($CBrF_3$)	1053	8.4
5*	1445-1503	34.1	980	290/6.2	20	4900	31.0
5	1400-1415	10.0	980	290/6.2	134($CBrF_3$)	731	4.6
6*	1515-1530	32.8	980	290/6.8	14	7000	49
7	1545-1635	25.3	1180	290/5.4	239	494	2.3
9*	1630-1715	70.9	1500	290/4.6	110	1364	4.2
10*	1630-1737	67.4	1500	300/4.2	121	1240	3.5
10	1630-1737	57.0	1500	300/4.2	331($CBrF_3$)	416	1.2
11*	1731-1815	73.5	1500	290/4.8	250	600	1.9
				AVE.	136		
Test 3 (9/5/76)							
3	0213-0259	51.7	700	280/6.2	774	90	0.8
8	0414-0545	47.4	690	280/4.7	649	106	0.7
10	0432-0517	39.5	700	270/5.2	558	125	0.9
14*	0637-0647	37.2	740	306/3.3	118	627	2.8
				AVE.	525		

---

* Traverse data indicate that only a portion of the plume was traversed.

TABLE 10 (cont.)

TRACER MASS BALANCE RESULTS

Trav	Time	X (km)	L (m)	u (m/sec)	% tracer observed	L_{pred} (m)	u_{pred} (m/sec)
Test 4 (9/6/76)							
2	2130-2217	50.9	600	280/4.4	515	117	0.9
4	2200-2248	50.9	600	270/4.6	440	136	1.0
6	2232-2320	54.5	570	270/4.6	400	143	1.2
7	2315-2400	58.8	545	300/3.8	307	178	1.2
				AVE.	416		
Test 5 (9/9/76)							
1	1255-1315	9.4	3000	31/1.8	198	1515	0.9
2	1314-1330	9.4	3000	31/1.8	189	1587	1.0
4*	1351-1405	17.7	3000	9/1.1	66	4545	1.7
5*	1356-1428	24.3	3000	338/0.8	47	6383	1.7
6	1359-1416	10.6	3000	252/1.0	195	1538	0.5
7	1413-1426	18.5	3000	338/0.8	53	5660	1.5
8	1436-1450	18.6	3000	338/0.8	61	4918	1.3
				AVE.	116		
Test 6 (9/10/76)							
3*	1001-1051	47.6	540	115/1.1	3	18000	37
5*	1030-1115	47.6	810	272/1.1	4	20000	28
8*	1106-1203	45.8	930	270/2.1	7	13000	30
Airborne							
4	1044-1052	37.2	810	260/5.5	89	909	6.2
10	1000-1039	43.3	540	260/5.5	15	3666	37
12	1200-1239	43.8	1200	270/3.0	21	5669	14
				AVE.	23		

TABLE 10(cont.)

TRACER MASS BALANCE RESULTS

Trav	Time	X (km)	L (m)	u (m/sec)	% tracer observed	L_{pred} (m)	u_{pred} (m/sec)
Test 7 (9/13/76)							
1	0924-0956	15.3	300	230/1.5	95	316	1.6
3	1113-1217	50.7	1475	290/3.0	160	922	1.9
4*	1130-1146	22.0	400	290/2.8	70	571	4.0
6	1340-1414	22.4	1500	230/1.3	151	993	0.9
7	1429-1451	47.4	1100	310/4.1	33	3333	12.4
8	1450-1706	54.7	1500	270/4.5	243	617	1.9
9	1458-1522	52.7	960	280/3.6	7	14000	51
10	1537-1611	22.9	1500	280/3.5	56	2679	6.3
11*	1654-1820	65.9	545	260/4.5	24	2271	18.7
12*	1835-1901	42.8	500	260/4.8	30	1667	16.0
				AVE.	87		
Airborne							
6	0945-0958	17.1	300	310/0.9	8	3807	11.4
8	1327-1343	61.6	244=ℓ_1	280/1.7	4		
9	1348-1404	61.4	122=ℓ_2	280/1.7	3	113 total	
11	1428-1456	61.7	2134=ℓ_3 L=2500	290/1.3	106	2212	1.5
12	1759-1812	72.7	2500	280/4.2	120	2079	3.5
				AVE.	80		

TABLE 10 (cont.)

TRACER MASS BALANCE RESULTS

Trav	Time	X (km)	L (m)	u (m/sec)	% tracer observed		L_{pred} (m)	U_{pred} (m/sec)
Test 8 (9/14/76)								
1	0906-0931	14.4	350	270/2.2	110		318	2.0
2	0941-1007	15.7	480	270/2.2	61		787	3.6
3	1047-1151	48.9	800	240/4.2	168		476	2.5
4	1154-1218	18.4	300	270/3.1	13		2308	23.8
				AVE.	88			
Airborne								
3	0858-0911	17.4	350	270/3.6	18		1951	20.1
4	0942-0955	17.4	$114=\ell_1$	220/3.6	2			
5	0959-1012	17.2	$122=\ell_2$	190/6.3	20	102 total		
6	1016-1028	17.2	$244=\ell_3$	190/6.3	80		471	6.2
			L=480	AVE.	60			

Overall Average: 154% of tracer
observed in 51 crosswind traverses

With Tests 3 and 4 omitted,
Overall Average: 95% of tracer
observed in 43 crosswind traverses

4.5 Analysis of Dispersion

The results of the Gaussian best-fit procedure for the automobile traverse data can be used to determine the relationship of the dispersion parameters, σ_y and σ_z, to the transport distance, x. In terms of the usual dispersion coefficients, these relationships are given by

$$\sigma_y = ax^b \tag{13}$$

and

$$\sigma_z = cx^d \tag{14}$$

where x is taken to be in meters. The values of the coefficients a, b and c, d can be found by plotting each dispersion parameter as a function of x and determining a linear least-squares fit to the data. Typical results of this calculation are shown in Figures 69 - 72; dispersion data for every tracer test are given in Volume II, Part A, Section 3.11. The dispersion coefficients associated with each tracer release are listed in Table 11.

We have considered only the automobile traverse data in this analysis. The results for Tests 2 and 7 were determined separately for each of the release points. Generally, the scatter in the σ_y data is reasonably small, and the best-fit lines provide good representations of the dispersion data. The best-fit of Test 2 data does not include two points at 0.8 km; effects of the local terrain appear to dominate the dispersion at close downwind distances. In the Test 7 results, the scatter is larger and the line serves only as a rough approximation to the data. During Test 7, no single well-defined plume was observed; tracer released from Pinole diverged widely across the Delta Region and into the Livermore-Stockton area. Automobile traverses in several cases did

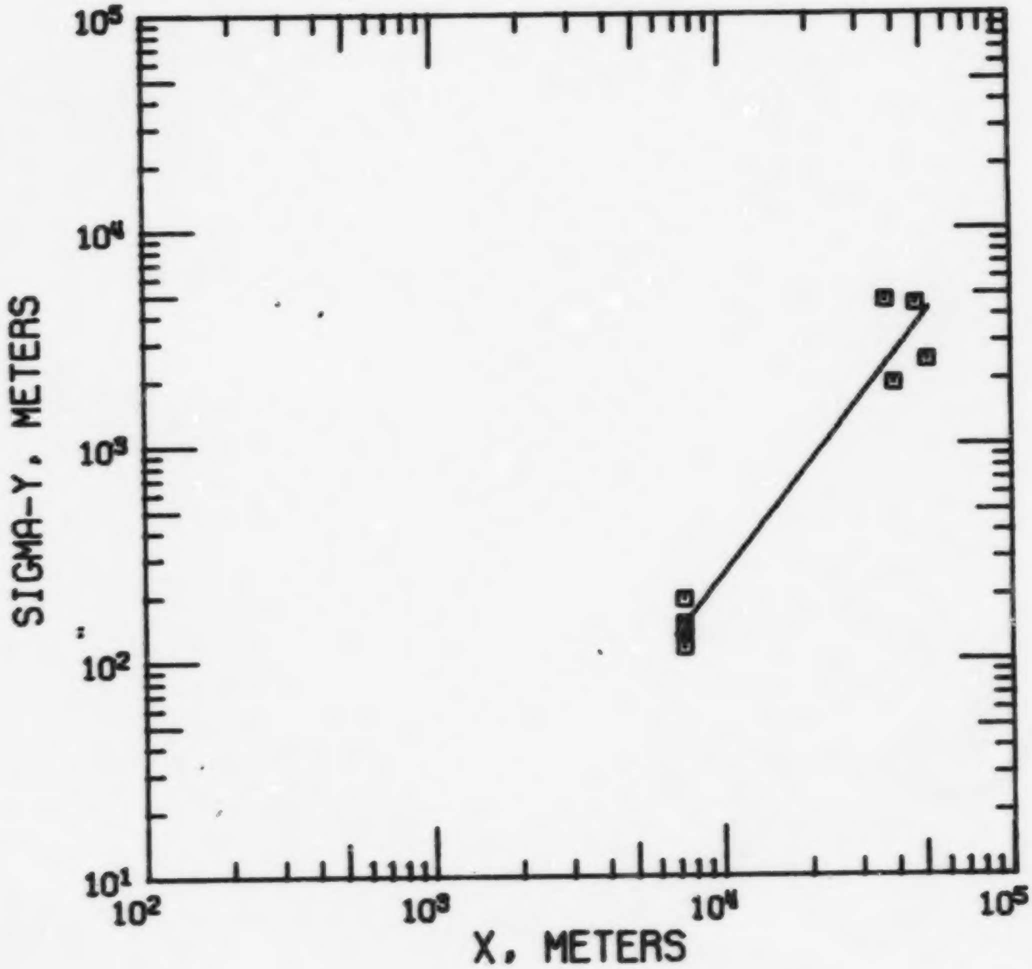

CAL. DELTA TEST 3

Dow Auto Traverse

Figure 69. Horizontal crosswind dispersion parameter, σ_y, as a function of distance downwind of the Dow site.

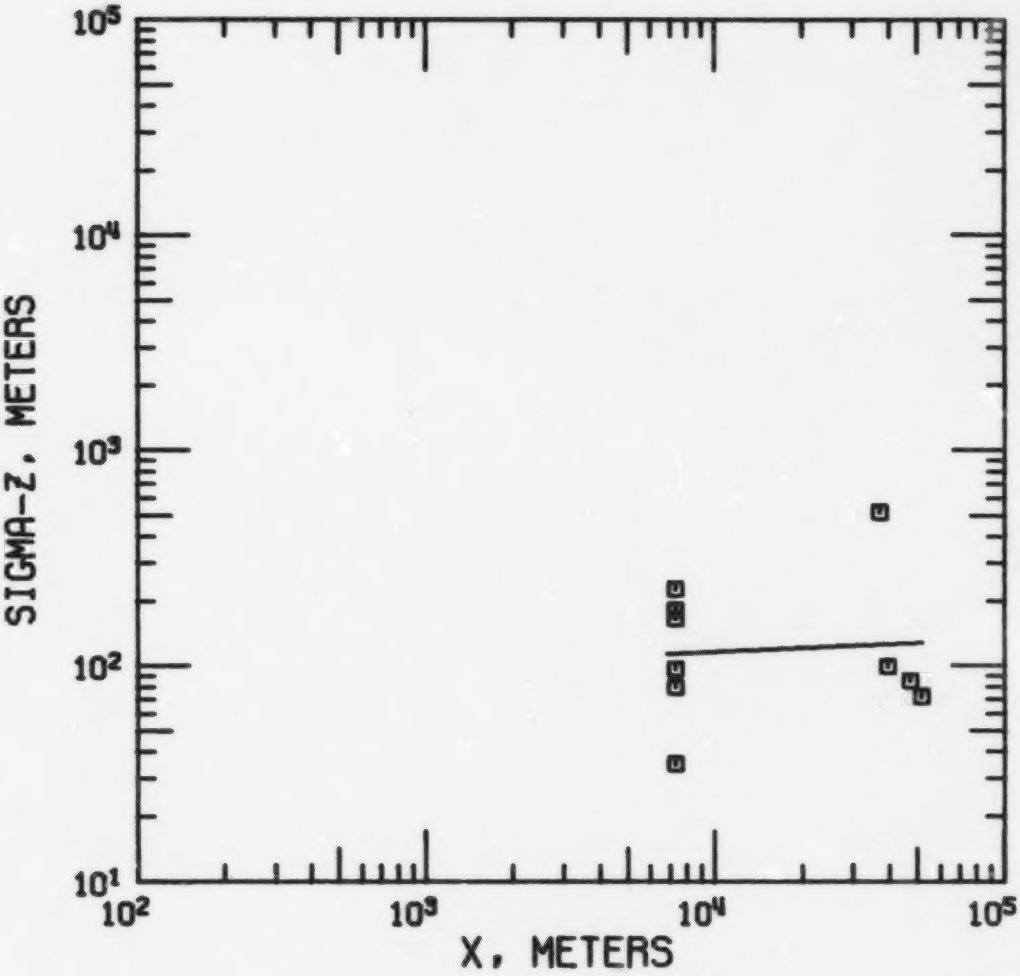

CAL. DELTA TEST 3

Dow Auto Traverse

Figure 70. Vertical crosswind dispersion parameter, σ_z, as a function of distance downwind of the Dow site.

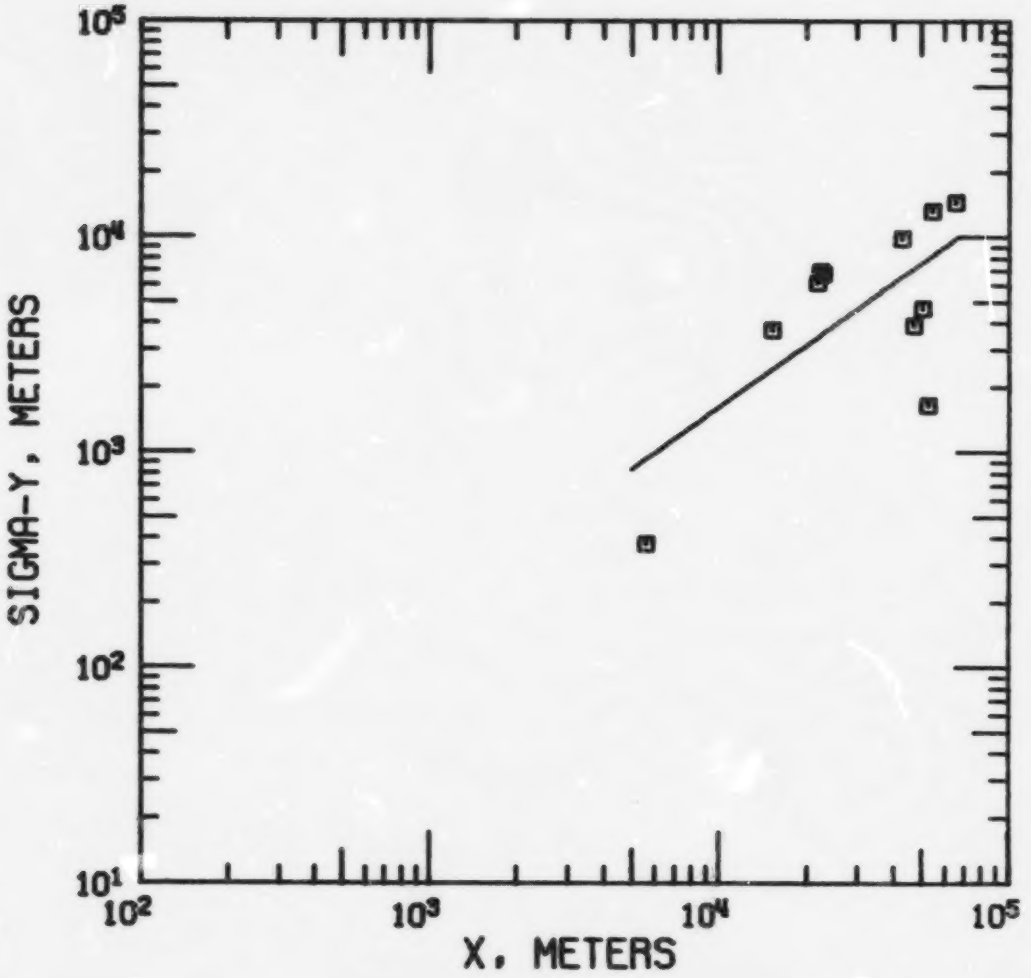

CAL. DELTA TEST 7

Pinole Auto Traverse

Figure 71. Horizontal crosswind dispersion parameter, σ_y, as a function of distance downwind of Pinole.

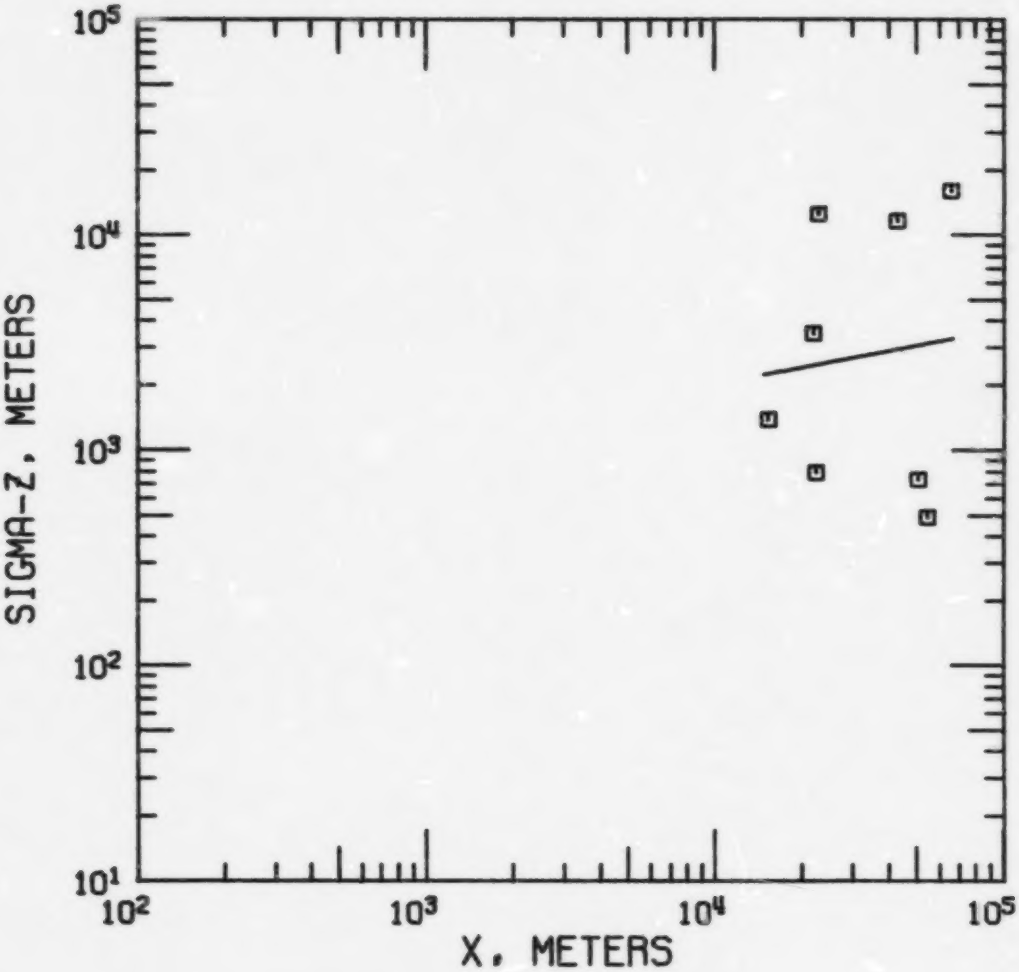

CAL. DELTA TEST 7

Pinole Auto Traverse

Figure 72. Vertical crosswind dispersion parameter, σ_z, as a function of distance downwind of Pinole.

TABLE 11

HORIZONTAL CROSSWIND DISPERSION COEFFICIENTS

$$\sigma_y = a\,X^b$$

Test, Release Point	a m^{1-b}	b	σ (std. dev. about best-fit line)* (m)
Test 1, Dow	$5.31 \cdot 10^{-2}$	1.11	284
Test 2, Dow	$1.12 \cdot 10^{-5}$	1.84	230
Test 2, Martinez	$1.31 \cdot 10^{-8}$	2.50	3710
Test 3, Dow	$3.71 \cdot 10^{-5}$	1.71	1030
Test 4, Dow	$8.17 \cdot 10^{-4}$	1.37	428
Test 5, Dow	$7.09 \cdot 10^{-1}$	0.784	362
Test 6, Dow	$6.52 \cdot 10^{-6}$	1.87	331
Test 7, Dow	-	-	
Test 7, Pinole	$2.40 \cdot 10^{-1}$	0.958	3850
Test 8, Pinole	$5.33 \cdot 10^{-4}$	1.48	75

$$*\ \sigma = \left[\frac{\sum_{i=1}^{n} (\sigma_{y_i} - \sigma_y)^2}{n-1}\right]^{1/2}$$ where σ_{y_i} are the data points and $\sigma_y = aX^b$

Meteorological Period, Release Point	a	b	σ (m) (std. dev. about best-fit line)
Pre-Sea Breeze, Dow	$8.34 \cdot 10^{-5}$	1.62	344
Pre-Sea Breeze, Pinole	$4.54 \cdot 10^{-2}$	1.08	1960
Sea Breeze, Dow	$4.74 \cdot 10^{-2}$	1.07	1230
Sea Breeze, Martinez	$1.31 \cdot 10^{-8}$	2.50	3710
Sea Breeze, Pinole	$4.06 \cdot 10^{-2}$	1.12	4330
Sea Breeze, Pinole & Martinez	$3.57 \cdot 10^{-3}$	1.34	5050
Sea Breeze Tail, Dow	$8.17 \cdot 10^{-4}$	1.37	428
Nighttime, Dow	$3.71 \cdot 10^{-5}$	1.71	1030

TABLE 11 (cont.)

Pasquill Stability Class	a[*]	b[*]
A (very unstable)	0.40	0.85
B (unstable)	0.40	0.87
C (slightly unstable)	0.23	0.89
D (neutral)	0.14	0.89
E (slightly stable)	0.11	0.89
F (stable)	0.072	0.89

[*] Determined from dispersion curves given by Turner (1970); x is taken to be in meters.

TABLE 11 (cont.)

VERTICAL CROSSWIND DISPERSION COEFFICIENTS

$$\sigma_z = c\, X^d$$

Test, Release Point	c m^{1-b}	d	σ (std. dev. about best-fit line)* (m)
Test 1, Dow	$3.37 \cdot 10^{-1}$	0.681	45
Test 2, Dow	-	-	-
Test 2, Martinez	$6.61 \cdot 10^{-2}$	0.847	246
Test 3, Dow	$6.83 \cdot 10^{1}$	0.0582	146
Test 4, Dow	1.46	0.400	14
Test 5, Dow	-	-	-
Test 6, Dow	-	-	-
Test 7, Dow	-	-	-
Test 7, Pinole	$1.90 \cdot 10^{2}$	0.257	5228
Test 8, Pinole	-	-	-

$$* \sigma = \left[\frac{\sum_{i=1}^{n} (\sigma_{z_i} - \sigma_z)^2}{n-1}\right]^{1/2}$$ where σ_{z_i} are the data points and $\sigma_z = cX^d$

- -

Meteorological Period, Release Point	c	d	σ (m) (std. dev. about best-fit line)
Pre-Sea Breeze, Dow	-	-	-
Pre-Sea Breeze, Pinole	-	-	-
Sea Breeze, Dow	4.93	0.424	194
Sea Breeze, Martinez	$6.61 \cdot 10^{-2}$	0.847	246
Sea Breeze, Pinole	$4.96 \cdot 10^{1}$	0.414	8529
Sea Breeze, Pinole & Martinez	$2.52 \cdot 10^{-2}$	1.04	6570
Sea Breeze Tail, Dow	1.46	0.400	14
Nighttime, Dow	$6.83 \cdot 10^{1}$	0.0582	146

TABLE 11 (cont.)

*$\sigma_z = \exp[a_0 + a_1 \ln X + a_2 (\ln X)^2 + a_3 (\ln X)^3]$

Pasquill Stability Class	a_0	a_1	a_2	a_3
A (very unstable)	6.10	2.11	0	0
B (unstable)	4.70	1.09	$9.12 \cdot 10^{-3}$	$-2.14 \cdot 10^{-3}$
C (slightly unstable)	4.10	0.940	$-7.56 \cdot 10^{-3}$	$2.86 \cdot 10^{-4}$
D (neutral)	3.46	0.662	$-1.28 \cdot 10^{-2}$	$-1.12 \cdot 10^{-3}$
E (slightly stable)	3.12	0.592	$-9.61 \cdot 10^{-3}$	$-4.24 \cdot 10^{-3}$
F (stable)	2.63	0.651	$-6.08 \cdot 10^{-2}$	$2.03 \cdot 10^{-3}$

*Best-fit expression for Pasquill dispersion curves, determined from Turner (1970); x is taken to be in kilometers.

not appear to cross the entire width of the plume. The scatter in the vertical dispersion data is generally worse than that for the horizontal dispersion data. This can be attributed to the dependence of the accuracy of σ_z upon estimations of the mixing height and average wind speed.

The automobile traverse data can be grouped into the four meteorological periods based upon the time of the traverse. Data from Tests 1, 2 and the latter part of Test 7 (7-5 through 7-12) were obtained during the Sea Breeze period. Traverses during Tests 6, 7 (7-1 through 7-4) and 8 occurred during the Pre-Sea Breeze period. Tests 3 and 4 were conducted during the Nighttime and Sea Breeze Tail periods, respectively. Typical horizontal and vertical dispersion data for the meteorological periods are presented in Figures 73 - 78. The remainder of the data is shown in Volume II, Section 3.11, Part A. Data for the Martinez and Pinole tracer releases have been plotted together to represent a northeastern Bay Area source. The dispersion coefficients of the best-fit lines for the meteorological periods are given in Table 11. Grouping data from different test days together increases the scatter about the best-fit lines. Scatter in the horizontal data for the combined Pinole-Martinez plot does not appear excessive; the scatter in the vertical data is worse. The best-fit lines generally give a reasonable approximation of the dispersion data.

The horizontal and vertical dispersion characteristics of the atmosphere during the study period are compared to the empirical dispersion relationships associated with the standard Pasquill stability classes as given by Turner (1970) in Figures 79 - 92 for each tracer test.

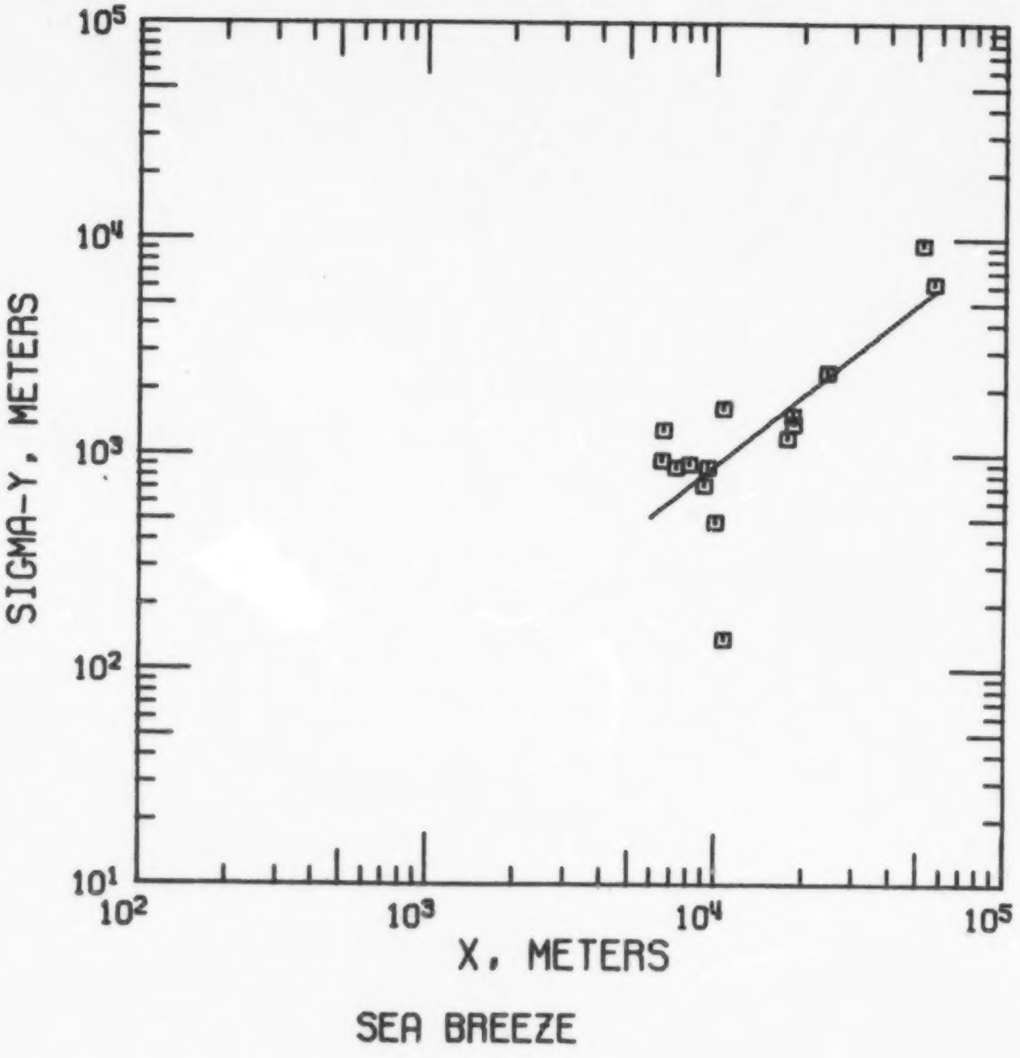

Dow Auto Traverse

Figure 73. Horizontal crosswind dispersion parameter, σ_y, as a function of distance downwind of the Dow site.

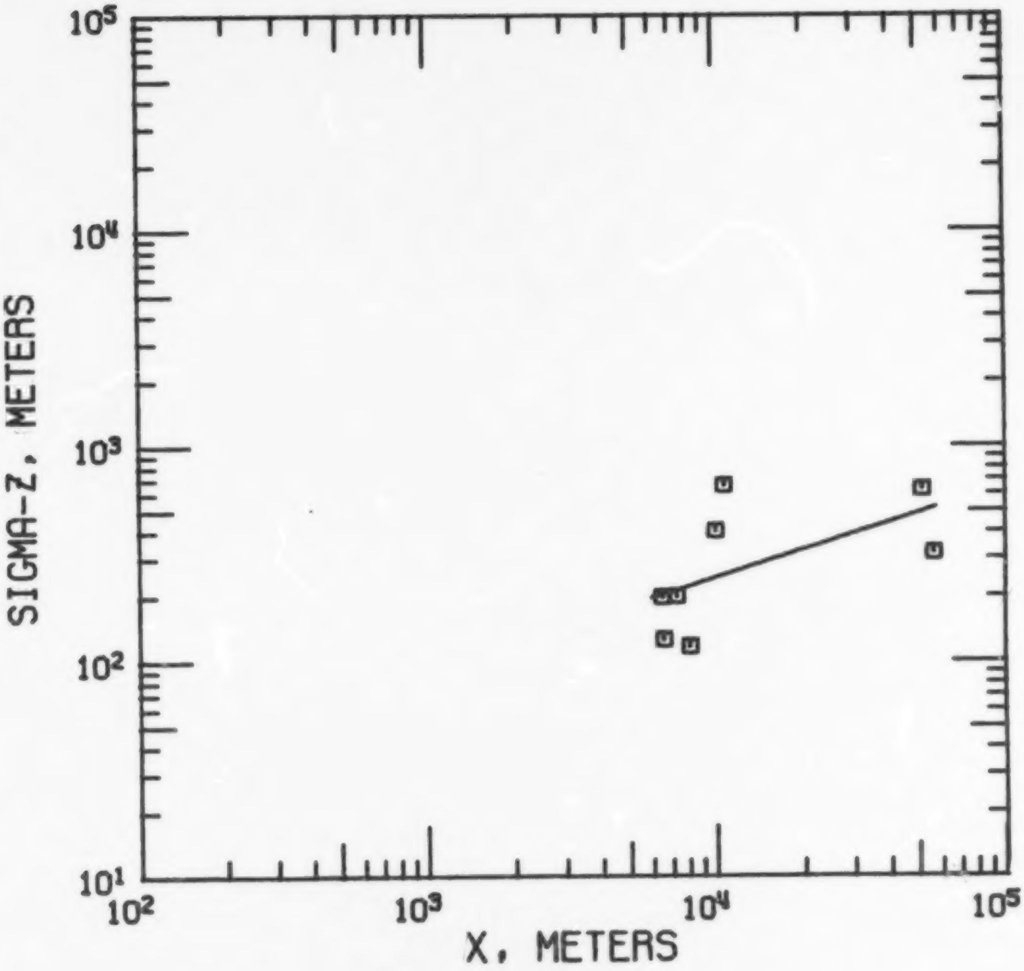

SEA BREEZE

DOW AUTO TRAV.

Figure 74. Vertical crosswind dispersion parameter, σ_z, as a function of distance downwind of the Dow site.

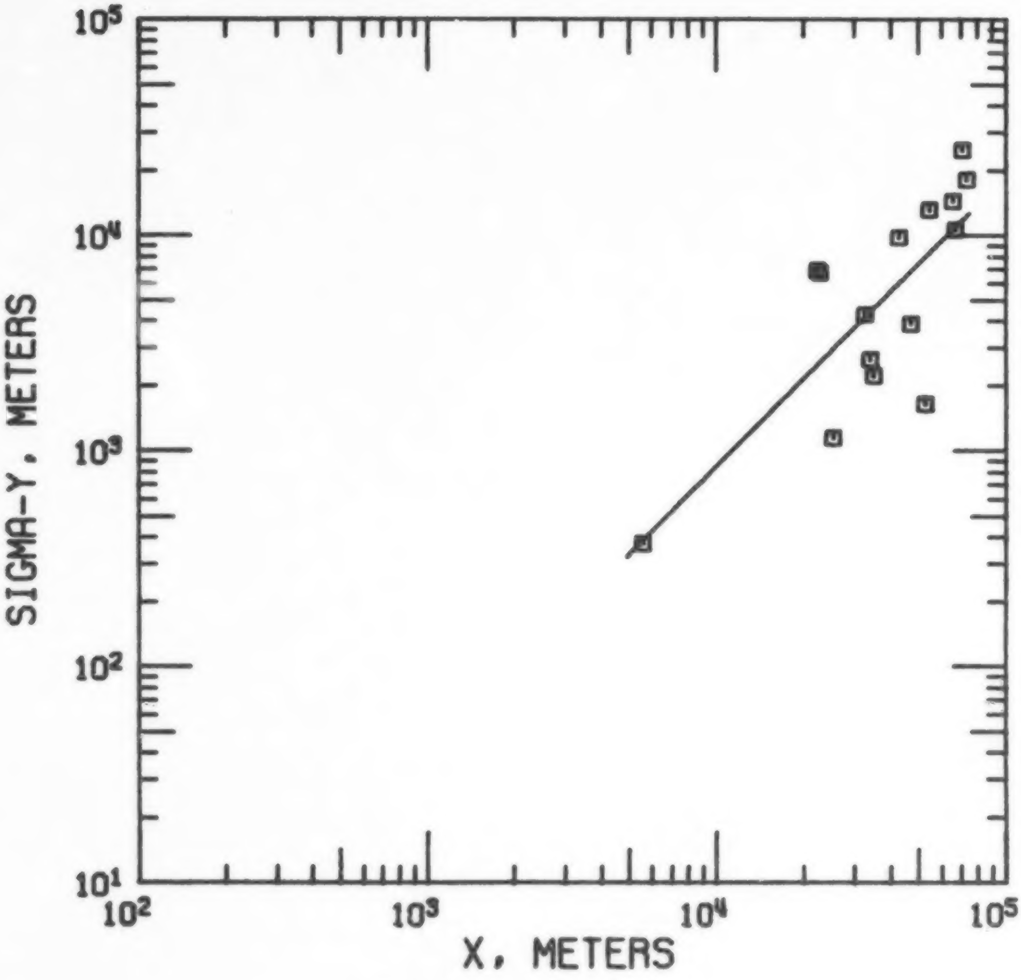

SEA BREEZE

Pinole-Martinez Auto Traverse

Figure 75. Horizontal crosswind dispersion parameter, σ_y, as functions of distance downwind of Pinole and Martinez.

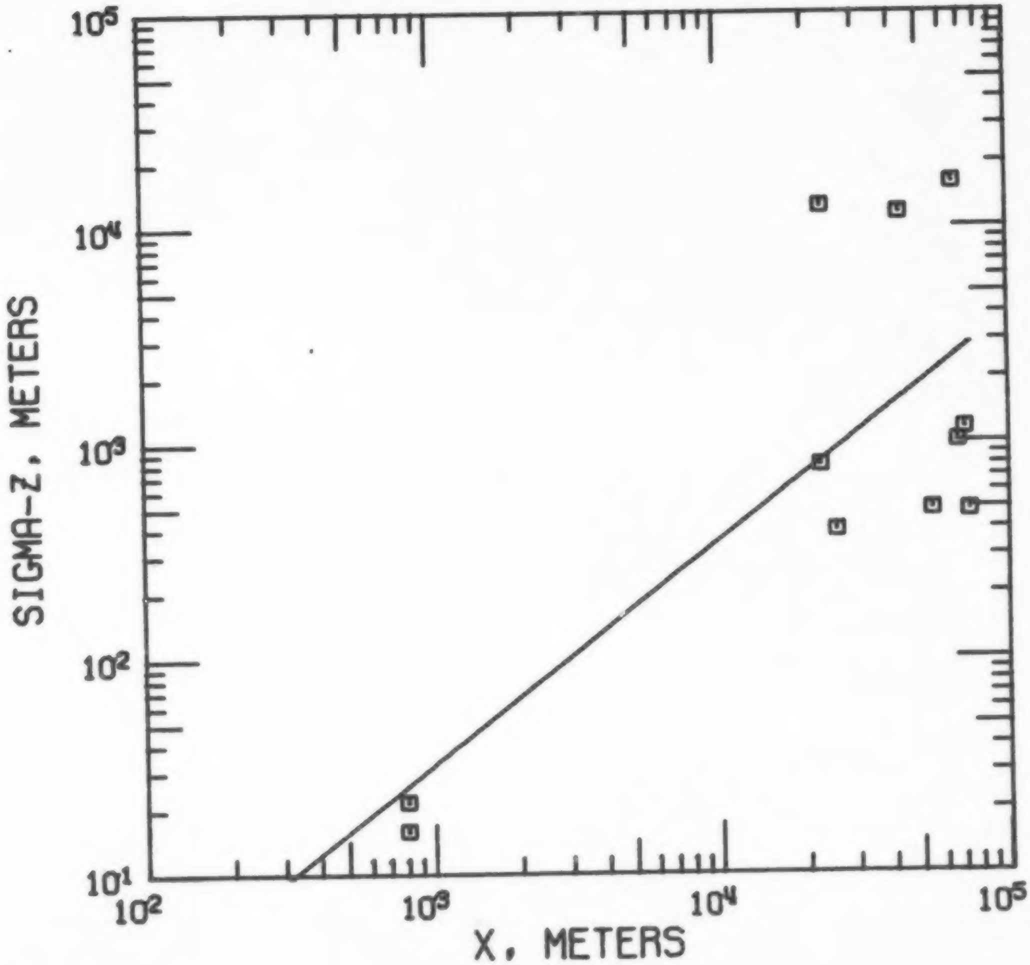

SEA BREEZE
PINOLE-MART AUTO TRAV.

Figure 76. Vertical crosswind dispersion parameter, σ_z, as a function of distance downwind of Pinole and Martinez.

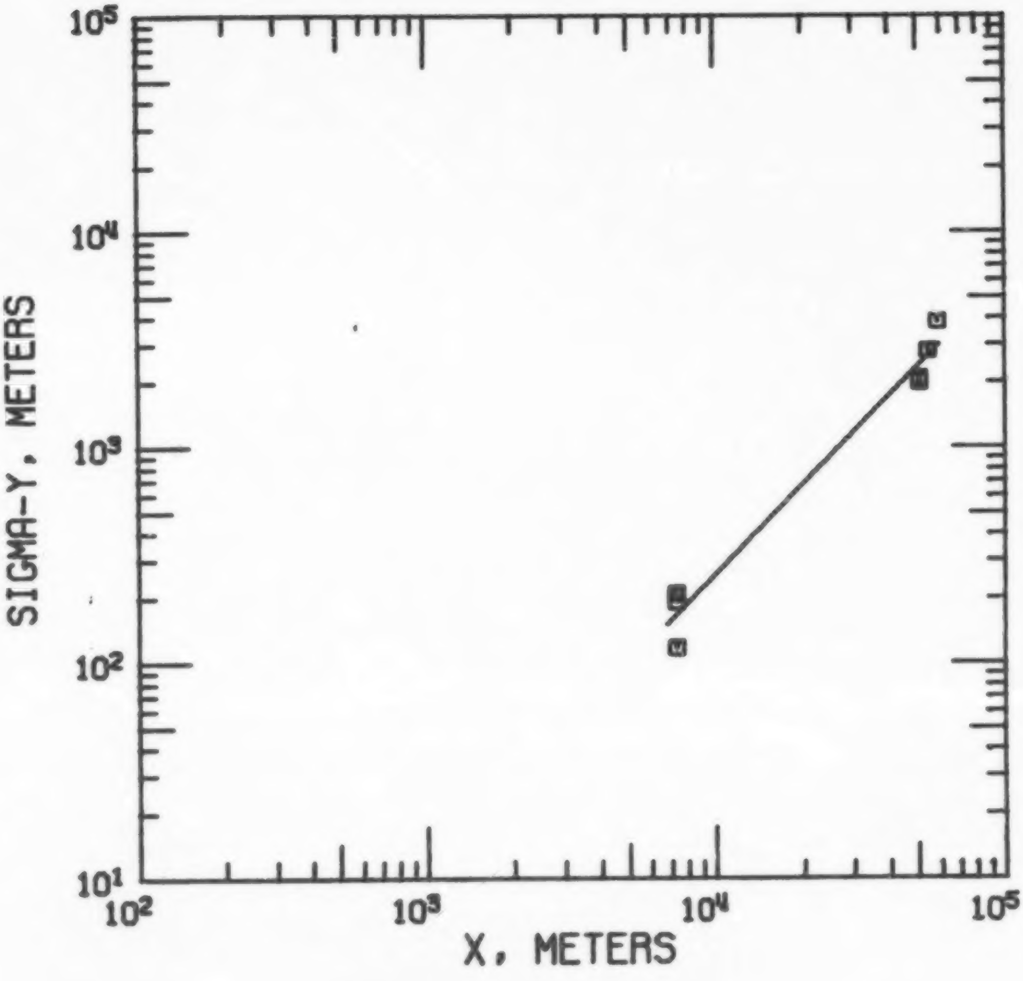

SEA BREEZE TAIL

Dow Auto Traverse

Figure 77. Horizontal crosswind dispersion parameter, σ_y, as a function of distance downwind of the Dow site.

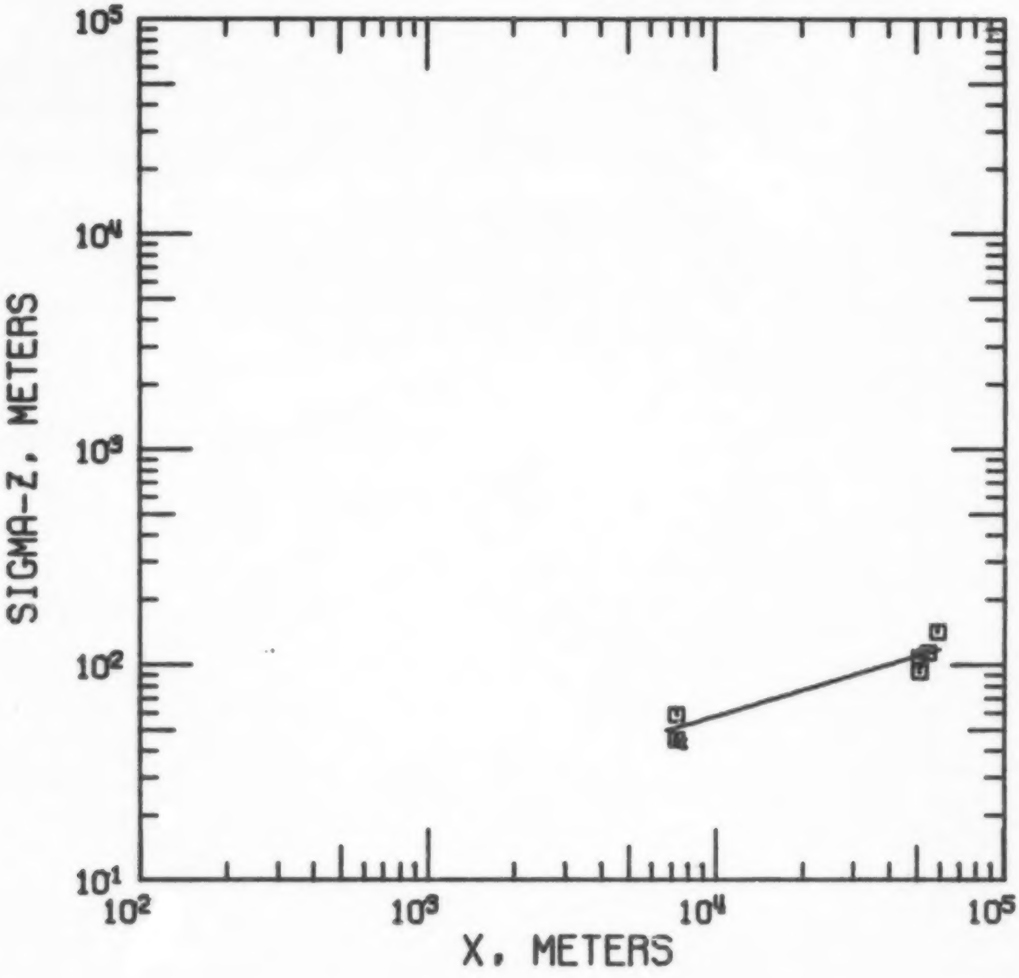

SEA BREEZE TAIL
DOW AUTO TRAV.

Figure 78. Vertical crosswind dispersion parameter, σ_z, as a function of distance downwind of the Dow site.

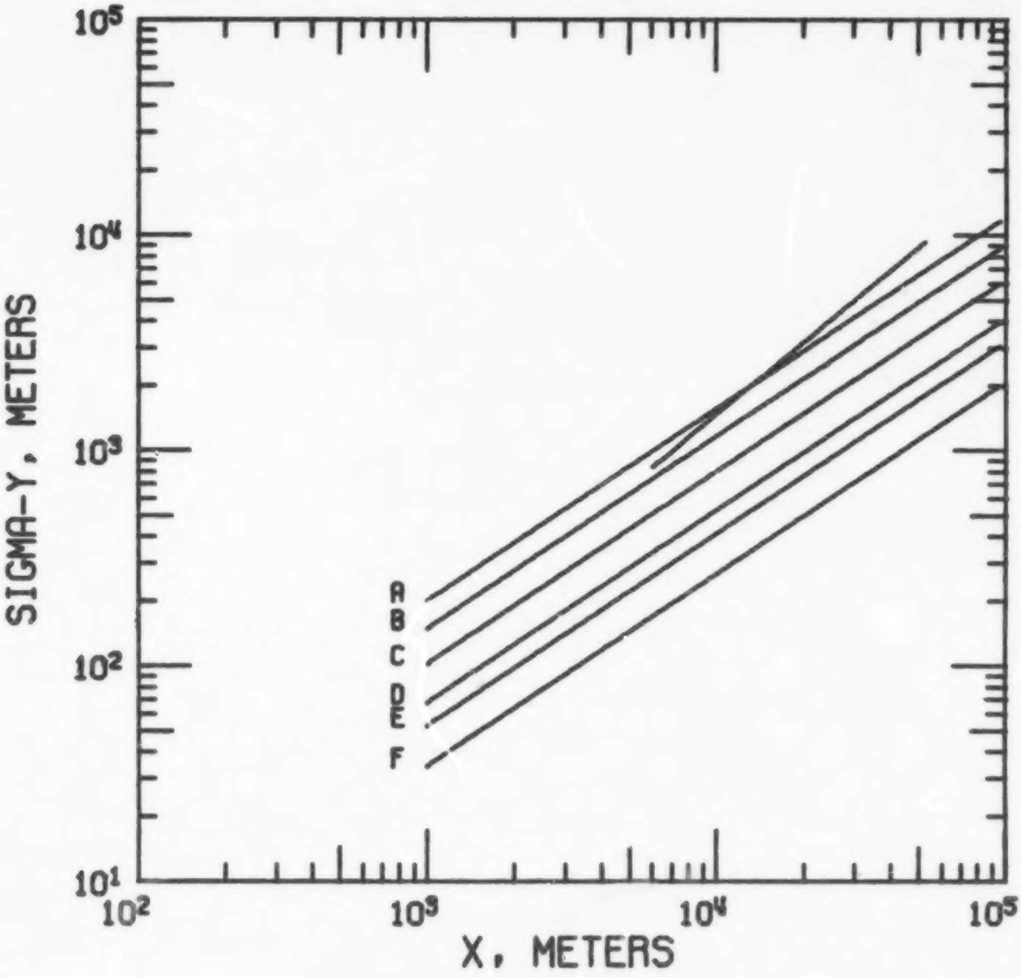

CAL. DELTA TEST 1

DOW AUTO TRAV.

Figure 79. Comparison of horizontal dispersion of plumes emitted from the Dow site with the horizontal dispersion of plumes associated with Pasquill atmospheric stability classes.

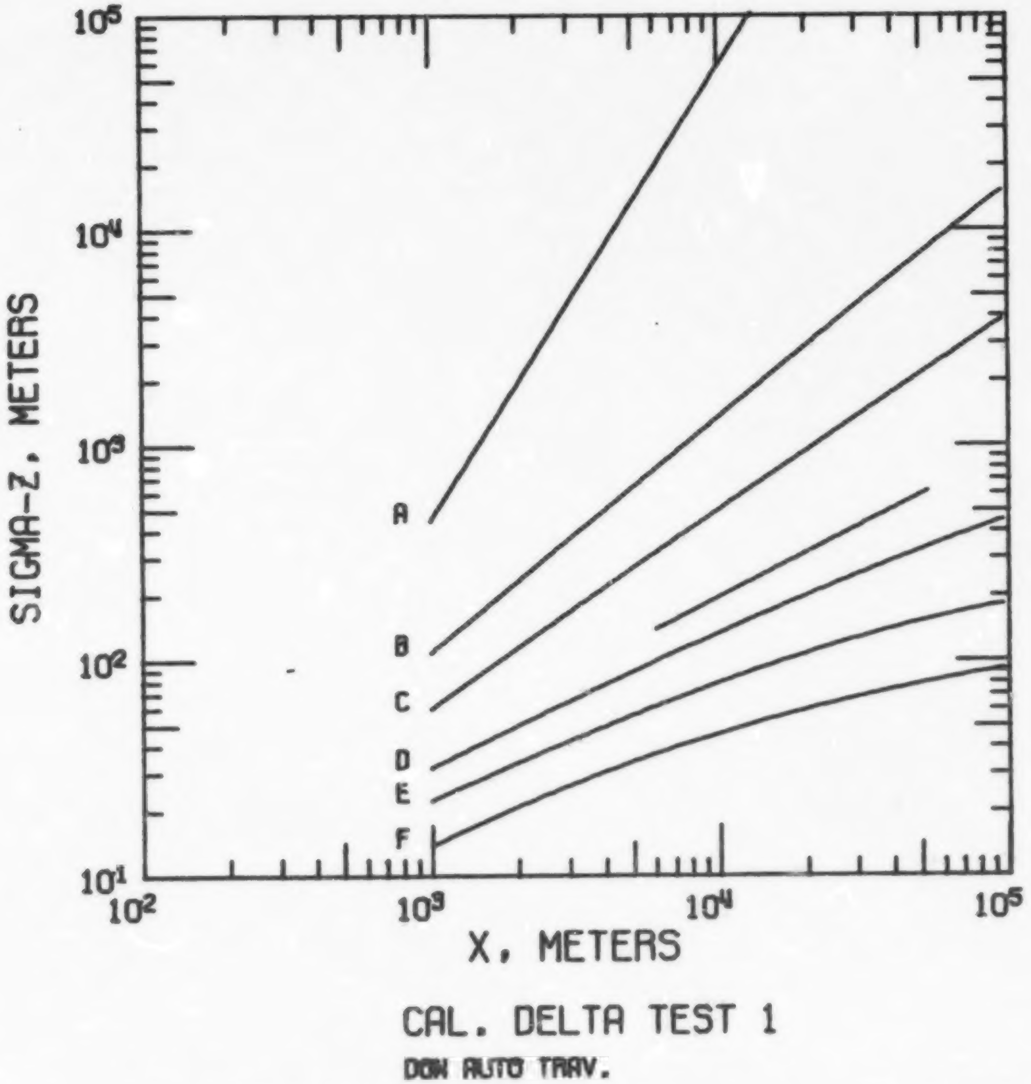

Figure 80. Comparison of vertical dispersion of plumes emitted from the Dow site with the vertical dispersion of plumes associated with Pasquill atmospheric stability classes.

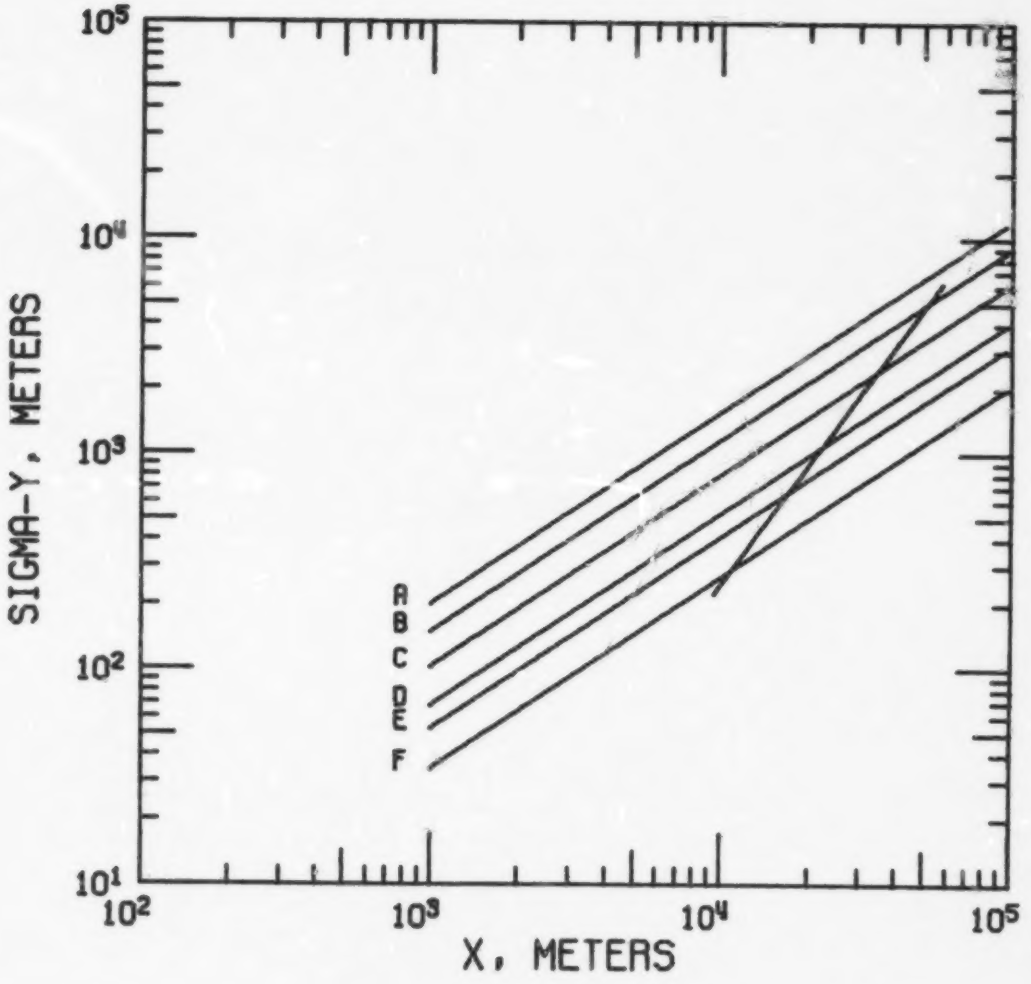

CAL. DELTA TEST 2

DOW AUTO TRAV.

Figure 81. Comparison of horizontal dispersion of plumes emitted from the Dow site with the horizontal dispersion of plumes associated with Pasquill atmospheric stability classes.

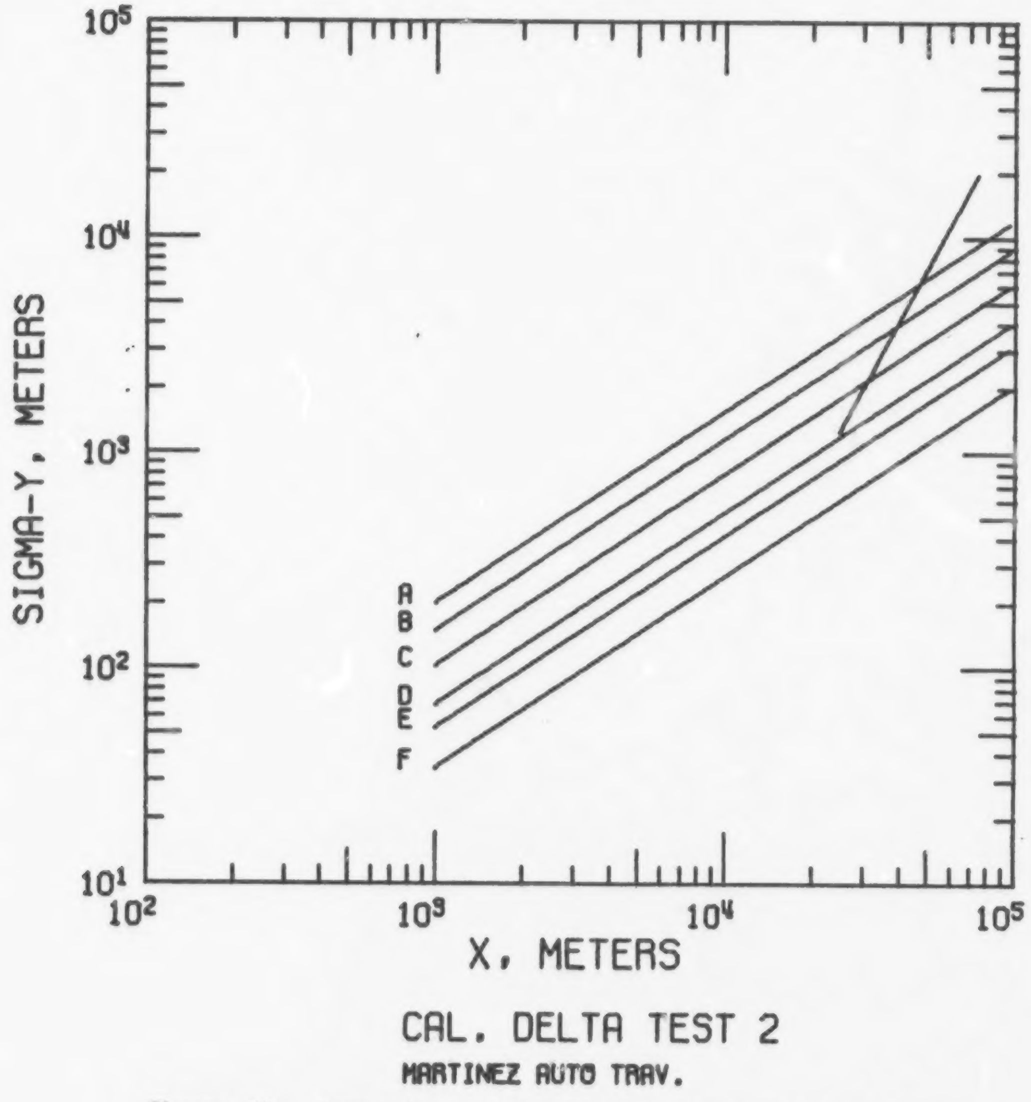

Figure 82. Comparison of horizontal dispersion of plumes emitted from Martinez with the horizontal dispersion of plumes associated with Pasquill atmospheric stability classes.

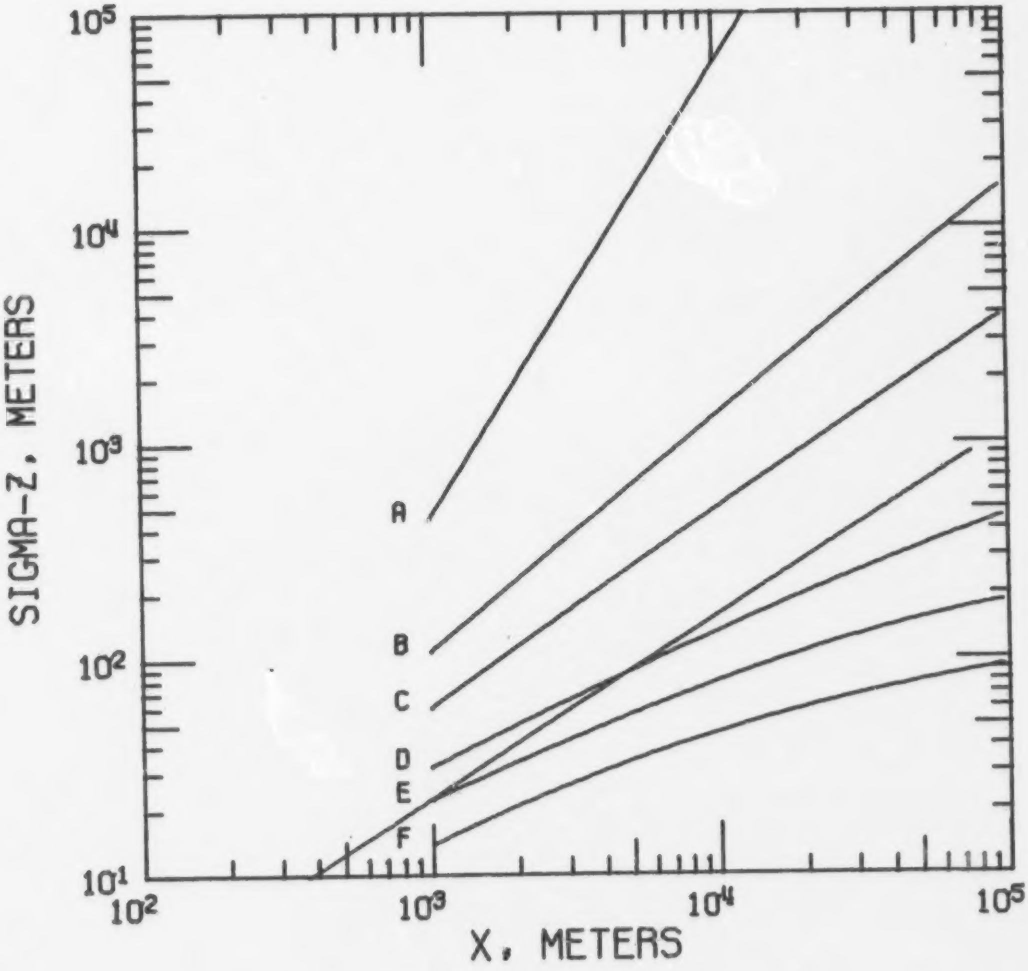

CAL. DELTA TEST 2

MARTINEZ AUTO TRAV.

Figure 83. Comparison of vertical dispersion of plumes emitted from Martinez with the vertical dispersion of plumes associated with Pasquill atmospheric stability classes.

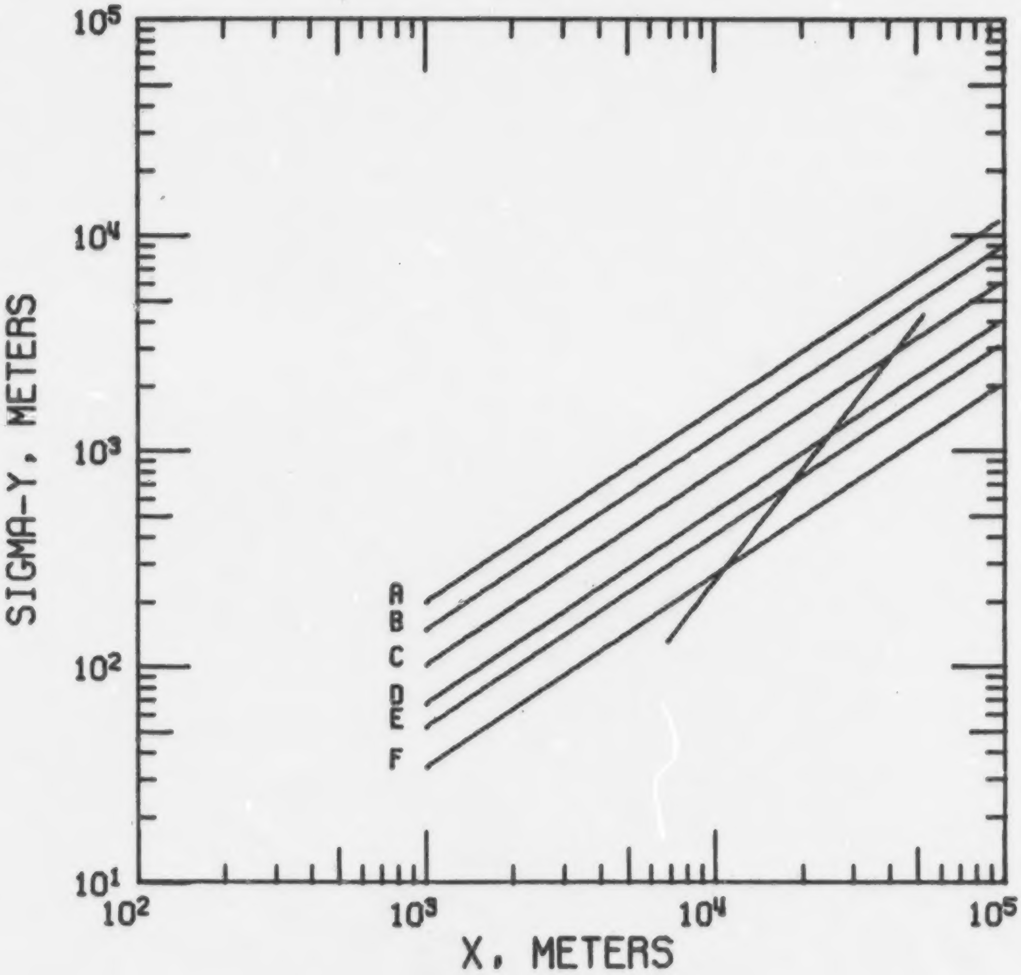

CAL. DELTA TEST 3

DOW AUTO TRAV.

Figure 84. Comparison of horizontal dispersion of plumes emitted from the Dow site with the horizontal dispersion of plumes associated with Pasquill atmospheric stability classes.

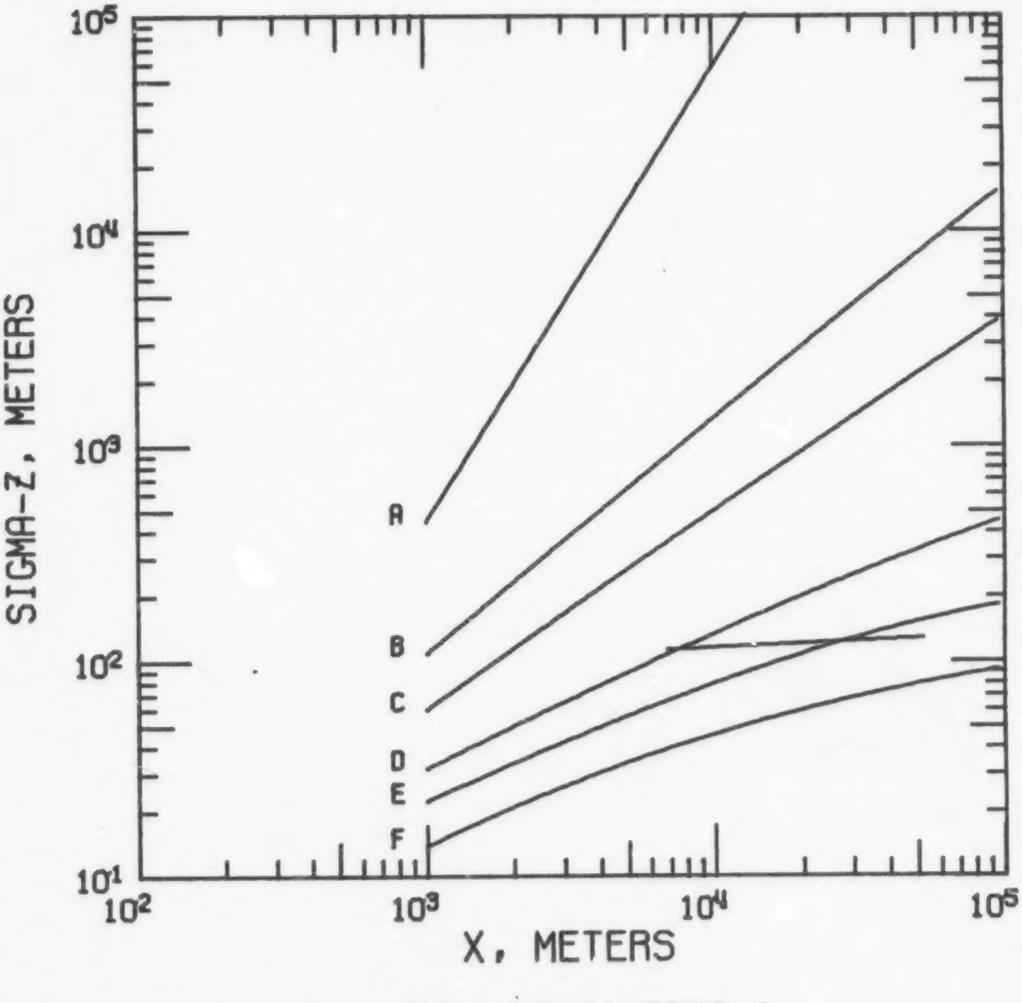

CAL. DELTA TEST 3

DOW AUTO TRAV.

Figure 85. Comparison of vertical dispersion of plumes emitted from the Dow site with the vertical dispersion of plumes associated with Pasquill atmospheric stability classes.

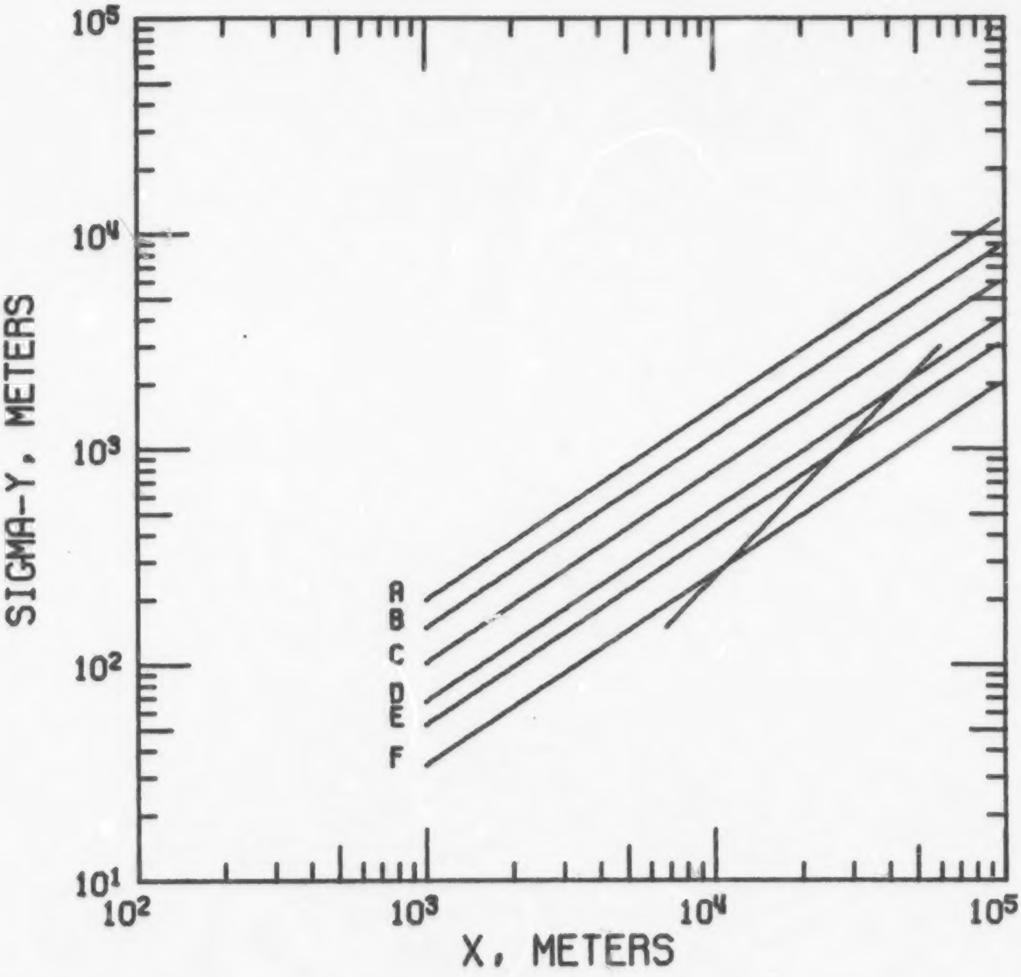

CAL. DELTA TEST 4

DOW AUTO TRAV.

Figure 86. Comparison of horizontal dispersion of plumes emitted from the Dow site with the horizontal dispersion of plumes associated with Pasquill atmospheric stability classes.

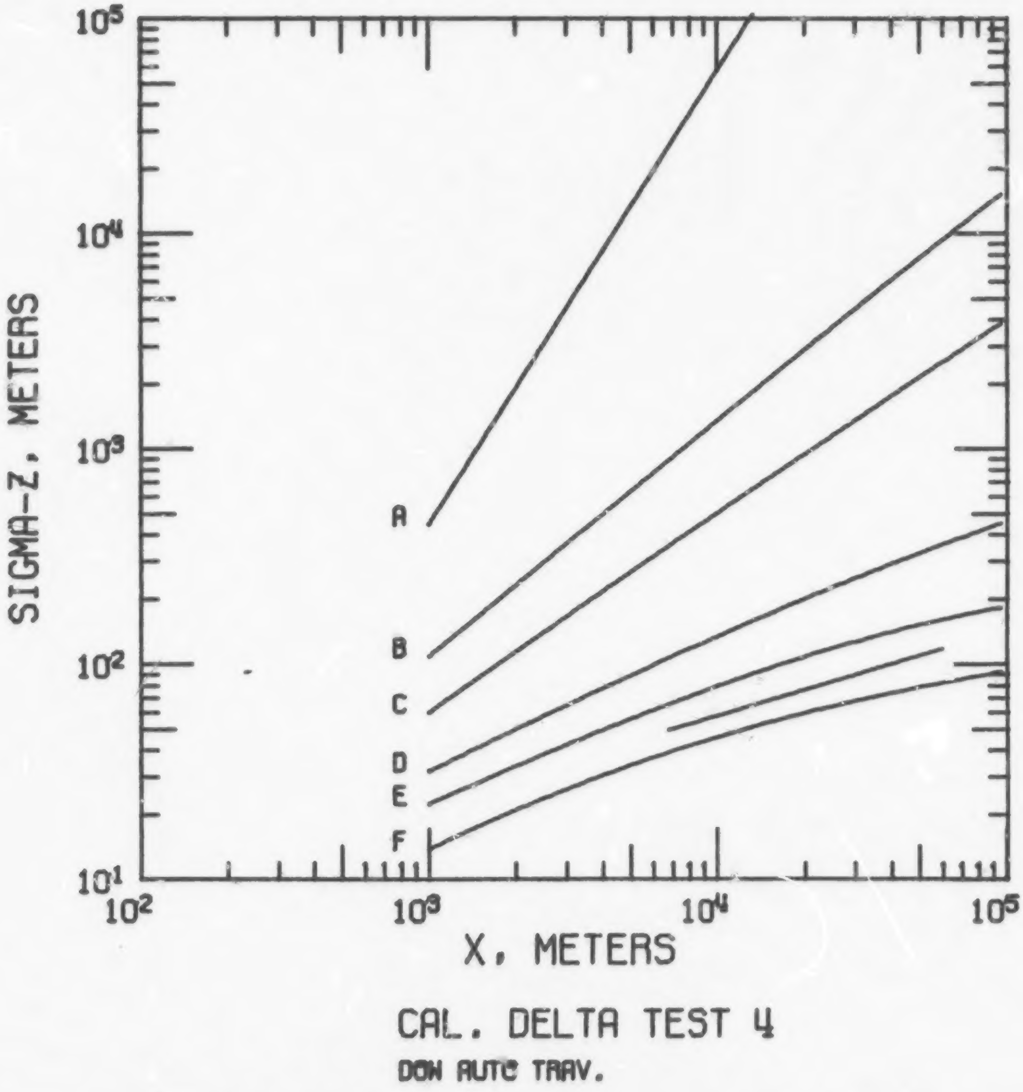

Figure 87. Comparison of vertical dispersion of plumes emitted from the Dow site with the vertical dispersion of plumes associated with Pasquill atmospheric stability classes.

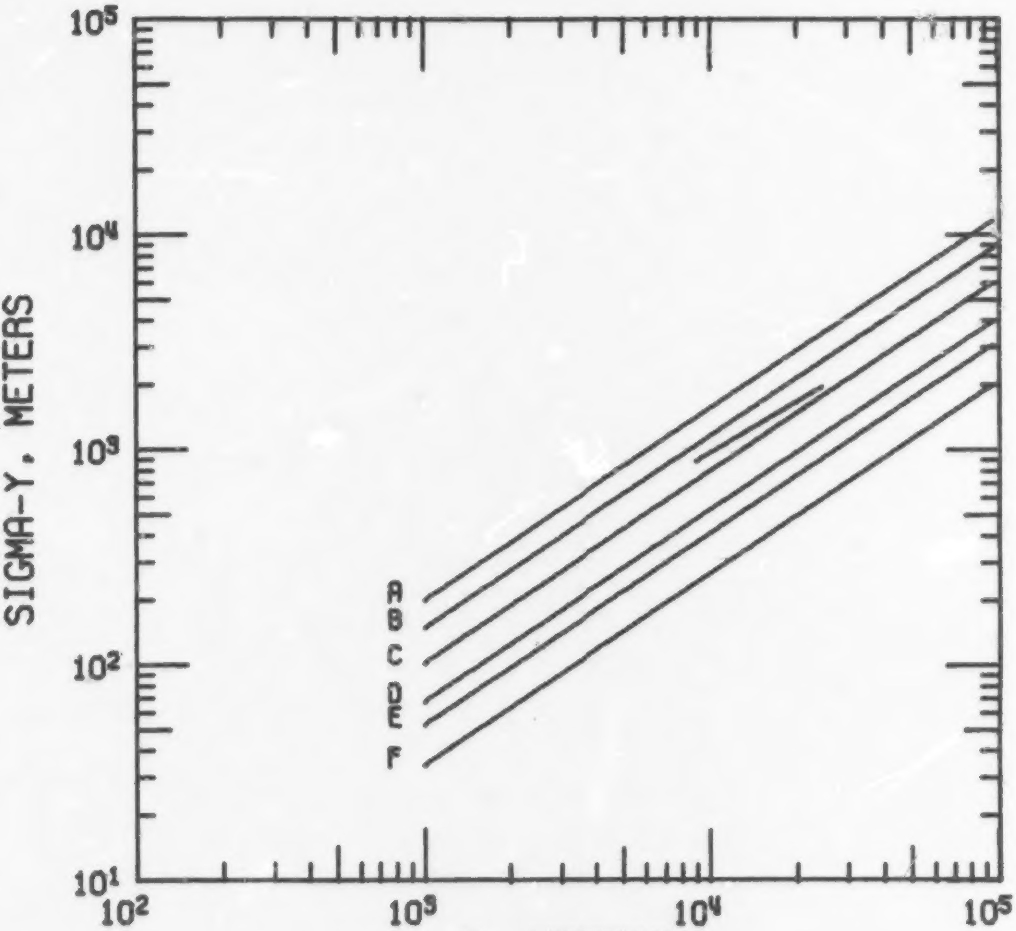

CAL. DELTA TEST 5

DOW AUTO TRAV.

Figure 88. Comparison of horizontal dispersion of plumes emitted from the Dow site with the horizontal dispersion of plumes associated with Pasquill atmospheric stability classes.

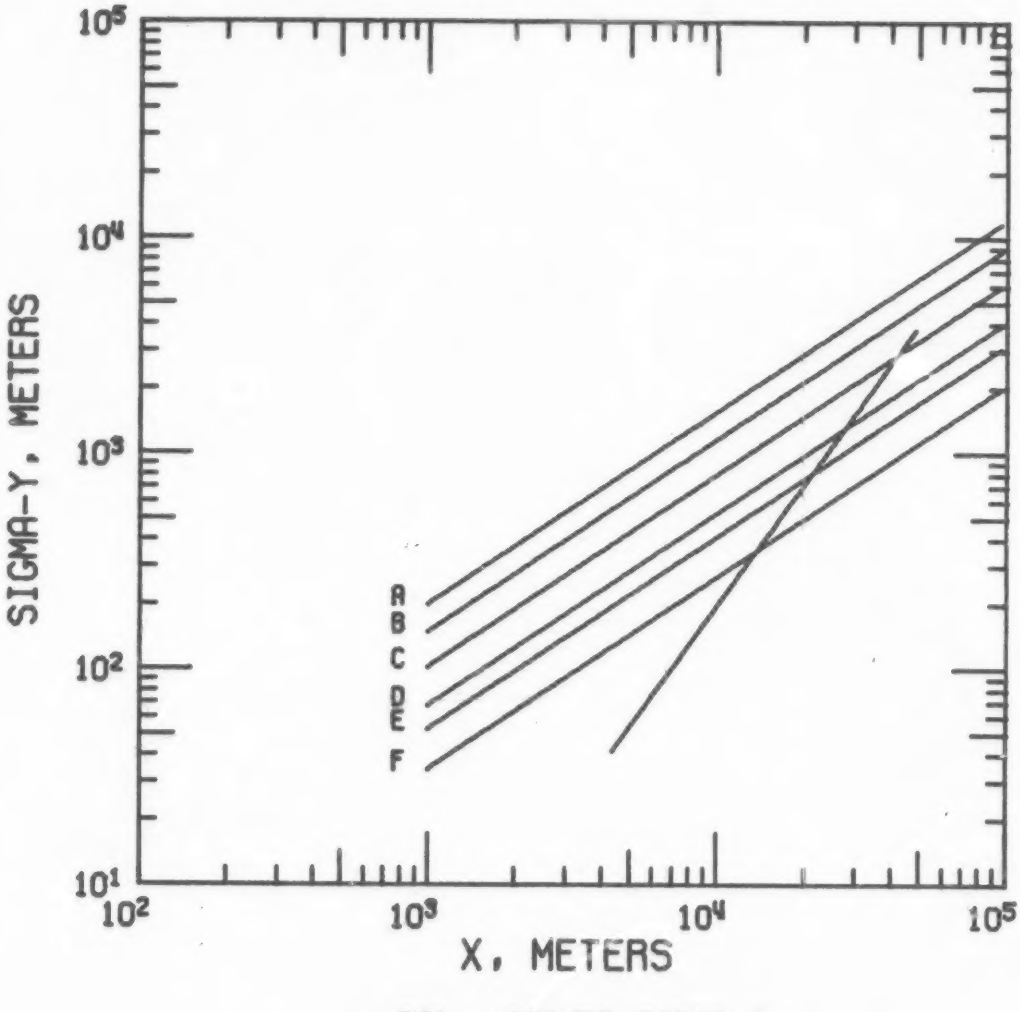

CAL. DELTA TEST 6

DOW AUTO TRAV.

Figure 89. Comparison of horizontal dispersion of plumes emitted from the Dow site with the horizontal dispersion of plumes associated with Pasquill atmospheric stability classes.

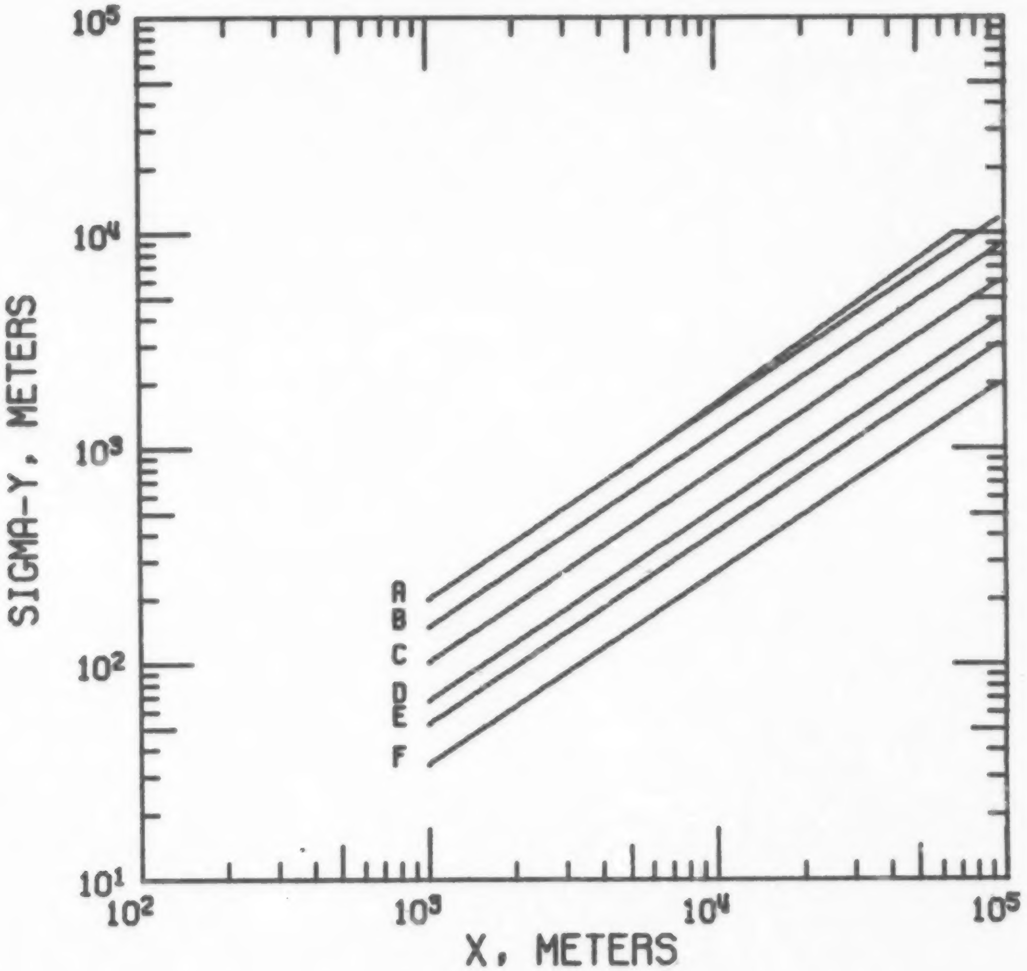

CAL. DELTA TEST 7

PINOLE AUTO TRAV.

Figure 90. Comparison of horizontal dispersion of plumes emitted from Pinole with the horizontal dispersion of plumes associated with Pasquill atmospheric stability classes.

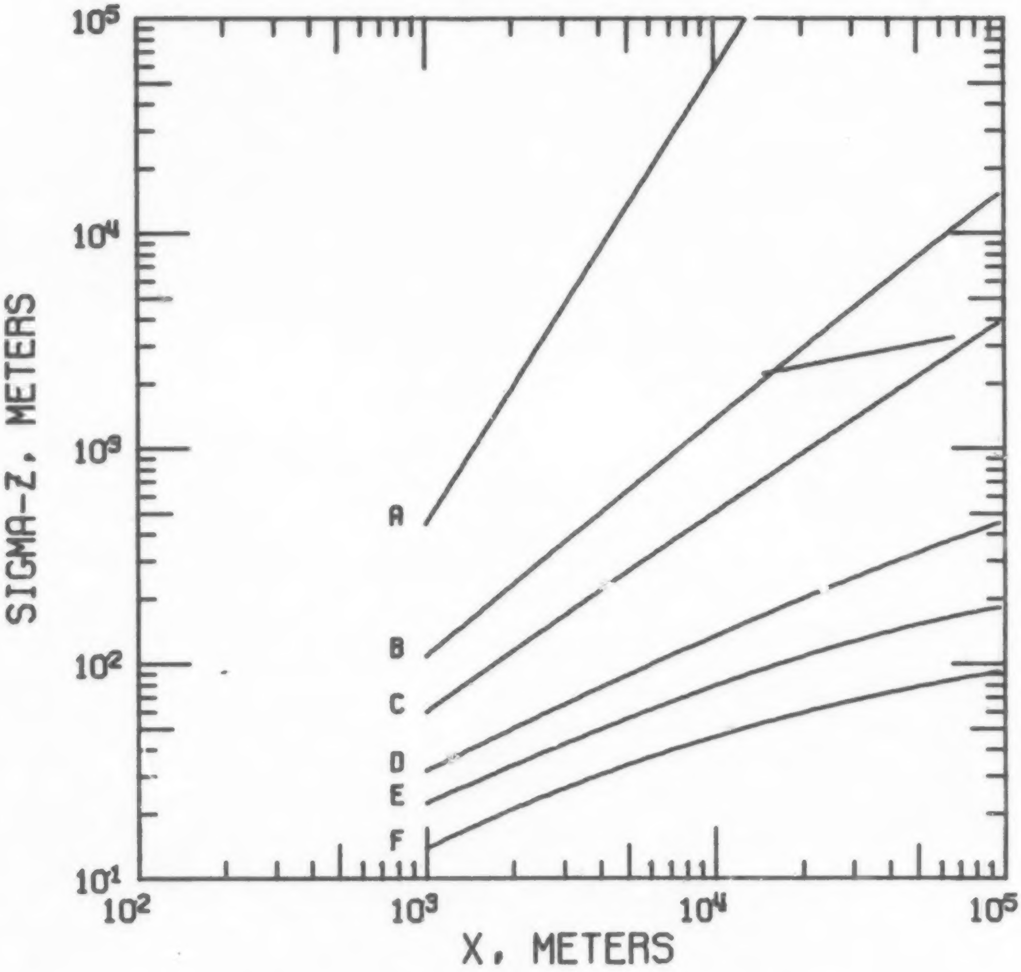

CAL. DELTA TEST 7

PINOLE AUTO TRAV.

Figure 91. Comparison of vertical dispersion of plumes emitted from Pinole with the vertical dispersion of plumes associated with Pasquill atmospheric stability classes.

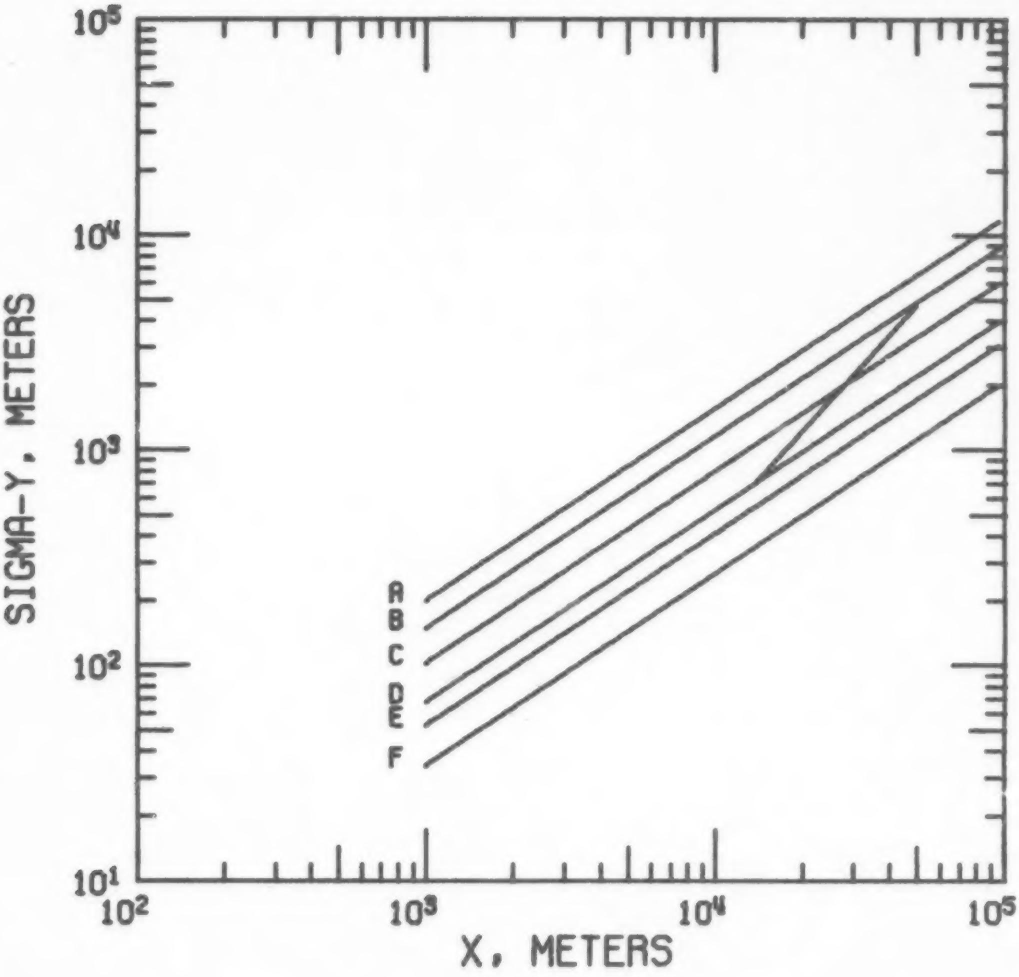

CAL. DELTA TEST 8

PINOLE AUTO TRAV.

Figure 92. Comparison of horizontal dispersion of plumes emitted from Pinole with the horizontal dispersion of plumes associated with Pasquill atmospheric stability classes.

The dispersion coefficients corresponding to the dispersion curves for σ_y and σ_z from Turner (1970) are listed in Table 11. The horizontal dispersion curves from every test, except Tests 5 and 7, indicate that atmospheric stability decreases with increasing distance. Results from Test 1 show that conditions were comparable to class B immediately downwind at the Dow site, and less stable than class A at far downwind distances. This pattern is more obvious in Tests 2, 3, 4, 6 and 8. Conditions range from very stable near the source to very unstable at far downwind distances. These curves suggest that the strong jet of wind passing through the Carquinez Strait and over the Dow site has a very large effect on the dispersion of pollutants at close downwind distances from the source. Typically, the plumes crossing Highway 160, 10 km downwind of the Montezuma Hills, are very narrow; during the seven Dow releases, the plume centerlines observed in the automobile traverse data crossed Highway 160 within a 2.1 km crosswind zone (see Figure 118, Section 4.8 of this volume). However, the plumes observed crossing Highway 99, 50 km downwind of the Montezuma Hills, were relatively broad, and their trajectories crossed Highway 99 in a zone extending from Lodi to Tracy during the seven tests.

The slopes of the experimental horizontal dispersion curves are roughly a factor of 2 greater than the slopes of the corresponding curves given by Turner. Thus, the rate of spreading under the field test meteorological conditions was a factor of 2 greater than the dispersion associated with the classical Pasquill stability categories. However, the horizontal dispersion curves generally begin under more stable conditions than would be predicted from wind speed and insolation considerations. Conditions during Test 1 were assumed to be Pasquill classes B-C; the horizontal dispersion curve for Test 1 ranges from class B near the source to class A far from the source. During Test 2, stability conditions were predicted to be Pasquill classes B-C; the horizontal stability according to dispersion data for the Dow releases ranged from class F near the source to class B far downwind. Stability conditions were assumed to be classes D-F for Tests 3 and 4; the stability conditions suggested by the horizontal dispersion curves ranged from more stable than class F, 7 km from the Dow site, to approximately class C at 50 km downwind. The horizontal dispersion curve from Test 6 begins under more stable conditions than class F at 5 km downwind, and ranges to class C conditions at 50 km downwind. The existing stability conditions were predicted to be class D conditions. Near the Dow site the atmosphere appears to be very stable; 50 km east of the Dow site, conditions approach those predicted from meteorological data.

Data from Test 5 for a Dow release and Test 7 for the Pinole release appear to follow the classical Pasquill curves. The predicted stability conditions during Test 5 were classes B-C; the experimental curve lies between classes B-C. The predicted conditions during Test 7 were B-C; the experimental curve is practically coincident with the Pasquill class A curve. Data obtained for Test 8 from Pinole indicated stability conditions to be B-C; the dispersion curve ranged from class D to class B.

The vertical dispersion data do not show the same stability pattern apparent in the horizontal data. Generally, the vertical dispersion curves follow the classical Pasquill curves. For Test 1, the experimental curve lies between the Pasquill class C and D curves; this is in a range slightly more stable than the classes B-C predicted for the test. Classes D-F were assumed to exist during Test 4; the vertical dispersion curve lies between the curves for classes E and F. The scatter in the vertical dispersion data for Test 7 was rather large. The data points lie between classes A and D, and the best-fit line lies between classes B and C. Stability conditions during the day were predicted to be classes B-C. For Test 3 conducted at night, the vertical dispersion data suggest that vertical mixing was almost independent of the transport distance. This is in agreement with the results of the mass balance analysis for the nighttime test. Even after moving distances of 50 km, the plumes extended to approximately the same height as that found at 7 km.

The relative dispersive capabilities of the atmosphere among the four meteorological regimes are summarized in Figures 93 and 94 for Dow releases and in Figures 95 and 96 for Pinole-Martinez releases. The Dow horizontal dispersion data clearly show the effects of daytime heating upon the regional dispersion processes. The afternoon Sea Breeze curve ranges from class C near Dow to class B far downwind. The other daytime period and the evening and nighttime periods are characterized by a dispersion process which is more stable than the Pasquill class F, 7 km from the Dow site, and close to class C at 50 km downwind. The large difference between the Sea Breeze curve and the remaining curves at short downwind distances can be attributed to the increased vertical mixing which prevails during the sunny, warm afternoon period. During the tracer releases, aside from Test 5, average wind speeds at the Dow site ranged from 4.6 to 9.3 m/sec (10 to 21 mph). These high wind speeds account for the extremely stable conditions apparent in the dispersion curves at close downwind distances.

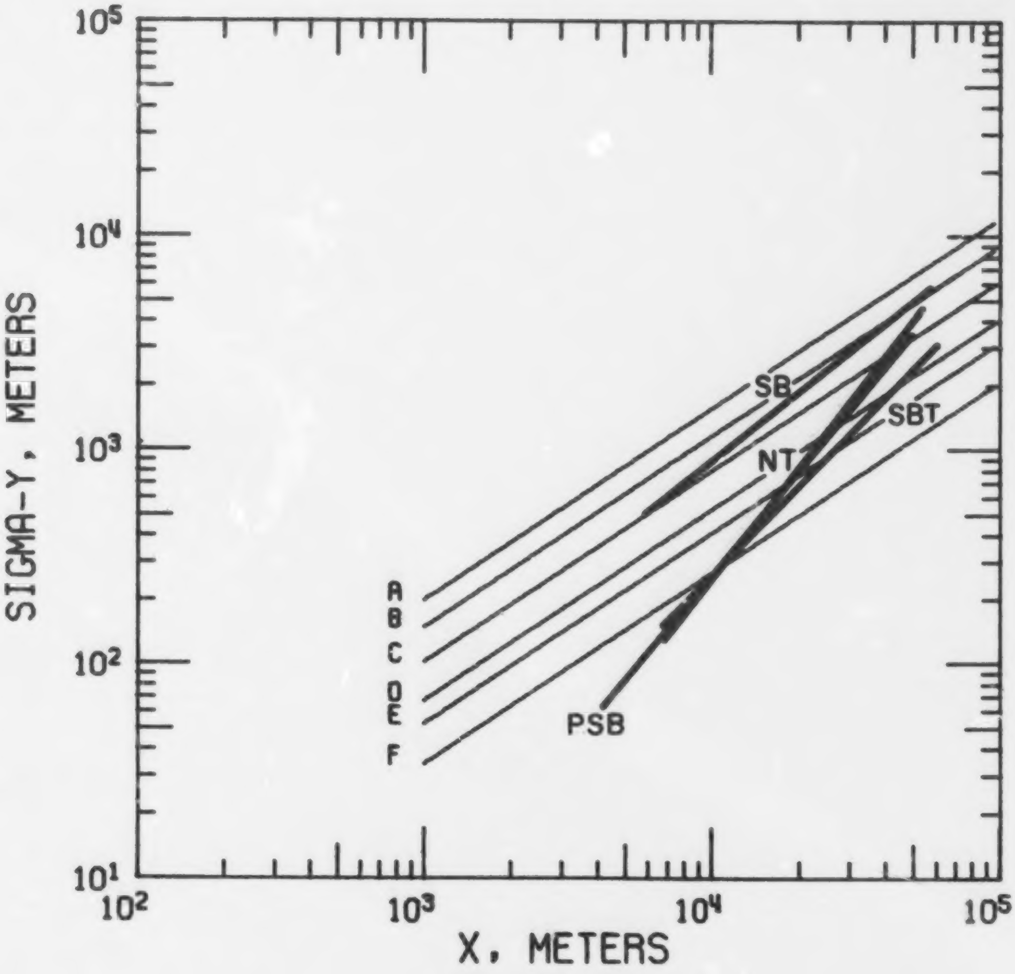

DOW AUTO TRAV.

Figure 93. Horizontal crosswind dispersion parameter, σ_y, as a function of distance downwind of the Dow site during Pre-Sea Breeze (PSB), Sea Breeze (SB), Sea Breeze Tail (SBT), and Nighttime (NT) conditions, and the horizontal dispersion parameter associated with Pasquill atmospheric stability classes.

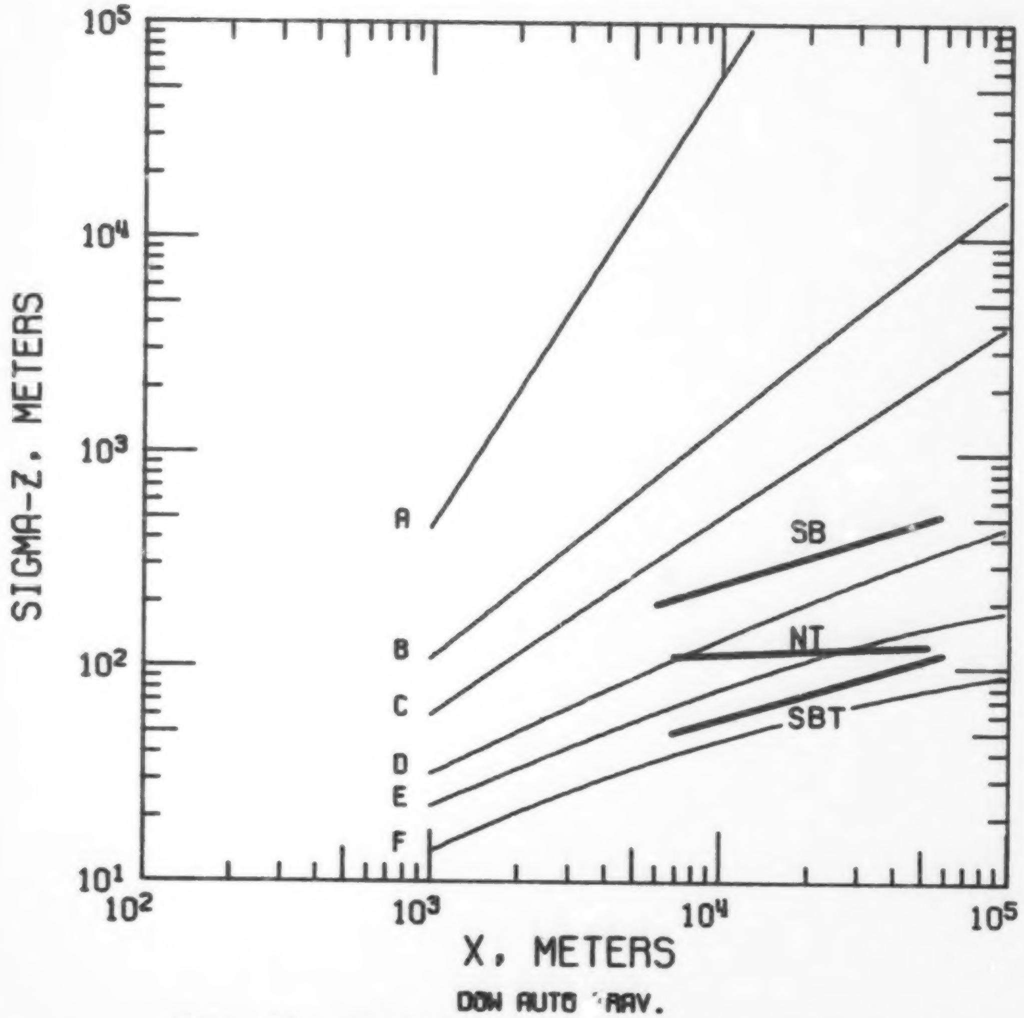

Figure 94. Vertical crosswind dispersion parameter, σ_z, as a function of distance downwind of the Dow site during Sea Breeze (SB), Sea Breeze Tail (SBT), and Nighttime (NT) conditions, and the vertical dispersion parameter associated with Pasquill atmospheric stability classes.

Reproduced from best available copy.

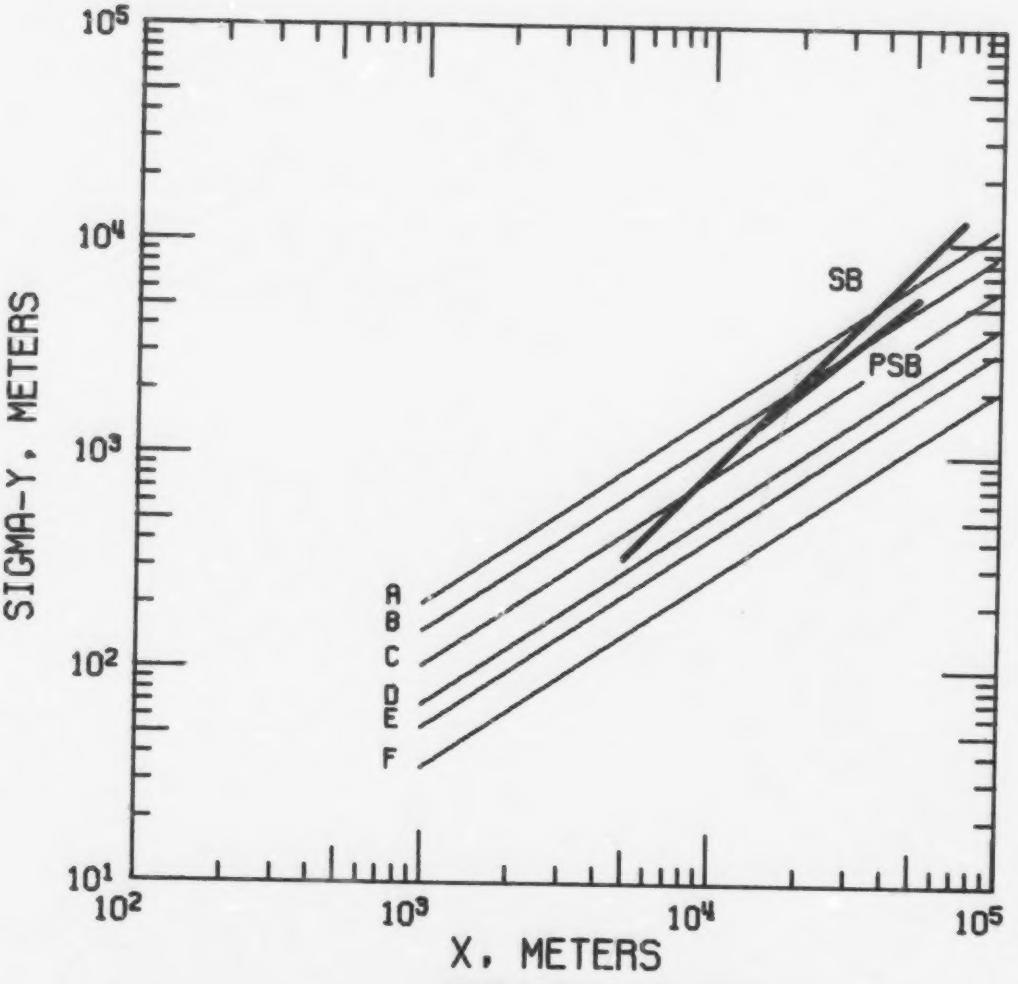

Figure 95. Horizontal crosswind dispersion parameter, σ_y, as a function of distance downwind for tracer releases from Pinole and Martinez during Sea Breeze (SB) and Pre-Sea Breeze (PSB) conditions, and the horizontal dispersion parameter associated with Pasquill atmospheric stability classes.

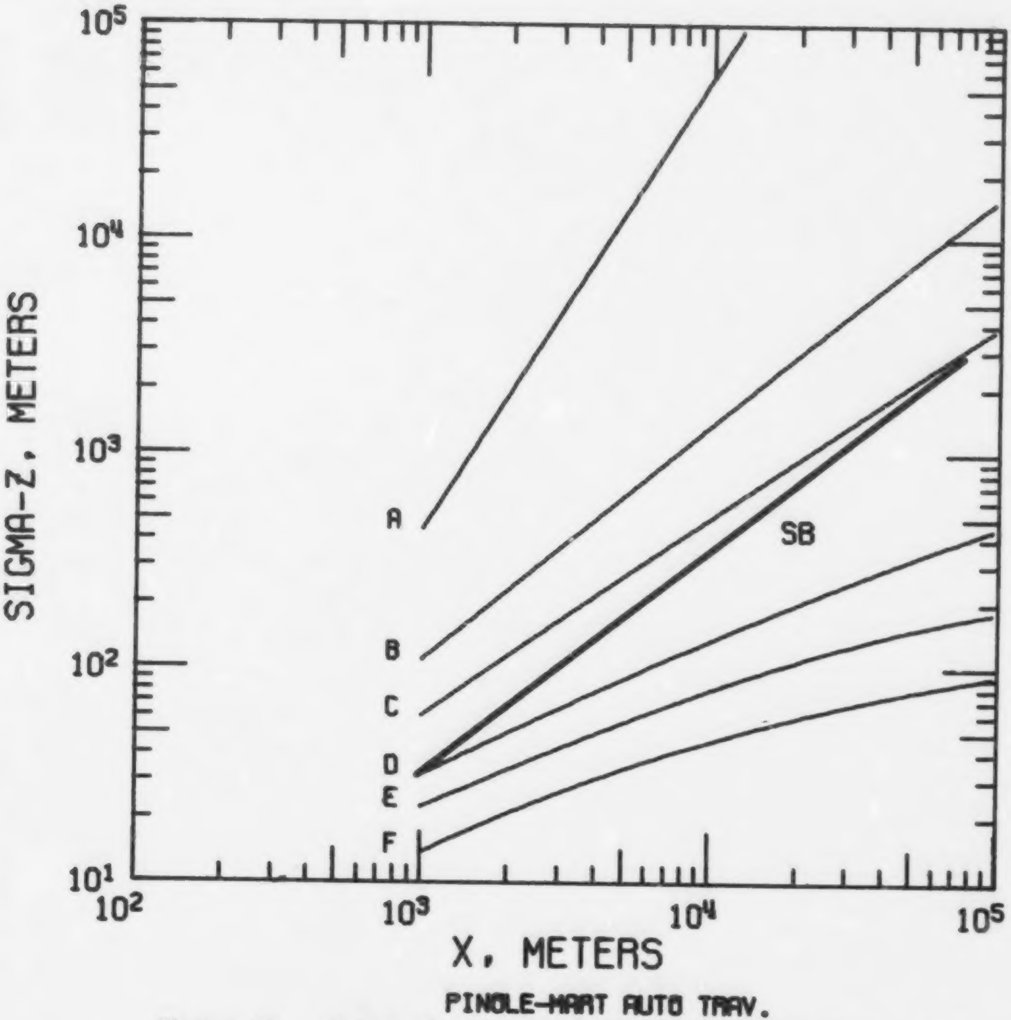

PINOLE-MART AUTO TRAV.

Figure 96. Vertical crosswind dispersion parameter, σ_z, as function of distance downwind for tracer release from Pinole and Martinez during Sea Breeze (SB) conditions, and the vertical dispersion parameter associated with Pasquill atmospheric stability classes.

The vertical dispersion curves for Dow releases are similar to the horizontal curves. Dispersion observed during Sea Breeze conditions is greater than that found during the other meteorological periods. However, for close downwind distances, the vertical dispersion data do not show the very stable nature of the atmospheric found in the horizontal dispersion curves. Under Sea Breeze and Sea Breeze Tail conditions, the vertical dispersion curves are approximately parallel to the curves associated with the Pasquill stability classes. Data obtained during the Nighttime period indicate that vertical dispersion is almost independent of the transport distance.

If one assumes that horizontal dispersion is only a function of changes in the horizontal wind field and vertical dispersion is only a function of the turbulent vertical heat exchange between the land and the atmosphere, then it appears that the dispersion processes near the Dow site are governed by a balance between the abnormally strong and steady winds and a relatively classical air-ground heat transfer. During the Sea Breeze period, the vertical mixing associated with the afternoon heating of the ground overrides the stabilizing effects of the steady winds. Stability conditions near the Dow site are reasonably close to those expected from insolation considerations. At other times, when the effects of heating are smaller, horizontal dispersion is sharply limited because of the steadiness and strength of the winds. However, during Sea Breeze Tail conditions when the land is cooling from the afternoon sun, vertical dispersion follows the classical Pasquill pattern. At night when wind speeds increase, horizontal and vertical dispersion near Dow are both very limited.

The dispersion data associated with the Pinole and Martinez tracer tests indicate that horizontal and vertical dispersion increased with distance at rates greater than those for Pasquill stability classes. This is similar to the pattern observed in the data obtained during the Dow releases. The horizontal dispersion curves obtained from Pre-Sea Breeze data is very similar to the curve derived from the Sea Breeze data. Both curves lie in the range of stability which was assumed to exist during the tests. The vertical dispersion curve indicates that conditions were one Pasquill class more stable than those predicted from the meteorology. It appears that strong and steady winds moving through the Carquinez Strait created a more stable atmosphere near the release points than was assumed to exist.

In summary, this analysis of the observed dispersion of the tracer indicates that the strong winds measured during the tracer tests generally cause horizontal dispersion to be limited near the release point. During the daytime, vertical dispersion follows the classical Pasquill dispersion curves; at night, vertical dispersion appears to be independent of downwind distance. The available data for Pinole and Martinez releases yield results which are similar to the results of the Dow dispersion analysis. At downwind distances of 50 km, the extent of horizontal dispersion under all periods approaches or exceeds that predicted from the meteorology using Pasquill stability classes.

It is very important to realize that these results are based on eight tracer tests covering a two-week period in September. We do not imply in this section that these results are necessarily representative of typical or worst case meteorological conditions. However, as we noted in the description of the tracer tests, the wind patterns observed during the field study were generally similar to those which occurred most frequently according to Smalley (1957). Mixing depth patterns were similar to those attributed to typical conditions by Miller (1968). A more complete discussion of typical and worst case conditions which occur in the Delta region is presented in the MRI report concerning the field study.

4.6 Use of Field Study Data for Air Quality Model Development

The tracer and meteorological data collected during the California Delta field tests offer a very comprehensive data base describing the transport and dispersion characteristics of the region. In this report, particularly in Volume II, we have presented all of the pertinent, available data which might be necessary for development and testing of atmospheric dispersion models.

All of the tabulated tracer and meteorological data in Volume II has been compiled on computer cards and is available from the California Air Resources Board upon request. Also available are digital topography data in 200 foot increments for the region extending from 37° to 39° latitude and 121° to 123° longitude; this encompasses all of the San Francisco Bay Area and the California Delta Region as far east as Sacramento and Stockton.

In the next section we present a short analysis of the applicability of a simple air quality model. This analysis is an example of how the field study data can be used to calibrate or validate other atmospheric models.

4.7 Applicability of the Gaussian Plume Model in the California Delta Region

The commonly used Gaussian plume model provides a simple and rapid means of predicting pollutant concentrations downwind of a continuous point source. Although the Gaussian model is restricted by assumptions related to stationary and homogeneous turbulence, and by the availability of empirical dispersion parameters, it is often used by industrial planners and regulatory agency personnel as a means of estimating the impact of industrial emissions. For this reason, we will test the Gaussian model in the California Delta Region by using it to predict the tracer data. In this manner, we can estimate the suitability of the Gaussian model as an impact analysis tool for industrial development in the California Delta Region.

The Gaussian plume model may be used in the form given by Turner (1970):

$$C = \frac{Q}{2\pi\,\sigma_y\sigma_z u}\exp\left[-\tfrac{1}{2}\left(\frac{y}{\sigma_y}\right)^2\right]\left\{\exp\left[-\tfrac{1}{2}\left(\frac{Z+H}{\sigma_z}\right)^2\right]+\right.$$

$$\exp\left[-\tfrac{1}{2}\left(\frac{Z-H}{\sigma_z}\right)^2\right]+\sum_{n=1}^{4}\left(\exp\left[-\tfrac{1}{2}\left(\frac{z+H-2nL}{\sigma_z}\right)^2\right]+\right.$$

$$\exp\left[-\tfrac{1}{2}\left(\frac{z+H+2nL}{\sigma_z}\right)^2\right]+\exp\left[-\tfrac{1}{2}\left(\frac{z-H-2nL}{\sigma_z}\right)^2\right]+$$

$$\left.\left.\exp\left[-\tfrac{1}{2}\left(\frac{z-H+2nL}{\sigma_z}\right)^2\right]\right)\right\} \qquad (15)$$

where u is the average wind speed, Q is the release rate, H is the effective stack height, and L is the height of the mixing layer. The dispersion parameters, σ_y and σ_z, can be taken from the empirical curves given by Turner as functions of the Pasquill stability classes. These empirical curves were determined from data taken over flat, open terrain.

The topography of the Delta area can be characterized as relatively flat, open country. This description suggests that the Gaussian model used with the dispersion parameters from Turner (1970) may be suitable for application in the Delta region. However, the comparison of the tracer dispersion curves with Pasquill's curves in Section 4.5 indicate that the unique wind patterns of the region effect the dispersion to a much greater extent than might be expected. . Although the Gaussian model may be applicable, it appears that it may be best applied using the experimental dispersion parameters. To test the Gaussian model and the two available sets of dispersion parameters, the Gaussian expression was used to predict the centerline tracer concentrations from the automobile traverses for each test. In this prediction, σ_y and σ_z were taken from the best-fit lines through the tracer data for each test. If a curve for σ_z were not available, the curve from Turner was used. The effective stack height, H, was set equal to the release height, 5 m, and the release rate, Q, was assumed to be equal to the average release rate for each test as given in Table 2 . The value of u for each test was obtained by vector averaging hourly wind data from all stations downwind of the tracer release point over the time of interest. The mixing height, L, was determined by averaging the hourly heights from the available stations for the test period.

The predicted results for the automobile traverse tracer data are given in Figures 97-109in terms of ground-level centerline concentrations as a function of downwind distance. In each figure, the experimental maximum 10-second and hourly averaged concentrations are also plotted as a function of downwind distance. Additionally, predicted concentrations using the dispersion curves from Turner are shown for each test.

The predicted results based on Turner's σ_y and σ_z fall very close to the measured concentrations in Test 1 for class C stability. The curve based on the experimental dispersion data underestimates the concentrations

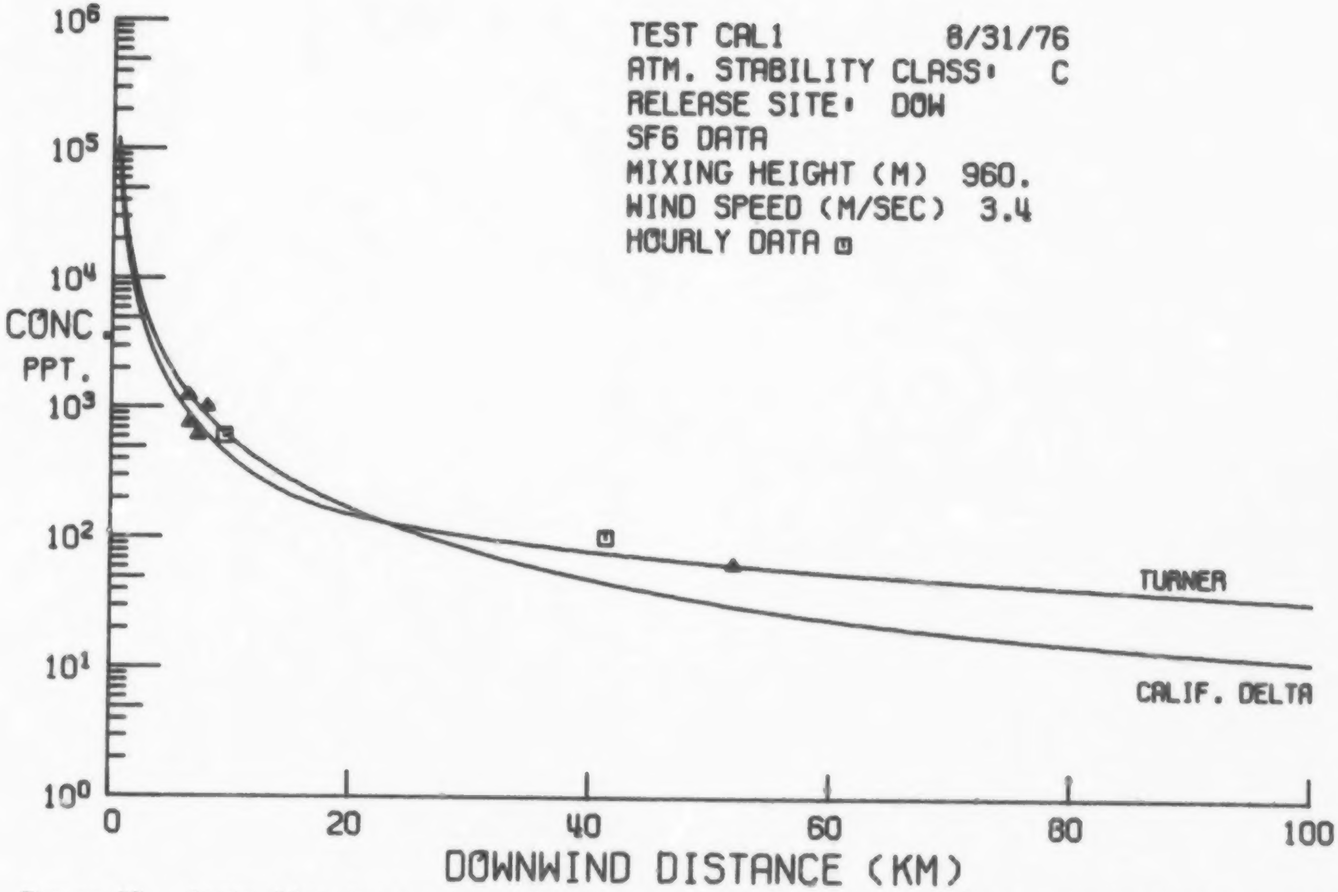

Figure 97. Centerline tracer concentrations compared with centerline concentrations predicted using the Gaussian plume model. The "Turner" curve is based upon Pasquill dispersion parameters given by Turner (1970); the "Calif. Delta" curve is based upon experimental dispersion parameters.

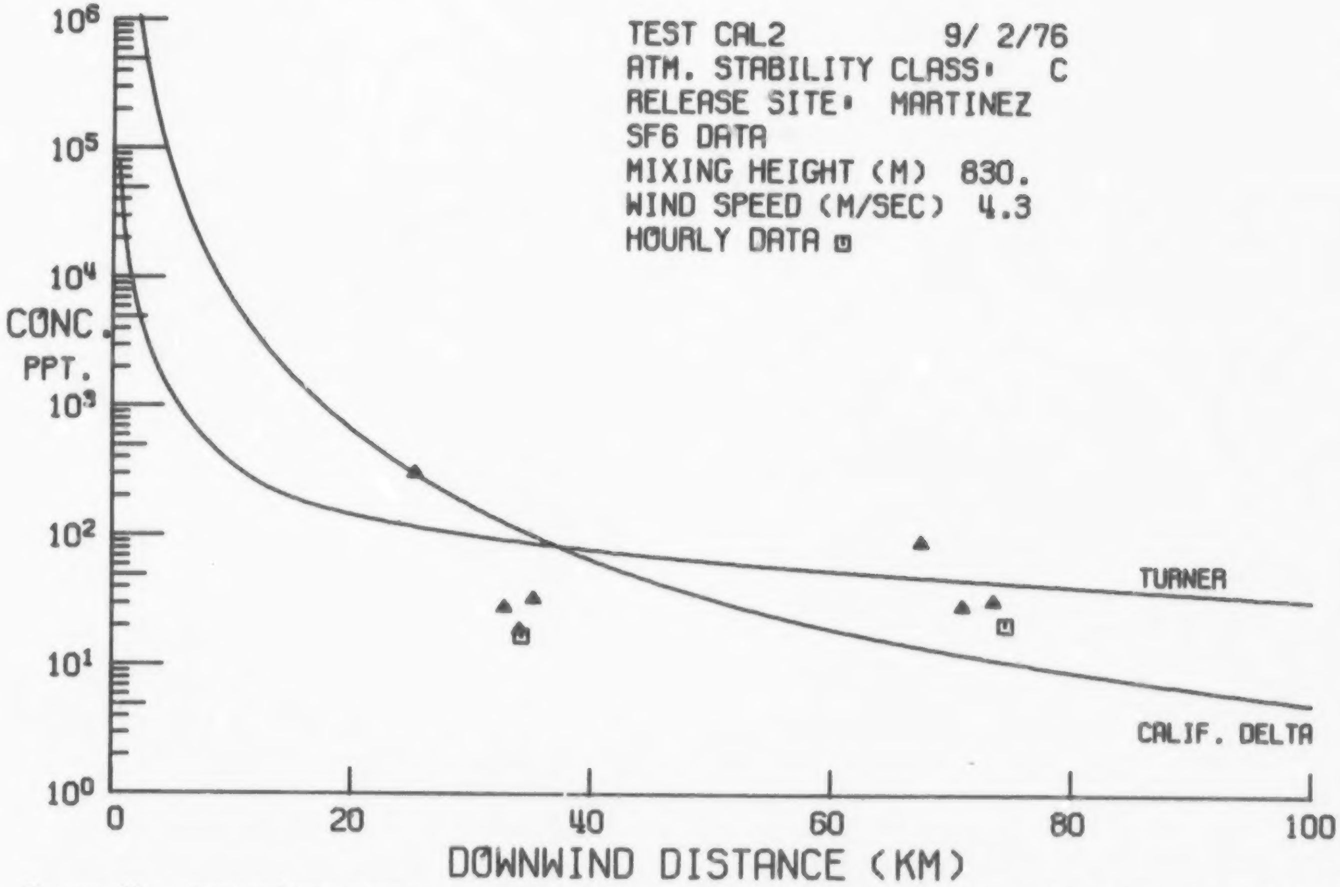

Figure 98. Centerline tracer concentrations compared with centerline concentrations predicted using the Gaussian plume model. The "Turner" curve is based upon Pasquill dispersion parameters given by Turner (1970); the "Calif. Delta" curve is based upon experimental dispersion parameters.

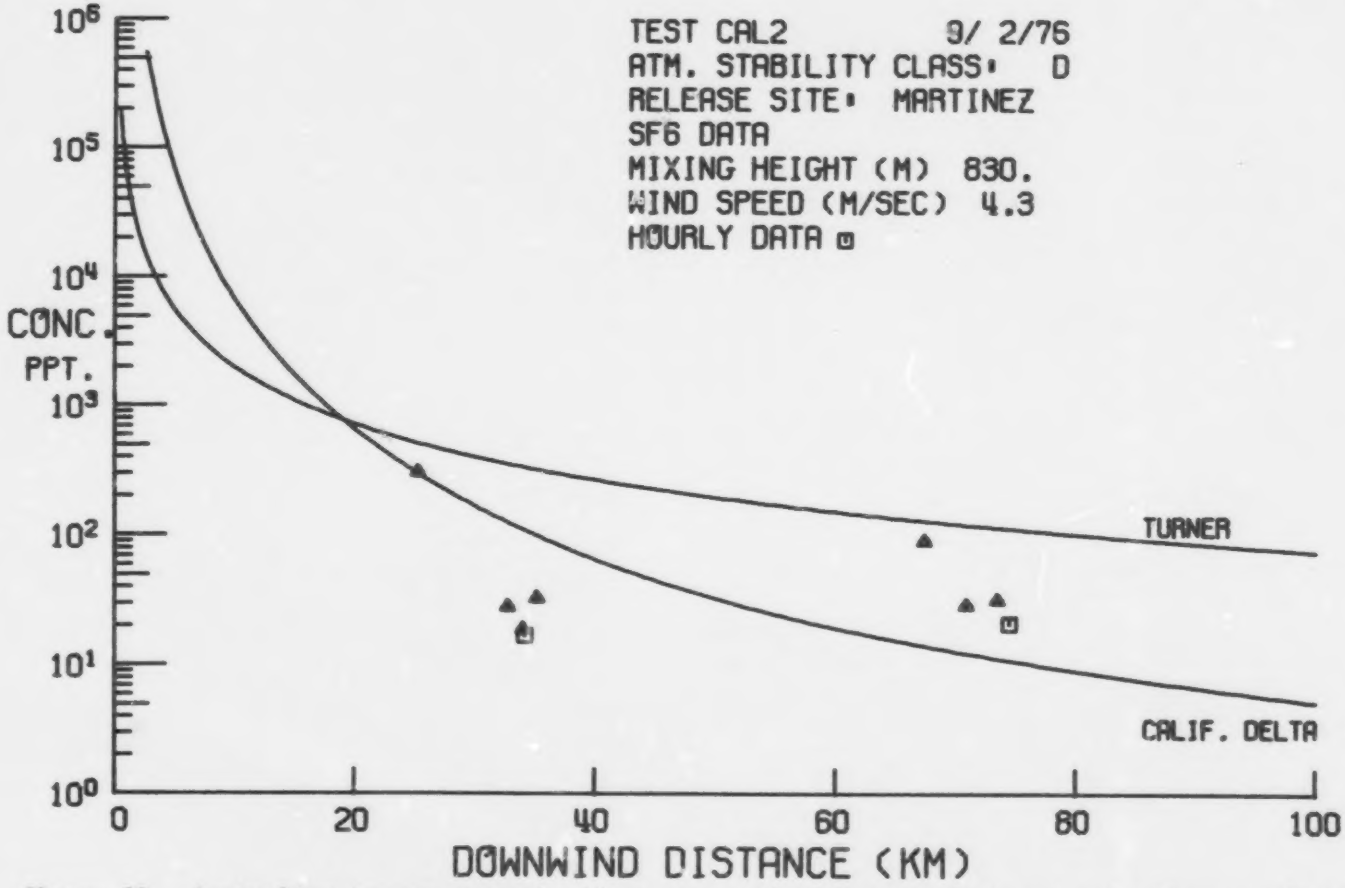

Figure 99. Centerline tracer concentrations compared with centerline concentrations predicted using the Gaussian plume model. The "Turner" curve is based upon Pasquill dispersion parameters given by Turner (1970); the "Calif. Delta" curve is based upon experimental dispersion parameters.

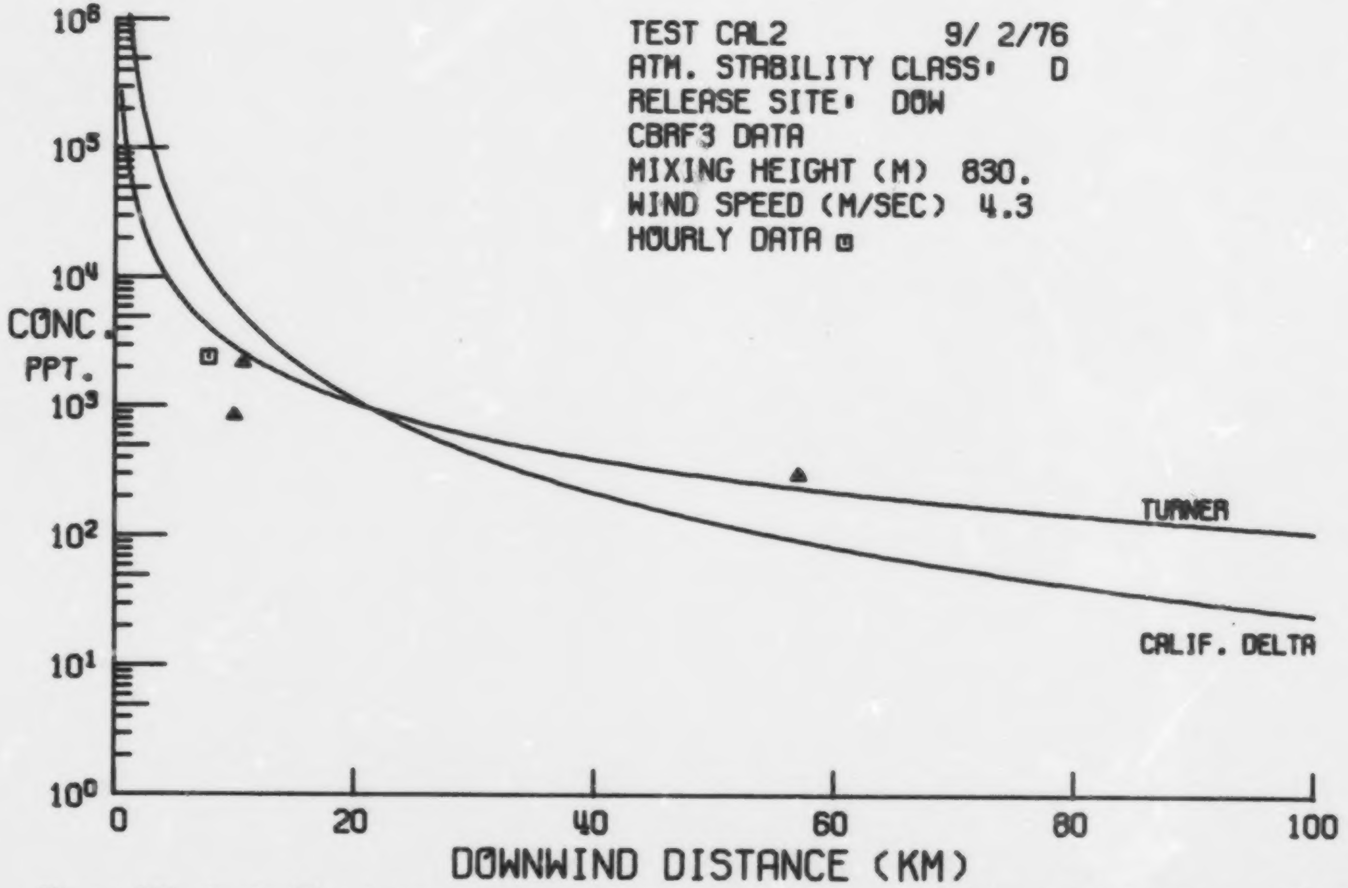

Figure 100. Centerline tracer concentrations compared with centerline concentrations predicted using the Gaussian plume model. The "Turner" curve is based upon Pasquill dispersion parameters given by Turner (1970); the "Calif. Delta" curve is based upon experimental dispersion parameters.

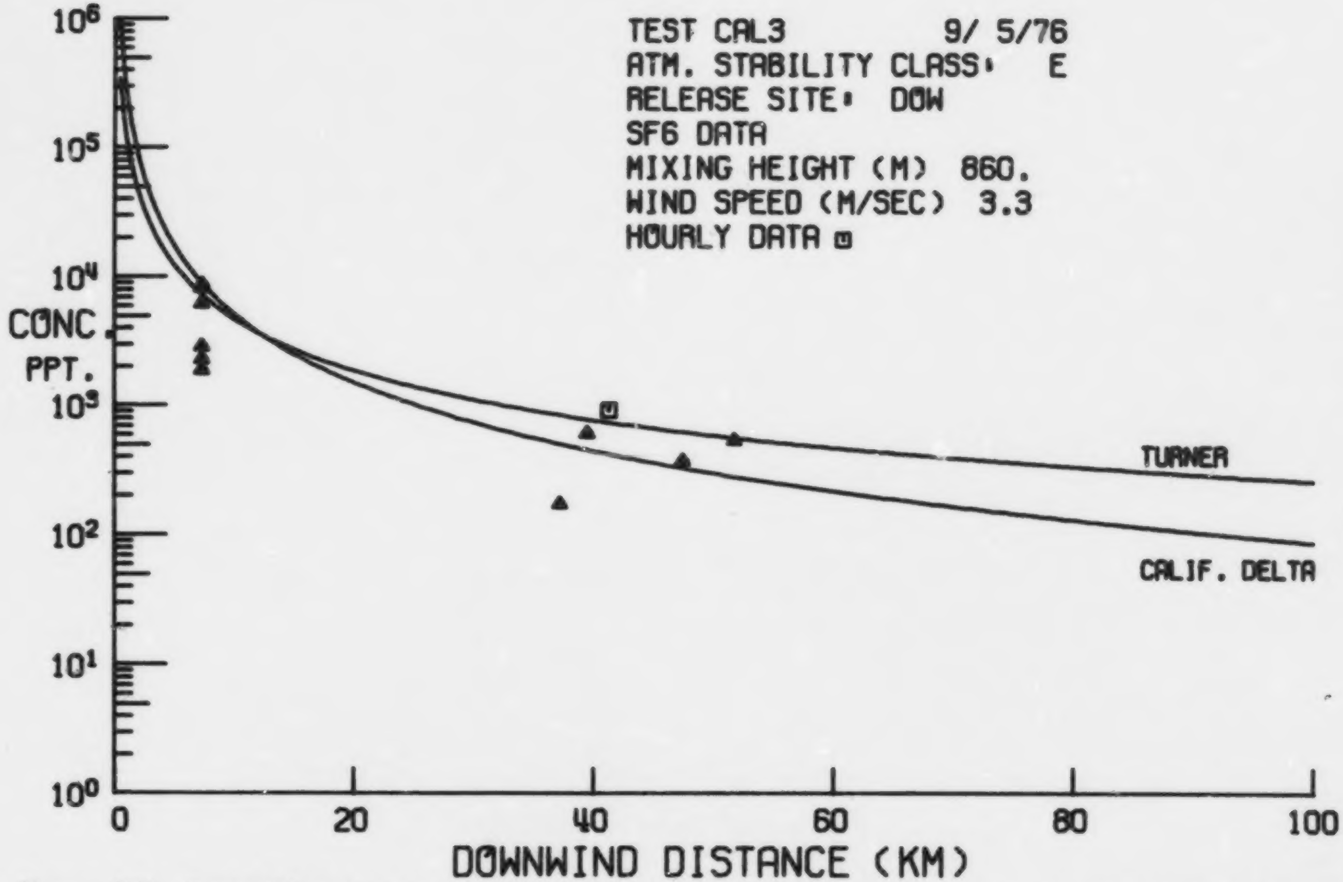

Figure 101. Centerline tracer concentrations compared with centerline concentrations predicted using the Gaussian plume model. The "Turner" curve is based upon Pasquill dispersion parameters given by Turner (1970); the "Calif. Delta" curve is based upon experimental dispersion parameters.

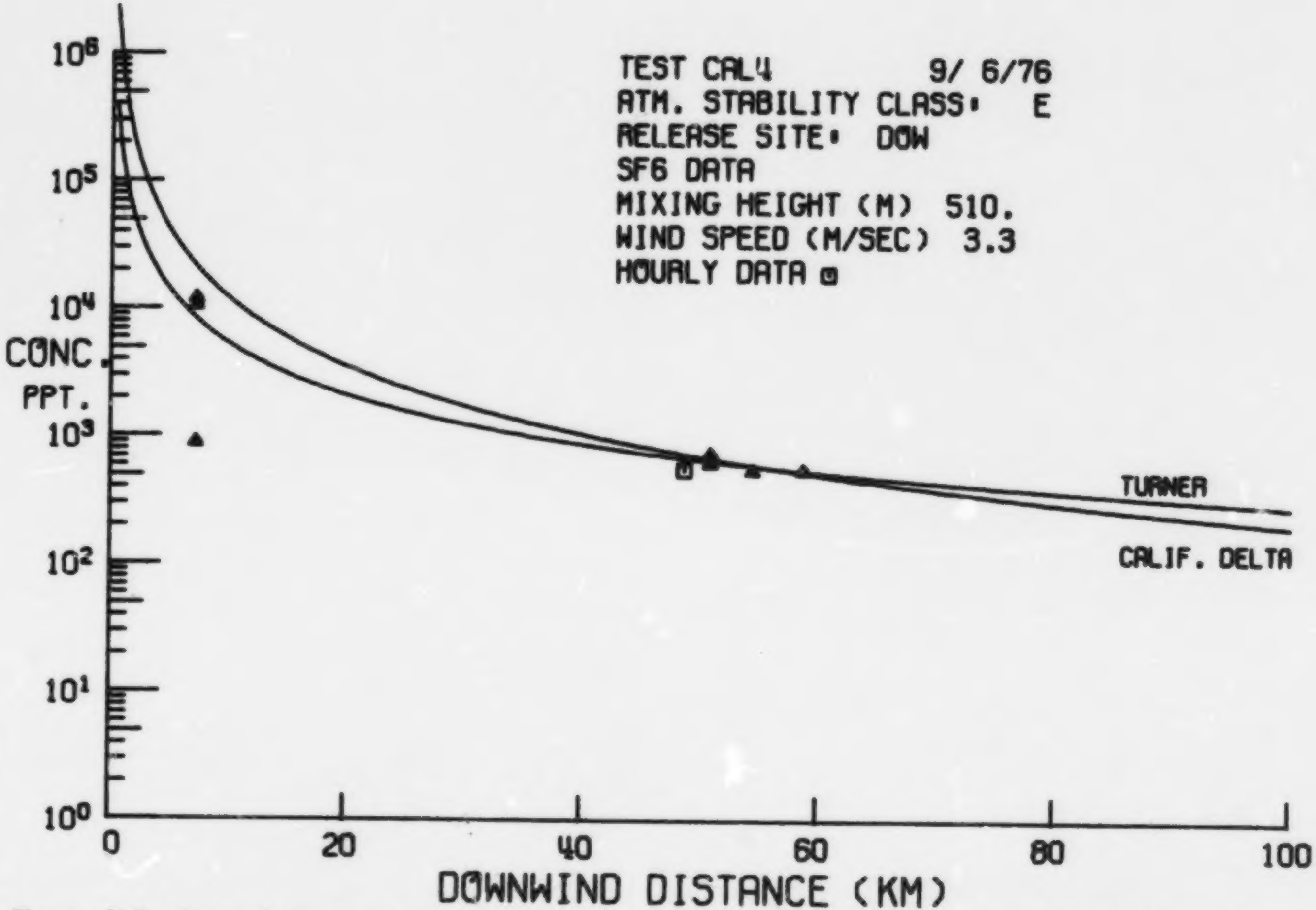

Figure 102. Centerline tracer concentrations compared with centerline concentrations predicted using the Gaussian plume model. The "Turner" curve is based upon Pasquill dispersion parameters given by Turner (1970); the "Calif. Delta" curve is based upon experimental dispersion parameters.

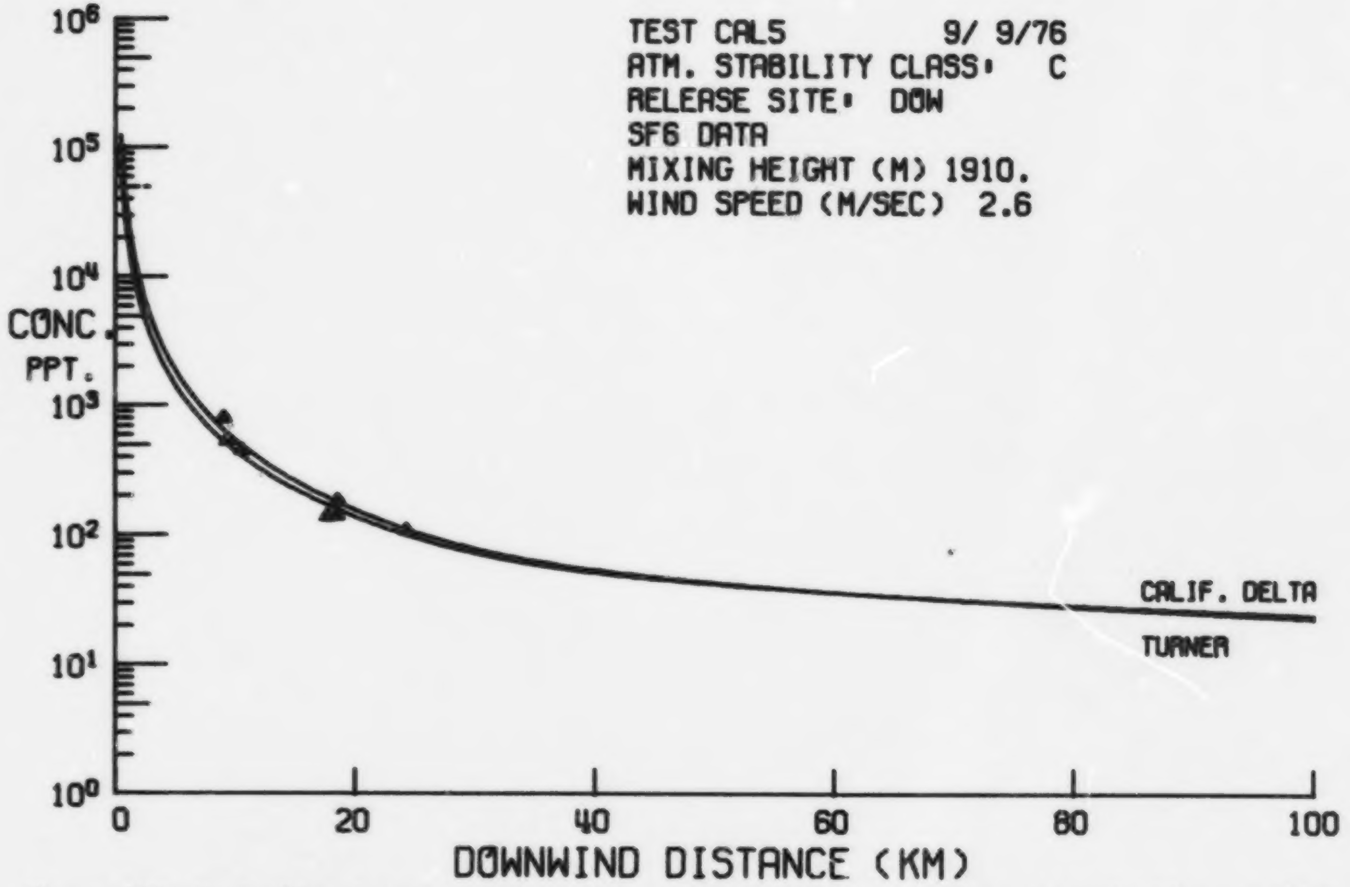

Figure 103. Centerline tracer concentrations compared with centerline concentrations predicted using the Gaussian plume model. The "Turner" curve is based upon Pasquill dispersion parameters given by Turner (1970); the "Calif. Delta" curve is based upon experimental dispersion parameters.

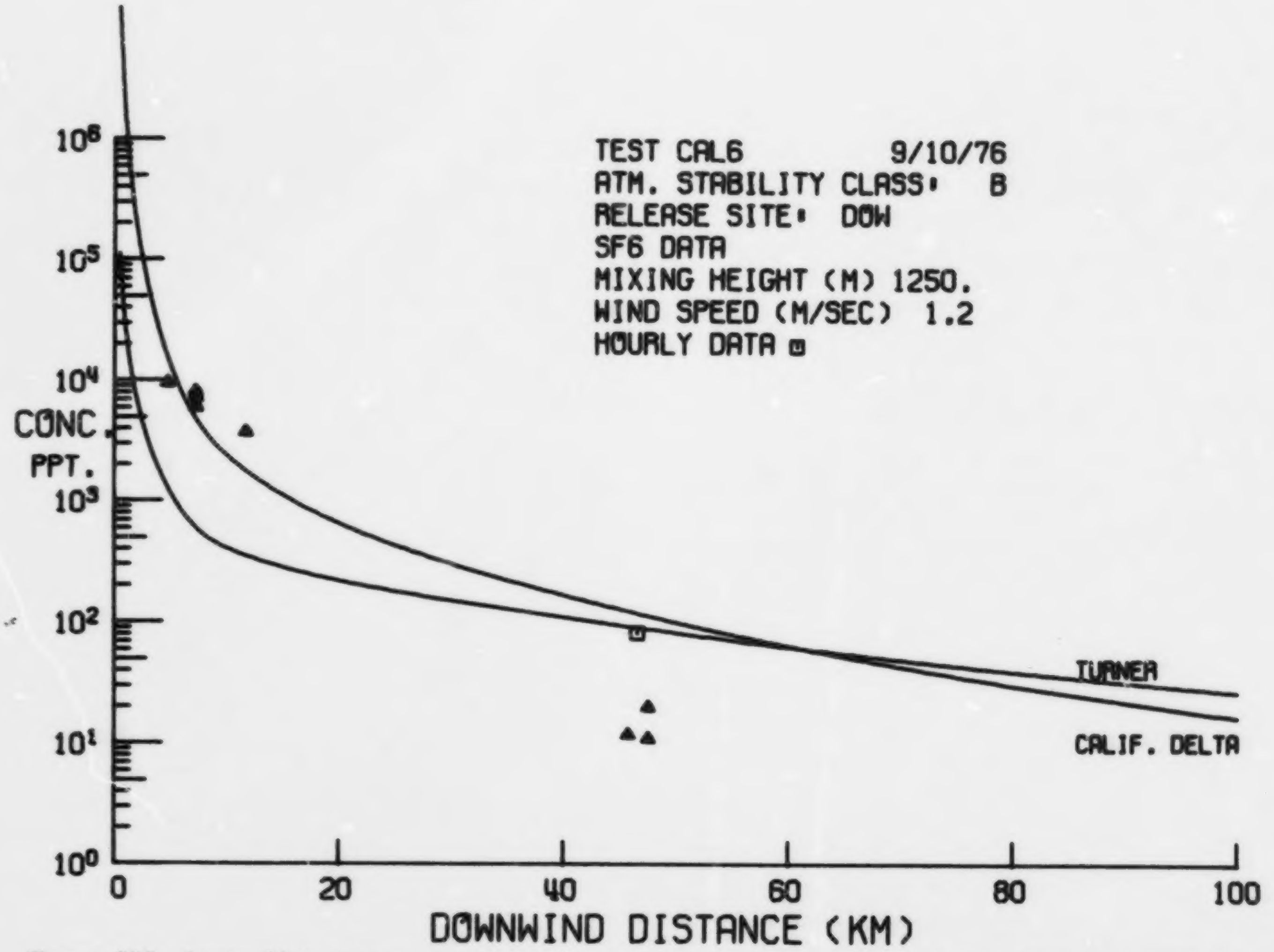

Figure 104. Centerline tracer concentrations compared with centerline concentrations predicted using the Gaussian plume model. The "Turner" curve is based upon Pasquill dispersion parameters given by Turner (1970); the "Calif. Delta" curve is based upon experimental dispersion parameters.

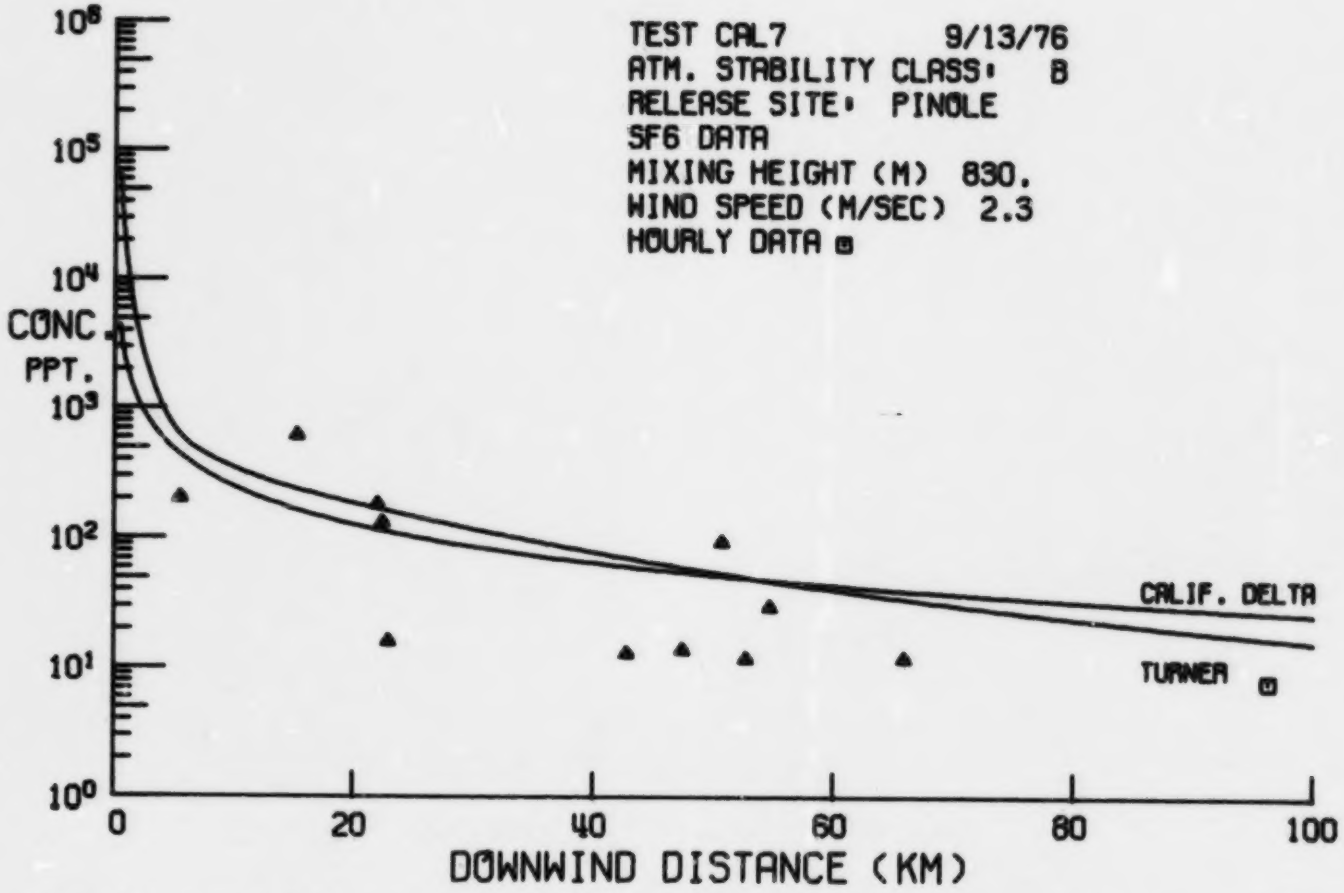

Figure 105. Centerline tracer concentrations compared with centerline concentrations predicted using the Gaussian plume model. The "Turner" curve is based upon Pasquill dispersion parameters given by Turner (1970); the "Calif. Delta" curve is based upon experimental dispersion parameters.

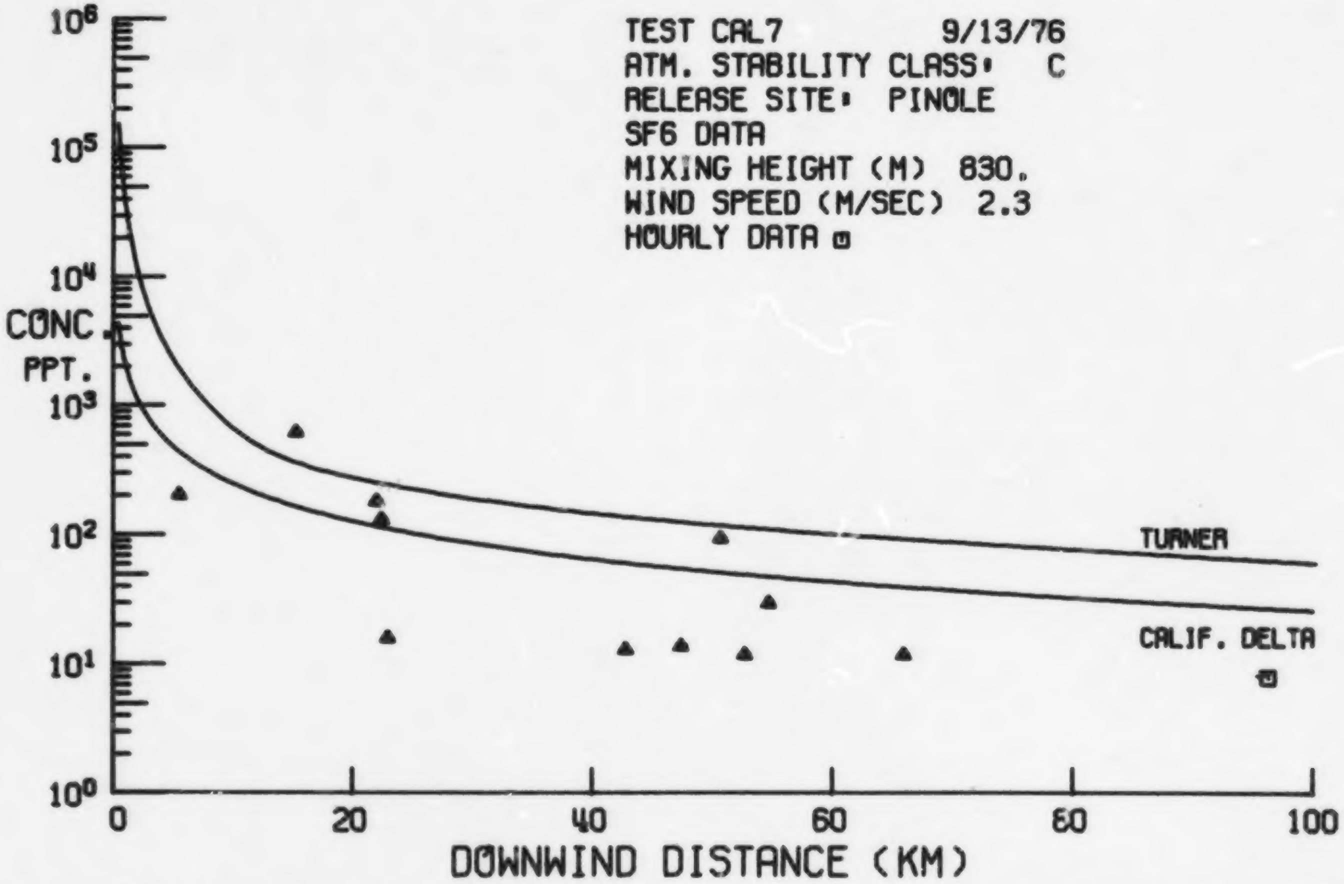

Figure 106. Centerline tracer concentrations compared with centerline concentrations predicted using the Gaussian plume model. The "Turner" curve is based upon Pasquill dispersion parameters given by Turner (1970); the "Calif. Delta" curve is based upon experimental dispersion parameters.

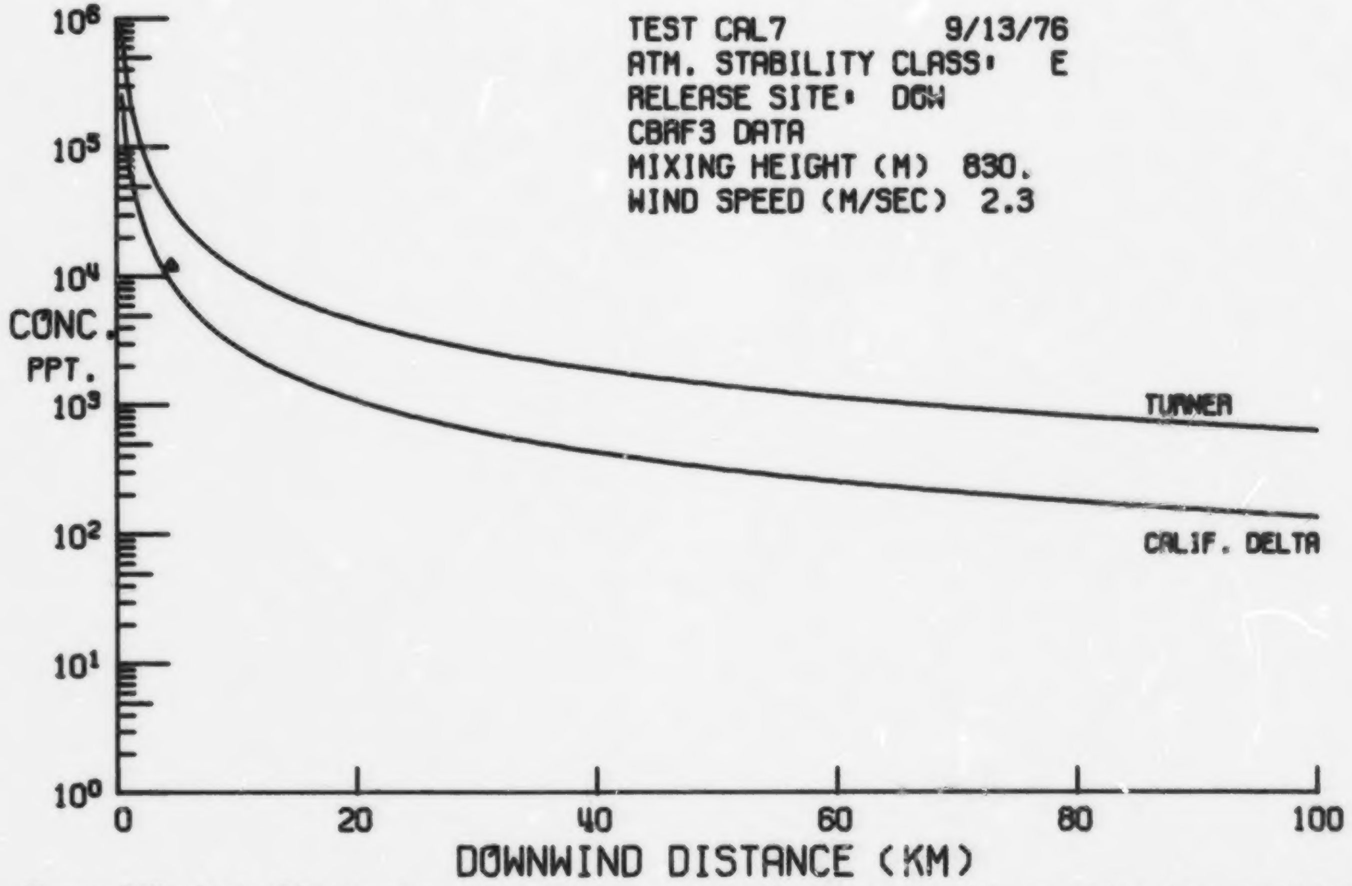

Figure 107. Centerline tracer concentrations compared with centerline concentrations predicted using the Gaussian plume model. The "Turner" curve is based upon Pasquill dispersion parameters given by Turner (1970); the "Calif. Delta" curve is based upon experimental dispersion parameters.

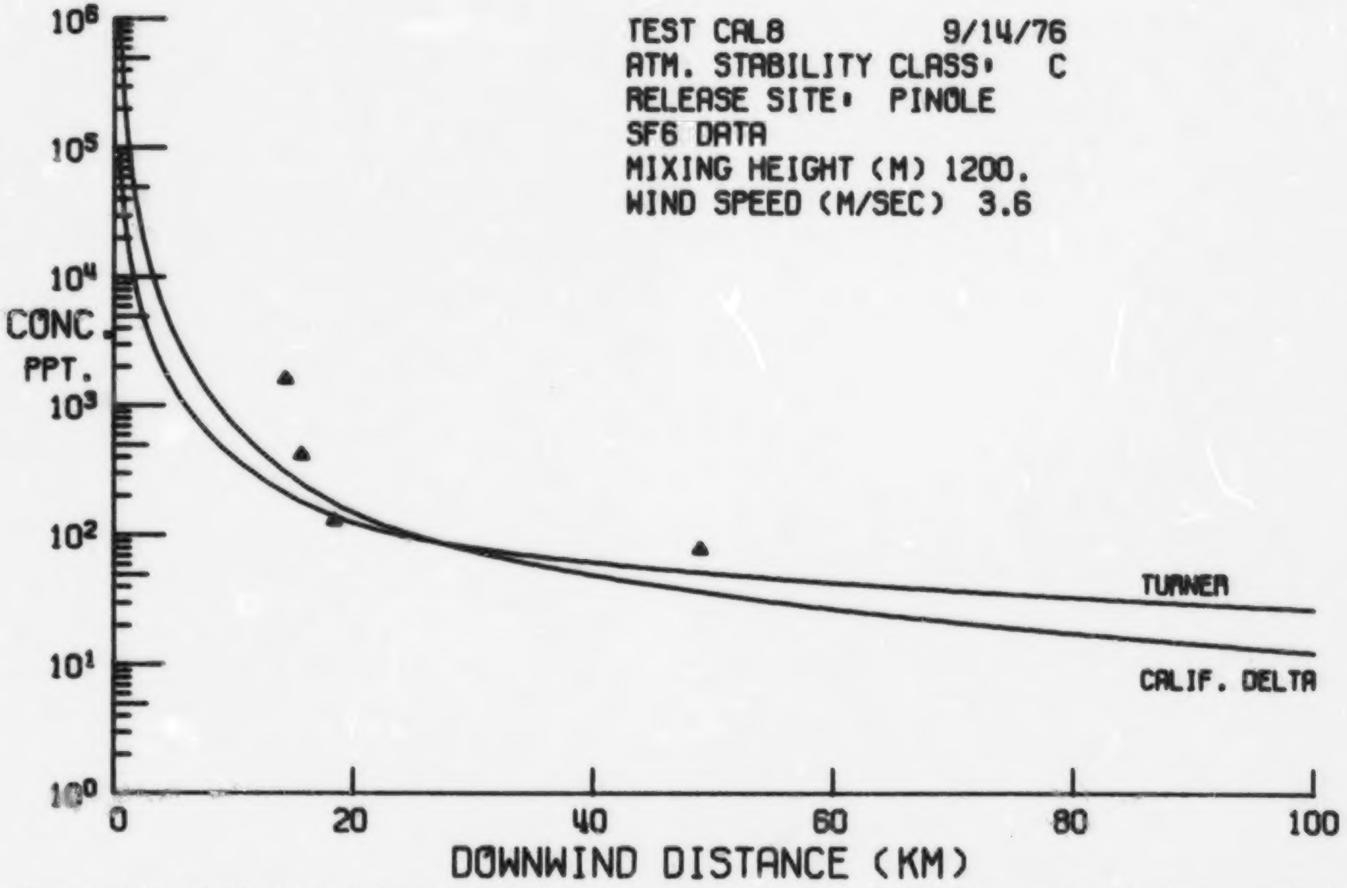

Figure 108. Centerline tracer concentrations compared with centerline concentrations predicted using the Gaussian plume model. The "Turner" curve is based upon Pasquill dispersion parameters given by Turner (1970); the "Calif. Delta" curve is based upon experimental dispersion parameters.

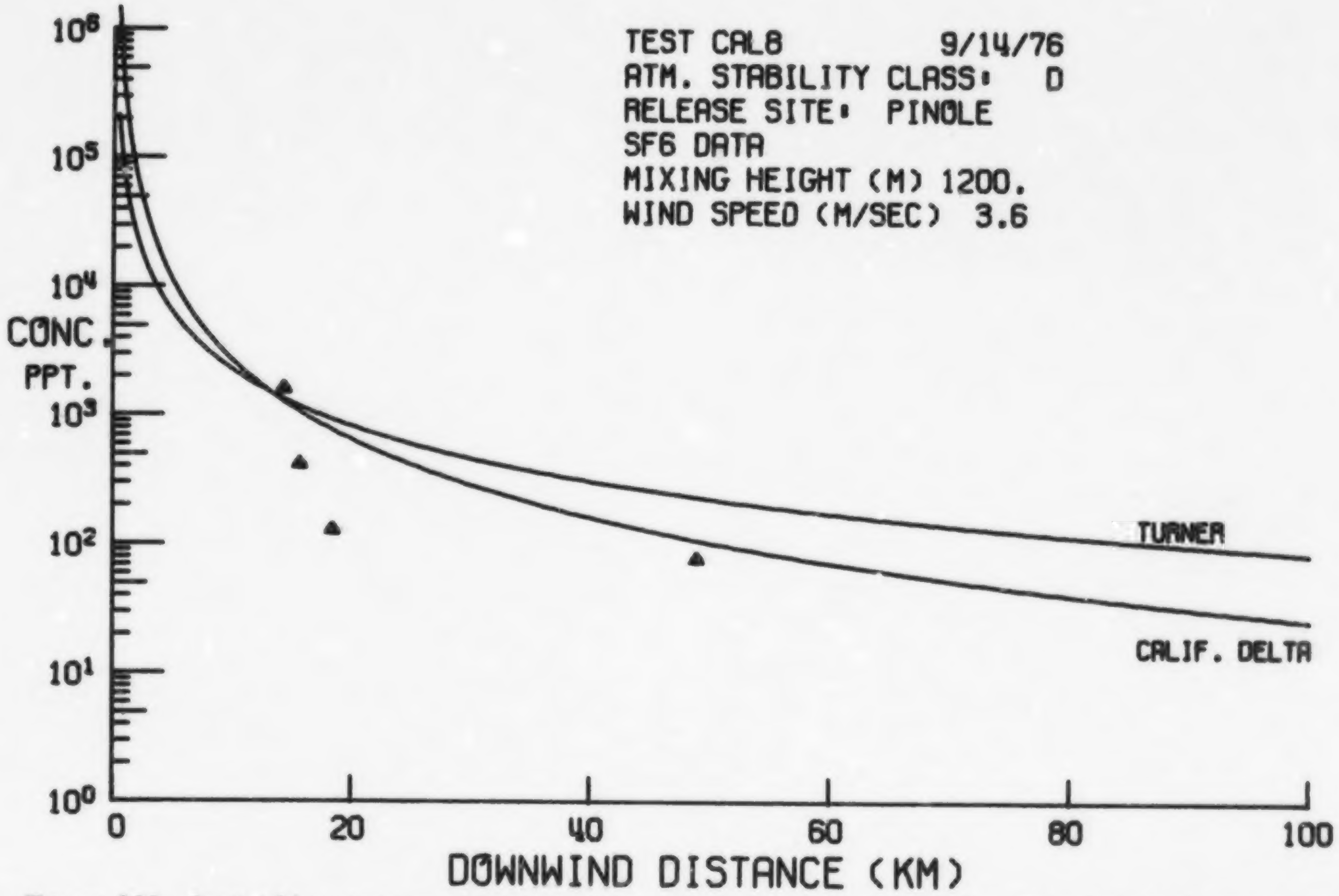

Figure 109. Centerline tracer concentrations compared with centerline concentrations predicted using the Gaussian plume model. The "Turner" curve is based upon Pasquill dispersion parameters given by Turner (1970); the "Calif. Delta" curve is based upon experimental dispersion parameters.

at 40 to 65 km but predicts the experimental concentrations very closely at 10 km. Note that there is essentially no difference between the 10-second and hourly averaged experimental concentrations. Test 1 stability conditions were determined to be close to classes B-C from the meteorology. The predicted curves for the Test 2 release from Martinez for class C conditions do not fall very near the experimental data. The Turner curve under class D conditions serves as an upper bound on the data. Conditions during Test 2 were Pasquill classes B-C. The Turner curves for the Test 2 release from Dow lies fairly close to the experimental data under class D stability. The California Delta curve overestimates concentrations less than 20 km from Dow and underestimates the data point taken 60 km from Dow. The predicted results for Test 3 using Turner's σ_y and σ_z represent the data relatively well under class E conditions. The curve obtained from the experimental dispersion data correctly predicts the tracer concentrations between 40 and 50 km downwind, but the curve overestimates the data at 10 km. The California Delta curve comes much closer to the data in Test 4. However, the Turner curve also fits the Test 4 data fairly well under class E stability. The data from Test 5 is predicted almost exactly by both calculated curves under class C stability conditions. The California Delta curve for Test 6 fits the tracer concentrations at 10 km fairly well, but the curve overestimates the data obtained at 45 km. The curve from the Turner parameters provides a very poor fit of the data under the same conditions. The tracer data from Test 7 is widely scattered and appears to be fitted best by the California Delta curve. Results for class C conditions indicate that the curve using the parameters from Turner serves as an upper bound for the data. The single data point from the Test 7 Dow release is predicted quite closely by the California Delta curve. Note that the curve from Turner could be made to predict the data point by adjusting the stability condition and wind speed. The data from Test 8 is not represented very closely by either calculated curve for classes C or D. The Turner curve for class D conditions serves as an approximate upper bound to the data.

The results of the Gaussian prediction show that in most of the cases considered, the Gaussian plume model predicts the experimental data reasonably well. Where the model was used with the empirical dispersion curves from Turner and for the stability classes determined from the meteorology, reasonable fits of the tracer data were obtained for Tests 1, 3, 4, 5, 7 and 8. In cases where the experimental dispersion parameters were used, reasonable fits of the tracer data were obtained for Tests 1, 3, 4, 5, 6, 7 (Pinole) and 7(Dow).

It appears that both sets of dispersion parameters can be used with the Gaussian plume model with a measurable degree of success. Notably, the predictions appear to fit the tracer data best under the more stable evening and nighttime conditions; these are the periods where it appears worst-case impact can occur. During the daytime in Test 5, the data are perfectly predicted. However, weak northerly winds prevailed during the day and the strong jet of air over Montezuma Hills was not present. In the absence of the strong westerly flow, the dispersion process appeared to follow the classical Pasquill dispersion pattern. Data obtained during the Martinez and Pinole releases were more scattered than for Dow releases. In the Bay Area releases, plumes appeared to diverge widely across the Delta region; the automobile traverses in some cases did not cover the entire width of the plume. During Test 7, the data suggest that the plume split into at least two streams upwind of the Montezuma Hills. It is very difficult to apply the Gaussian model under these conditions.

This presentation of predicted and experimental results indicate that averaging the wind field and mixing heights is a reasonable and, probably the most straightforward method of supplying the necessary input data to the model. In view of the large wind velocity gradients present in the region, the apparent usefulness of average input values is somewhat surprising.

The availability of detailed concentration profiles as obtained from the automobile traverse data is extremely rare. Also, the Gaussian model is rarely used to predict more than plume centerline concentrations. However, because the data are available and the model can be used to determine concentration profiles, we have presented the calculated and experimental traverse profiles for four evening and nighttime traverses in Figures 110 -112. The input values for Figures 110 and 111 represent the overall average conditions during the test. The two smooth curves were calculated with the dispersion parameters from Turner and from the field study. In Test 3-Traverse 6, the Delta curve fits the data almost perfectly; the Turner curve underestimates the peak concentration and overestimates the plume width. Further downwind in Traverse 10, the Delta curve slightly underestimates the peak value, and gives a reasonable approximation of the plume width. The Turner curve again overestimates the maximum concentration, but predicts the plume width fairly well. The results from Test 4, 51 km downwind, are extremely impressive; using overall average input values, both curves predict the tracer data almost perfectly. In Traverse

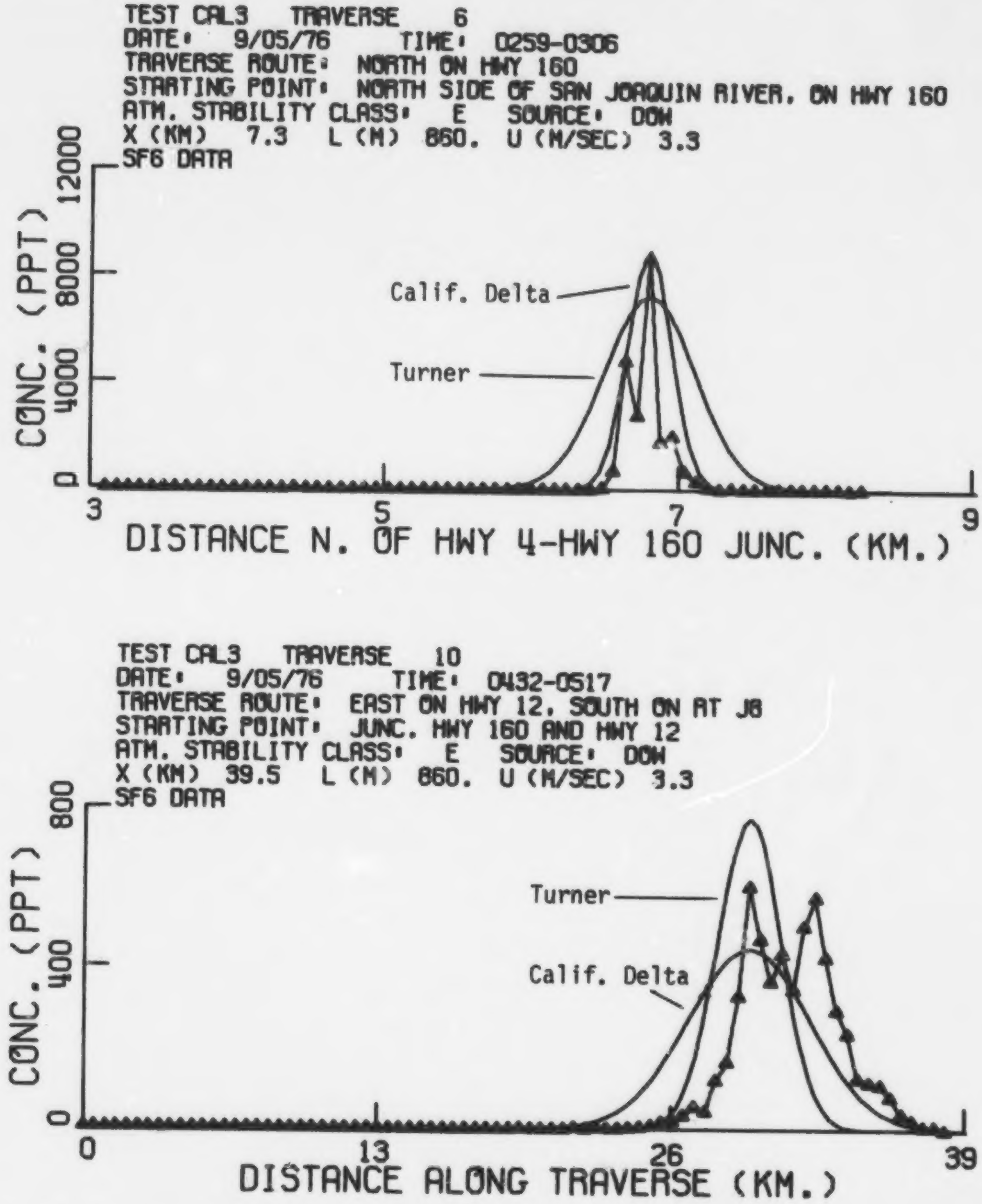

Figure 110. Crosswind tracer profiles compared with crosswind profiles predicted using the Gaussian plume model. The "Turner" curve is based upon Pasquill dispersion parameters given by Turner (1970); the "Calif. Delta" curve is based upon experimental dispersion parameters. Meteorological data represent the average values for the region during the test.

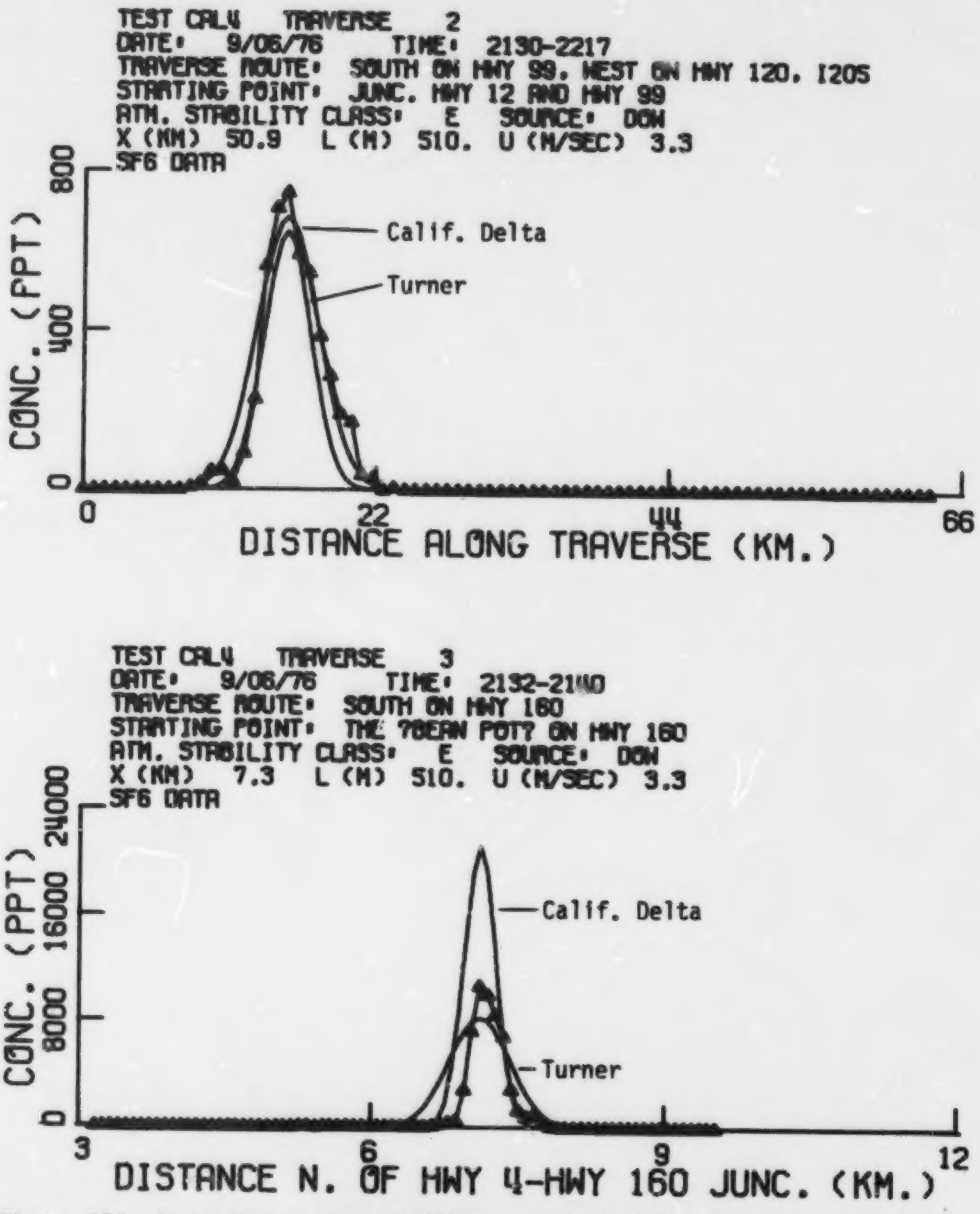

Figure 111. Crosswind tracer profiles compared with crosswind profiles predicted using the Gaussian plume model. The "Turner" curve is based upon Pasquill dispersion parameters given by Turner (1970); the "Calif. Delta" curve is based upon experimental dispersion parameters. Meteorological data represent the average values for the region during the test.

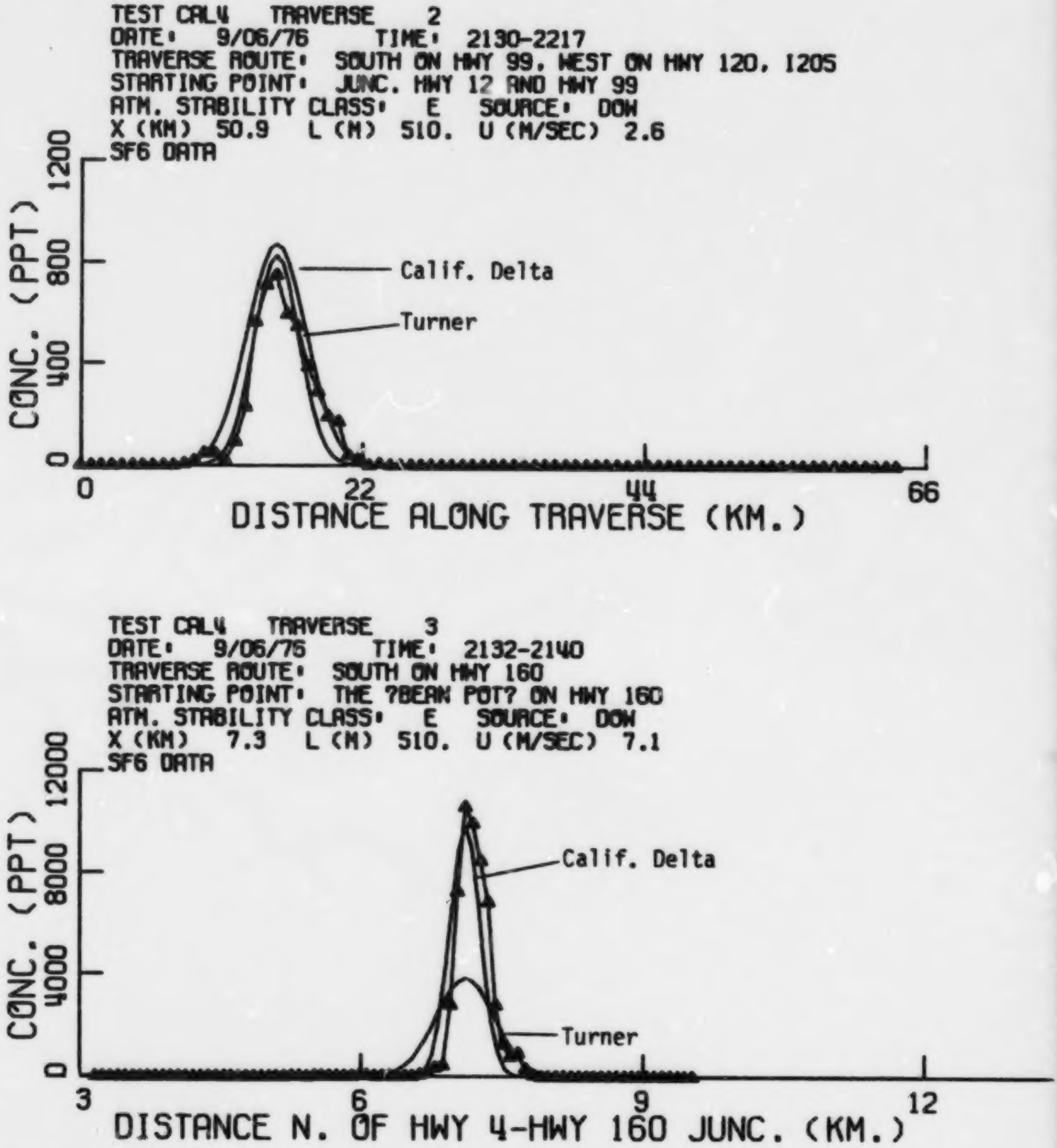

Figure 112. Crosswind tracer profiles compared with crosswind profiles predicted using the Gaussian plume model. The "Turner" curve is based upon Pasquill dispersion parameters given by Turner (1970); the "Calif. Delta" curve is based upon experimental dispersion parameters. Wind speeds for Traverse 2 and Traverse 3 were averaged from measurements taken at Venice Ferry and the Dow site, respectively.

3, just 7 km downwind, the Delta curve overestimates the peak concentration by a factor of two. In Figure 112 however, where average wind speed measured at the release point was used for Traverse 3, the Delta curve gives a very accurate description of the data. The average wind speed for Traverse 2 in Figure 112 was measured at Venice Ferry for the duration of the release. The use of this wind speed does not change the predicted results significantly.

This exercise in detailed Gaussian modeling indicates that under the test conditions, the Gaussian model provides a simple and accurate method for determining pollutant impact. Peak concentrations and plume widths were more than adequately predicted for these traverses. Calculations show that this is true for most of the data obtained during these tests.

Although tracers were released near the surface in every test, the results of the tracer tests can be extended to include effective stack heights which might be typical of industrial chemical facilities. We have seen that the Gaussian expression can be used to predict tracer concentrations given the average meteorological variables as input data. It is also possible to input stack characterisitics into an appropriate plume rise model to determine effective stack heights under a variety of wind and stability conditions. The resulting value of H, the effective stack height, can then be used in the Gaussian expression in order to determine the sensitivity of the regional dispersion processes to stack height. Preliminary design data available for the Dow project include stack heights, stack diameters, stack gas temperatures, and exit velocities (Moyer, 1977). These are listed in Table 12 . We have taken

TABLE 12

STACK CHARACTERISTICS FROM MONTEZUMA PLANT
(Moyer, 1977)

Source	Stack Height (m)	Stack Diameter (m)	Gas Exit Temperature (° K)	Exit Velocity (m/sec)
Stack 1 A	36.6	3.8	450	9.60
Stack 1 B	36.3	3.8	450	9.60
Stack 1 C	19.8	3.4	450	8.40
Stack 1 D	19.8	3.4	450	8.40
Stack 2	19.8	2.1	450	8.40
Stack 3 A	15	1.5	450	12.44
Stack 3 B	15	1.5	450	12.44
Stack 3 C	45	3.0	450	9.34
Stack 4	15	1.7	450	8.25
Stack 5	15	2.9	450	8.25
Stack 6	25	2.5	450	11.50

data for the tallest stack, 37 meters, for input into the Brigg's Plume Rise Model; for details concerning the model, see Briggs (1969) and (1972). The wind speed was taken as the average speed observed at the Dow site during each test, and the Pasquill stability conditions used in the previous modeling analysis were used. Effective stack heights calculated from this data base for each tracer test period ranged from 101 m during Test 3 under class E stability to 415 m during Test 5 under class C stability. The relatively high wind speeds normally observed in the Montezuma Hills cause the calculated plume rise to be smaller than might be expected. The value of H for each test period was used in the Gaussian expression to predict the tracer centerline concentrations.

Typical results are given in Figures 113-115. The agreement between predicted and experimental tracer concentrations for Test 1 and Test 6 is representative of all the tests except Tests 3 and 4. In most cases, the concentrations at both close and far downwind distances were predicted reasonably accurately. In Test 4, Figure 114, where conditions were stable, the maximum concentrations observed at 8 km were sharply underestimated by the calculated curves. As could be expected, under some conditions, plume rise decreases the maximum impact at close distances. However, further downwind, the predicted and experimental values are in excellent agreement. Thus, we see that the field study results can, in most cases, be extended directly to characterization of dispersion from stacks typical of possible industrial developments in the area.

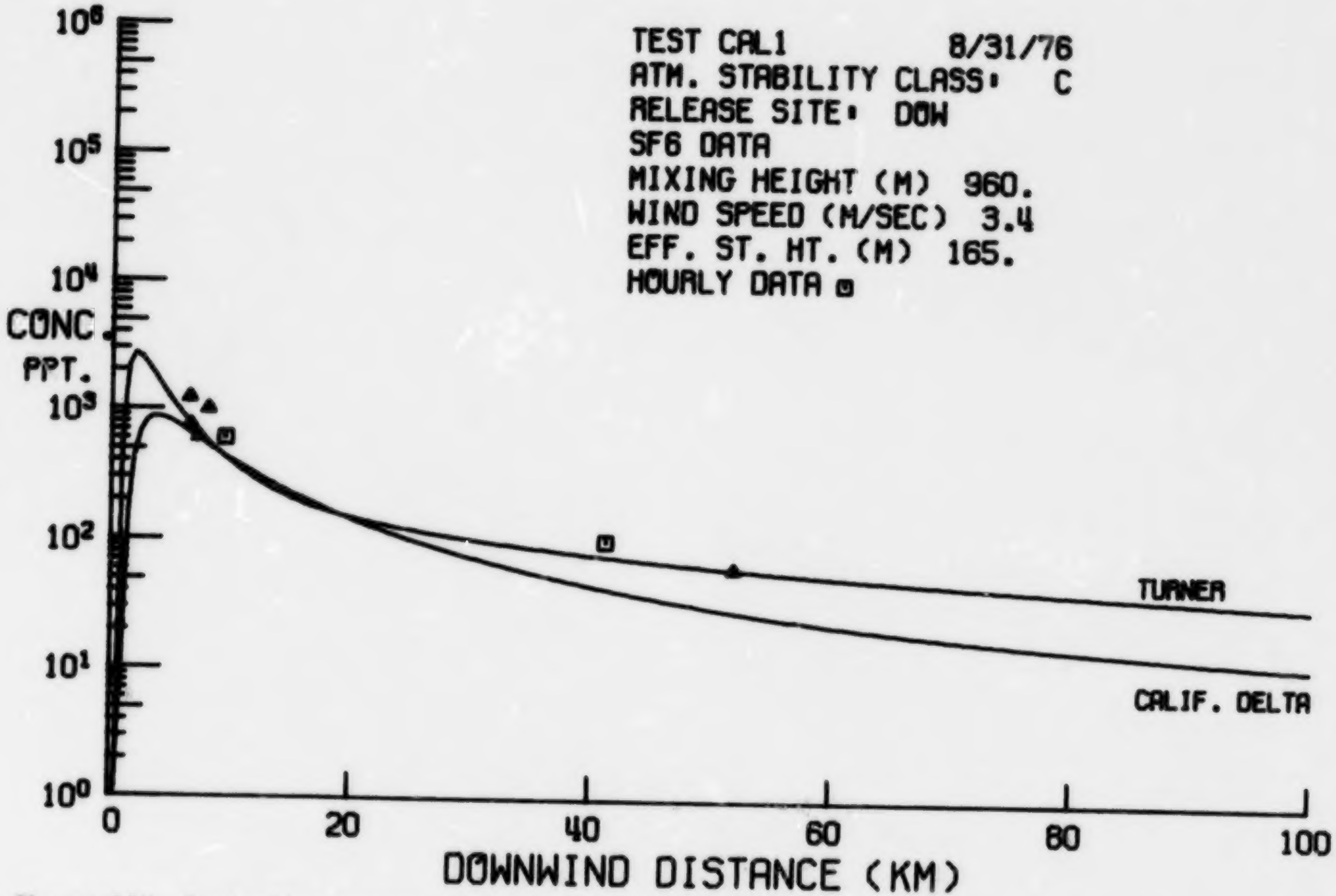

Figure 113. Centerline tracer concentrations compared with centerline concentrations predicted using the Briggs plume rise model and the Gaussian plume model. Stack characteristics were taken from design data for the Dow Montezuma Hills complex. The "Turner" curve is based upon Pasquill dispersion parameters given by Turner (1970); the "Calif. Delta" curve is based upon experimental dispersion parameters.

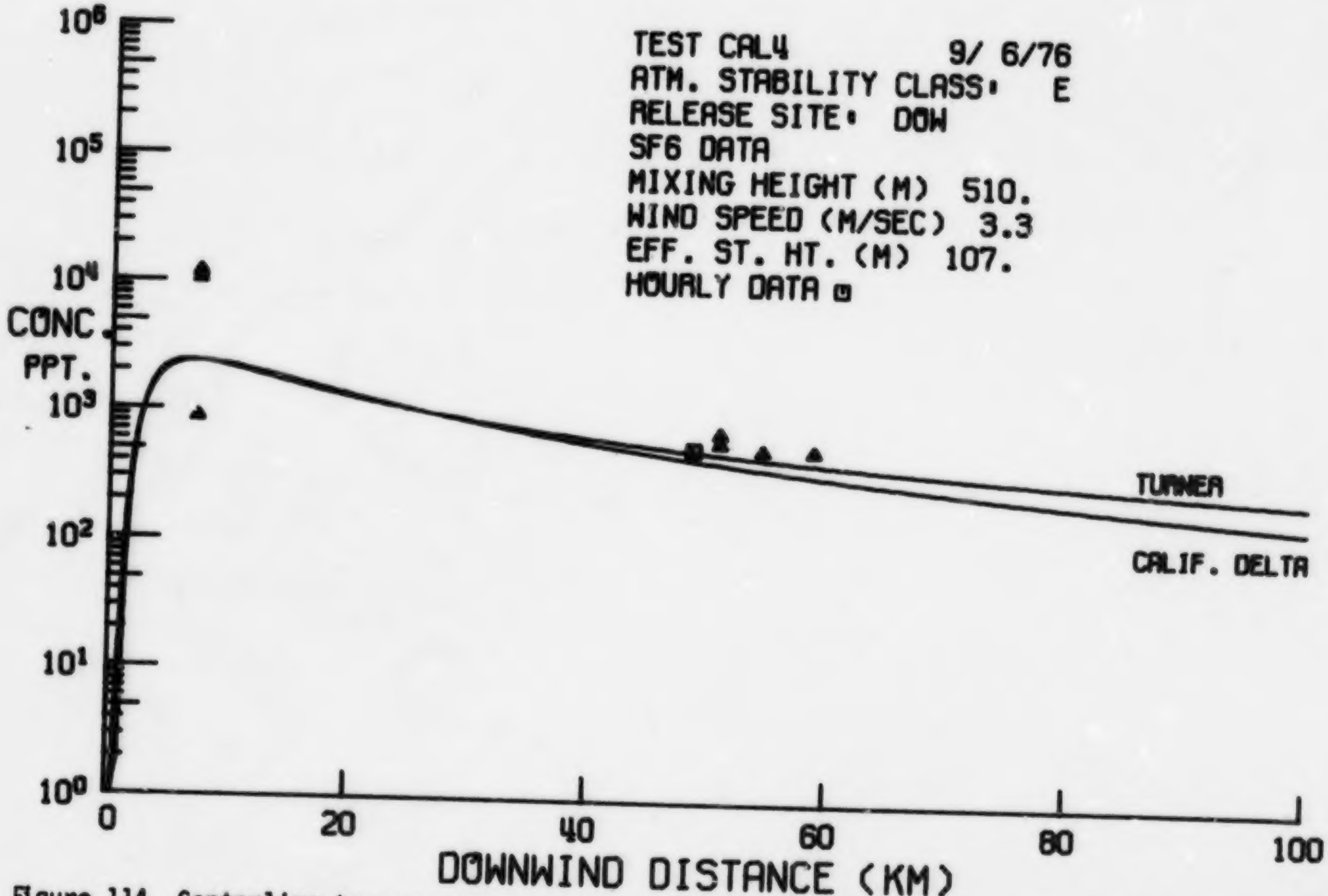

Figure 114. Centerline tracer concentrations compared with centerline concentrations predicted using the Briggs plume rise model and the Gaussian plume model. Stack characteristics were taken from design data for the Dow Montezuma Hills complex. The "Turner" curve is based upon Pasquill dispersion parameters given by Turner (1970); the "Calif. Delta" curve is based upon experimental dispersion parameters.

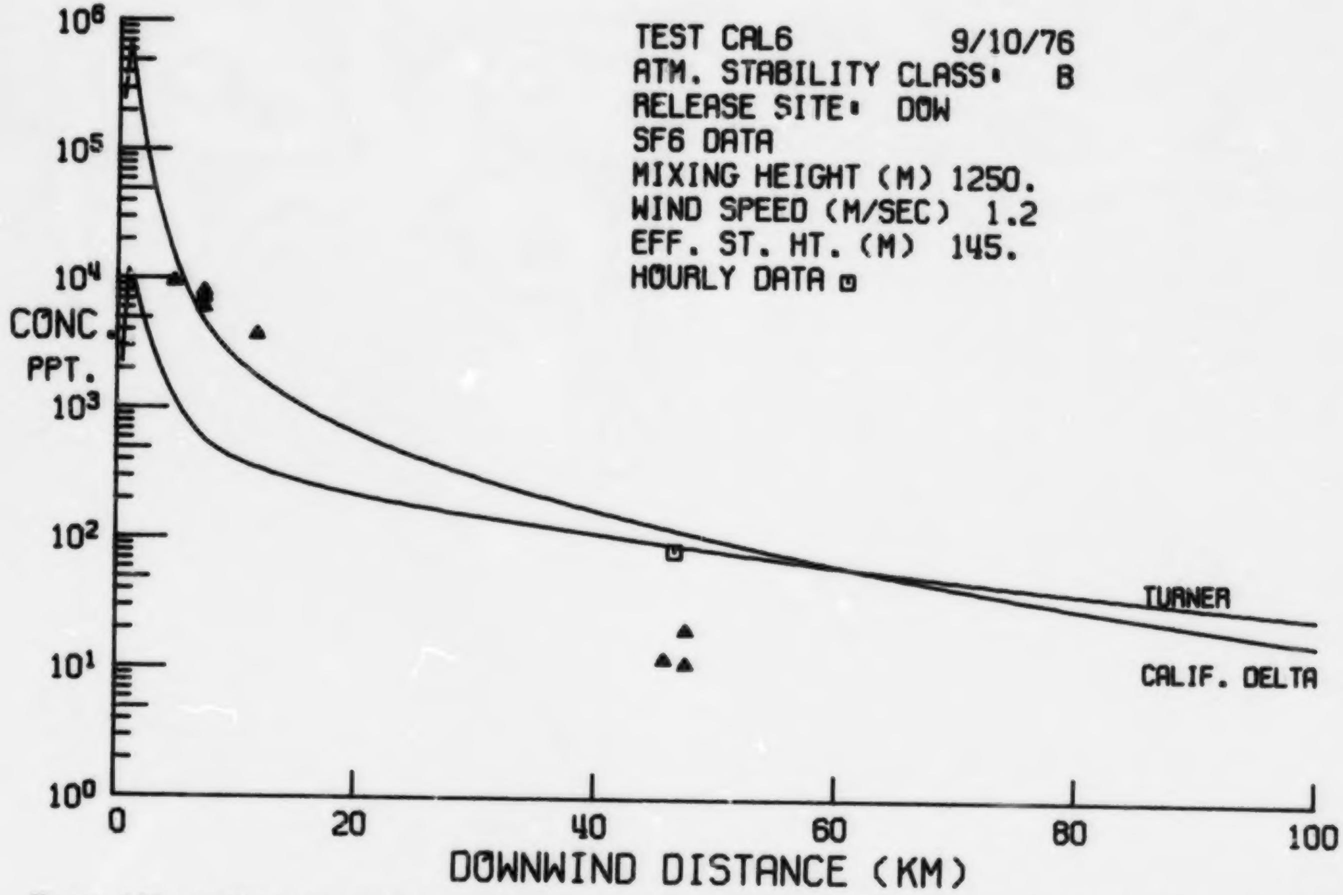

Figure 115. Centerline tracer concentrations compared with centerline concentrations predicted using the Briggs plume rise model and the Gaussian plume model. Stack characteristics were taken from design data for the Dow Montezuma Hills complex. The "Turner" curve is based upon Pasquill dispersion parameters given by Turner (1970); the "Calif. Delta" curve is based upon experimental dispersion parameters.

4.8 Relation of Dispersion Data to Fluctuations of the Wind

Wind data measured by Rockwell at two levels at the Dow site (10 meters and 56 meters) and at Brentwood (10 meters) and data obtained from MRI for the Rancho Seco Nuclear Plant site (61 meters) can be formulated in terms of the hourly horizontal standard deviation of the winds, σ_θ. Hourly values of σ_θ for Dow and Brentwood were calculated using 5-minute averaged wind directions. Values of σ_θ from the Rancho Seco tower were obtained in tabulated form; no information is available concerning the calculation procedure. All of the data are tabulated in Volume II, Part B, Table 17.

A summary of the wind fluctuation data is presented in Figures 116 and 117 for the four locations. The data are plotted for all eight tracer tests as σ_θ versus time of day. Gifford (1968) categorized the magnitude of σ_θ in terms of the Pasquill stability classes. The values of σ_θ corresponding to Pasquill classes are shown in each figure.

The steady nature of the horizontal winds passing over the Montezuma Hills is very apparent in Figure 116. The average values of σ_θ during the test period at the Dow site for the lower and upper heights were 10° and 9°, respectively. At distances 19 km downwind of the Montezuma Hills at Brentwood and 65 km at Rancho Seco, the respective averages during the eight tests were 34° and 17°.

The effects of the steadiness of the winds over the Montezuma Hills upon pollutant transport are readily apparent in Figure 118. The plume centerlines observed in traverses along Highway 160 during the releases from the Dow site, on the average, crossed Highway 160 7.6 km north of the

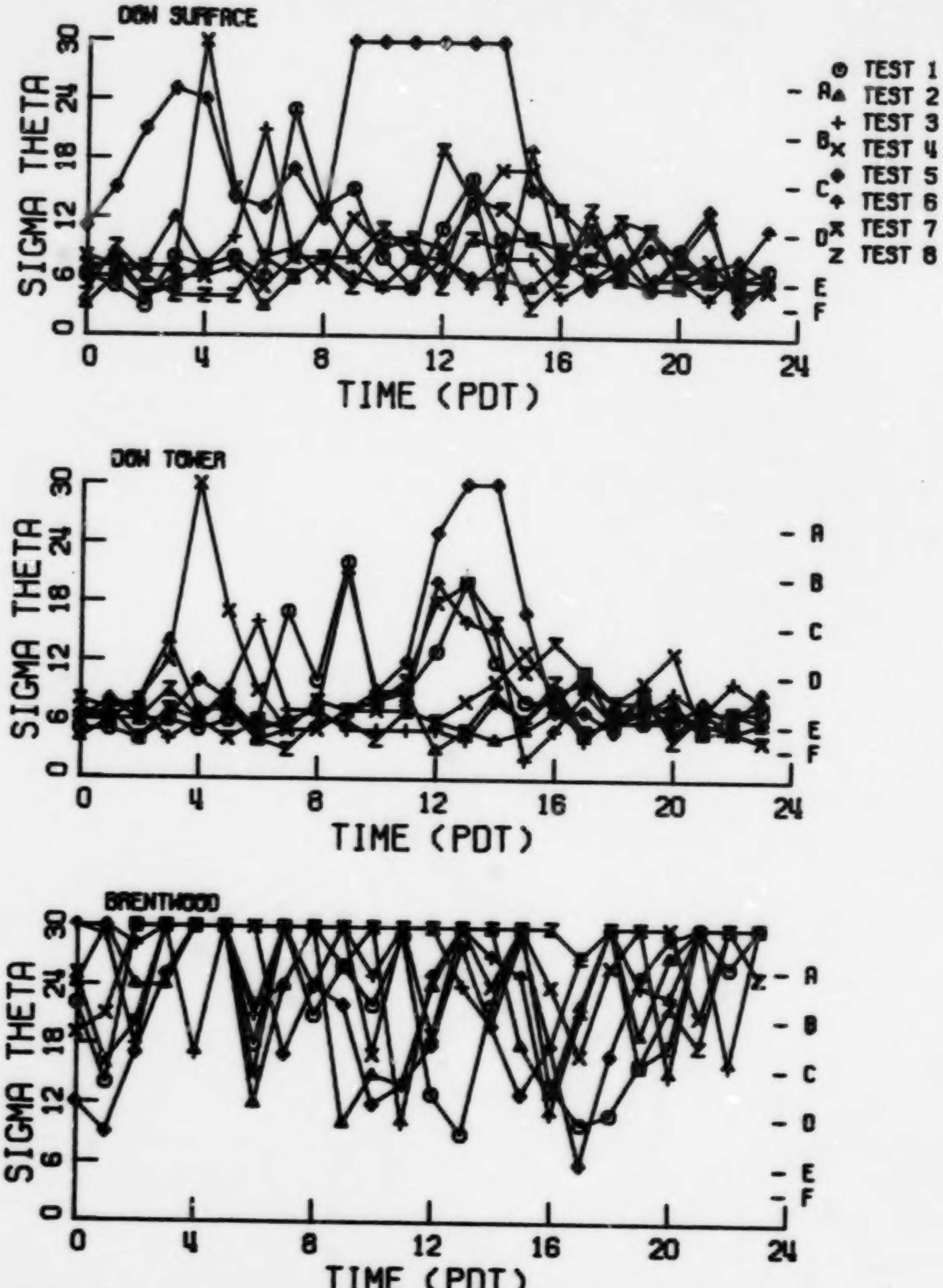

Figure 116. Horizontal standard deviation of the wind as a function of time of day.

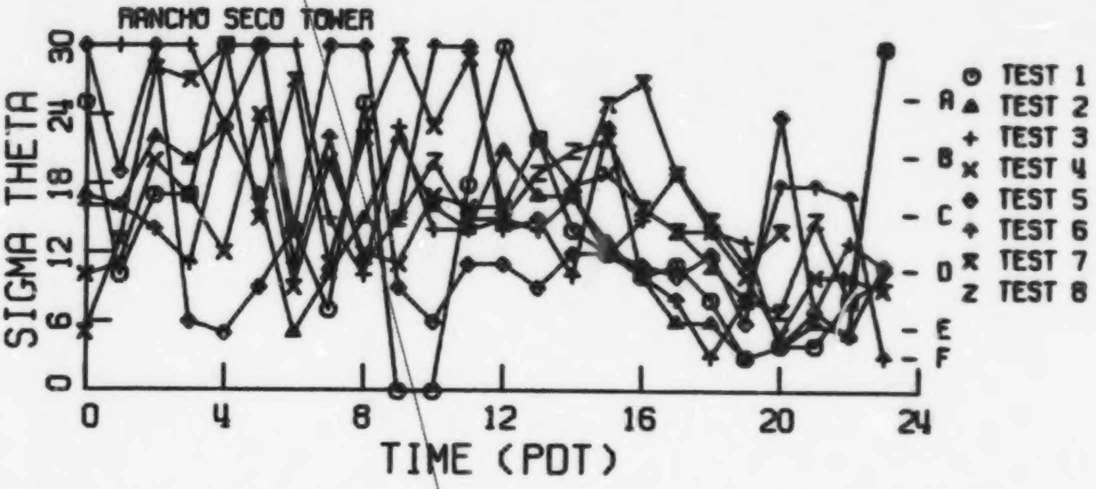

Figure 117. Horizontal standard deviation of the wind as a function of time of day.

Highway 160-Highway 4 junction. The standard deviation of the centerline locations was only ±1.05 km. Thus, the plume centerlines of pollutants emitted from the Dow site under the test period meteorological conditions would have crossed Highway 160 within a 2.1 km zone, 8 km downwind.

Performing a similar analysis upon the traverse and hourly averaged data obtained along Highway 99 yields Figure 119. In this case, the average plume centerline crossed Highway 99 approximately 72 km south of Sacramento or 5 km south of Stockton. The transport zone across Highway 99 calculated from the standard deviation of the centerline locations extended 28 km along the highway. A straight line can be drawn from the release point in the Montezuma Hills to the average centerline position of the plume crossing Highway 160. The extension of this line intersects Highway 99 approximately 2 km north of the observed centerline position. On the average, plumes emitted from the Montezuma Hills during the test periods were transported southeast directly over Stockton. The average plume centerlines from the Dow site to Highway 160 and from Highway 160 to Highway 99 are shown in Figure 120; the standard deviations associated with the centerline positions are also shown. The area enclosed by the standard deviations of the plume centerline positions correspond to the area of major impact which was observed during the eight tracer tests. This area also appears to be closely related to the area swept out by the average value of σ_θ during the field study. The angle associated with the standard deviation

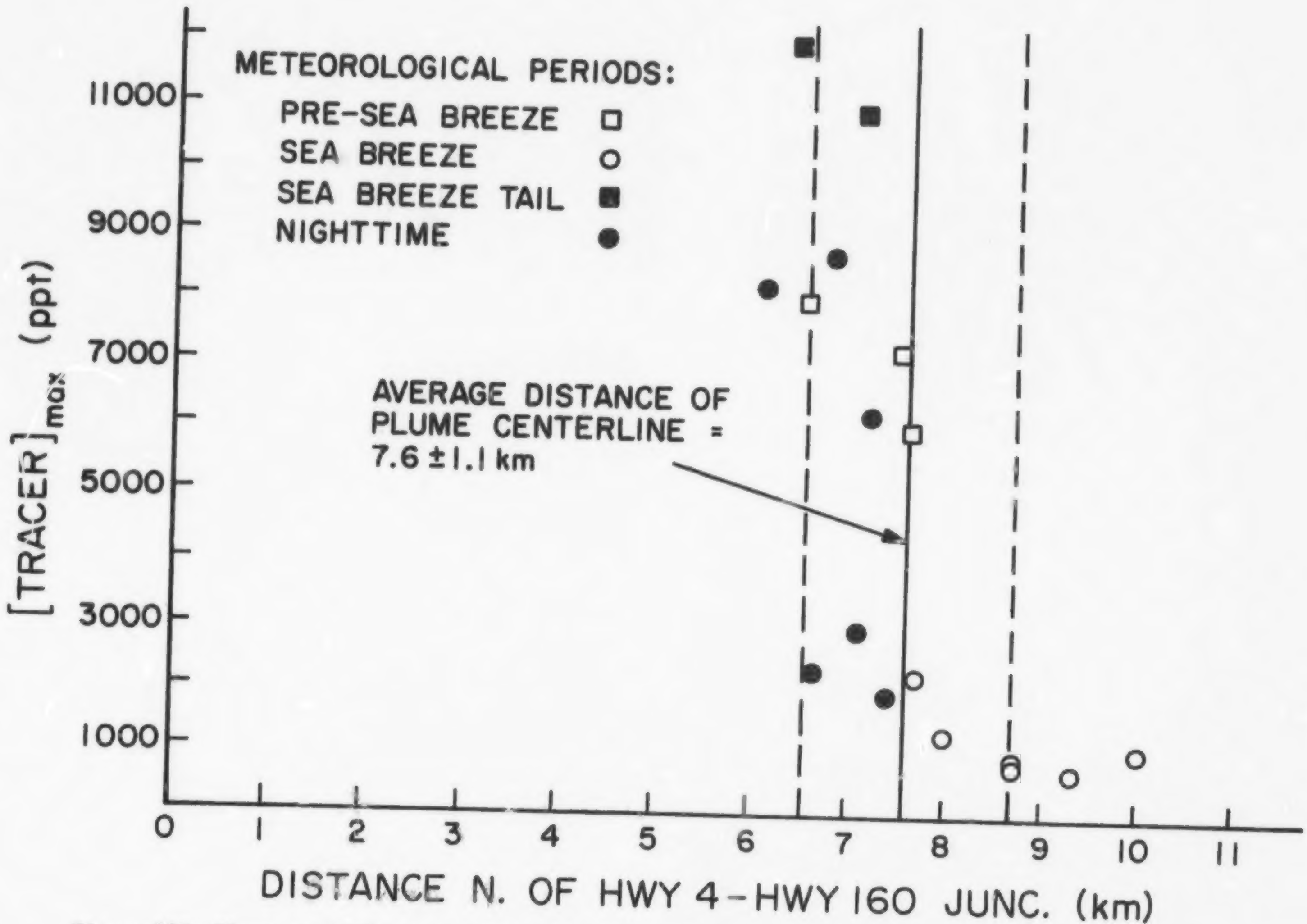

Figure 118. Plume centerline concentration as a function of distance north of the Highway 4 - Highway 160 junction taken from automobile traverse data for Dow tracer releases.

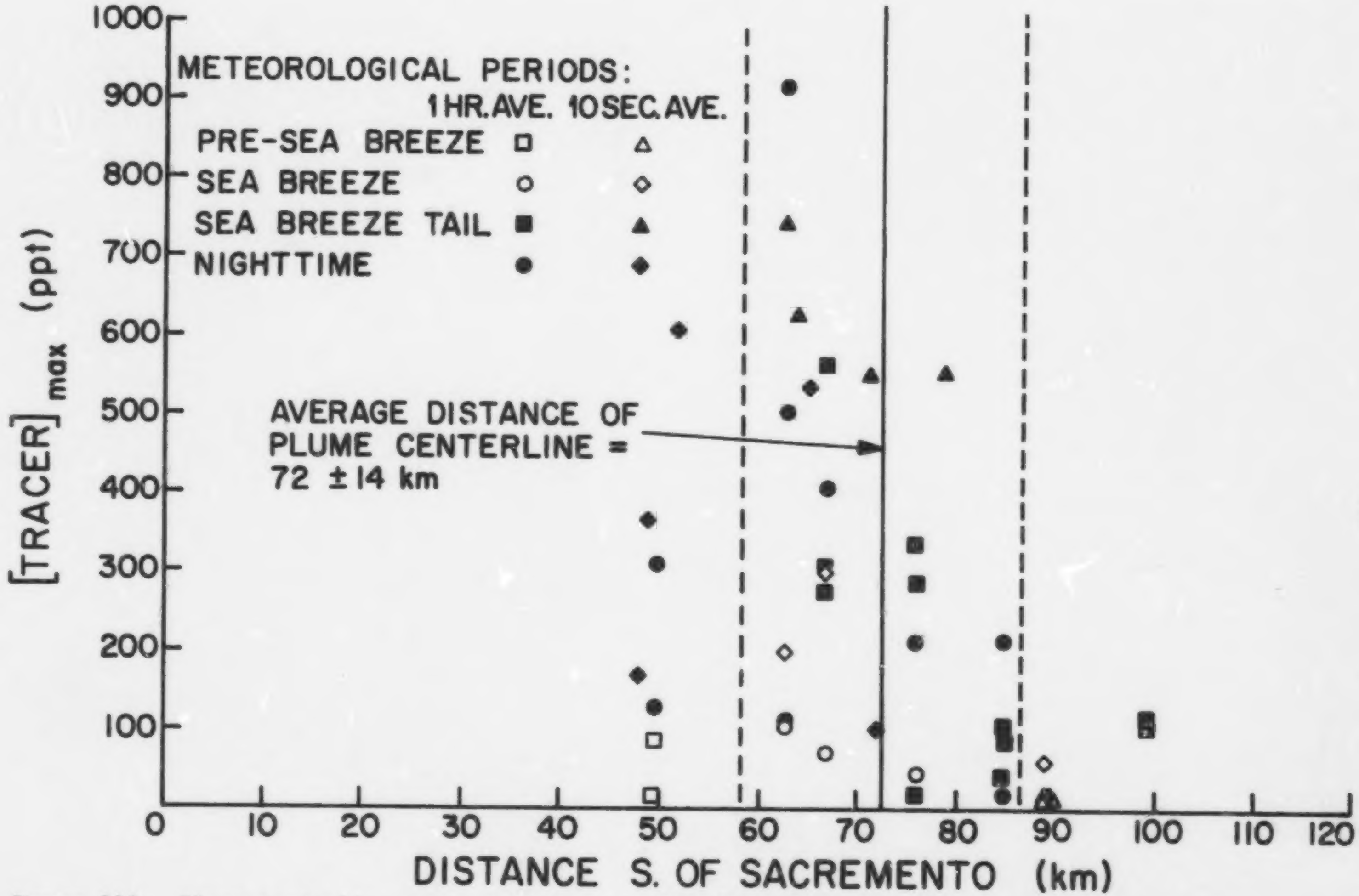

Figure 119. Plume centerline concentration as a function of the distance south of Sacramento along Highway 99 taken from automobile and hourly averaged crosswind tracer profiles.

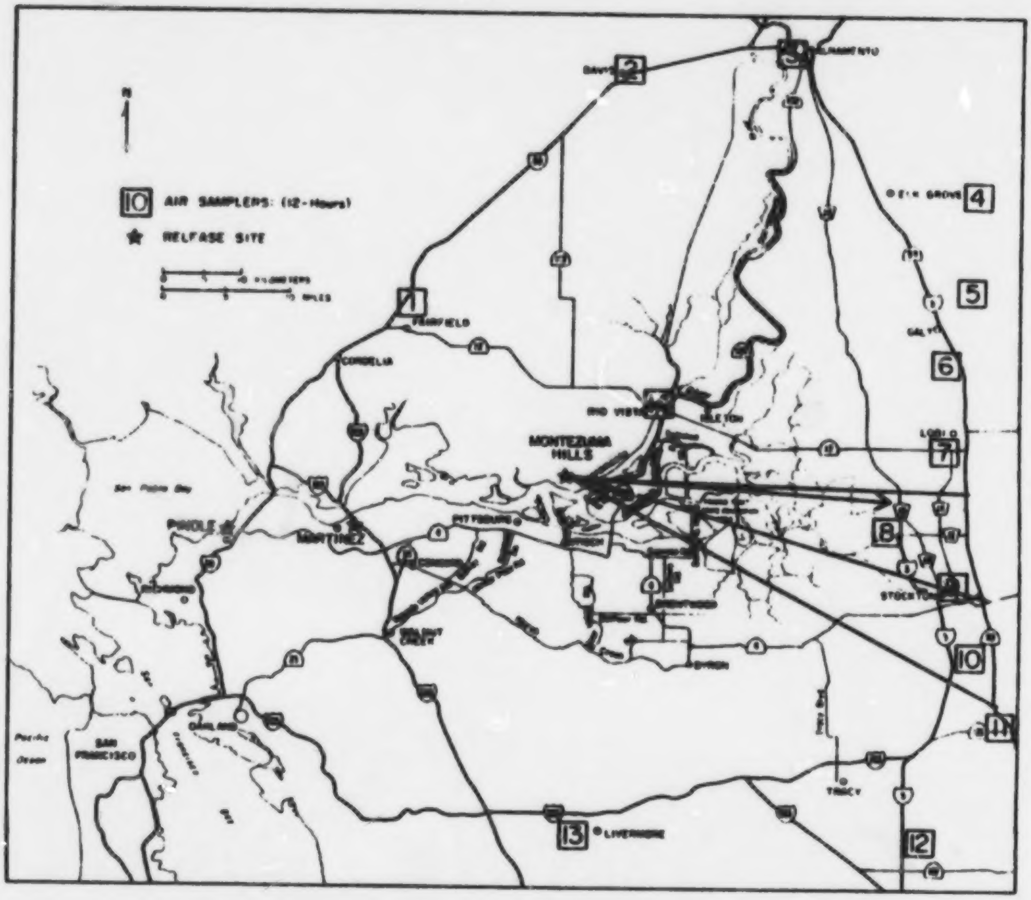
N
10 AIR SAMPLERS: (12-Hours)
★ RELEASE SITE
10 KILOMETERS
10 MILES
DAVIS 2
SACRAMENTO 3
ELK GROVE 4
5
GALT
6
LODI
7
8
STOCKTON 9
10
11
12
TRACY
13 LIVERMORE
1 FAIRFIELD
CORDELIA
RIO VISTA
ISLETON
MONTEZUMA HILLS
San Pablo Bay
PINOLE
MARTINEZ
PITTSBURG
WALNUT CREEK
BRENTWOOD
BYRON
OAKLAND
SAN FRANCISCO
Pacific Ocean

Figure 120. Average plume centerline positions for plumes emitted from the Dow site in the Montezuma Hills. The outer lines represent the standard deviations associated with the average centerline positions. The wind vector represents the vector averaged wind direction during the seven tracer releases from the Montezuma Hills.

of the centerline locations along Highway 160 is 8°; the average value of σ_θ during the tests was 9°. Although the average value of σ_θ agrees very well with the angle determined from the traverse centerline fluctuations, the vector-averaged wind direction during the seven Dow releases does not coincide with the average centerline locations along Highway 160 and Highway 99. The average wind direction was 275°; the angle associated with the location of the average centerline was approximately 285°. The location of maximum impact predicted from the average Dow wind direction is 11 Km north of the location of the average centerline along Highway 99. It appears that curvature of the winds immediately downwind of the Dow site causes the plumes emitted from the Montezuma Hills to turn slightly more to the southeast than expected. As we will see in Section 5, this curvature does appear when wind data from stations downwind of Dow are included in a plume trajectory analysis.

A further result of the nature of the winds over the Delta region is the relationship observed between maximum tracer concentrations in the 10-second and hourly averaged data. Hino (1968) states that the "maximum or axial time-mean concentration of effluent generally decreases with increasing sampling time because the lateral dispersion of effluent increases with time." Hino found in an analysis of a variety of diffusion data that the relationship between maximum concentrations and sampling times generally followed:

$$\frac{C_1}{C_2} = \left(\frac{t_1}{t_2}\right)^{-1/5} \quad \text{for sampling times less than 10 minutes} \tag{16}$$

and

$$\frac{C_1}{C_2} = \left(\frac{t_1}{t_2}\right)^{-1/2} \quad \text{for sampling times from 10 minutes to several hours.} \tag{17}$$

Hino showed that the exponent of -½ in the second relationship was predicted from theoretical grounds as well as from experimental data. The value of -1/5 for short sampling times had been recommended by Nonhebel (1960) and was confirmed in the Hino analysis.

In view of these relationships, conversion of the 10-second averaged maximum concentrations to hourly averaged values should follow the combined relationship:

$$\frac{C_{HR}}{C_{10\,s}} = \left(\frac{t_{10m}}{t_{10s}}\right)^{-1/5} \left(\frac{t_{HR}}{t_{10m}}\right)^{-1/2} \tag{18}$$

where C_{HR} is the hourly value, C_{10s} is the 10-second value, t_{10m} equals 10 minutes, t_{10s} equals 10 seconds, and t_{HR} equals 3600 seconds. Equation (18) results from converting C_{10s} to a 10-minute value using Equation (16) and substituting the converted concentration into Equation (17). The final result may be written as

$$\frac{C_{HR}}{C_{10s}} = 0.18 \tag{19}$$

Thus, according to Hino, maximum hourly averaged concentrations should be approximately one-fifth of the 10-second averaged maximum concentrations. This relationship can be checked easily for the Delta region by comparing the traverse results along Highway 160 and Highway 99 with the hourly averaged data for the hours in which traverses were completed. The results of this comparison are tabulated in Table 13; the ratio of C_{HR}/C_{10s} for each case is also listed. No comparisons were made for the last three tracer tests because traverses were not taken during the hours where maximum hourly values were found.

In view of our previous discussion concerning the steadiness of the winds over the Delta region, the results are not at all surprising. Instead of changes in concentrations by the factor of 5 suggested by Hino, the hourly values are generally no more than a factor of 2 less than the 10-second maximum concentrations. The overall average of the experimental ratio is

$$\frac{C_{HR}}{C_{10s}} = 0.7 \tag{20}$$

These results indicate that the 10-second averaged maximum tracer data can be converted to hourly averaged values rather simply and with reasonable accuracy. This will allow us to estimate maximum hourly averaged pollutant concentrations using the traverse σ_y and σ_z data with the Gaussian plume model. Such estimations will be useful in determining where and when air quality standards might be violated due to emissions from an industrial facility. Presentation of this analysis follows in Section 4.9.

TABLE 13

COMPARISON OF 10-SECOND AND HOURLY AVERAGED MAXIMUM TRACER CONCENTRATIONS

Date	Time PDT	C_{10s} PPT	C_{HR} PPT	C_{HR}/C_{10s}
8/31/76	1347-1447	611	241	0.394
		1013	241	0.238
	1447-1547	756	470	0.622
	1547-1647	1223	602	0.492
	1700-1800	64	44	0.688
			Ave. =	0.487 ± 0.180
9/2/76	1336-1435	33	17	0.515
	$CBrF_3$	2168	2427	1.119
	1436-1536	19	11	0.579
		28	11	0.393
	$CBrF_3$	840	1905	2.27
	1600-1700	29	12	0.414
	1700-1800	91	13	0.143
	1800-1900	32	21	0.656
			Ave. =	0.761 ± 0.671
9/5/76	0200-0300	537	504	0.939
	0400-0500	370	309	0.835
		608	309	0.508
			Ave. =	0.761 ± 0.225
9/6/76	2100-2200	746	305	0.409
	2200-2300	628	566	0.901
		553	566	1.024
	2300-2400	553	333	0.602
			Ave. =	0.734 ± 0.280

Overall average = 0.687 ± 0.452

The preceding results suggest that it is possible to relate the magnitude of the wind fluctuations to the magnitude of the horizontal dispersion parameter in a straightforward manner. If one assumes that the centerline of a plume fluctuates within the angle of the standard deviation of the wind as we have seen, then an ideal crosswind dispersion distance can be defined as

$$A = X \tan(\sigma_\theta) \simeq X \sigma_\theta \tag{21}$$

where σ_θ is measured in radians and A is simply half the crosswind distance through which the plume centerline moves in an hour, measured at the downwind distance, X. In other words, A represents an ideal dispersion parameter based only upon the crosswind fluctuation of the plume centerline. To see how the experimental dispersion parameter is related to values of σ_θ in the Delta region, σ_y for each traverse is plotted in Figure 121 as a function of σ_θ. Values of A were based upon the value of σ_θ measured at the surface on the Dow site for the hour in which the traverse was taken. The best-fit line through the data in Figure 121 indicates that σ_y can be written as a simple function of σ_θ :

$$\sigma_y \simeq 0.6 X \sigma_\theta . \tag{22}$$

Values of σ_θ were calculated from 5-minute averaged wind directions.

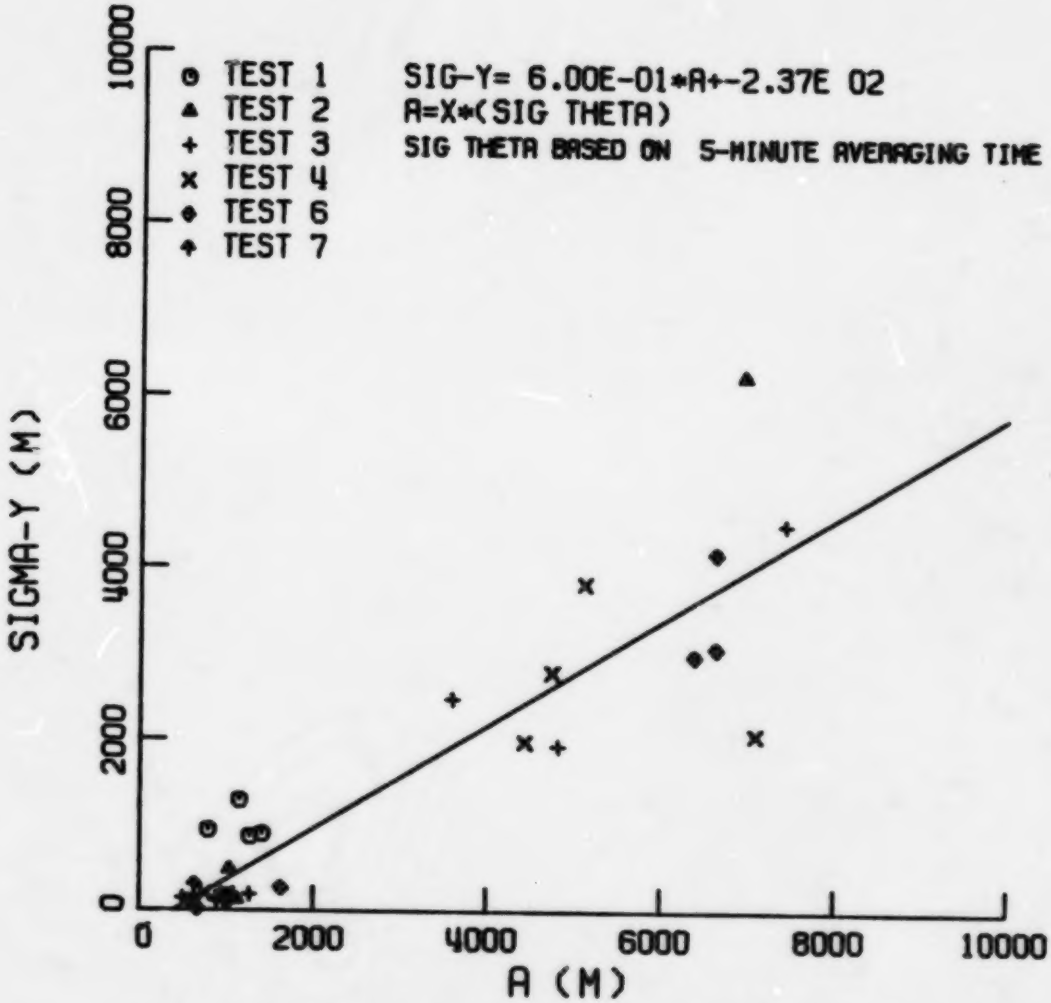

Figure 121. Horizontal Crosswind Standard Deviation (σ_y) as a function of the horizontal standard deviation of the wind (σ_θ) measured at the Dow site in the Montezuma Hills.

This relationship is very similar to an equation given by Islitzer (1961) for an unstable atmosphere:

$$\sigma_y = 0.81 X \sigma_\theta \tag{23}$$

where σ_θ was based on 5-second averaged wind directions and σ_y was measured at downwind distances up to 3.2 km. In a later work, Islitzer and Dumbauld (1963) found that values of σ_y equaled $X \sigma_\theta$ for unstable atmospheres if values of σ_θ were based on averaging times dependent upon the travel time from the source to the receptor. These times were determined to be a function of β, the ratio of the Lagrangian to Eulerian time scales.

The difference between the results of these earlier works and the relationship predicted from the field study can possibly be explained by noting that the wind direction averaging times were considerably different and the transport distances in the Delta study were considerably greater than in those cited above. Islitzer, recalling work by Hay and Pasquill (1959), states that the correct averaging time is determined from the proper part of the spectrum of turbulence by

$$s = T/\beta \tag{24}$$

where β is taken to equal 5 and T is the transport time, X/u. In the Delta field study values of s were of order 7 minutes at 8 km and 50 minutes at 50 km. The actual averaging time used was 5 minutes.

The 5-minute wind direction averages can be summed and averaged to give 10-minute and longer averaging times. These average directions can then be used to determine the hourly standard deviation of the winds based on a new averaging time. To investigate the effects of longer averaging times upon the relationship between σ_y and σ_θ, we have calculated hourly averaged values of σ_θ based on 10-minute, 15-minute, and 20-minute averaging times. The results for all eight tests are given in Figure 122. The general effect of longer averaging times is to decrease the standard deviation of the wind during an hour. The new relationships between σ_y and σ_θ for increasing averaging times are shown in Figures 123 - 125 .

The slopes of the best-fit lines for the three averaging times appear to go through a maximum for σ_θ (15-minutes). The respective relationships for the increasing values of s are:

$$\sigma_y = 0.60 \times \sigma_\theta \text{ (5-minutes)}, \tag{25}$$

$$\sigma_y = 0.65 \times \sigma_\theta \text{ (10-minutes)}, \tag{26}$$

$$\sigma_y = 0.76 \times \sigma_\theta \text{ (15-minutes)}, \tag{27}$$

and

$$\sigma_y = 0.75 \times \sigma_\theta \text{ (20-minutes)}. \tag{28}$$

These results indicate that the proportionality coefficient between σ_y and $\sigma_\theta(s)$ is very sensitive to the magnitude of s. If, indeed, $\sigma_y = X\ \sigma_\theta\ (s)$ for a specified value of s, then the results of this analysis suggest that s lies close to 15 minutes for the dispersion data under consideration. Of course, it is possible that the difference between s = 15 and s = 20 is insignificant, and the correct value of s is larger than 20 minutes. At any rate, it does appear that the initial

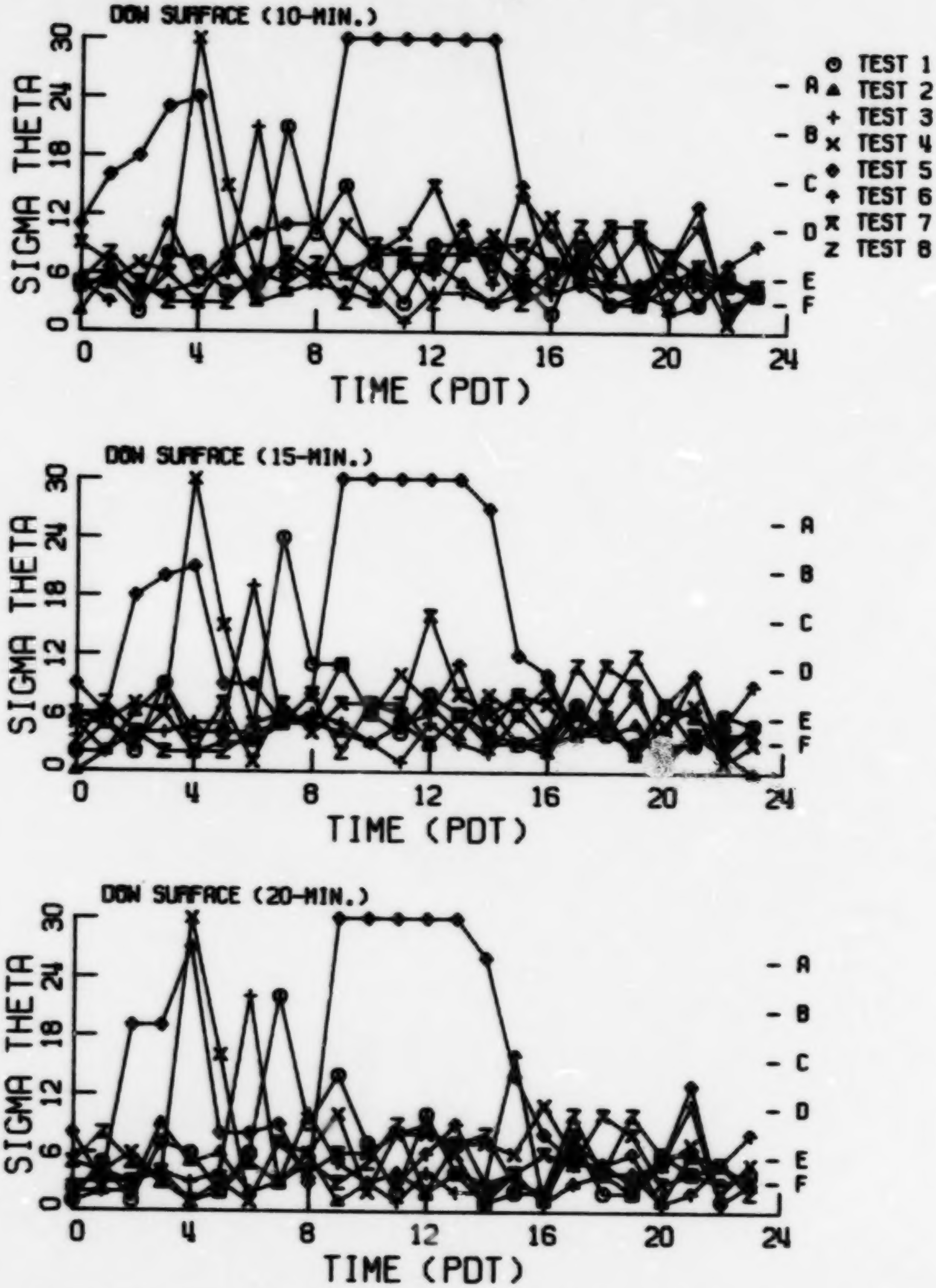

Figure 122. Horizontal standard deviation of the wind, σ_θ, as a function of time of day for different averaging periods.

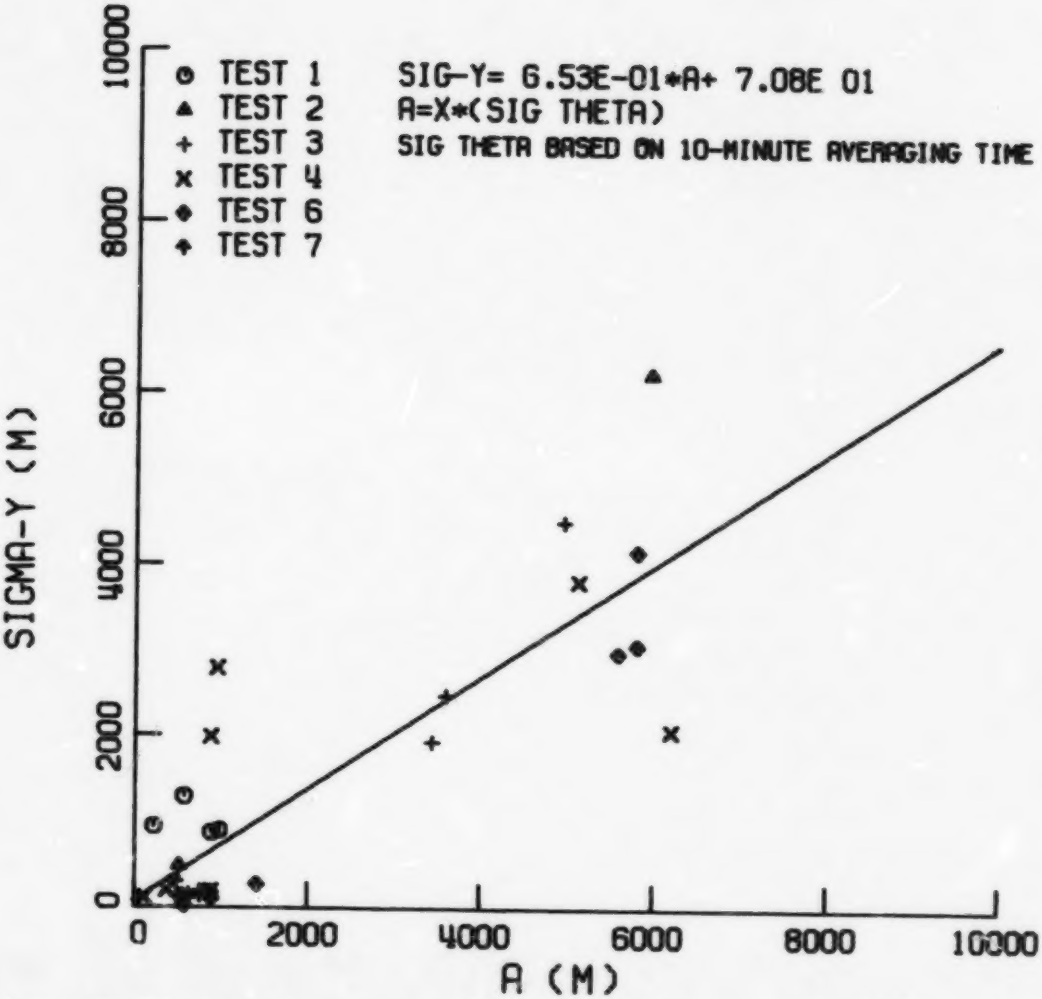

Figure 123. Horizontal crosswind standard deviation, σ_y, as a function of the horizontal standard deviation of the wind, σ_θ, measured at the Dow site in the Montezuma Hills.

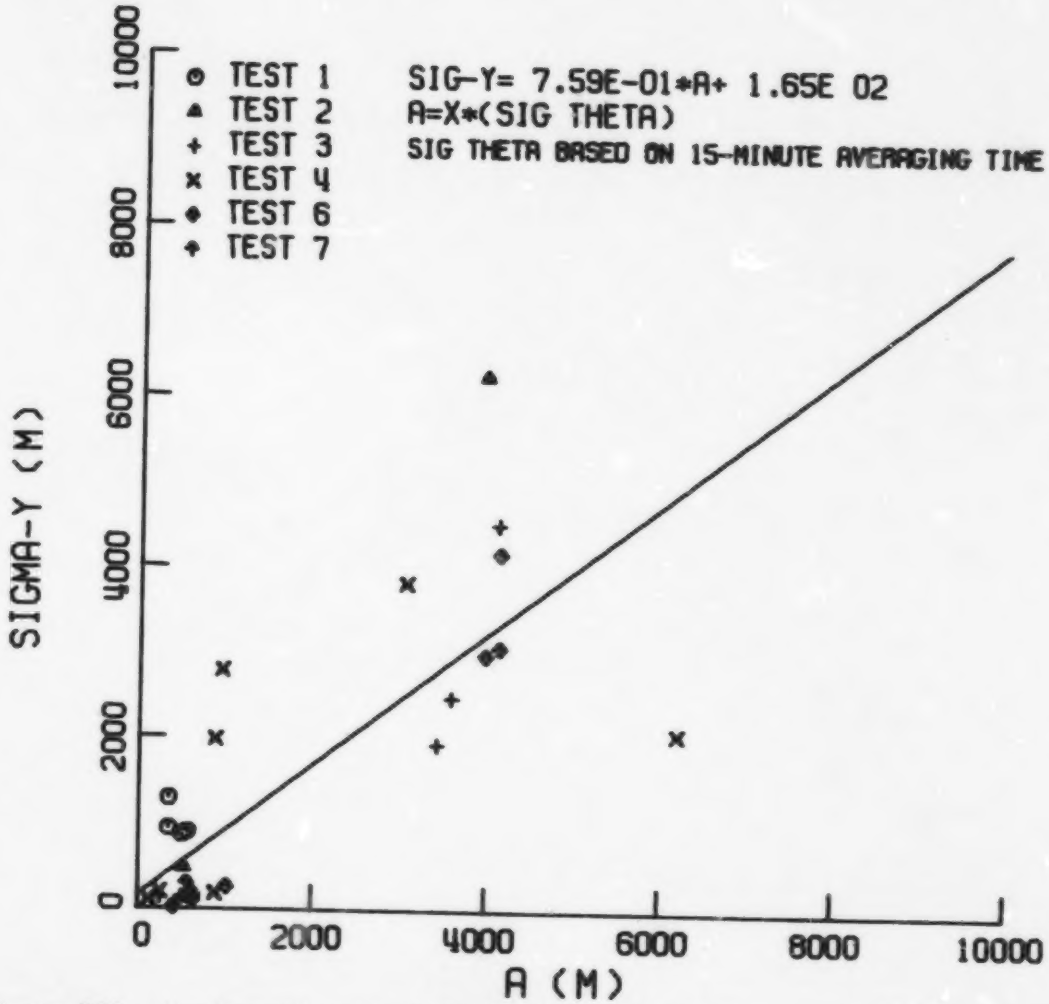

Figure 124. Horizontal crosswind standard deviation, σ_y, as a function of the horizontal standard deviation of the wind, σ_θ, measured at the Dow site in the Montezuma Hills.

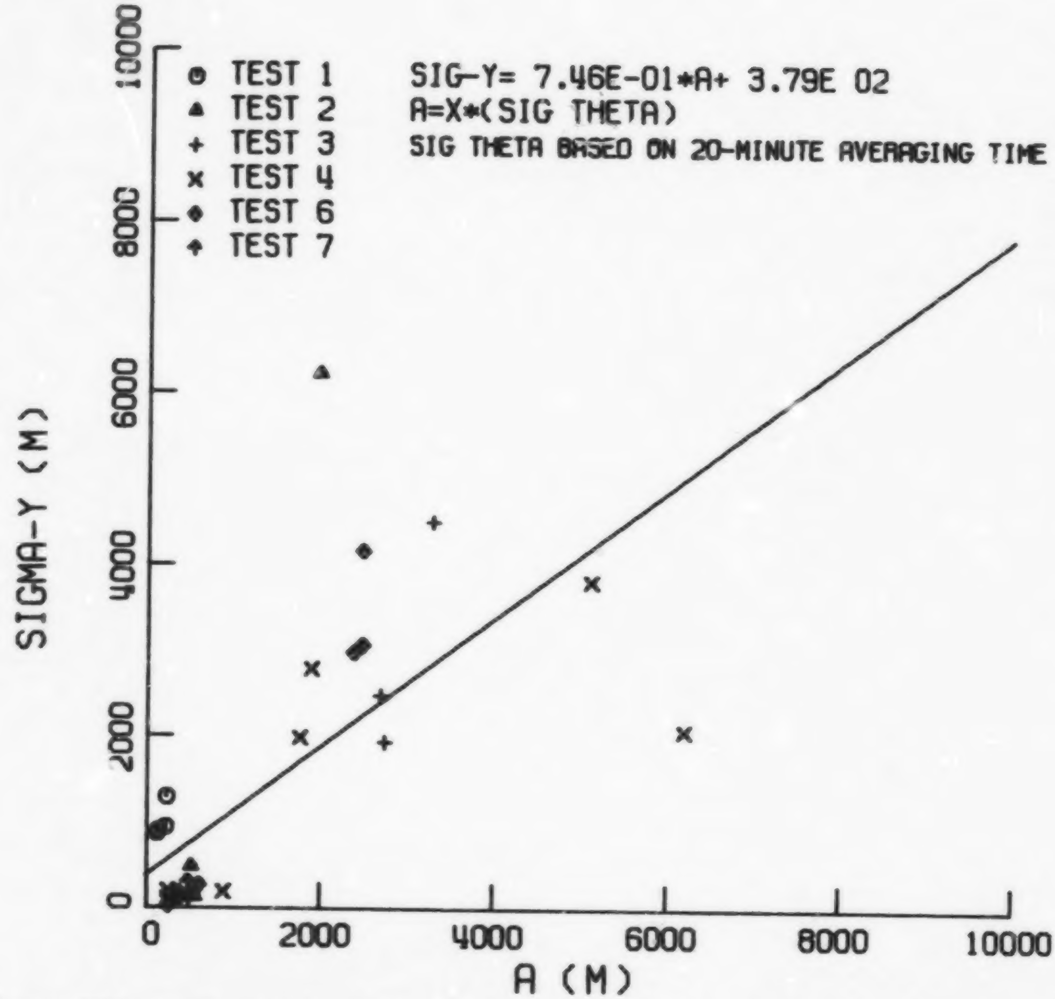

Figure 125. Horizontal crosswind standard deviation, σ_y, as a function of the horizontal standard deviation of the wind, σ_θ, measured at the Dow site in the Montezuma Hills.

relationship determined from a 5-minute average time can be improved by considering the proper range of averaging times. However, this improvement is limited since the wind data is available only in 5-minute increments. For the distances and transport times under consideration in the Delta region, a better averaging time for wind fluctuation measurements might be 1 minute. Summation of 1-minute intervals would provide a more flexible means of determining the proper averaging time.

Even though the available wind fluctuation data does not yield a one-to-one relationship between σ_y and X σ_θ, it appears that the experimental extent of horizontal dispersion in the Delta region can be determined for other periods of the year by simply acquiring the appropriate wind fluctuation data. Although it may prove difficult to obtain a suitable amount of historical σ_θ data in the area, acquiring a data base in the future will only be a matter of operating a wind anemometer and strip-chart recorder at the appropriate times and places. The acquisition of a suitable data base and the application of the simple relationship between σ_y and σ_θ to the data provide a simple, but important method of extending the results of the California Delta tracer tests to other periods of the year.

4.9 Estimated Maximum Pollutant Concentrations

The tracer data can be used with the nomographs and projected Dow emissions in Section 4.1 to estimate the maximum pollutant concentrations which would have been measured during the test periods if the Dow facility were in operation. The maximum tracer concentrations which were measured during the study and the corresponding pollutant concentrations are given in Table 14. The values of the California air quality standards are also listed. Emissions of NO are assumed to be rapidly converted to NO_2 . Results due to the Dow + turbine emissions are also given.

Comparison of the calculated pollutant concentrations and the air quality standards indicate that only the standard for NO_2 appears to be in danger of violation. Both SO_2 and CO levels are far below the respective standards. For NO_2, the observed hourly averaged data indicate that the standard would not have been violated during the test period. Except for the first two tests, the hourly data were all collected 50 km downwind along Highway 99. In 10-second data, much higher concentrations were measured approximately 10 km downwind. However, in no case based on the Dow emissions were tracer concentrations great enough to cause the NO_2 standard to be violated. The possibility of a standard violation appears more likely if the Dow facility were to include a gas turbine. If the sampling time correction from Section 4.8 is applied to the 10-second data for the Dow + turbine emissions, the data indicate that the NO_2 standard might have been violated during Tests 3, 4, 6, and 7 at downwind distances of approximately 10 km. Converted NO_2 10-second concentrations greater than 357 ppb are in violation of the standard. Worst-case conditions, according to this data, occur during the evening Sea Breeze Tail period.

TABLE 14

MAXIMUM POLLUTANT CONCENTRATIONS DUE TO PROJECTED DOW EMISSIONS

Test	$[\text{Tracer}]_{max}$ ppt	$[\text{Pollutant}]^{*}_{max}$ ppb					
		Dow Emissions			Dow + Turbine Emissions		
	10-second	$[NO_2]^{**}$	$[SO_2]$	[CO]	$[NO_2]$	$[SO_2]$	[CO]
1	1,013	30	3	5	74	3	25
2	2,168	42	4	7	103	4	35
3	8,660	286	24	49	701	28	241
4	11,900	346	29	59	848	34	290
5	801	23	2	4	57	2	20
6	9,526	284	24	49	698	28	241
7	12,140	238	20	41	584	23	201
	1-hour						
1	602	18	2	3	43	2	15
2	2,427	46	4	8	112	4	38
3	918	30	3	5	74	3	26
4	566	16	1	3	40	2	14
5	-						
6	83	3	.2	.4	6	.2	2
7	-						

California Hourly Air
Quality Standards: 250 ppb (NO_2); 500 ppb (SO_2); and 40,000 ppb (CO).

$$^{*}\ \text{Pollutant}_{max} = \text{Tracer}_{max} \cdot \frac{MW_T}{RR_T} \cdot \frac{RR_p}{MW_p}$$

MW_T and MW_p are the tracer and pollutant molecular weights, respectively; RR_T and RR_p are the tracer and pollutant emission rates, respectively.

** Emissions of NO have been assumed to react rapidly to form NO_2.

The Gaussian model predictions can be used to estimate the extent that the Dow project might influence existing air quality in the area. It appears that the air quality standard for NO_2 could possibly be violated at downwind distances of 10 km during stable evening and nighttime periods. It is of interest to determine how far downwind emissions of NO might produce levels of NO_2 greater than those that currently exist. During the two-week test period, maximum NO_2 concentrations in the area reached 0.06 ppm. By utilizing the nomograph in Section 4.1 and the predicted concentration curve for the evening test shown in Figure 126, we estimate that hourly averaged NO_2 concentrations due to Dow emissions were greater than 0.06 ppm up to 24 km downwind. This estimation assumes the conversion of NO to NO_2 is rapid and that hourly averaged values are related to the 10-second averaged data as given in Section 4.8. Similar use of the curves for the Sea Breeze period and for the Nighttime period indicate that NO_2 concentrations were greater than 0.06 ppm up to 4 km and 14 km, respectively. The emission rate of NO from the Dow site was taken to be 9.4 tons/day. These distances would increase if the projected Dow + turbine emission rate of 23 tons/day were used. The estimated impact of projected Dow emissions could double NO_2 concentrations over a significant distance downwind of Montezuma Hills.

The results of the analysis of maximum NO_2 concentrations due to projected Dow emissions are summarized in Table 15. The ambient NO_2 levels and the tracer-converted NO_2 data are compared with Gaussian model predictions presented by Dow and the predictions presented in this report. The Dow-predicted value of NO_2 at 10 km was taken from data presented by Dow officials as testimony during State of California

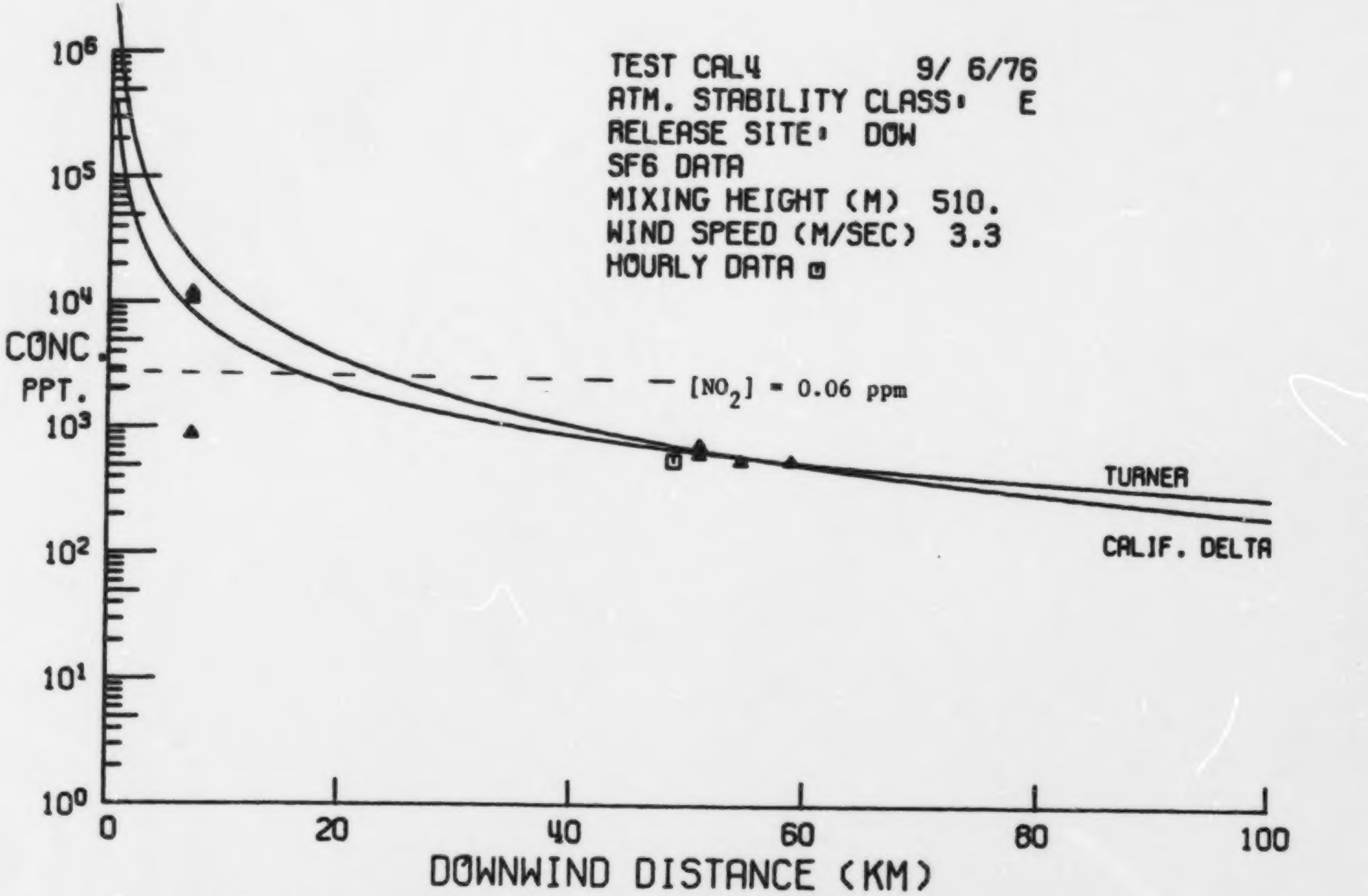

Figure 126. Estimation of distance downwind of the Montezuma Hills where the concentration of NO_2 (caused by projected Dow emissions) equals maximum ambient levels.

TABLE 15

COMPARISON OF NO_2 CONCENTRATION MEASUREMENTS AND PREDICTIONS

$[NO_2]_{max}$
ppb

Test	Ambient Measurements[1] Montezuma Hills		Estimated from Tracer Data[2] (hourly average) 10 Km		Predicted by Dow[3]	Predicted Using Tracer Dispersion Data[4] 10 Km	
	Montezuma Hills	Stockton	10 Km	50 Km		10 Km	50 Km
1	50	70	18	3.0	5.8 at 10 Km from tracer release	12	0.7
2	60	80	46	-		81	2
3	40	70	(200)	30		105	6
4	50	60	(242)	16		250	17
5	70	-	(16)	-		9	1
6	70	80	(199)				
7	10	60	(167)	-		-	2
8	40	60	-	-		-	-

[1] Ambient hourly averaged concentrations collected by Rockwell at Montezuma Hills and the San Joaquin APCD at Stockton during the test period.

[2] NO_2 concentrations estimated using maximum observed hourly-averaged tracer concentrations and projected Dow emission rates. Values in parentheses are hourly values estimated from 10-second data, $C_{HR}/C_{10s} = 0.7$.

[3] Predicted by Dow for worst-case conditions using the Gaussian plume model. Data presented as testimony during State of California multi-agency hearings, December, 1976.

[4] NO_2 concentrations predicted using the experimental σ_y and σ_z values and projected Dow emissions in the Gaussian plume model. Although σ_y and σ_z were obtained from 10-second average tracer data, comparison of 10-second and hourly averaged tracer data indicate that $C_{HR}/C_{10s} = 0.7$. The values given above have been converted to hourly averaged levels.

(California air quality standard for NO_2 equals 250 ppb, hourly average) multi-agency hearings, December, 1976 (State of California, 1976). No information is available concerning the calculation procedures employed by Dow.

The summary indicates that maximum levels of NO_2 due to projected Dow emissions are generally within a factor of 4 of the ambient levels. Measured tracer data and predicted concentrations based on the dispersion data suggest that the air quality standard for NO_2 could be violated during the evening meteorological period at distances downwind of the Montezuma Hills of approximately 10 km. This analysis has not considered the impact of NO emissions upon ambient levels of ozone downwind of the proposed construction sites.

5. Calculation of the Surface Wind Field

The rather comprehensive set of surface wind data provides a data base for calculating hourly wind fields in terms of hourly wind vectors based upon a numerical solution of the mass balance equation. The determination of the hourly surface wind vectors, in turn, provide a basis for performing an air parcel trajectory analysis of the tracer tests. In this section, we present results of wind field and trajectory calculations covering the first tracer release. The computer programs used for these calculations were developed and kindly provided by William Goodin (1977).

The numerical solutions of the mass balance equation were determined for the 4 km square grid system shown in Figure 127. The surface and upper air wind stations and the tracer release sites are marked on the grid. The numerical procedure is designed to account for the presence of topographical barriers in the grid system. Barrier lines appropriate to the Bay and Delta topography are shown in Figure 127. The program is designed to accept digital topography data. The data for the Bay Area is available, but was not used in the results presented here.

The program accepts one hour of wind data and calculates a wind vector for each grid square. If several hours of data are processed, forward air parcel trajectories can be determined from the calculated vectors. A starting point and time must be specified. The program then determines how far and in what direction an air parcel would move in an hour according to the hourly wind vectors. The trajectory develops as the parcel is moved according to each succeeding hour of data. As an example of this procedure, the surface wind data for August 31, 1976,

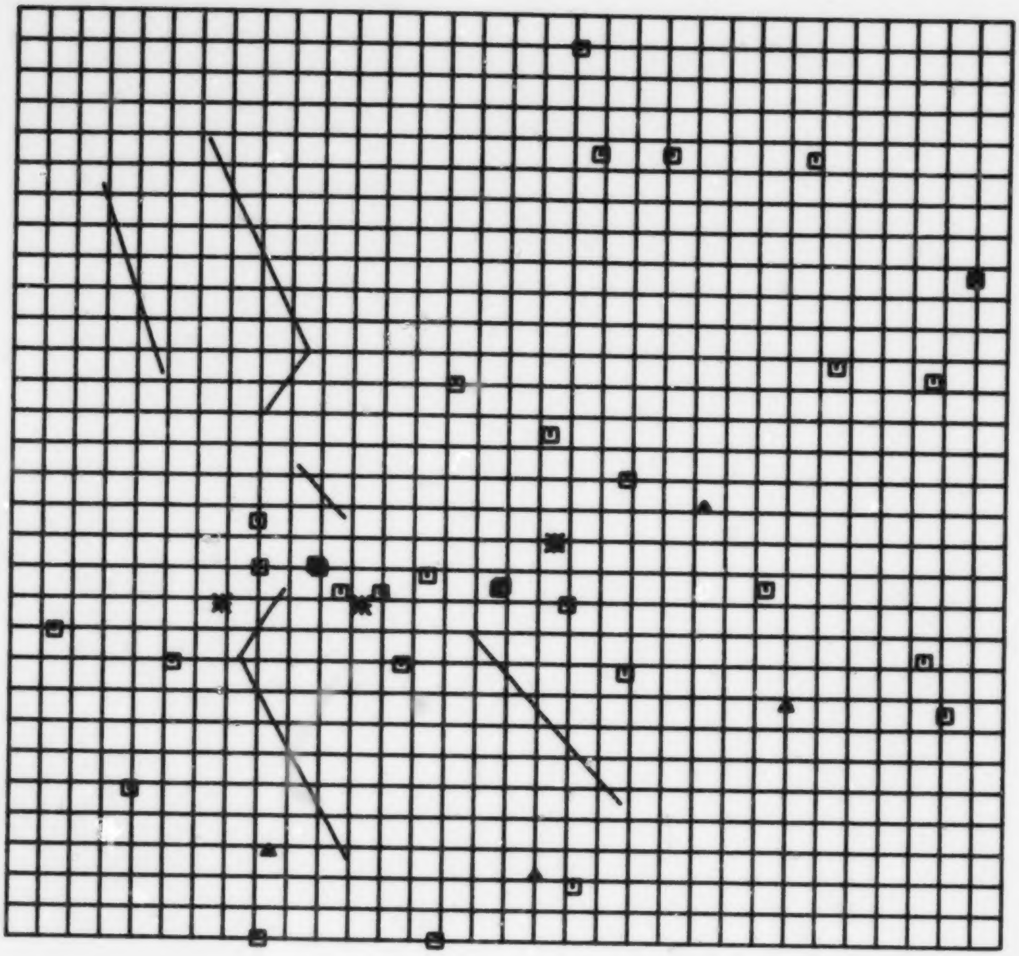

▣ SURFACE WIND STATIONS

▲ UPPER AIR WIND STATIONS

⁕ TRACER RELEASE POINTS

/ TOPOGRAPHICAL BARRIERS

Figure 127. Grid system for calculation of wind fields over the California Delta Region. Grid squares are 4 Km x 4 Km.

from 1200 to 2300 PDT were used to calculate the wind fields given in Figures 128-139. Because no data were available for the northwestern corner of the grid, a dummy wind station using data from the Davis station was placed in the corner for calculation purposes. Although the wind vectors in the northwestern sector are meaningless, the effects of the dummy data upon the remainder of the grid are considered negligible.

The major features apparent in the complex flow patterns which occurred during the first tracer test include the turning of the marine air into the northern Bay Area and the subsequent channeling of air through the Carquinez Strait. From 1200 to 1500 PDT, flow over the Delta was directed to the southeast; after 1600 PDT, the winds at the Montezuma Hills straightened towards the east. Immediately downwind of the Montezuma Hills, the flow diverged to the northeast and southeast. From 1700 to 2000 PDT, an exceptionally strong flow to the south appeared in the Stockton-Tracy area.

Upper air data obtained for the first release day were used to determine the average wind fields in 3 layers extending from 300 to 900 feet, from 900 to 1500 feet, and from 1500 to 3000 feet above the surface. The surface wind field was assumed to extend to 300 feet above the surface. The resulting three-dimensional wind field is presented in Figures 140-142 for 1700 PDT. Comparison of these upper air wind fields with the surface wind field at 1700 PDT readily illustrates the effects of the complex topography upon the gradient westerly flow. Above the surface layer, flow is uniformly from the west throughout the region. Note that if the digital topography data were used to specify the boundary condition

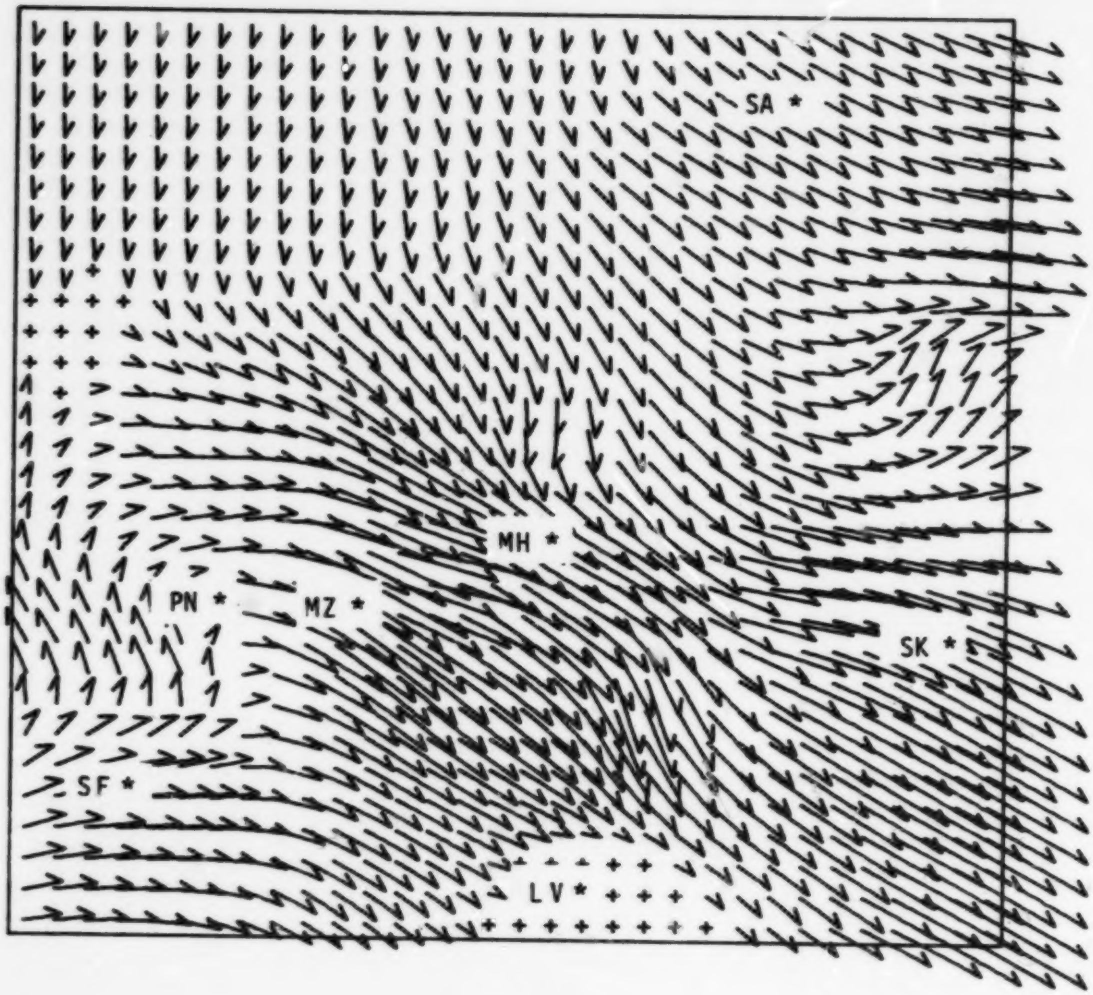

Figure 128. Hourly surface wind vectors, 1200 PDT, 8/31/76. Reference locations: Martinez (MZ), Montezuma Hills (MH), Pinole (PN), Sacramento (SA), San Francisco (SF), Stockton (SK), Livermore (LV).

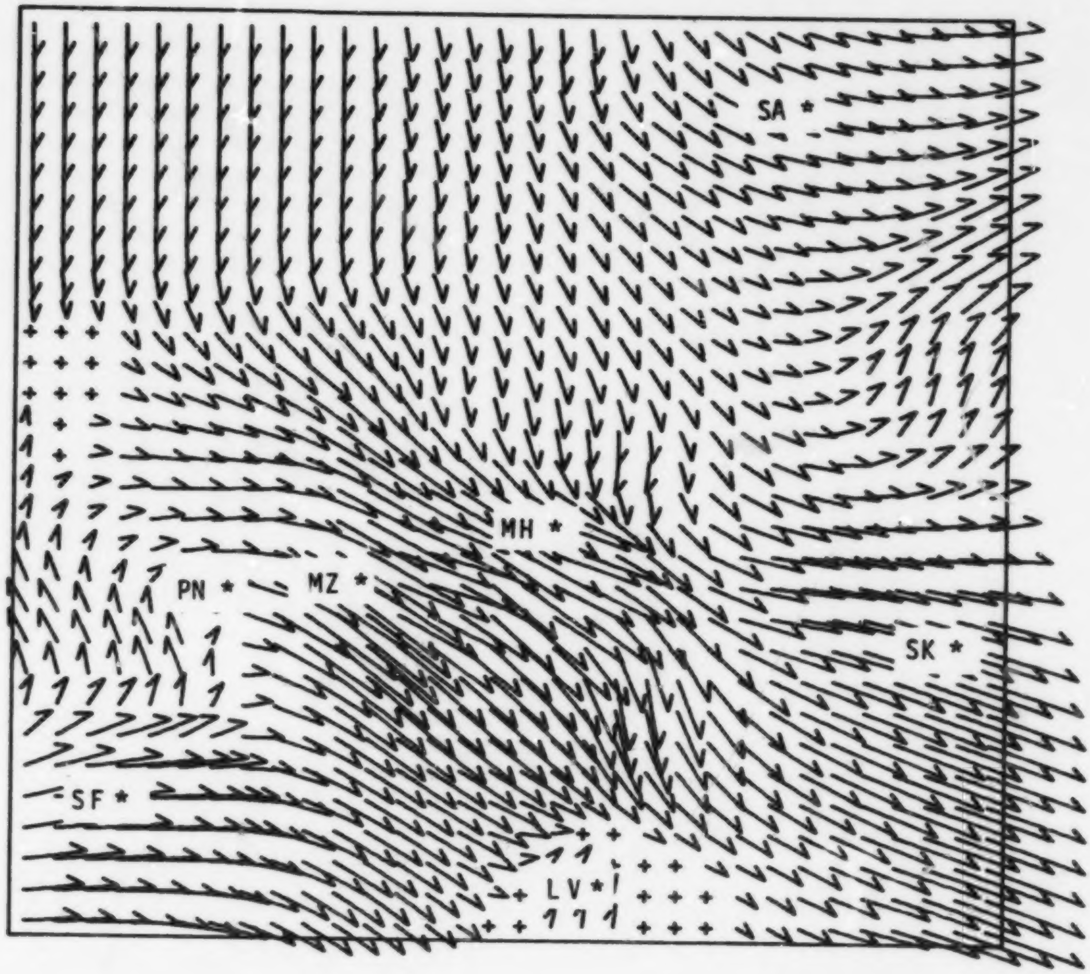

Figure 129. Hourly surface wind vectors, 1300 PDT, 8/31/76. Reference locations: Martinez (MZ), Montezuma Hills (MH), Pinole (PN), Sacramento (SA), San Francisco (SF), Stockton (SK), Livermore (LV).

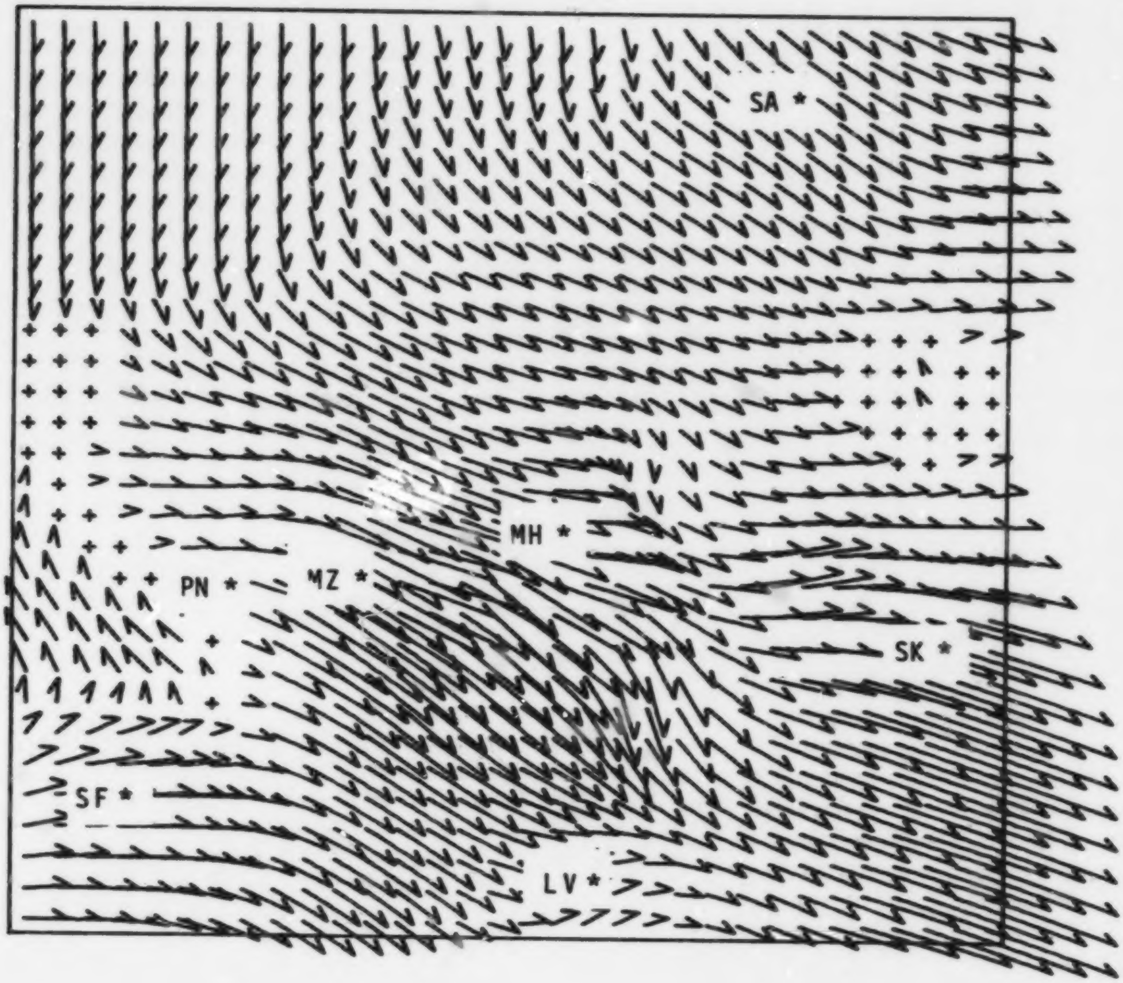

Figure 130. Hourly surface wind vectors, 1400 PDT, 8/31/76. Reference locations: Martinez (MZ), Montezuma Hills (MH), Pinole (PN), Sacramento (SA), San Francisco (SF), Stockton (SK), Livermore (LV).

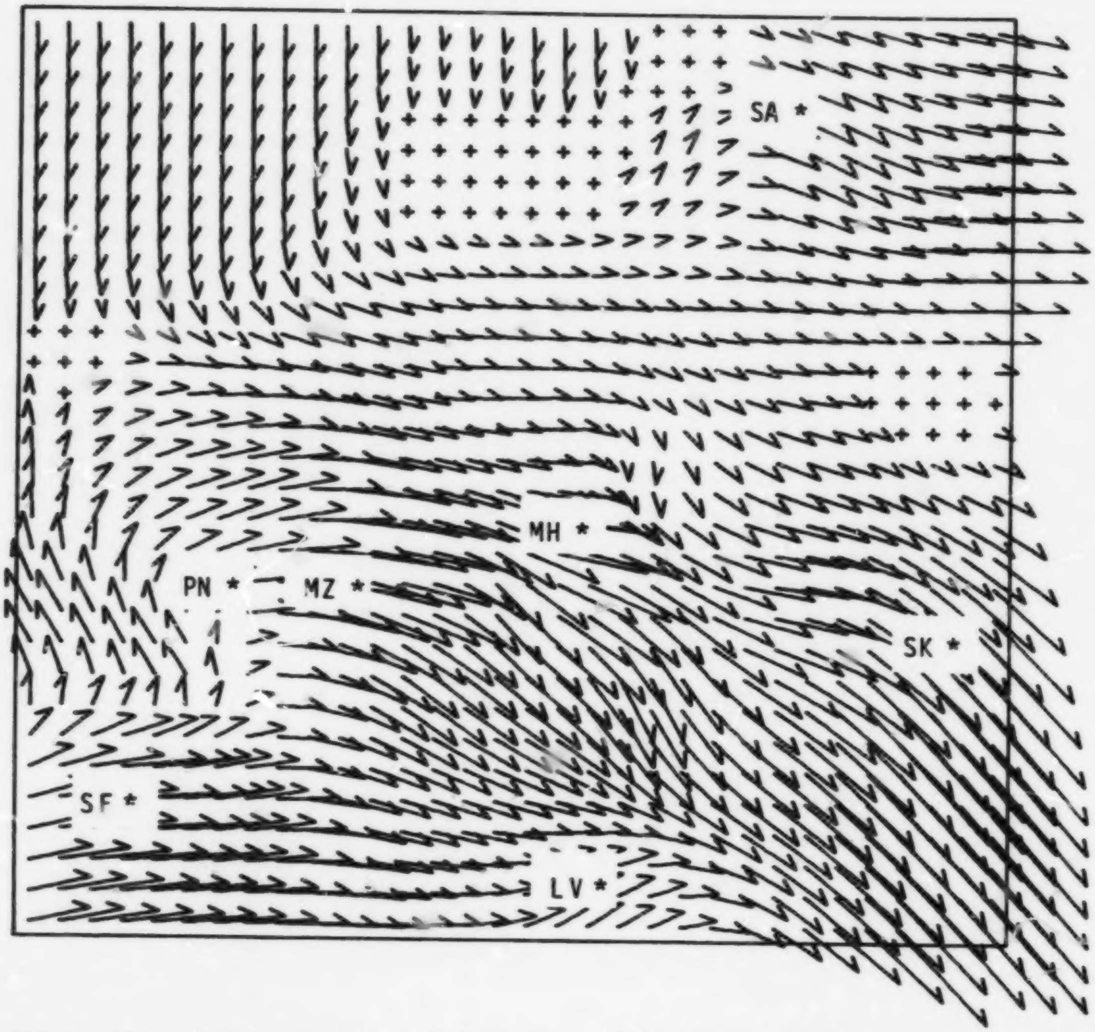

Figure 131. Hourly surface wind vectors, 1500 PDT, 8/31/76. Reference locations: Martinez (MZ), Montezuma Hills (MH), Pinole (PN), Sacramento (SA), San Francisco (SF), Stockton (SK), Livermore (LV).

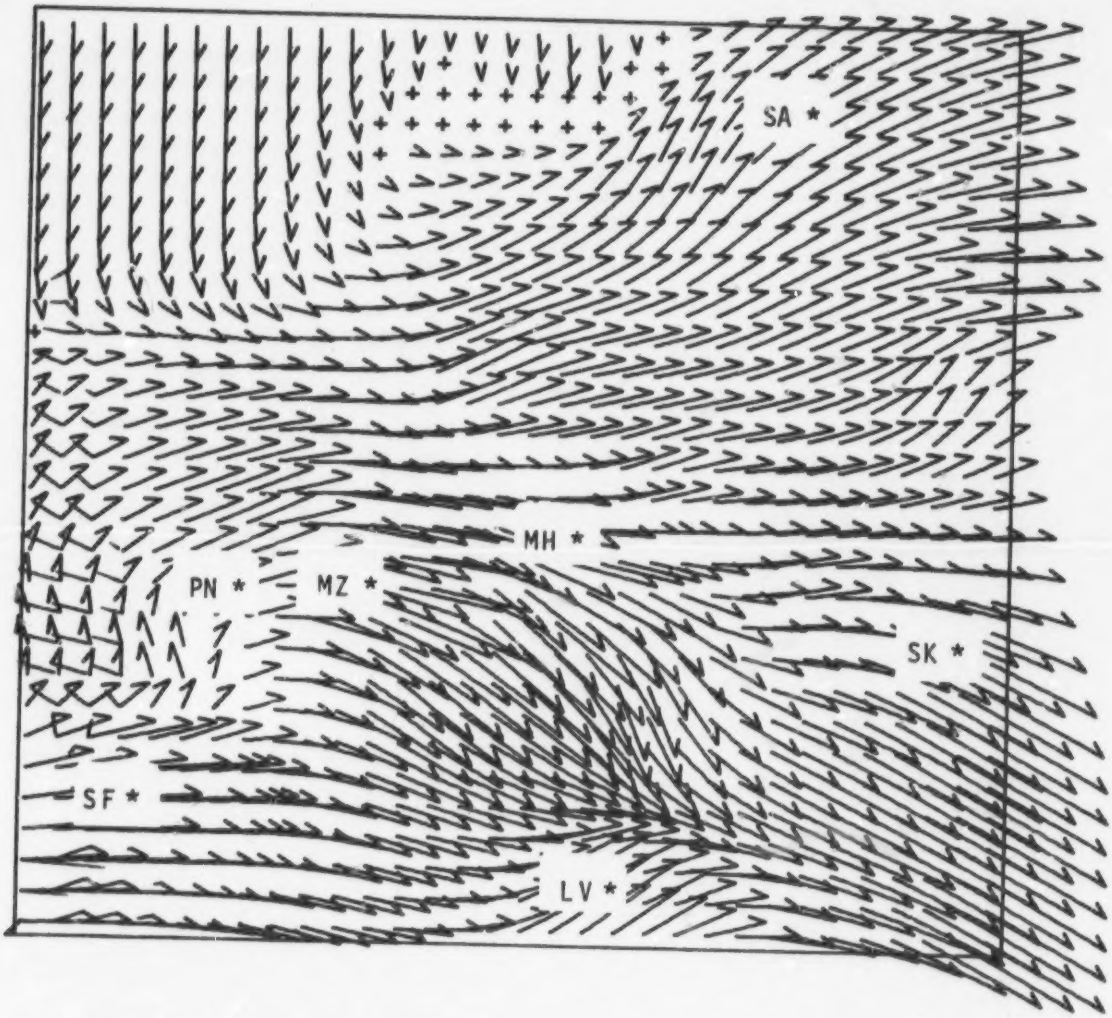

Figure 132. Hourly surface wind vectors, 1600 PDT, 8/31/76. Reference locations: Martinez (MZ), Montezuma Hills (MH), Pinole (PN), Sacramento (SA), San Francisco (SF), Stockton (SK), Livermore (LV).

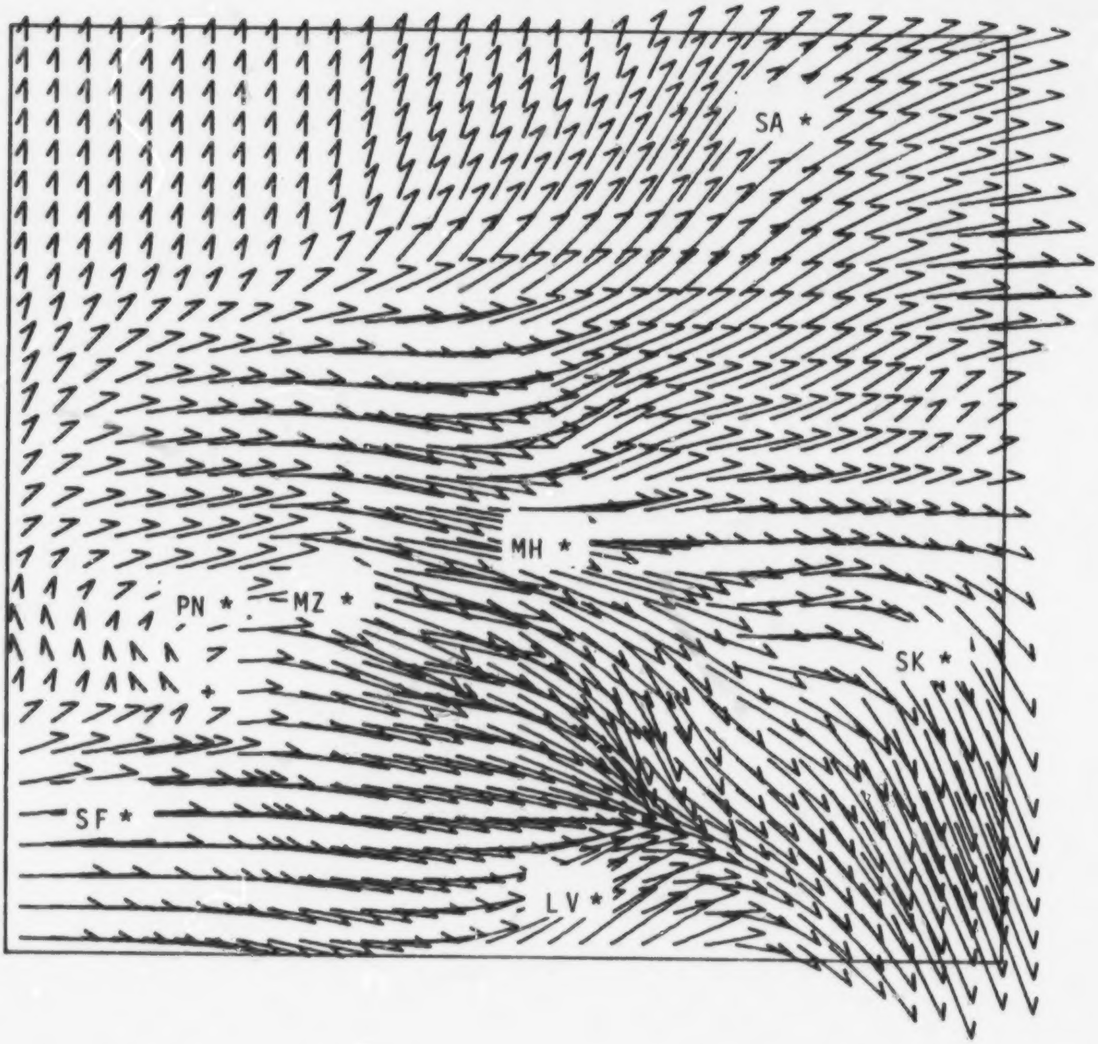

Figure 133. Hourly surface wind vectors, 1700 PDT, 8/31/76. Reference locations: Martinez (MZ), Montezuma Hills (MH), Pinole (PN), Sacramento (SA), San Francisco (SF), Stockton (SK), Livermore (LV).

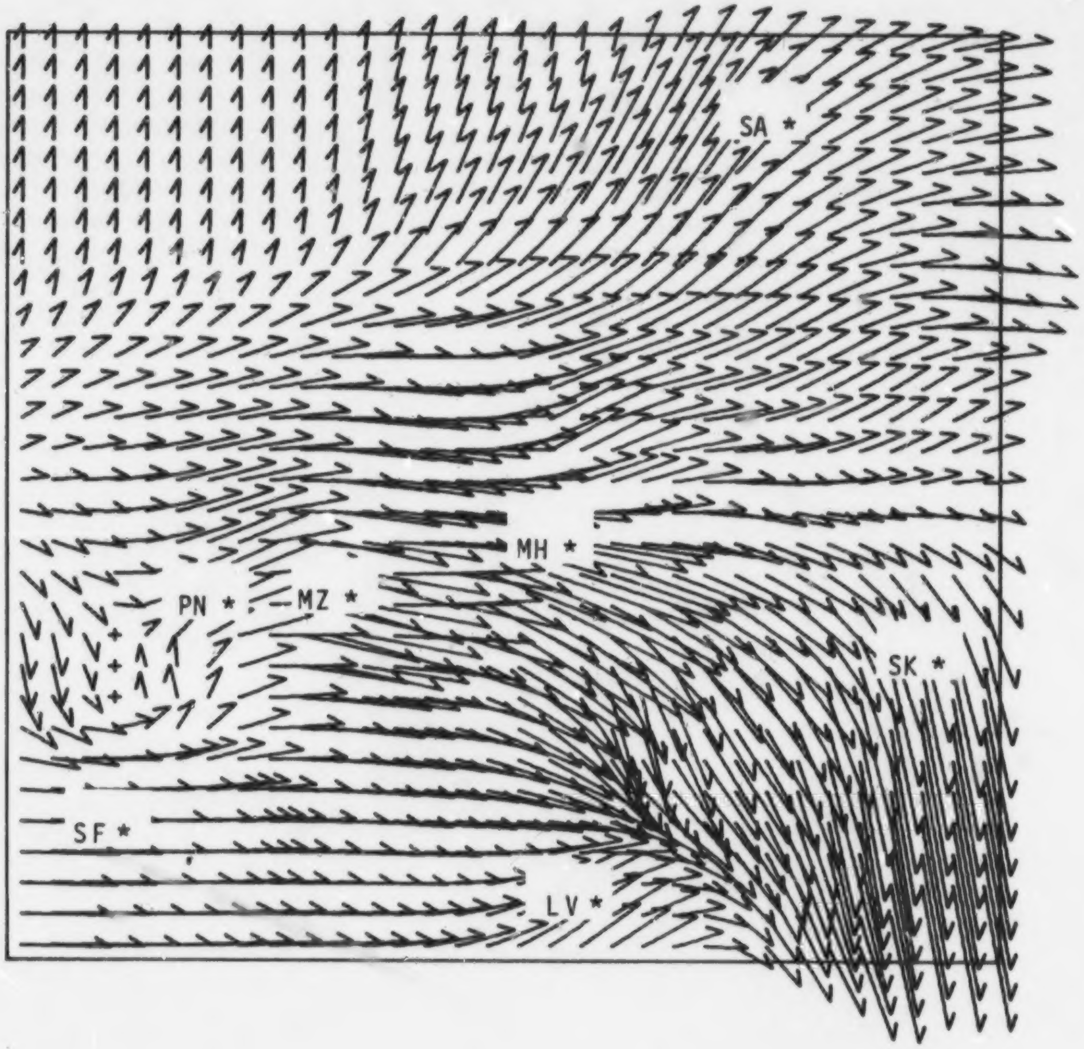

Figure 134. Hourly surface wind vectors, 1800 PDT, 8/31/76. Reference locations: Martinez (MZ), Montezuma Hills (MH), Pinole (PN), Sacramento (SA), San Francisco (SF), Stockton (SK), Livermore (LV).

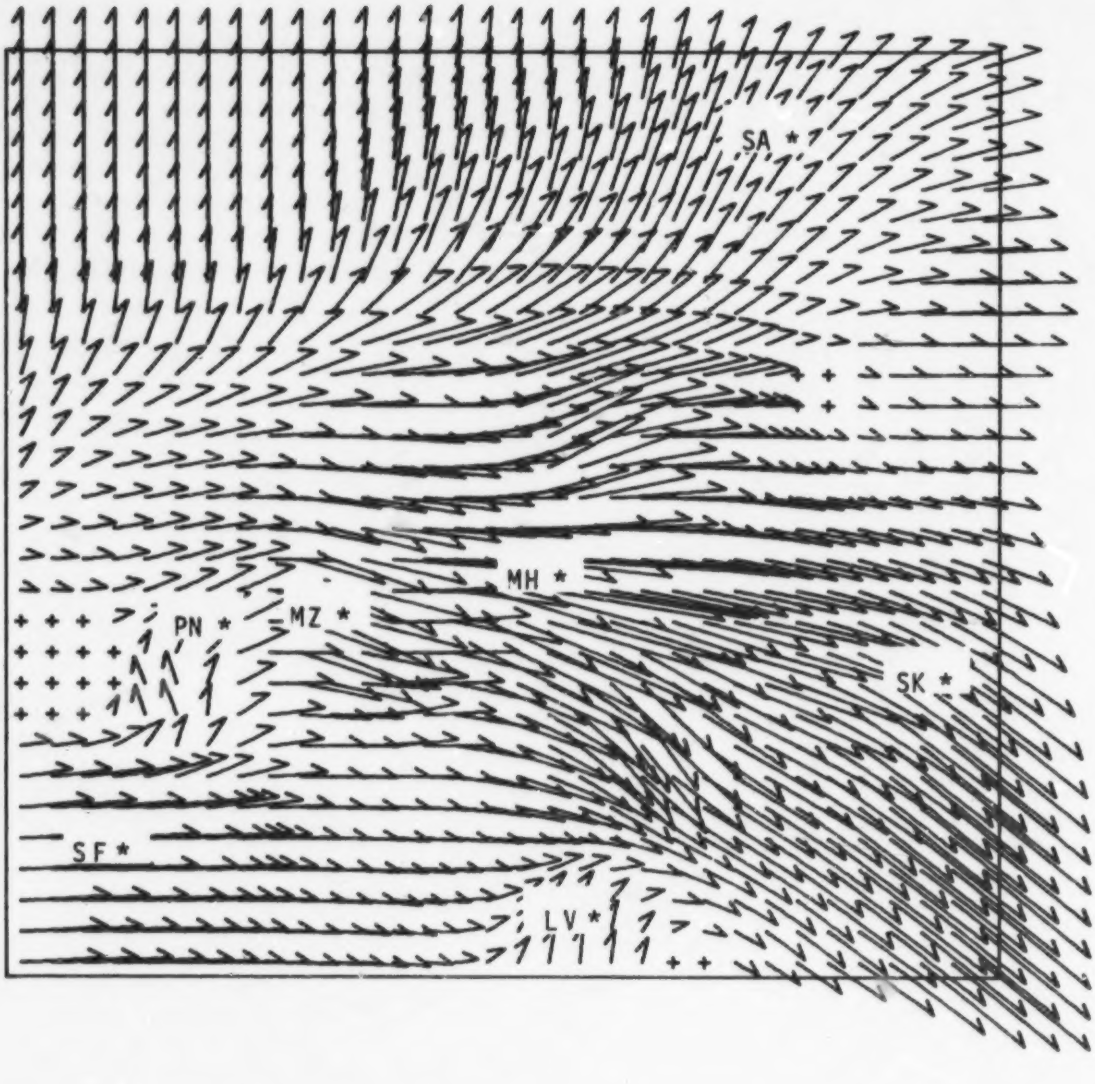

Figure 135. Hourly surface wind vectors, 1900 PDT, 8/31/76. Reference locations: Martinez (MZ), Montezuma Hills (MH), Pinole (PN), Sacramento (SA), San Francisco (SF), Stockton (SK), Livermore (LV).

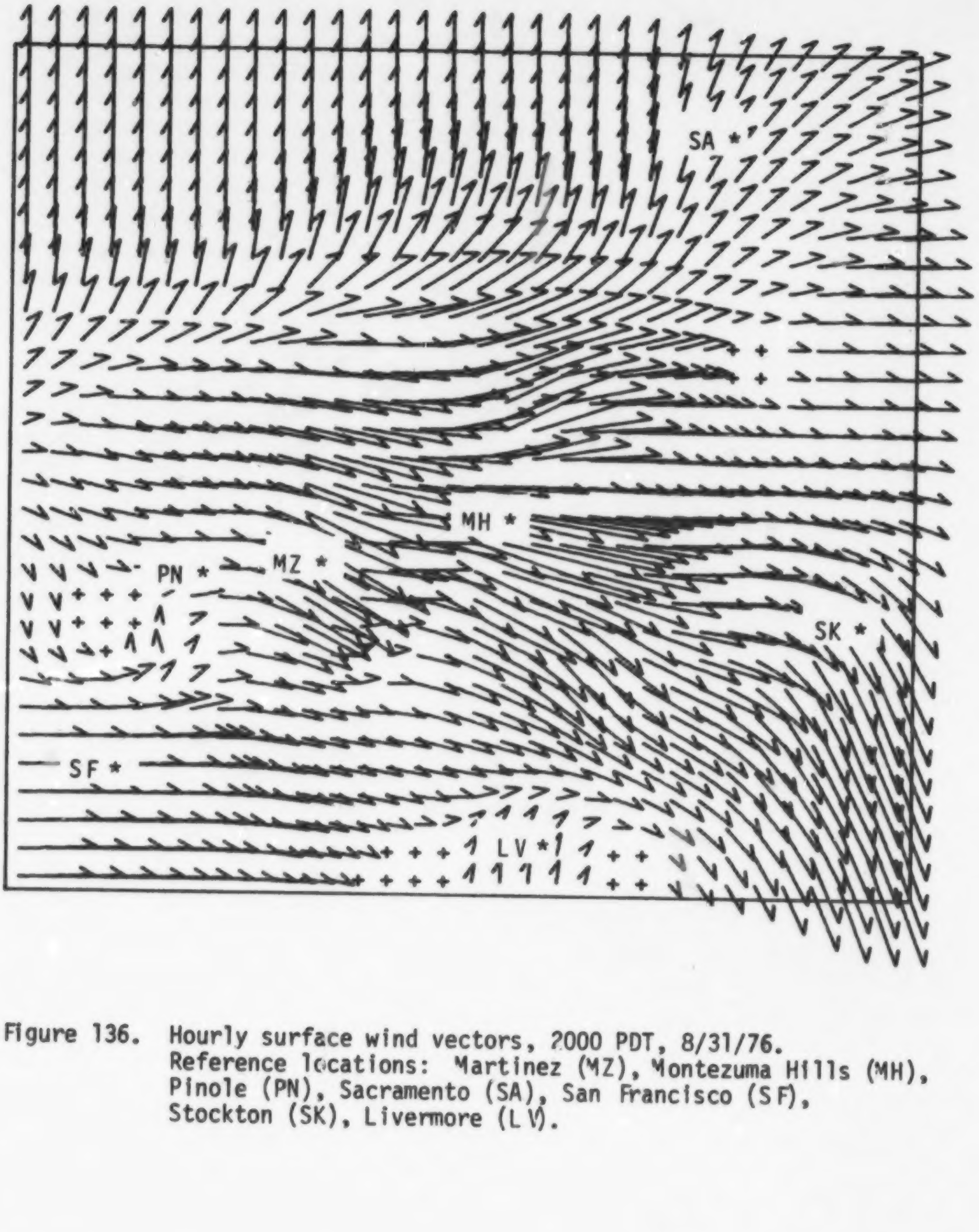

Figure 136. Hourly surface wind vectors, 2000 PDT, 8/31/76. Reference locations: Martinez (MZ), Montezuma Hills (MH), Pinole (PN), Sacramento (SA), San Francisco (SF), Stockton (SK), Livermore (LV).

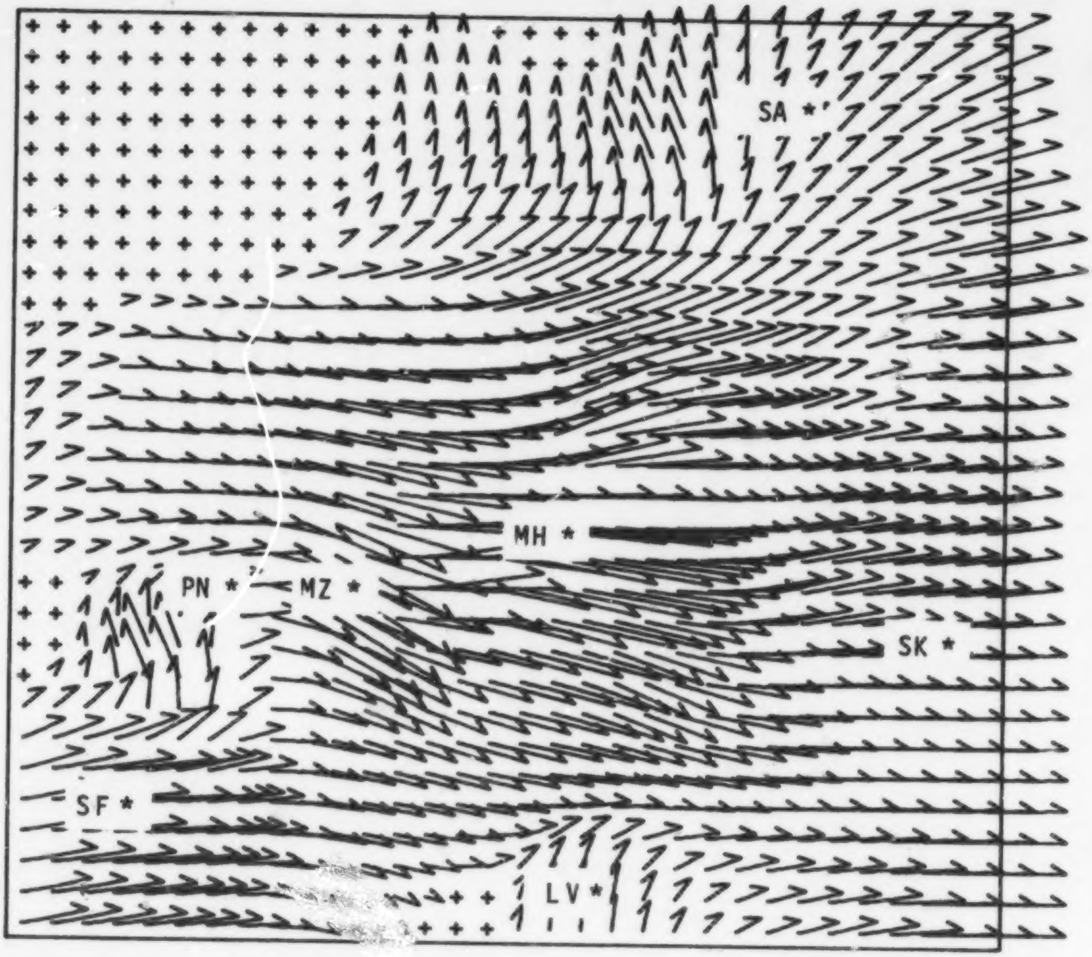

Figure 137. Hourly surface wind vectors, 2100 PDT, 8/31/76. Reference locations: Martinez (MZ), Montezuma Hills (MH), Pinole (PN), Sacramento (SA), San Francisco (SF), Stockton (SK), Livermore (LV).

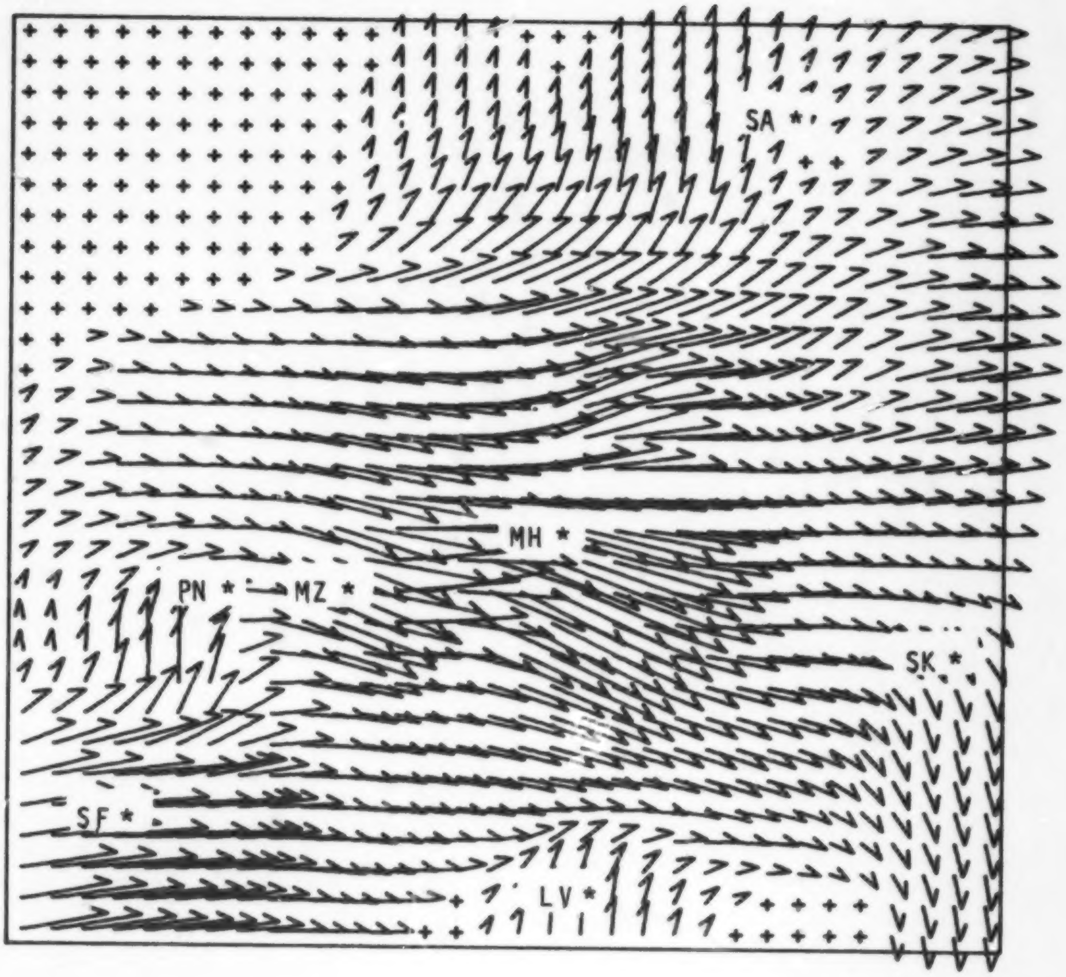

Figure 138. Hourly surface wind vectors, 2200 PDT, 8/31/76. Reference locations: Martinez (MZ), Montezuma Hills (MH), Pinole (PN), Sacramento (SA), San Francisco (SF), Stockton (SK), Livermore (LV).

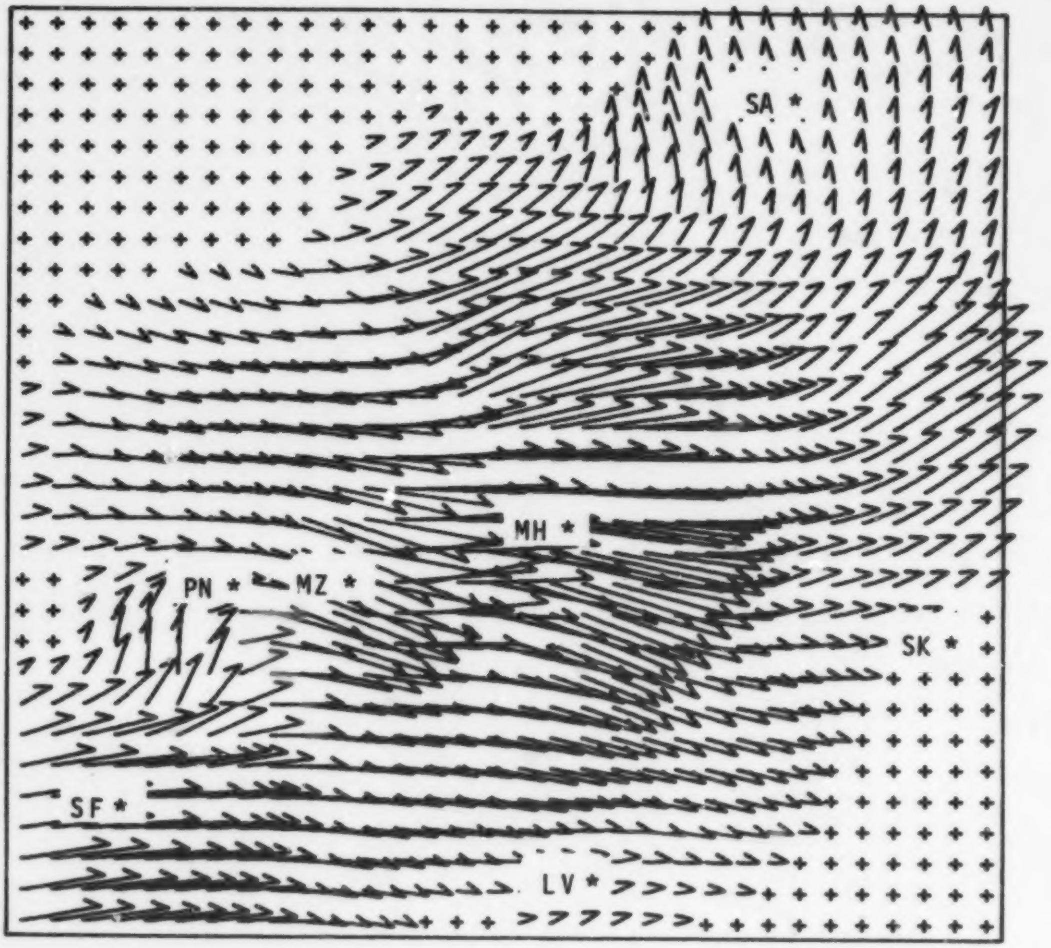

Figure 139. Hourly surface wind vectors, 2300 PDT, 8/31/76. Reference locations: Martinez (MZ), Montezuma Hills (MH), Pinole (PN), Sacramento (SA), San Francisco (SF), Stockton (SK), Livermore (LV).

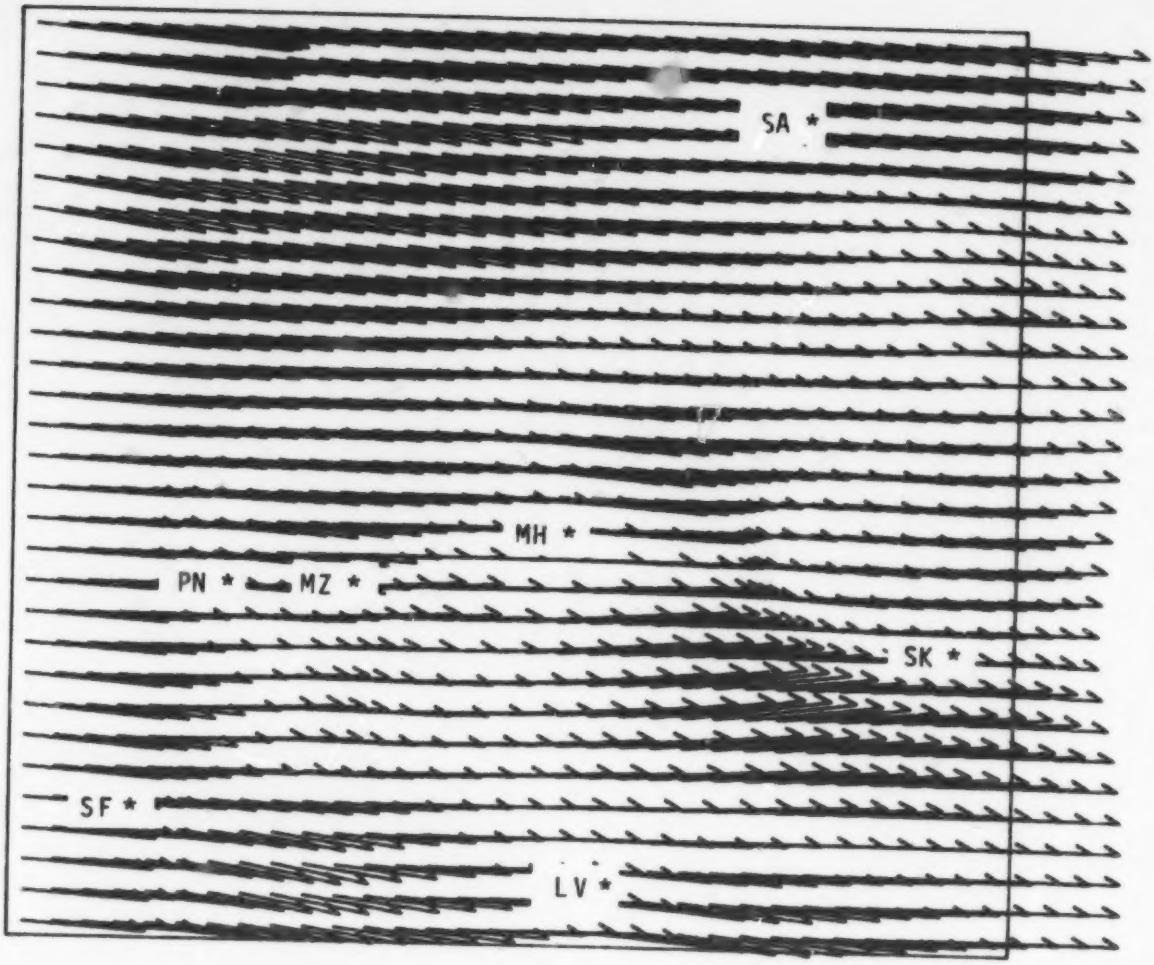

Figure 140. Hourly upper air wind vectors, average wind field from 300 to 900 feet, 1700 PDT, 8/31/76.
Reference locations: Martinez (MZ), Montezuma Hills (MH), Pinole (PN), Sacramento (SA), San Francisco (SF), Stockton (SK), Livermore (LV).

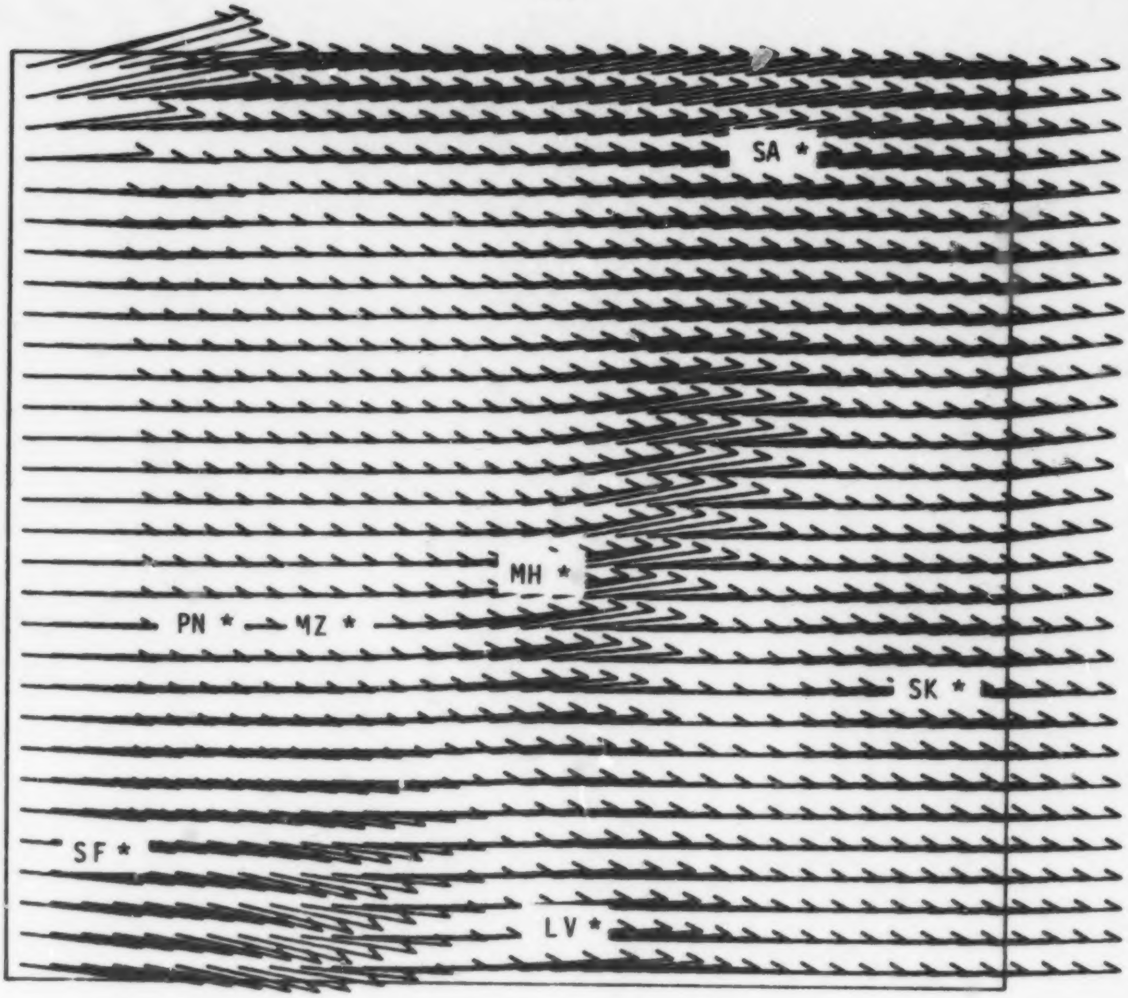

Figure 141. Hourly upper air wind vectors, average wind field from 900 to 1500 feet, 1700 PDT, 8/31/76.
Reference locations: Martinez (MZ), Montezuma Hills (MH), Pinole (PN), Sacramento (SA), San Francisco (SF), Stockton (SK), Livermore (LV).

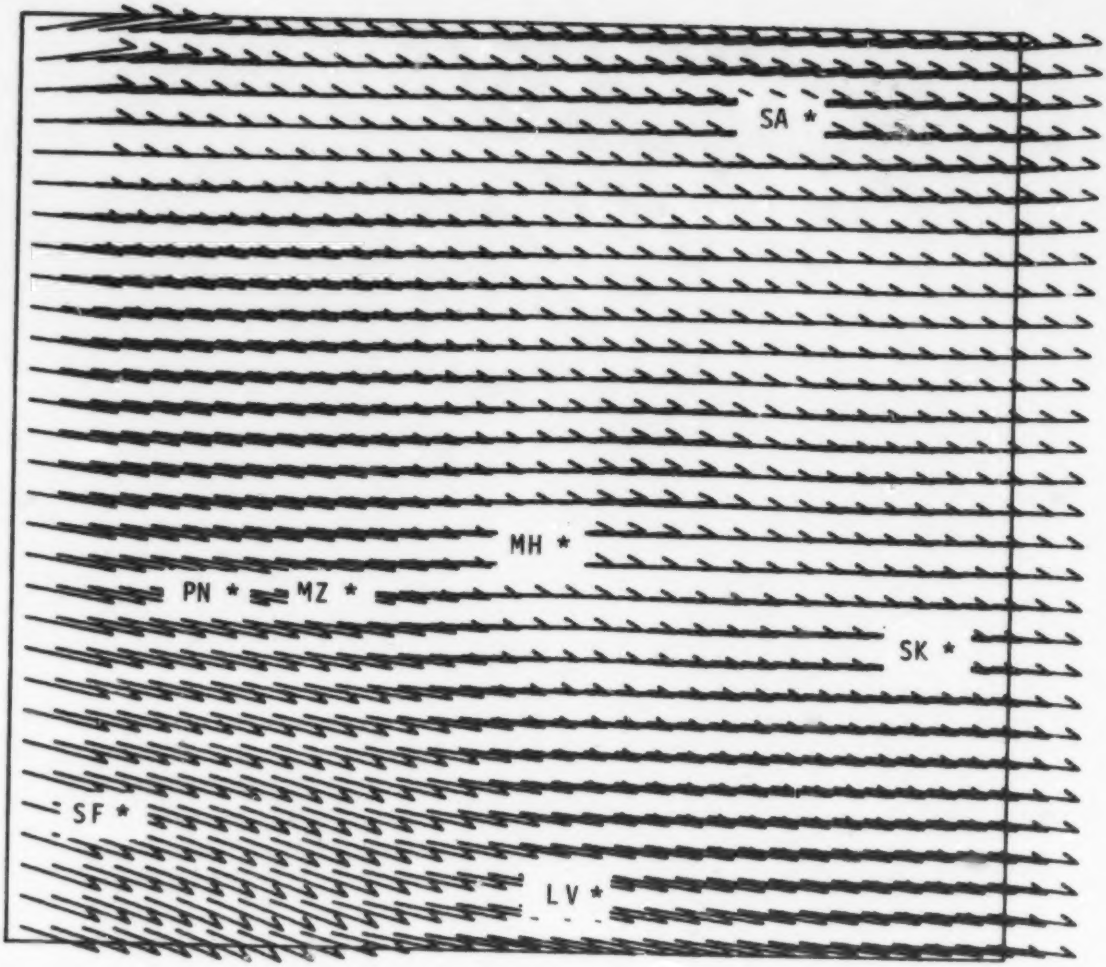

3

Figure 142. Hourly upper air wind vectors, average wind field from 1500 to 3000 feet, 1700 PDT, 8/31/76. Reference locations: Martinez (MZ), Montezuma Hills (MH), Pinole (PN), Sacramento (SA), San Francisco (SF), Stockton (SK), Livermore (LV).

at the surface, then more complex flow would probably appear in all of the upper air wind fields. The terrain surrounding the Bay Area reaches to over 1000 feet in places; Mt. Diablo rises to an elevation of 3849 feet (16 km south of Pittsburg).

Forward hourly air parcel surface trajectories beginning at the Dow site in the Montezuma Hills were calculated from the surface wind fields for starting times from 1200 to 1700 PDT. As indicated in Figure 143, all of the surface trajectories moved southeast to the Stockton-Tracy area. The effects of stagnant conditions in Stockton at 2300 PDT are apparent in the later trajectories. The paths and transport times of the surface trajectories are in excellent agreement with observations made from the traverse tracer data along Highway 99. Tracer and calculated trajectories both appeared to pass between Tracy and Stockton beginning at 1700 PDT. The maximum hourly averaged SF_6 concentration occurred between 1800 and 1900 PDT 4 km north of Stockton. Crosswind hourly profiles indicated that the SF_6 plume fluctuated through a zone extending from Lodi to Tracy between 1700 and 2000 PDT. Although the calculated surface trajectories are in agreement with the automobile traverse data at 1700 PDT, it appears that the impact zone was wider than that predicted from the trajectories. We have seen that the calculated air flow above 300 feet was directed almost due east throughout the Delta region. Airborne tracer data collected during the sixth tracer test indicated that the tracer can be mixed vertically at least as high as 600 feet after being transported from the Dow site to Highway 99. One may envision a tracer plume at the surface moving southeast towards Tracy. As tracer is mixed vertically due to the afternoon heating of the

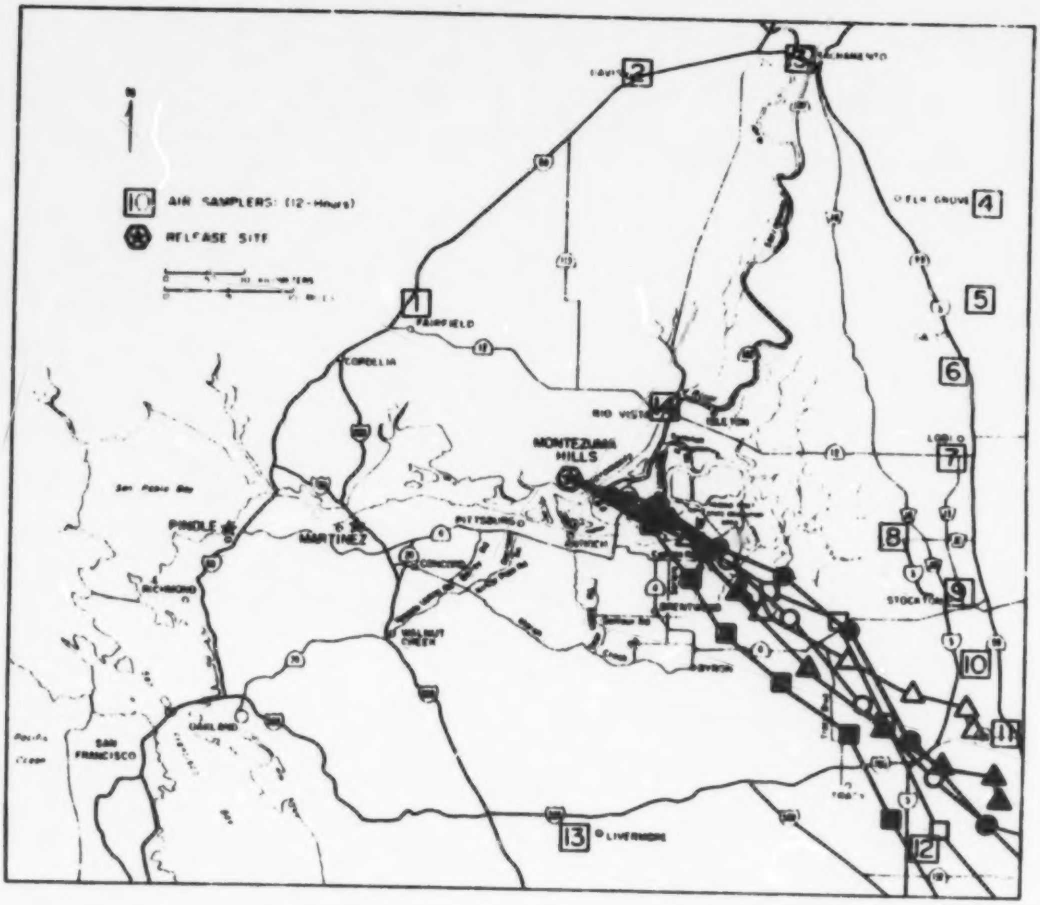
N
10 AIR SAMPLERS (12-Hours)
RELEASE SITE
SACRAMENTO
DAVIS
ELK GROVE
FAIRFIELD
CORDELIA
RIO VISTA
ISLETON
MONTEZUMA HILLS
LODI
San Pablo Bay
PINOLE
MARTINEZ
PITTSBURG
CONCORD
RICHMOND
WALNUT CREEK
BRENTWOOD
BYRON
STOCKTON
OAKLAND
SAN FRANCISCO
Pacific Ocean
TRACY
LIVERMORE
1
2
3
4
5
6
7
8
9
10
11
12
13
14

Figure 143. Forward air parcel surface trajectories; each point represents one hour of transport, 8/31/76. Trajectories were started from the Dow site in the Montezuma Hills at the following times:

1200 PDT ■

1300 PDT □

1400 PDT ●

1500 PDT ○

1600 PDT ▲

1700 PDT △

Reproduced from best available copy.

land, upper air flow from the west carries tracer east across Highway 99 in a zone from Lodi to Tracy. Although this explanation may explain the relationship between observed and calculated plume behavior, further work utilizing the digital topographical data and the three-dimensional aspects of the numerical procedure should be performed.

The surface wind fields were also used to construct air parcel trajectories beginning at Martinez and Pinole for two release times during the first tracer test. Even though we did not conduct tracer releases from these points during the first test, it is of interest to determine the transport paths of pollutants emitted in the northern Bay Area for the sake of comparison. The results for trajectories starting at 1200 and 1700 PDT from each point are shown in Figure 144. There appears to be a significant difference in paths initiated at 1200 and those started at 1700 PDT. The earlier releases from both Martinez and Pinole traveled south of Concord into the Tracy area. Winds at 1700 PDT forced the trajectories beginning at that time to move further east through Pittsburg before they turned southeast towards Tracy. Neither set of trajectories were carried over the Montezuma Hills. These patterns are very similar to those observed during Test 2 and Test 7. The trajectories which began at 1200 PDT reached Tracy at about the same time as those released from the Montezuma Hills at 1600 and 1700 PDT. Both the trajectories initiated from the Pinole-Martinez area and the trajectories started from the Montezuma Hills indicate that pollutants emitted from these points into the afternoon sea breeze can be transported into the mouth of the San Joaquin Valley.

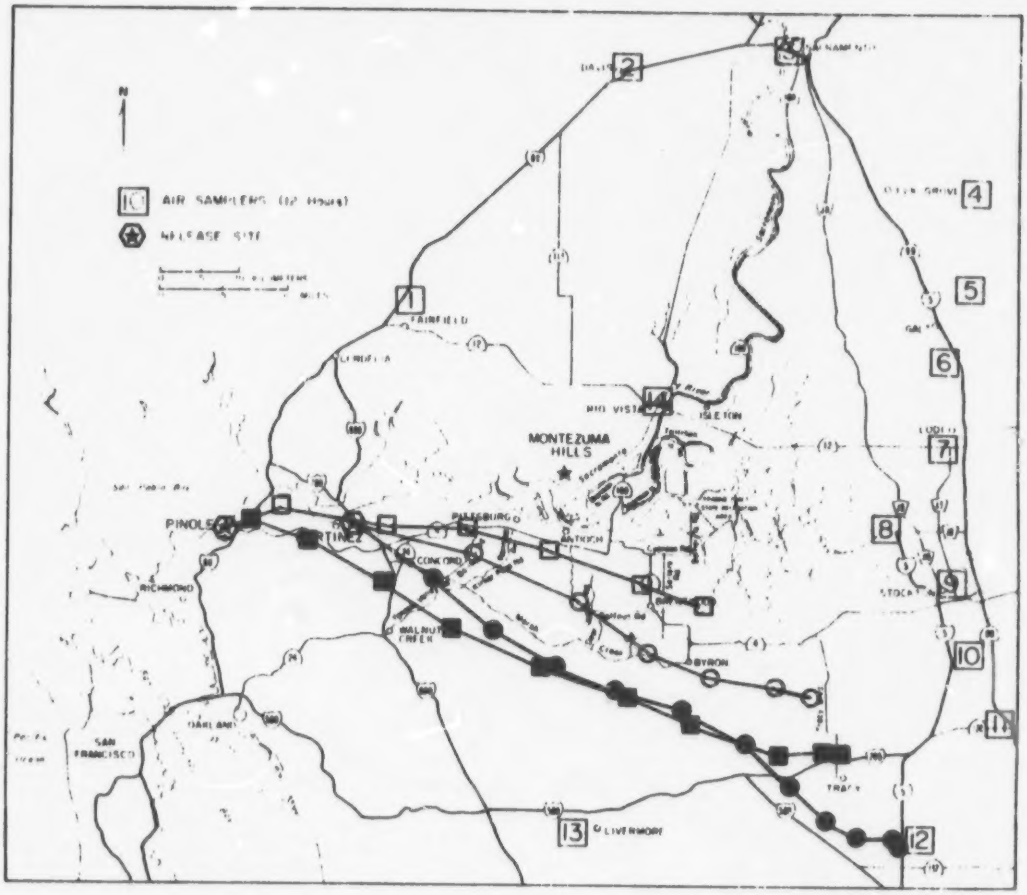
N
AIR SAMPLERS (12 Hours)
RELEASE SITE
DAVIS
2
SACRAMENTO
ELK GROVE
4
5
6
LODI
7
1
FAIRFIELD
CORDELIA
RIO VISTA
14
ISLETON
MONTEZUMA HILLS
PINOLE
MARTINEZ
PITTSBURG
ANTIOCH
CONCORD
RICHMOND
WALNUT CREEK
BYRON
8
STOCKTON
9
10
11
TRACY
12
13
LIVERMORE
OAKLAND
SAN FRANCISCO
Pacific Ocean

Figure 144. Forward air parcel surface trajectories; each point represents one hour of transport, 8/31/76. Trajectories were started from Pinole and Martinez at the following times:

Pinole	1200 PDT	■
	1700 PDT	□
Martinez	1200 PDT	●
	1700 PDT	○

Appendix A

Calibration of the twelve chromatographs (designated Z1-Z10, Y1 and Y2) was accomplished by means of a well-mixed exponential dilution system. Calibrations were completed prior to the field study on 8/21/76 and following the test on 9/28/76 and 9/29/76. The results of the calibrations are listed as KF values (integrator peak area in μV-sec/ppt tracer) in Table A-1. Several times during the field study, cross-check tests were performed among the gas chromatographs. A constant concentration sample was analyzed in several gas chromatographs in order to determine the standard deviation associated with the reproducibility of the analysis. The results of the cross-check tests are given in Table A-2.

TABLE A-1

GAS CHROMATOGRAPH CALIBRATION RESULTS

Chromatograph	SF_6			$CBrF_3$		
	KF Values		ΔKF(%)	KF Values		ΔKF(%)
	8/21/76	9/28/76				
Z5	102	102	0			
Z6	145	140	3			
Z7	101	87	14			
		Average =	7%			
Z8	100	91	9			
	8/21/76	9/29/76		8/21/76	9/29/76	
Z9	456	424	7	29	27	7
Z10	270	169	37	7	5	29
Y1	430	316	27	20	16	20
Y2	497	352	29	17	13	24
		Average =	25%		Average =	20%

TABLE A-2

GAS CHROMATOGRAPH CROSS-CHECK RESULTS

Date	Test	Chromatographs	% Std. Deviation of measured Concentrations		Average Tracer Concentration (ppt)	
8-31-76	CC-1	Z8, Z9, Y1	20		24	(SF_6)
	CC-2	Z5,Z6,Z7,Z10	20		24	(SF_6)
9-2-76	CC-3	Y1,Y2,Z10	21		2693	(SF_6)
	CC-4	Y1,Y2,Z10	3		2060	(SF_6)
	CC-5	Y1,Z9,Z10	22		2253	($CBrF_3$)
	CC-6	Y1,Y2,Z9	14		932	($CBrF_3$)
	CC-7	Z5,Z6	6		294	(SF_6)
	CC-8	Z5,Z7,Z8	13		273	(SF_6)
	CC-9	Y1,Y2,Z9,Z10	11		332	(SF_6)
				using 9-29-76 KF Values		
9-13-76	CC-10	Y1,Z5	17	(5%)	534	(SF_6)
	CC-11	Y2,Z6	24	(1%)	430	(SF_6)
	CC-12	Z8,Z9	23	(18%)	491	(SF_6)
	CC-13	Z7,Z10	28	(5%)	513	(SF_6)

Appendix B

Calculation of Plume Parameters from Crosswind Traverses

Plumes are often modeled by assuming they have a gaussian shape; that is, the concentration along a crosswind traverse follows an equation:

$$C(y) = C_o \exp\left[-\frac{1}{2}\left(\frac{y-Y_o}{\sigma}\right)^2\right] \qquad \text{(B-1)}$$

where Y_o is the distance coordinate of the center of the plume, C_o is the concentration at the center of the plume, and σ is the standard deviation of the plume. From standard data analysis techniques, equations relating σ and Y_o to the data obtained ($C(y)$ and y) are:

$$Y_o = \frac{\int_{-\infty}^{\infty} yC(y)dy}{\int_{-\infty}^{\infty} C(y)dy} \qquad \text{(B-2)}$$

and

$$\sigma = \left[\frac{\int_{-\infty}^{\infty} y^2C(y)dy}{\int_{-\infty}^{\infty} C(y)dy} - Y_o^2\right]^{\frac{1}{2}} \qquad \text{(B-3)}$$

A value for C_o can also be calculated once Y_o and σ have been calculated:

$$\int_{-\infty}^{\infty} C(y)dy = C_o\,\sigma\sqrt{2\pi} \qquad \text{(B-4)}$$

or, rearranging terms,

$$C_o = \frac{\int_{-\infty}^{\infty} C(y)dy}{\sqrt{2\pi}\,\sigma} \qquad \text{(C-5)}$$

These parameters (C_o, Y_o, σ) when used in Equation (B-1) represent a best-fit of the data ($C(y)$, y) to the equation.

Three major sources of error appear in the actual use of these equations: one is the error inherent in the data itself; another is due to the data being for discrete points rather than for all y; and finally, due to limitation on the sampling locations, one or both edges of the plume might be chopped off (the integration cannot be carried out to the limits, $-\infty$, ∞). The errors in the data cannot be reduced once the data is taken, but errors in application of the above formulas can be estimated and reduced to some extent.

The error involved in calculating the integrals is dependent upon the method used, but the error involved in chopping off the edges of the plume can be treated generally and is considered first. By assuming a perfect gaussian plume and calculating the parameters from equations (B-2)-(B-5), but with limits of integration Y_a and Y_b instead of $-\infty$ and $+\infty$, the following expressions for error of the results can be found:

$$(5)\; Y_o' = Y_o - \frac{\sigma\, e^{-\frac{1}{2}u^2}\Big|_{u_a}^{u_b}}{\sqrt{2\pi}\, P_{(u)}\Big|_{u_a}^{u_b}} \qquad \text{(B-6)}$$

$$(6)\; \sigma' = \sigma\left[1 - \frac{u\, e^{-\frac{1}{2}u^2}\Big|_{u_a}^{u_b}}{\sqrt{2\pi}\, P_{(u)}\Big|_{u_a}^{u_b}} - \frac{1}{2\pi}\left(\frac{e^{-\frac{1}{2}u^2}\Big|_{u_a}^{u_b}}{P_{(u)}\Big|_{u_a}^{u_b}}\right)^2\right]^{\frac{1}{2}} \qquad \text{(B-7)}$$

$$u = \left(\frac{Y - Y_o}{\sigma}\right)$$

$$P_{(u)} = \frac{1}{\sqrt{2\pi}} \int_{-\infty}^{u} e^{-\frac{1}{2}v^2}\, dr$$ (note $P_{(u)}$ is the Normal Probability function.)

where σ and Y_o are the actual parameters of the plume, and σ' and Y_o'

are the parameters calculated using formulas (B-2)-(B-5) with limits of integration Y_a and Y_b. No simple expressions for Y_o and σ in terms of Y_o' and σ' could be found; however, equations (B-6) and (B-7) can be applied in an iterative manner so that successively better approximations of Y_o and σ can be found.

$$Y_{o(n+1)} = Y_{o(o)} + \frac{\sigma(n)\, e^{-\frac{1}{2}u^2}\Big|_{ua(n)}^{ub(n)}}{\sqrt{2\pi}\, P_{(u)}\Big|_{ua(n)}^{ub(n)}} \qquad \text{(B-8)}$$

$$\sigma_{(n+1)} = \sigma_{(o)}\left[1 - \frac{u\, e^{-\frac{1}{2}u^2}\Big|_{ua(n)}^{ub(n)}}{\sqrt{2\pi}\, P_{(u)}\Big|_{ua(n)}^{ub(n)}} - \frac{1}{2\pi}\left(\frac{e^{-\frac{1}{2}u^2}\Big|_{ua(n)}^{ub(n)}}{P_{(u)}\Big|_{ua(n)}^{ub(n)}}\right)^2\right]^{-\frac{1}{2}} \qquad \text{(B-9)}$$

$$U_{n(n)} = \left(\frac{Y_y - Y_{o(n)}}{\sigma_n}\right) \qquad \text{(B-10)}$$

where the small subscript in ( ) refers to the number of times the iteration was performed to arrive at that approximation, (o) refers to initially calculated values.

Traverse data are usually taken at even intervals along the traverse which simplifies the integration considerably. The method we chose was Simpson's method; Simpson's Rule is written as follows:

$$\int_{Y_o}^{Y_{2n}} f(x)\, dx = \frac{h}{3}\left[f_o + f_{2n} + 4\sum_{i=1}^{n}(f_{2i-1}) + 2\sum_{i=1}^{n-1}(f_{2i})\right] + \varepsilon \qquad \text{(B-11)}$$

where h is the difference between any two x_i, $f_i = f(x_i)$, and 2n+1 is the number of data points. The error term ε is shown below:

$$\varepsilon = \frac{nh^5}{90} \frac{d^4 f}{dx^4}(x) \qquad \text{where } X_0 < \varepsilon < X_{2n} \tag{B-12}$$

Since ε is unknown only a minimum and maximum error can be found. If f(x) is of the form of a gaussian curve, the minimum and maximum errors are

$$\varepsilon_{min} = -.02061 \frac{C_0 nh^5}{\sigma^4} \qquad \varepsilon_{max} = \frac{nh^5 C_0}{30\sigma^4} \tag{B-13}$$

The curves we deal with are not exactly gaussian, so this error loses much of its significance; however, it is calculated as a check on the data (a grossly large error could mean that the data is bad).

Literature Cited

1. Angell, J. K., D. H. Pack, G. C. Holzworth, and C. R. Dickson (1966) "Tetroon Trajectories in an Urban Atmosphere," *J. Appl. Meteor*. *5*, 565-572.

2. Ang[illegible], J. K., C. R. Dickson, and W. H. Hoecker, Jr. (1976) "Tetroon Trajectories in the Los Angeles Basin Defining the Source of Air Reaching the San Bernardino-Riverside Area in Late Afternoon," *J. Appl. Meteor*. *15*, 197-204.

3. Briggs, G. A. (1969) *Plume Rise* USAEC Critical Review Series TID-25075, National Technical Information Service, Springfield, Va. 22151.

4. Briggs, G. A. (1972) "Discussion on Chimney Plumes in Neutral and Stable Surroundings," *Atmos. Environ*. *6*, 507-510.

5. California State (1976) Transcripts from State Consolidated Hearings concerning the Dow Petrochemical Project, December 8-9, 1976, State Lands Commission, 1807 13th Street, Sacramento, California 95814.

6. Drivas, P. J. (1974) "Investigation of Atmospheric Disperion Problems by Means of a Tracer Technique," Ph.D. Thesis, California Institute of Technology, 16-26.

7. Drivas, P. J., and F. H. Shair (1974) "A Tracer Study of Pollutant Transport and Dispersion in the Los Angeles Area," *Atmos. Environ*. *8*, 1155-1163.

8. Drivas, P. J. and F. H. Shair (1975) "The Chemistry, Dispersion, and Transport of Air Pollutants Emitted from Fossil Fuel Power Plants in California; Transport and Dispersion of Plumes Associated with Coastal Meteorology," Final Report for the California State Air Resources Board, Contract No. ARB 3-915, 1709 11th Street, Sacramento, California 95814

9. Fosberg, M. A., D. G. Fox, E. A. Howard, and J. D. Cohen (1976) "Nonturbulent Dispersion Processes in Complex Terrain," *Atmos. Environ*. *10*, 1053-1055.

10. Fosberg, M. A., and M. J. Schroeder (1966) "Marine Air Penetration in Central California," *J. Appl. Meteor.* *5*, 573-589.

11. Frenzel, C. W. (1962) "Diurnal Wind Variations in Central California," *J. Appl. Meteor*. *1*, 405-512.

12. Gifford, F. A., Jr. (1968) "An Outline of Theories of Diffusion in Lower Layers of the Atmosphere," in D. H. Slade (ed), "Meteorology and Atomic Energy, 1968," U. S. Atomic Energy Commission, Oak Ridge, Tenn. 101-103.

13. Giroux, H. D., L. E. Hausner, L. H. Teuscher, and P. Testerman (1974) "Power Plant Plume Tracing in the Southern California Marine Layer," from Proceedings of the Symposium on Atmospheric Diffusion and Air Pollution. Amer. Meteor. Soc., Boston, Mass. 02108 238-245.

14. Goodin, W. (1977), Environmental Quality Laboratory, California Institute of Technology, Pasadena, Calif. 91125, personal communication.

15. Hay, J. S., and F. Pasquill (1959) "Diffusion from a Continuous Source in Relation to the Spectrum and Scale of Turbulence," Advances in Geophys. 6, 345-364.

16. Hinds, W. T. (1970) "Diffusion Over Coastal Mountains of Southern California," Atmos. Environ. 4, 107-124.

17. Hino, M. (1968) "Maximum Ground-level Concentrations and Sampling Times," Atmos. Environ. 2, 149-165.

18. Islitzer, N. F. (1961) "Short-Range Atmospheric Dispersion Measurements from an Elevated Source," J. of Meteor. 18, 443-450.

19. Islitzer, N. F., and R. K. Dumbauld (1963) "Atmospheric Diffusion-deposition Studies Over Flat Terrain," Intern. J. Air Water Poll. 7, 999-1022.

20. Lamb, B. K., and F. H. Shair (1977) "Tracer Study of Power Plant Emission Transport and Dispersion from the Oxnard/Ventura Plain," California State Air Resources Board, Contract No. ARB-5-306, 1709 11th Street, Sacramento, Calif. 95814.

21. Liu, M., D. Durran, P. Mundkar, M. Yocke, and J. Ames (1976) "The Chemistry, Dispersion, and Transport of Air Pollutants Emitted from Fossil Fuel Power Plants in California: Data Analysis and Emission Impact Model," California State Air Resources Board, Contract No. ARB-4-258, 1709 11th Street, Sacramento, Calif. 95814.

22. MacReady, P. B., Jr., L. B. Baboolal, and P. B. S. Lissaman (1974) "Diffusion and Turbulence Aloft over Complex Terrain," from the Proceedings of the Symposium on Atmospheric Diffusion and Air Pollution, Amer. Meteor. Soc., Boston, Mass. 02108, 218-225.

23. Miller, A. (1968) "Wind Profiles in West Coast Temperature Inversions," Report No. 4, San Jose State College, Dept. of Meteor., San Jose, Calif.

24. Moyer, N. (1977) California State Air Resources Board, personal communication.

25. Nonhebel, G. (1960) "Recommendations on Heights for New Industrial Chimneys," J. Inst. Fuel. 33, 479-511.

26. Pasquill, F. (1974) Atmospheric Diffusion. John Wiley and Sons, New York, 298-300.

27. Peters, L. K., and L. W. Richards (1977) "Extension of Atmospheric Dispersion Models to Incorporate Fast Reversible Reactions," Atmos. Environ. 11, 101-108.

28. Reynolds, S. D., P. M. Roth, and J. H. Seinfeld (1973) "Mathematical Modeling of Photochemical Air Pollution - I," Atmos. Environ. 7, 1033-1061.

29. Roberts, P. T. (1975) "Gas-To-Particle Conversion: Sulfur Dioxide in a Photochemically Reactive System," Ph.D. Thesis, California Institute of Technology, Pasadena, Calif. 91125.

30. Roffman, A., and R. Grimble (1974) "A Time-Dependent Air Quality Model With Terrain Corrections," from the Proceedings of the Symposium on Atmospheric Diffusion and Air Pollution, Amer. Meteor. Soc., Boston, Mass. 02108, 311-317.

31. Sandberg, J. S., W. J. Walker, and R. H. Thuiller (1970) "Fluorescent Tracer Studies of Pollutant Transport in the San Francisco Bay Area," J. Air Poll. Contr. Assoc. 20, 593-598.

32. Seinfeld, J. H. (1975) Air Pollution: Physical and Chemical Fundamentals McGraw-Hill, Inc., New York, 260-351.

33. Smalley, C. (1957) "A Study of Air Flow Patterns in the San Francisco Bay Area," Information Bulletin 6-15-70, Technical Services Division, Bay Area Air Pollution Control District, San Francisco, Calif.

34. Smith, T. B. (1977) Meteorology Research, Inc., Altadena, Calif. personal communication.

35. Start, G. E., C. R. Dickson, and N. R. Ricks (1974) "Effluent Dilutions Over Mountainous Terrain and Within Mountain Canyons," from the Proceedings of the Symposium on Atmospheric Diffusion and Air Pollution, Amer. Meteor. Soc., Boston, Mass. 02108 226-232.

36. Turner, D. B. (1961) "Relationships Between 24-Hour Mean Air Quality Measurements and Meteorological Factors in Nashville, Tennessee," J. Air Poll. Contr. Assoc. 11, 483-489.

37. Turner, D. B. (1970) "Workbook of Atmospheric Dispersion Estimates," Environmental Protection Agency, Research Triangle Park, North Carolina.